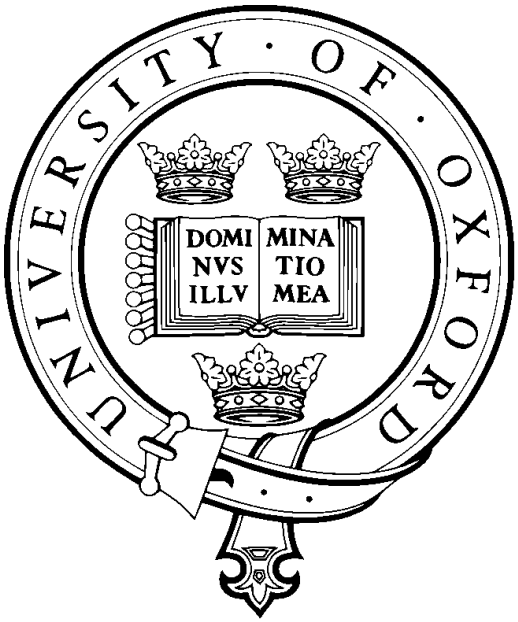
Novel Molecular Therapies for the Treatment of Familial Hypercholesterolaemia

Alastair Kerr

Department of Physiology, Anatomy and Genetics
and
Cardiovascular Medicine



A thesis submitted for the degree of Doctor of Philosophy in Cardiovascular Science

St Cross College

University of Oxford

Michaelmas Term 2016

Abstract

Familial hypercholesterolaemia (FH) is an autosomal dominant genetic disorder characterised by elevated levels of plasma low density lipoprotein (LDL) cholesterol. Loss-of-function mutations in the Low-Density Lipoprotein Receptor (LDLR) gene are responsible for ~85% of all FH cases. Heterozygous FH (HeFH) affects 1 in 200-500 individuals world-wide, while homozygous FH (HoFH) has a prevalence of one in a 160000-1000000. Elevated levels of LDL-cholesterol in the blood lead to an accelerated development of atherosclerosis and progression to coronary heart disease.

The work presented in this thesis investigates two novel molecular therapies for the treatment of FH. A small molecule approach for the treatment of HeFH and a non-viral gene therapy for the treatment of HoFH.

Small molecule: Through a compound screen, we identified a series of small molecules able to upregulate the LDLR at nanomolar potencies, via a mechanism distinct from statins. We then went on to elucidate the mechanism of action as inhibitors of squalene synthase and demonstrated, that when used in combination with statins, these compounds give a much greater increase in LDLR expression than can be achieved with statins alone. By carrying out extensive structure-activity relationship studies we improved the potency and pharmacokinetics of our lead compound and demonstrated *in vivo* efficacy.

Non-viral gene therapy: We have previously generated mini-gene vectors carrying the human *LDLR* cDNA, driven by 10 kb of genomic DNA from the native human *LDLR* locus, encompassing the promoter region. To further enhance *LDLR* transgene expression, a miRNA, targeting Hmgcr (miR82) was cloned into the same vector, generating a combinatorial RNAi-*LDLR* vector. *In vivo,* we show the RNAi-*LDLR* vector is able to significantly reduce total and LDL-cholesterol in *Ldlr*$^{-/-}$ mice fed a high cholesterol diet twelve weeks post-delivery. The LDL-cholesterol lowering resulted in reduced atherosclerosis in the RNAi-*LDLR* vector treated mice. Here we demonstrate for the first time, that an episomal non-viral vector is able to significantly reduce LDL-cholesterol and slow the progression of atherosclerosis in a mouse model of FH.

Acknowledgements

First and foremost, I would like to thank my supervisors, Richard Wade-Martins and Keith Channon, for taking a punt on me and giving me the opportunity to carry out my DPhil in their labs. I feel very lucky to have had two very different but excellent scientists to have learnt from and attempt to mould myself against. The support Richard has provided me throughout my DPhil has been invaluable, the way you have helped me look towards the future experiment and big picture of the work is something I will take forward for the rest of my scientific career. Just as valuable, has been your sound career advice and how to get yourself noticed in this sometimes flooded market. Your door always seemed open and I would of not progressed my career outside of the lab without you. To Keith, I owe so much in how I try and think about an individual scientific problem, being part of your lab meetings and listening to you dissect each element of a result apart is something I have been in awe of and still am now.

My second thanks go to Lawrence who raised me scientifically through the troublesome teething years and was eternally patient while I learnt what happens when you label all your tubes of clear liquid ‘later’. Special garage pirate radio shout outs to Brent and Hugo for mad analytical insight they be sharing and science real talk, whenever, wherever. To the office crew, still going strong since 2k12. We have lost members over the years to factions such as ISIS and weird places no one has even heard of before, like Canada, but it has been a pleasure to sit on the science front line and share true war horror stories of ill-loaded western blots with you all. In particular, Nora for a lot of helpful science chat and teaching me about the apartheid that should exist between types of food. Rozzy, James and Sarah for your science and life (relationship) advice and Gabriella for making Ecuador my favourite South American country. Thanks to Becky for never letting a man do a strawpedo solo, Ben for showing me the quickest way to get home from a Christmas party and Dayne for showing me there is at least one Arsenal fan that understands football. The post-doc offices and all its members for advice on many a problem, including Amy, Natalie, Oscar, Ruth, Mic, Ana, Charmaine, Siv and Tara, it has been a pleasure. A special shout out is reserved for Milena, who has helped me so much over the four years with all animal work,

you made doubling up in those fume hoods for hours, a joy. Everyone in the Wade-Martins lab and Channon lab past and present deserve a thank you, as I have never gone to someone who has not taken the time to help me and I hope you all felt the same with me.

I would like to thank Mark, Eileen and Jyoti for putting up with constant science queries and always taking time away from your work to patiently talk through any questions I may have had. Thanks to Gillian for help with planning and preparation of most of my animal experiments. To Ash, for always seemingly making time to help me with my work no matter how much you had on, it was a pleasure to spend mornings and afternoons in the procedure rooms trying to brainstorm when Villa might put pick up their next three points. A huge thanks to the chemistry team for all their help with the small molecule work, especially Angela, Graham, Carole and Joe. I still don't know much about chemistry but thanks to you I am much better at pretending I do.

I would like to thank my flatmate Will for helping me run the roads during the Piffley patrol era, and showing Oxford how a reel badman don't take no bek chat. You made living in Oxford an absolute pleasure and I have had some of my funniest times in that house. I know we will stay mates for a long time.

A shout out to my London raving crew, Liam, Stefan, Lia, Lindah and Annisha for reminding me there is a life outside the lab and helping me recharge ready to get back in the lab on Monday. In particular, Stef and Liam, you have been my sound council through all the ups and downs over the years. Love you boys.

Finally, a huge, huge thank you to my parents and brother for their unwavering support of me throughout the DPhil, I could never have achieved any of this without your guidance and love. I dedicate this thesis to all three of you.

Declaration

I hereby declare that this thesis is the product of my own work and that were others have contributed every effort has been made to acknowledge the contribution. This work has not been submitted for any other degree.

Publications

Publications

Kerr AG, Tam LCS, Hale AB, Cioroch M, Douglas G, Channon KM and Wade-Martins R. **Episomal non-viral gene therapy vectors slow progression of atherosclerosis in a model of familial hypercholesterolemia.** (2016) Accepted for publication Molecular Therapy: Nucleic Acids

Kerr AG, Tam LCS, Hale AB, Cioroch M, Douglas G, Agkatser S, Hibbitt O, Mason J, Holt-Martyn J, Batille C, Wynne G, Channon KM, Russell A, Wade-Martins R. **A novel series of squalene series inhibitors able to enhance the upregulation of the low-density lipoprotein receptor seen with statins.** Manuscript in preparation

Table of Contents

Abstract **1**

Chapter 1: Introduction **21**

1.1 Cardiovascular disease **21**

1.2 Cholesterol **21**

1.3 Lipoproteins **22**

1.4 Low-density lipoprotein receptor **26**

1.4.1 Structure and function of the low-density lipoprotein receptor 26

1.4.2 Regulation of the low-density lipoprotein receptor 28

1.5 LDL-cholesterol and cardiovascular disease **30**

1.5.1 Evidence for LDL-cholesterol's role in cardiovascular disease 30

1.5.2 Atherosclerosis 31

1.5.3 LDL-cholesterol and its role in atherosclerosis 33

1.6 Familial hypercholesterolaemia **34**

1.6.1 Identification of familial hypercholesterolaemia 34

1.6.2 Prevalence and genetic causation of familial hypercholesterolaemia 35

1.6.3 Clinical diagnosis and prognosis 36

1.6.4 Current therapies for familial hypercholesterolaemia 37

1.7 Gene therapy for familial hypercholesterolaemia **46**

1.7.1 Gene therapy 46

1.7.2 A liver targeted gene therapy for familial hypercholesterolaemia 46

1.8 Aims of thesis **55**

Chapter 2: Materials and Methods 57

2.1 Cell culture of immortalised cell lines 57

2.1.1 Cell Culture 57

2.1.2 Drug treatment 57

2.1.3 Cryopreservation of cells 58

2.1.4 Thawing of frozen cell stocks 58

2.2 Plasmid transfection 58

2.3 In vitro luciferase activity assay 58

2.4 Protein quantification 59

2.5 Cytotoxicity assay 59

2.6 Analysis of mRNA expression 59

2.6.1 RNA isolation 59

2.6.2 cDNA synthesis 60

2.6.3 Quantitative real time polymerase chain reaction (qRT-PCR) 60

2.6.4 qRT-PCR expression analysis 61

2.7 Western blot analysis of protein expression 62

2.7.1 Protein extraction 62

2.7.2 Western blot 62

2.8 HMG-CoA Reductase activity assay 64

2.9 Squalene Synthase activity assay 64

2.10 Animal husbandry, breeding and experimental procedures 65

2.11 Pharmacokinetic measurement of compounds in mouse plasma 66

2.11.1 Preparation of compounds for delivery 66

2.11.2 Dosing and collection of samples 67

2.11.3 HPLC analysis of compounds in plasma 67

2.12 Vector cloning 67

2.12.1 Miniprep 67

2.12.2 Endotoxin free megaprep 68

2.12.3 Restriction digest of plasmids 68

2.12.4 Agarose gel electrophoresis 69

2.13 In vivo luciferase activity assay 69

2.13.1 Hydrodynamic delivery 69

2.13.2 Luciferase imaging 69

2.14 Plasma analysis of lipids and proteins 70

2.15 Immunohistochemistry 70

2.15.1 Fixation and processing of heart and liver samples 70

2.15.2 Immunofluorescent detection of LDLR 71

2.15.3 Immunohistochemical detection of Galectin-3 72

2.16 Aortic root plaque size analysis 72

2.17 Oil red-O lipid staining 73

2.17.1 En face aorta plaque analysis 73

2.17.2 Fixation and processing frozen liver samples 73

2.17.3 Oil red-O staining on frozen liver sections 74

2.18 Plasmid rescue assay 74

2.18.1 Isolation of total DNA from liver 74

2.18.2 Electrocompetent cells 75

2.18.3 Electroporation of DNA into electrocompetent cells 75

2.18.4 Plasmid rescue 75

2.19 Statistical analysis 76

Chapter 3: Identification of a novel series of small molecules able to upregulate the low-density lipoprotein receptor 77

3.1 Introduction 77

3.1.1 The need for further small molecules able to upregulate the low-density lipoprotein receptor 77

3.1.2 Potential mechanisms underlying the side effects of statins 78

3.1.3 Squalene synthase 80

3.1.4 Squalene synthase inhibitors as hypocholesterolaemic agents 81

3.1.5 A compound screen to identify novel molecules which upregulate the low-density lipoprotein receptor..... 83

3.2 Results 85

3.2.1 Identification of a novel set of small molecules which drive expression through the LDLR promoter 85

3.2.2 Compounds 15a, 65 and 90 do not inhibit HMG-CoA reductase 87

3.2.3 Compounds 15a and 65 are able to increase the LDLR at the mRNA and protein level in hepatocyte cell lines..... 89

3.2.1 Compound 40 and Compound 15a inhibit squalene synthase..... 92

3.2.1 A squalene synthase inhibitor and statin used in combination causes a synergistic drive in expression from the LDLR promoter 95

3.3 Discussion 97

Chapter 4: Demonstration of in vivo efficacy of a novel squalene synthase inhibitor.....101

4.1 Introduction 101

4.1.1 Squalene synthase and other cholesterol biosynthesis inhibitors in animal models 101

4.1.2 Development of a functional in vivo reporter assay for the determination of compound efficacy 103

4.1.3 Hydrodynamic delivery of a non-viral plasmid to the liver 103

4.2 Results 104

4.2.1 Compound 15a has a low half-life when spiked into mouse liver microsomes 104

4.2.2 Compound 40 is a more potent analogue of Compound 15a with improved pharmacokinetics 106

..... 108

4.2.3 Compound 40 can be detected in mouse plasma 6 hours post administration 109

4.2.4 After hydrodynamic delivery the right median lobe shows the highest level of transgene expression 114

4.2.5 β-cyclodextrin causes increased expression of the human LDLR promoter in vivo 116

4.2.6 Corn oil with Kolliphor EL can act as a vehicle for compound 40 .. 118

4.2.7 Compound 40 is able to upregulate the human LDLR promoter in vivo 120

4.3 Discussion 122

Chapter 5: Characterisation of a novel non-viral combinatorial vector in an animal model of familial hypercholesterolaemia....126

5.1 Introduction 126

5.1.1 Development of the pLDLR-LDLR 2nd generation mini-gene vector 126

5.1.2 Development of the pLDLR-LDLR-miR82 3rd generation mini-gene vector 127

..... 129

5.1.3 Animal models of familial hypercholesterolaemia 131

5.2 Results 133

5.2.1 Characterisation of a 1% high cholesterol diet as a model of familial hypercholesterolaemia 133

5.2.2 LDLR-Hmgcr-RNAi results in lipid lowering and sustained LDLR upregulation in 1% HC-fed Ldlr$^{-/-}$ mice 135

5.2.3 A meta-analysis of diet intervention in the Ldlr$^{-/-}$ mouse..... 140

5.2.4 Characterisation of a more moderate hypercholesterolaemic diet as a model for familial hypercholesterolaemia 144

5.2.5 LDLR-Hmgcr-RNAi vector treatment results in long term lipid lowering and reduced atherosclerosis 148

5.3 Discussion 157

Chapter 6: Discussion 162

6.1 Small molecule squalene synthase inhibitor 163

6.2 Combinatorial non-viral gene therapy 167

Figure 1 – Chemical structure of cholesterol. 21

Figure 2 – General structure of a lipoprotein 22

Figure 3 - Overview of lipoprotein metabolism (Kwiterovich 2000) 25

Figure 4 - Schematic representation of the LDLR gene (A), mRNA (B) and protein (C) (Al-Allaf et al. 2010). 28

Figure 5 – Graphical representation of the effect of age and cumulative LDL-cholesterol on onset of CHD (Sniderman, Tsimikas and Fazio 2014). 31

Figure 6 – Cholesterol biosynthesis pathway demonstrating where statins inhibit 41

Figure 7- Enzymatic reaction involving HMG-CoA Reductase 64

Figure 8 - Identification of three novel small molecules which upregulate LDLR promoter activity. 84

Figure 9 - Compounds 15a, 65 and 90 dose dependently increase luciferase expression in the CHO-pLDLR-Luc cell line 86

Figure 10 – Compounds 15a, 65 or 90 do not stabilise or interact with D-Luciferin or luciferase nor do they fluoresce themselves. 87

Figure 11 - Compounds 15a, 65 or 90 do not inhibit HMG-CoA reductase activity. 88

Figure 12 – Compounds 15a and 65 significantly upregulate LDLR mRNA expression in a human hepatocyte cell line 90

Figure 13 – Compounds 15a and 65 both increase Ldlr protein expression in a mouse hepatocyte cell line 91

Figure 14 – Compound 15a structure could mimic pre-squalene diphosphate and inhibit squalene synthase 93

Figure 15 - Compounds 15a and 40 competitively inhibit squalene synthase through binding in the active site. 94

Figure 16 – A statin and squalene synthase inhibitor produce a synergistic effect further upregulating LDLR promoter activity 96

Figure 17 – Tamoxifen increases LDLR promoter activity in the CHO-pLDLR-Luc cell line. 100

Figure 18 – Compound 15a has a half-life of less than 5 minutes in mouse liver microsomes. 105

Figure 19 – Identification of compound 40 a more potent analogue of compound 15a 108

Figure 20 – Compound 40 has superior metabolic stability compared to compound 15a and other heterobiaryl derivatives. 109

Figure 21 – Compound 40 can be detected in mouse plasma up to 10nM using HPLC 111

Figure 22 - A 40mg/kg dose of compound 40 in β-cyclodextrin produces high plasma concentrations of the drug. 112

Figure 23 – Compound 40 can be detected up to 6 hours post I.P injection in CD-1 male mice. 113

Figure 24 – Volume and speed of hydrodynamic injection is essential for expression in MF-1 male mice 115

Figure 25 – β-cyclodextrin causes an increase in human LDLR promoter activity in vivo 117

Figure 26 – Corn oil with Kolliphor EL will be the vehicle used for future compound 40 dosing studies 119

Figure 27- Compound 40 is able to drive expression of the human LDLR promoter in a mammalian system 121

Figure 28 - Vector maps for pEHZ (A), pLDLR-LDLR (B), pLDLR-Luc (C) and pLDLR-LDLR-miR82 (D) 129

Figure 29 - The pLDLR-LDLR-miR82 vector reduces Hmgcr and elevates LDLR expression in vitro and in vivo. 130

Figure 30 - A 1% cholesterol diet causes hypercholesterolaemia and atherogenesis in a Ldlr$^{-/-}$ male mice after 12- weeks diet intervention. 134

Figure 31 – pLDLR-LDLR-miR82 decreases Hmgcr and subsequently increases LDLR expression 4 weeks post delivery..... 136

Figure 32 - pLDLR-LDLR-miR82 significantly reduces total and LDL cholesterol in a mouse model of FH. 137

Figure 33 - LDLR mini-gene vectors had no significant effect on atherosclerotic plaque progression in the aortic arch after 4-weeks therapeutic intervention. 138

Figure 34 - LDLR mini-gene vectors had no significant effect on atherosclerotic plaque progression in the aortic root or macrophage infiltration after 4-weeks therapeutic intervention. 139

Figure 35 – A meta-analysis of aortic root atherosclerotic development, demonstrates the biggest difference in progression occurs between mice of total cholesterol levels between 10 and 20 mmol/L. 144

Figure 36 - A 0.25 and 0.5% cholesterol diet causes hypercholesterolaemia in Ldlr$^{-/-}$ male mice after 8- weeks diet intervention. 146

Figure 37 – A 0.25 and 0.5% high cholesterol (HC) diet is able to induce atherogenesis after 8-weeks 147

Figure 38 - Graphical representation of the long term efficacy study 149

Figure 39 – LDLR mini-gene vectors result in prolonged LDLR transgene expression without causing lipid accumulation within Ldlr$^{-/-}$ mouse liver 150

Figure 40 - Delivery of LDLR vectors results in long-term cholesterol lowering.. 152

Figure 41 – LDLR mini-gene vectors slow the progression of atherosclerosis in a mouse model of familial hypercholesterolaemia..... 154

Figure 42 – LDLR mini-gene vectors had no significant effect on galectin-3 or collagen content of atherosclerotic plaques 155

Figure 43 – LDLR-mini gene vectors had no significant effect on atherosclerotic plaque development in the whole aorta..... 156

Table 1 - Classes of lipoprotein 23

Table 2 - Different classes of mutations in the LDLR resulting in FH 36

Table 3 - General properties for the most commonly used viral vectors for FH gene therapy 47

Table 4 - Primer sequences 61

Table 5 - qRT-PCR run conditions 61

Table 6 - Western blot running gel 62

Table 7 - Western blot stacking gel 63

Table 8 - List of vehicles used to dissolve Compound 40 66

Table 9 - Dehydration of tissue samples for paraffin embedding 70

Table 10 - Rehydration of paraffin embedded samples for immunofluorescence 71

Table 11 - Masson trichrome staining 73

Table 12 – Reference list of all studies included in meta-analysis of diet-intervention induced atherosclerotic lesion development. 143

Abbreviations

AAV - adeno-associated viruses

ABCA1 - ATP- binding cassette A1

ACAT - acyl-CoA:cholesterol acyltransferase

ALT - alanine aminotransaminase

ApoAI - apolipoprotein AI

ApoB-48 - apolipoprotein B-48

ApoB-100 - apolipoprotein B-100

APOBEC1 - ApoB mRNA editing complex

ApoE - apolipoprotein E

AST - aspartate aminotransferase

CAD - coronary artery disease

CHD - coronary heart disease

CHO – chinese hamster ovary

CETP - cholesterol ester transfer protein

CMV - cytomegalovirus

DMEM - dulbecco’s modified eagle’s medium

DS - dyad symmetry

EGF - epidermal growth factor

EBNA-1 - EBV nuclear antigen 1

EBV - epstein-Barr Virus

ER - endoplasmic reticulum

EtOH – ethanol

FR - family of repeats

FBS – fetal bovine serum

FH - familial hypercholesterolaemia

FPP - farnesyl pyrophosphate

Gal-3 – galectin-3

GPP - geranylgeranyl pyrophosphate

HC - high cholesterol

HDL - high-density lipoprotein

HeFH – heterozygous FH

HMGCR - HMG-CoA reductase

HNF1α - hepatocyte nuclear factor-1α

HoFH – homozygous FH

HSPG - heparin sulphate proteoglycan

HSV-1 - herpes simplex viruses-1

iBAC - infectious bacterial artificial chromosome

IDL - intermediate density lipoprotein

IDOL - inducible degrader of the LDL receptor

I.P - intraperitoneal

IPSCs - induced pluripotent stem cells

Insig - insulin induced gene

LCAT - lecithin-cholesterol acyl transferase

LDL - low density lipoprotein

LDLR – low density lipoprotein receptor

LDPS - lipoprotein deficient serum

LPL - lipoprotein lipase

LXR - liver X receptor

MoMLV - moloney murine leukemia virus

MTP - microsomal triglyceride transfer protein

NPC1L1 - niemann–pick C1-like 1

PCSK9 - proprotein convertase subtilisin/ kexin type 9

PPAR - peroxisome proliferator activated receptor

PGC-1α - PPAR γ coactivator-1α

RC - regular chow

SCAP - SREBP cleavage-activating protein

SD - standard deviation

SEM - standard error of the mean

S/MAR - scaffold/matrix attachment region

SQS - squalene synthase

SSIs - SQS inhibitors

SRE - sterol response elements

SREBP – sterol response element binding protein

ULN – upper limit of normal

VLDL - very low-density lipoproteins

TBG - thyroxine binding globulin

WHHL - watanabe heritable hyperlipidemic

WT – wildtype

WTD - western type diet

Chapter 1: Introduction

1.1 Cardiovascular disease

Cardiovascular disease is the number one cause of death worldwide (WHO 2016). Around 17.5 million people died from cardiovascular disease in 2012, which equated to 31% of all deaths worldwide. Cardiovascular disease encompasses coronary heart disease (CHD), cerebrovascular disease, peripheral arterial disease, deep vein thrombosis and pulmonary embolism. Of these CHD is the most prevalent, resulting from a blockage in the coronary arteries due to a plaque rupturing within the coronary vasculature (Epstein and Ross 1999). The central step to this plaque developing in the first place is the infiltration of cholesterol within the artery wall.

1.2 Cholesterol

Cholesterol is essential to virtually all living organisms including bacteria and is the major sterol in all vertebrate cells. Cholesterol is a cyclic hydrocarbon alcohol that is insoluble in water (Figure 1) and is a major component of the myelin sheath in neurons and plasma membrane of all eukaryotic cells. Cholesterol is also essential for the synthesis of vitamin D3, bile acids and various steroid hormones including: cortisol, cortisone, aldosterone, progesterone, estrogen and testosterone (Hanukoglu 1992).

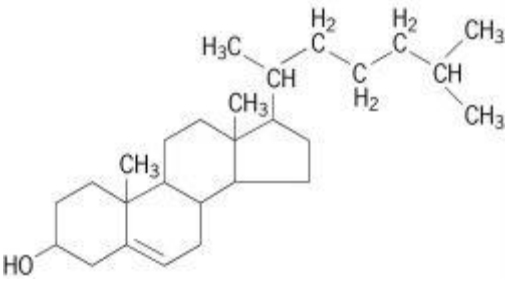


Figure 1 – Chemical structure of cholesterol.

Cholesterol is found in its free form in plasma membranes, where it interacts with the fatty acids of phospholipid molecules to reduce membrane fluidity and creates ‘rafts’ that concentrate signalling molecules (Goldstein and Brown 2010). Within cells and lipoproteins, cholesterol is found in its esterified form where it can be stored in lipid droplets ready for steroid synthesis or transported around the organism. Cholesterol is either acquired from the diet and absorbed through the intestine, primarily via Niemann–Pick C1-like 1 (NPC1L1) protein or can be synthesised from a double carbon molecule (acetyl CoA) through an enzymatic

reaction thought to involve over 40 cytosolic and membrane bound enzymes (Liscum 2008). Just over half of the body's cholesterol is synthesised *de novo* in the liver and intestine (depending on dietary intake, it can be much higher) however unlike mice, humans are unable to turn off the absorption of cholesterol from the diet (Dawson and Rudel 1999). Around 50% of cholesterol within the dietary tract is absorbed (Lecerf and de Lorgeril 2011) coming from either esterified cholesterol in food or reabsorption of free cholesterol in bile salts. Therefore, in a global sense, cholesterol is regulated throughout the body through absorption, *de novo* synthesis, catabolism and excretion, for which the liver is the master regulator of.

The liver is the only organ which expresses the enzyme cholesterol 7α-hydroxylase (CYP7A1), the first enzyme in a cascade to convert cholesterol into bile acids, where it can then be excreted in the faeces (Fuchs *et al.* 2003). The liver is also key in regulating the synthesis and release of lipoproteins, the major transport system for cholesterol throughout the body.

1.3 **Lipoproteins**

Lipoproteins are a biochemical assembly of lipids and proteins that are arranged in such a way to give a hydrophilic outer shell, with a hydrophobic inner core (Figure 2). A phospholipid bilayer with associated

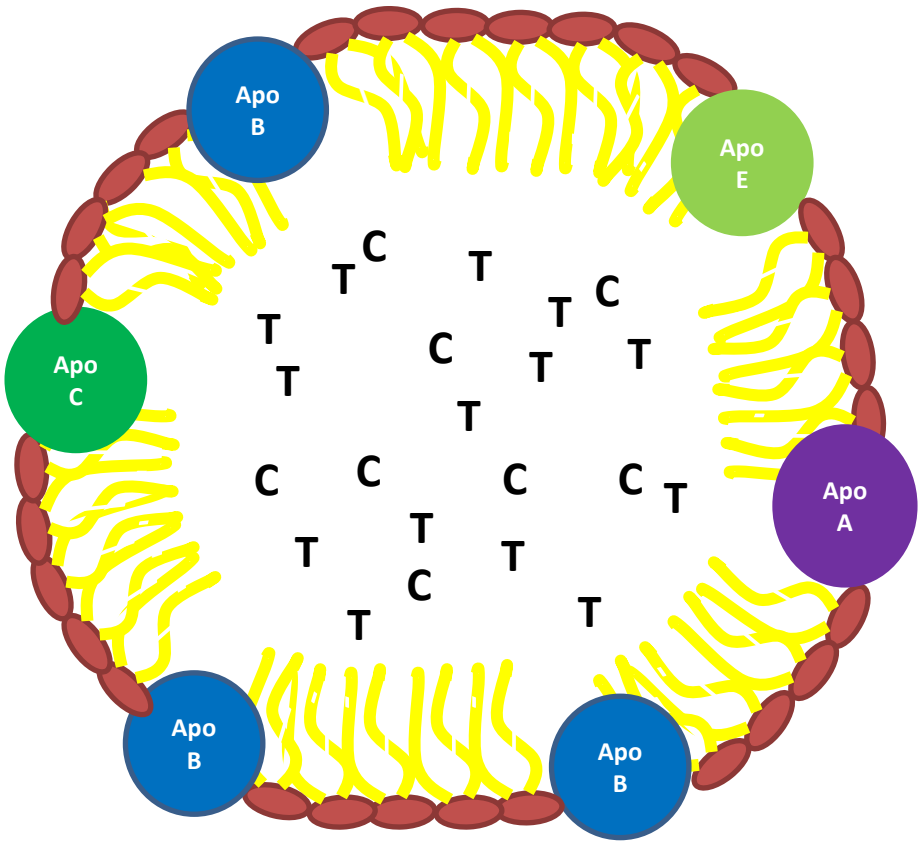


Figure 2 – General structure of a lipoprotein

apolipoproteins engulfs a lipid core full of triglycerides (T) and cholesterol (C). The best known function of the lipoproteins is their role in transporting lipids and sterols between the intestine, liver and peripheral tissues. It is becoming increasingly clear however their function may be much more diverse.

Transcriptomic and proteomic studies of different lipoprotein species has also implicated prominent roles in lipid transport, oxidation, inflammation, haemostasis, and immunity (Shah *et al.* 2016). Lipoproteins are separated into classes based on their density, with each class carrying different apolipoproteins on their outer shell (Table 1). The larger the content of triglyceride within the lipoprotein the larger the particle and lower the density.

Density (g/mL)	Lipoprotein class	Diameter (nm)	Protein (%)	Cholesterol (%)	Triglyceride (%)	Apolipoprotein
>1.063	HDL	5-15	33	30	4	AI, AII, AIV CI, CII, CIII E
1.019-1.063	LDL	18-28	25	50	8	B-100
1.006-1.019	IDL	25-50	18	29	31	B-100 C E
0.95-1.006	VLDL	30-80	10	22	50	B-100 CI, CII. CIII E
<0.95	Chylomicron	100-1000	<2	8	84	AI, AII, AIV B-48 CI, CII, CIII E

Table 1 - Classes of lipoprotein

Cholesterol, taken up in its free form by enterocytes is esterified by membrane bound acyl-CoA:cholesterol acyltransferases (ACAT), forming cholesterol esters.

Monoacylglycerols are esterified with free fatty acids by monoacylglycerol acyltransferase to form diacylglycerols, which are converted to triglycerides by diacylglycerol acyltransferases (Hussain 2014). These lipids are packaged into large triglyceride rich chylomicrons (less commonly known as UDL), containing a non-exchangeable apolipoprotein B-48 (ApoB-48) and other exchangeable apolipoproteins as seen in Table 1(Hussain *et al.* 1996). The chylomicron is released from the enterocyte, first into the lymph and then into the circulation, where it is acted upon by lipoprotein lipase (LPL) present in peripheral tissues. Apolipoprotein CII acts as a cofactor for LPL (Ramasamy 2014). LPL hydrolyses the triglycerides into free fatty acids, ready for energy production in muscle tissue and storage in adipocytes. The loss of triglyceride within the chylomicron, results in a much smaller particle known as a chylomicron remnant. The chylomicron remnant is removed by the liver through receptor mediated uptake via the low-density lipoprotein receptor (LDLR), heparin sulphate proteoglycan (HSPG) (MacArthur *et al.* 2007) or the LDLR related protein (LRP) binding to apolipoprotein E (ApoE) (Veniant *et al.* 1998) (Figure 3). It must be noted that Figure 3 is a simplified diagram and there appears to be a lot more heterogeneity than first thought, with many groups showing the LRP able to bind other apolipoproteins such as apolipoprotein AV (Nilsson *et al.* 2007).

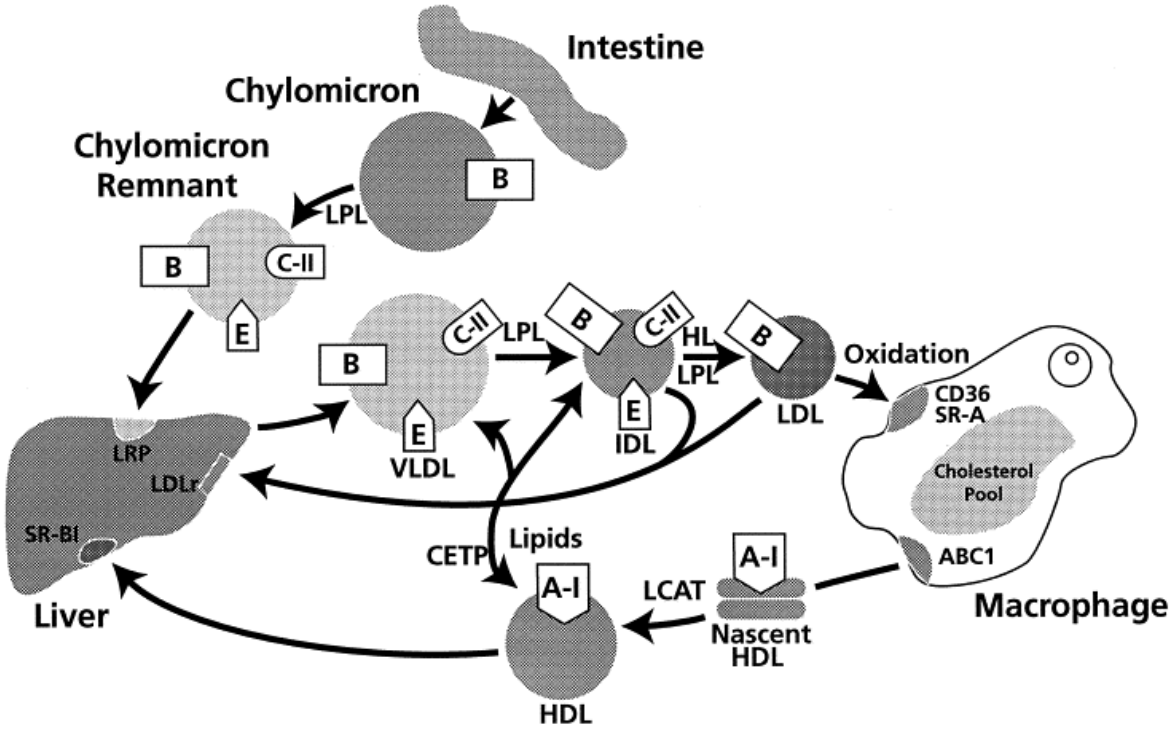


Figure 3 - Overview of lipoprotein metabolism (Kwiterovich 2000)

Cholesterol synthesised by the liver *de novo* or acquired through the uptake of chylomicrons is transported into very low-density lipoproteins (VLDL) by the microsomal triglyceride transfer protein (MTP) (Hussain *et al.* 2012). MTP is the major cellular protein involved in shuttling neutral lipids across membranes and is essential for the assembly of all ApoB containing lipoproteins (Hussain, Shi and Dreizen 2003). In humans, only ApoB-100 transcripts are produced in the liver, as the ApoB mRNA editing complex (APOBEC1) which forms a stop codon at approximately 48% of the full length coding sequence to produce ApoB-48 is not expressed (Lo *et al.* 2008). ApoB-48 lacks the C-terminus which contains the domain recognized by the LDLR (Veniant *et al.* 1998). VLDL is secreted by the liver where it delivers fatty acids to peripheral tissues, through LPL hydrolysis of its triglyceride rich core, much the same as described for chylomicrons. As the VLDL loses triglyceride, it becomes denser, forming an intermediate-density lipoprotein (IDL) (Figure 3). Once the IDL is formed, it is enriched with high-density lipoprotein (HDL) derived ApoE, which is cleared by the LDLR. If not cleared, IDL particles will undergo further hydrolysis forming low-density lipoprotein (LDL) particles, which are the most abundant lipoprotein found in man (Brown and Goldstein 1986).

LDL particles are taken up by the LDLR, importantly in the liver, where plasma cholesterol homeostasis can be maintained through production and degradation of lipoproteins. The movement of cholesterol from peripheral tissues back to the liver is termed reverse cholesterol transport and involves HDL (Glomset 1968). It is vital that other tissues are able to reduce their free cholesterol content, as a build-up is very cytotoxic (Cichon *et al.* 2004). Apolipoprotein AI (ApoAI) is secreted by the liver and intestines in a lipid poor form, where it then interacts with ATP- binding cassette A1 (ABCA1) protein on the cell surface of most cell types to form a HDL (Timmins *et al.* 2005). The major apolipoprotein in HDL is either ApoAI or ApoAII but it appears to be a very heterogeneous subfraction, with mass spectrometry analysis detecting apolipoproteins (AI, AII, AIV, B, (a), CI, CII, CIV, D, E, F, H, J, LI and M), which may provide very distinct functionalities for this class of lipoprotein (Davidsson *et al.* 2010). The HDL particle takes up free cholesterol from the cell, which is then esterified by lecithin-cholesterol acyl transferase (LCAT) to cholesteryl esters, which by the nature of their hydrophobicity move into the core of the HDL particle. This process forms the spherical HDL particle found in plasma (Spady 1999).

The cholesterol esters taken up from the peripheral tissues are then returned to the liver through two pathways, a proportion of the cholesterol ester is transferred to circulating LDL particles in exchange for a triglyceride molecule in the presence of cholesteryl ester transfer protein (CETP) (Barter *et al.* 2003a). In synergy with this, cholesterol ester is also taken up directly from the HDL particle from the liver by a non-endocytic pathway, which accounts for nearly 70% of all HDL cholesterol ester uptake (Spady *et al.* 1998).

1.4 Low-density lipoprotein receptor

1.4.1 Structure and function of the low-density lipoprotein receptor

The *LDLR* is a 45 kb sequence consisting of 18 exons and 17 introns and is mapped to chromosome 19 in bands p13.1-13.3 (Figure 4A) (Lindgren *et al.* 1985). A 5.3 kb mRNA is transcribed of which 2.6 kb codes for the 860 amino acid LDLR protein, with the other 2.7 kb coding for a 3’ untranslated region (Figure 4B)

(Yamamoto *et al.* 1984). The LDLR mRNA is translated by ribosomes on the rough endoplasmic reticulum (ER) into an immature protein with incomplete O-linked carbohydrate chains (Hobbs *et al.* 1990). After translation the LDLR protein is transported from the rough ER to the Golgi apparatus where the O-linked sugar chains are elongated and the mature 160kDa LDLR translocates to the plasma membrane.

As shown in Figure 4C, the LDLR is composed of five distinct domains. Exon 1 codes for a sequence directing the LDLR to the ER and is cleaved once reaching the ER (Hobbs *et al.* 1990). Exons 2-6 code for the ligand binding domain, made up of seven imperfect cysteine-rich tandem repeats of 40 amino acids, which can bind either ApoE or ApoB-100 (Fisher, Abdul-Aziz and Blacklow 2004). Attached to the ligand binding domain is the epidermal growth factor (EGF) precursor domain, which functions to ensure acid-dependent dissociation of the receptor from its ligand and subsequent recycling of the ligand-binding domain back to the cell surface (Jeon *et al.* 2001). Downstream of the EGF precursor domain is a serine and threonine rich region containing many O-linked carbohydrate chains, followed by the hydrophobic domain anchoring the receptor to the cell membrane. The last two exons, 17 and 18 code for a relatively short cytoplasmic tail that contains all the sequences required for receptor clustering in clathrin-coated pits and internalization (Malby *et al.* 2001). Once the LDLR is internalized, a drop in pH as the vesicle becomes a late endosome causes the dissociation of the receptors ligand and recycling back to the cell membrane. The LDLR can make a round trip from the cell surface to the endosome and back every 10 minutes, totalling several hundred in its 20 hour lifespan (Brown, Anderson and Goldstein 1983).

As the VLDL receptor is barely detectable in the liver, the LDLR is primarily responsible for the uptake and degradation of lipoproteins and thus the major governor of plasma cholesterol in man (Takahashi *et al.* 2004). Interestingly, an additional function of the LDLR has been demonstrated, where it is involved in hepatic VLDL assembly, promoting post-translational degradation, thus interfering with secretion of VLDL from the liver. This suggests an additional gatekeeping function for the receptor (Larsson, Skogsberg and Björkegren 2004).

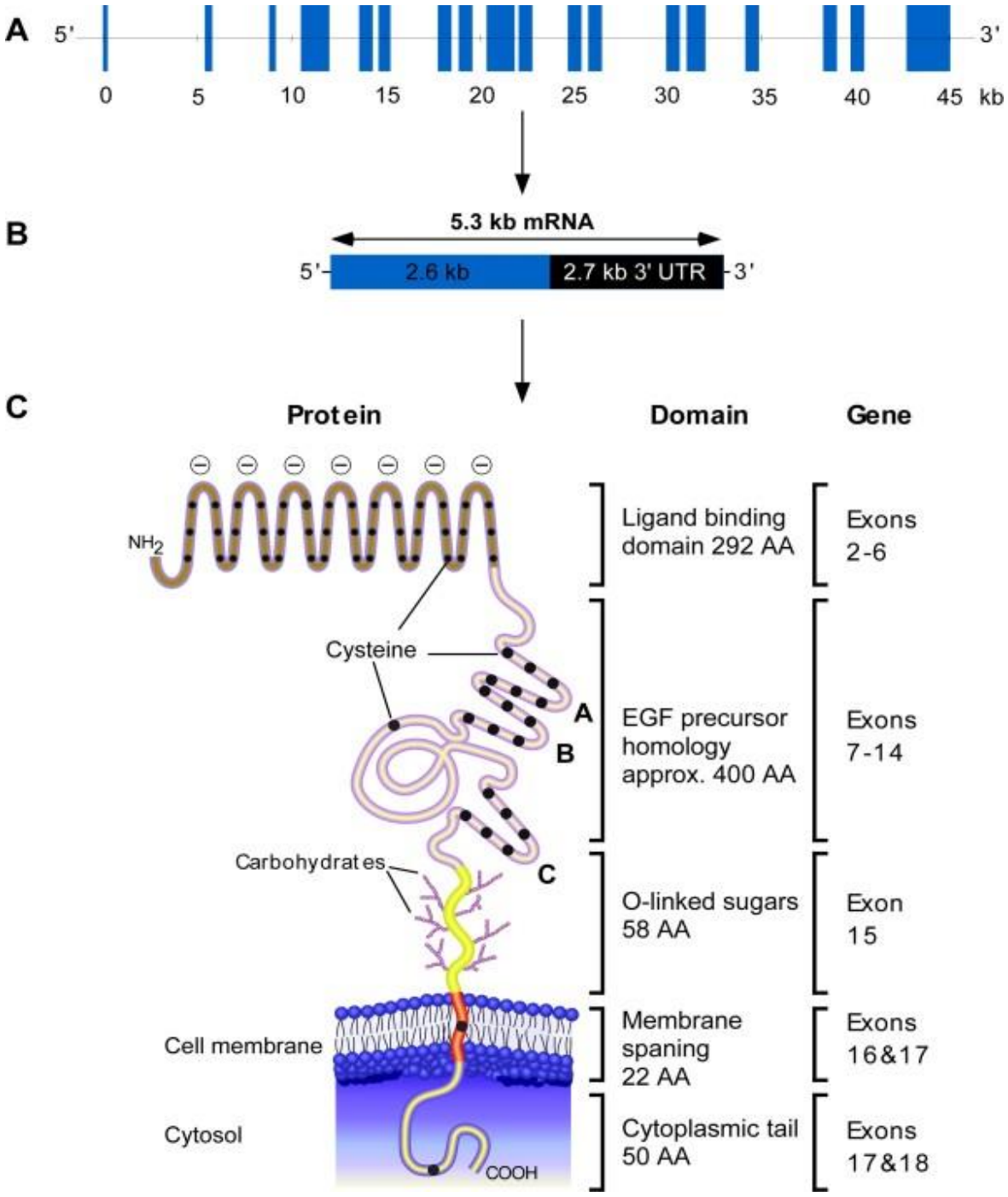


Figure 4 - Schematic representation of the LDLR gene (A), mRNA (B) and protein (C) (Al-Allaf *et al.* 2010).

1.4.2 Regulation of the low-density lipoprotein receptor

1.4.2.1 Transcriptional

In the promoter of the *LDLR* there are multiple 10 bp sequences called sterol response elements (SRE) that confer sterol regulated transcription (Südhof *et al.*

1987). The SRE sequences and generic Sp1 transcription factor binding sites are located within +58 and -234 bp of the LDLR promoter (Jeong, Cho and Pak 2009), with the SRE 53 bp upstream of the transcription start site (Briggs *et al.* 1993). The transcription factor, sterol response element binding protein-2 (SREBP-2) binds to this SRE to initiate transcription of the LDLR along with HMG-CoA Reductase (HMGCR) and 30 other genes involved in cholesterol regulation and biosynthesis (Horton *et al.* 2003). It should be noted there are also sterol independent response elements within the LDLR promoter, which appear to be regulated by peroxisome proliferator activated receptor (PPAR) γ coactivator-1α (PGC-1α) (Jeong, Cho and Pak 2009).

SREBP-2 is transcribed alongside a sterol sensing protein termed SREBP cleavage-activating protein (SCAP) (Hua *et al.* 1996). SCAP has a sterol sensing sequence in its transmembrane domain which binds to cholesterol or even more potently oxysterols such as 25-hydroxycholesterol (Nohturfft, Brown and Goldstein 1998). When there are high concentrations of sterols, they bind to SCAP and cause a conformational change, allowing insulin induced gene (Insig) to bind, tethering the complex to the ER. In conditions of low intracellular cholesterol, Insig cannot bind to the SCAP/SREBP-2 complex and prevent translocation to the Golgi apparatus (Adams *et al.* 2004). In the Golgi, SREBP-2 is cleaved by two proteases, S1P and S2P, releasing the mature NH_2-terminal bHLH-Zip domain. The cleaved SREBP-2 enters the nucleus, where it activates genes including the *LDLR* (Brown and Goldstein 2009).

1.4.2.2 Post-transcriptional

Proprotein convertase subtilisin/ kexin type 9 (PCSK9) is a serine endoprotease, primarily synthesized and secreted from the liver (Seidah *et al.* 2003). PCSK9 negatively regulates LDLR expression, causing the receptor to be broken down through two separate pathways. In an intracellular pathway, nascent PCSK9 can bind to the LDLR and direct it from the trans-Golgi to lysosomes for degradation (Poirier *et al.* 2009). The second pathway involves the secretion of PCSK9 into the plasma, where it can bind to the EGF precursor domain, both these pathways inhibit recycling of the receptor, targeting it for lysosomal degradation (Lagace 2014). Therapies targeting plasma PCSK9 (Discussed in section 1.5.4.7) indicate

it is probably the latter which exerts the biggest influence on LDLR expression (Stein and Swergold 2013). PCSK9 has three transcription binding sites in its promoter region, although it is thought to be primarily regulated by SREBP-2 (Jeong *et al.* 2008). PCSK9 expression is therefore turned on when LDLR and cholesterol biosynthesis is turned on, representing a paradoxical regulator, whereby to limit LDLR expression. PCSK9 also contains a hepatocyte nuclear factor-1α (HNF1α) binding site, which appears to be insulin sensitive, PCSK9 expression increases due to hyperinsulinaemia and may cause the hyperlipidaemia associated with insulin resistance (Li, Brown and Goldstein 2010).

The LDLR is also regulated by inducible degrader of the LDL receptor (IDOL) protein. IDOL is an E3 ubiquitin ligase, which causes ubiquitination and degradation of the LDLR (Zhang *et al.* 2012a). IDOL is expressed under the cholesterol-sensing nuclear receptor liver X receptor (LXR). The LXRs act in a complementary fashion to the SREBP transcription factors to control intracellular cholesterol levels. When cholesterol levels rise, oxysterols are generated which are the ligands for the LXRs (Janowski *et al.* 1999). Activation of the LXRs activates genes involved in cholesterol efflux like ABCA1 and ApoE (Venkateswaran *et al.* 2000) and genes to perturb further cholesterol uptake such as IDOL.

1.5 LDL-cholesterol and cardiovascular disease

1.5.1 Evidence for LDL-cholesterol's role in cardiovascular disease

In 1913 a causal relationship between high cholesterol and the development of atherosclerosis was identified by Nikolaj Nikolajewitsch Anitschkow. He fed a cholesterol rich diet to rabbits and documented the development of atherosclerotic lesions in their arterial intima (Anitschkow 1913). Since then many longitudinal epidemiology studies, including the Framingham heart study (Ciocco 1957) have cemented LDL-cholesterol as one of the leading risk factors for CHD.

Figure 5 shows how exposure to different levels of LDL-cholesterol over a lifetime lead to a quicker or later onset of CHD. Patients with familial hypercholesterolaemia (FH), a monogenic disease leading to severely elevated LDL-cholesterol plasma levels, have a much earlier progression into CHD than

age-matched normal controls (Sniderman, Tsimikas and Fazio 2014). The inverse is also true, with patients who have loss of function mutations in PCSK9 having much lower LDL-cholesterol levels and later incidence of CHD, than age-matched controls. Figure 5 demonstrates how LDL-cholesterol levels directly correlate to CHD and with the use of statins (LDL-cholesterol lowering agents, discussed in section 1.6.4.1), the role of LDL-cholesterol in cardiovascular disease was undoubtedly proven. Many long term studies using statins showed that by directly lowering LDL-cholesterol, there was a decrease in cardiovascular events (Shepherd *et al.* 1995).

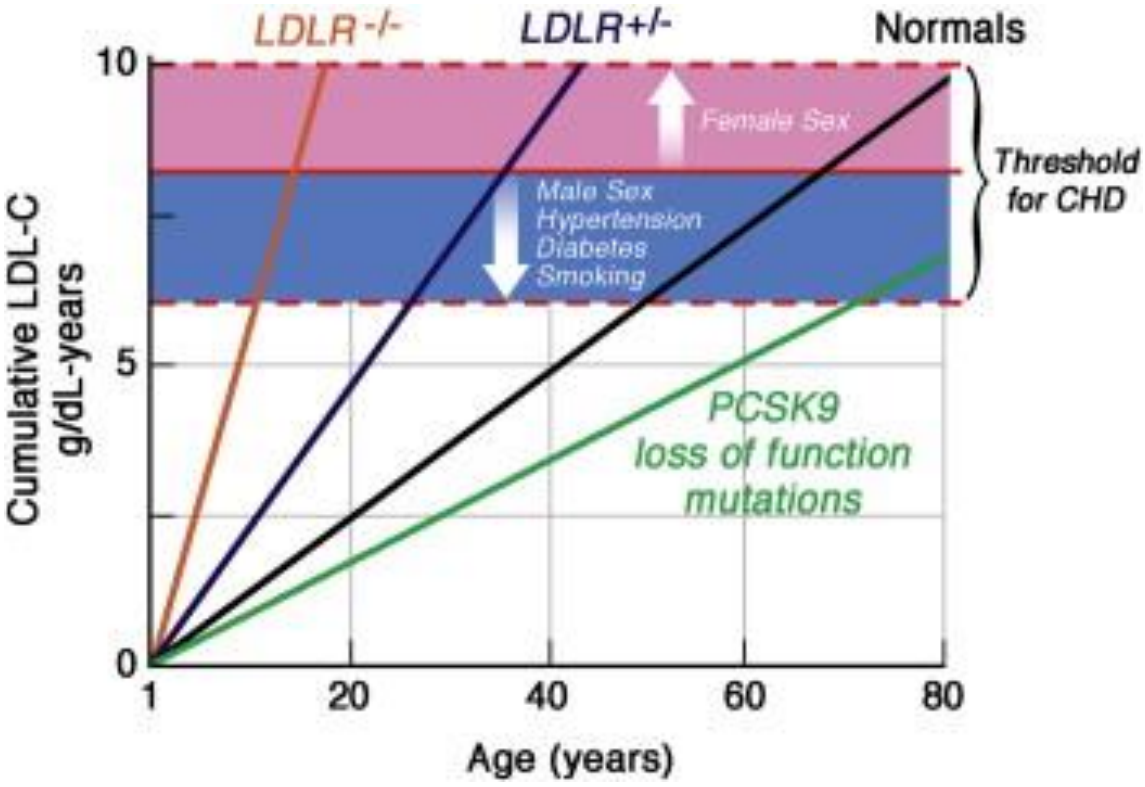


Figure 5 – Graphical representation of the effect of age and cumulative LDL-cholesterol on onset of CHD (Sniderman, Tsimikas and Fazio 2014).
An estimation of the likely onset of CHD in patients with HoFH ($LDLR^{-/-}$), HeFH ($LDLR^{+/-}$), loss of function PCSK9 mutations or normal controls. The horizontal red line represents a theoretical threshold of the cumulative LDL-C exposure required for development of CHD. The height of the red line will be lower in the presence of additional CHD risk factors.

1.5.2 Atherosclerosis

Atherosclerosis is a chronic inflammatory disease, that results from an imbalance in lipid metabolism and a maladaptive immune response driven by the

accumulation of cholesterol-laden macrophages in the artery wall (Moore, Sheedy and Fisher 2013). Over many years, atherosclerotic plaques develop in large and medium-sized elastic and muscular arteries, particularly in areas of perturbed laminar flow (Epstein and Ross 1999). These plaques can protrude into the arterial lumen and rupture or cause thrombosis, leading to ischaemia and a myocardial infarction or stroke.

Atherosclerotic lesions can be classed into different stages of pathology, type I and II lesions are the earliest identifiable and are the appearance of fatty streaks on the intima, with most of the lipid found in lipid loaded macrophages, called foam cells (Stary *et al.* 1994). Type III lesions, known as the intermediate lesion, display pools of extracellular lipid droplets alongside the foams cells and macrophages, greater intimal thickening, and replacement of intercellular matrix proteoglycans and fibres, driving smooth muscle cells apart (Stary *et al.* 1994). The next stage of lesions are deemed atheromas and considered the first advanced atherosclerotic lesions because the lipid core, intimal disorganization, and arterial deformity predispose to sudden lesion progression and ischemic events. Type IV lesions contain a large and dense area of extracellular lipid, known as the lipid core, causing severe intimal disorganization. Organelles within the smooth muscle cells may be calcified and calcium particles will be found within the lipid core. Lymphocytes and mast cells will be present and the region between the lipid core and the lesion surface will contain proteoglycans, macrophage foam cells, and isolated smooth muscle cells with minimal collagen, thus making Type IV lesions the first class vulnerable to rupture (Stary *et al.* 1995). Type V lesions are defined as lesions in which prominent new fibrous connective tissue has formed. Type V lesions are generally split into Va, Vb and Vc, with Vc lesions not having a lipid core and thought to be least vulnerable to rupture. In Type V lesions there is substantial increases in collagen and smooth muscle cells rich in rough-surfaced endoplasmic reticulum (Stary *et al.* 1995). A Type VI lesion is a Type IV or V lesion with one of the added complications: hematoma, haemorrhage or thrombosis.

1.5.3 LDL-cholesterol and its role in atherosclerosis

LDL-cholesterol is involved in the key initiating process of atherosclerotic lesion development. Sustained plasma levels of ApoB containing lipoproteins, cause entry and retention of this lipoprotein species in the subendothelium (Tabas, Williams and Borén 2007). Retention of these lipoproteins occurs through the interaction of the lipoproteins with subendothelial matrix molecules, principally proteoglycans. The most probable retention reaction involves the positively charged residues of the ApoB-100 interacting with the negatively charged sulfate groups on the proteoglycan sugars (Khalil, Wagner and Goldberg 2004). Studies using mice exclusively expressing ApoB-100, with site-directed mutations in their ApoB-proteoglycan-binding region showed greatly reduced atherogenesis (Borén *et al.* 1998) Though many other interactions have been demonstrated and contribute to LDL retention (Skålén *et al.* 2002). Once retained in the subendothelium, it is widely accepted that modifications of LDL such as oxidation (oxLDL), contribute to triggering maladaptive local inflammatory responses leading to chronic inflammatory disease (Moore, Sheedy and Fisher 2013). In oxLDL, the ApoB component is fragmented and lysine residues are covalently modified with reactive breakdown products of oxidized lipids (Young and McEneny 2001). When LDL is cultured *in vitro* alongside endothelial cells, it is modified to oxLDL and this form of LDL has been shown to be taken up by macrophages with a much higher affinity than LDL by the scavenger receptor (Steinbrecher *et al.* 1984). Unlike the LDLR, the scavenger receptor is not negatively regulated by cholesterol content, the macrophage continues to take up oxLDL until it is completely lipid loaded, becoming quiescent and forming fatty streaks (Steinberg and Witztum 2010). If the inflammatory response is not resolved, a further cascade of lipid and immune cell integration into the fatty streak results in the development of more advanced atherosclerotic lesions (Moore, Sheedy and Fisher 2013).

A highly atherogenic form of LDL called lipoprotein (a) has been associated with CHD (Anuurad *et al.* 2006), where high levels of lipoprotein (a) can increase CHD risk independent of LDL-cholesterol levels (Alonso *et al.* 2014). Lipoprotein (a) is structurally very similar to LDL apart from it has a apolipoprotein a molecule covalently attached to the ApoB-100 molecules (Anuurad *et al.* 2006). Lipoprotein (a) has increased retentive properties in the subendothelial space (Lundstam *et al.*

1999) and it appears to be rich in potentially atherogenic oxidized phospholipids, a property shown to be predictive of atherosclerotic vascular disease in humans (Tsimikas *et al.* 2005). All this evidence points to LDL-cholesterol and variants of itself through different lipoprotein composition or post translational modification being one of the key factors and initial steps in the development of atherosclerosis.

1.6 Familial hypercholesterolaemia

1.6.1 Identification of familial hypercholesterolaemia

A Norwegian clinician, Carl Muller first documented FH in 1938. Dr Muller noticed a certain population of patients with high blood cholesterol levels, which correlated with a high incidence of myocardial infarction, for which he reasoned was due to 'an inborn error of metabolism' (Muller 1938). In 1964, Dr Avedis Khachadurian described the two forms of FH, heterozygous and homozygous, recognizing FH as an autosomal dominant disorder (Khachadurian 1964). How this imbalance in cholesterol homeostasis was occurring however remained a mystery, until Dr Michael S. Brown and Dr Joseph L. Goldstein began working with FH patient fibroblasts in 1972, work that would win them the Nobel prize some 13 years later.

Dr Konrad Bloch had delineated cholesterol biosynthesis decades previously, himself winning the Nobel prize in 1964. Dr Bloch demonstrated that squalene is made from acetate, which in turn is converted to cholesterol, with one of the rate limiting enzymes in this process being HMGCR (Bloch 1965). Dr Brown and Dr Goldstein developed a micro-assay to measure HMGCR activity, first in healthy volunteer fibroblasts and found that the addition of LDL reduced the activity of HMGCR by ~50 fold (Brown, Dana and Goldstein 1973). When LDL was added to fibroblasts cultured from homozygous FH (HoFH) patients, the HMGCR activity was ~50-100 fold higher than in the fibroblasts from non FH patients (Brown, Dana and Goldstein 1974). However when cholesterol in its free form (dissolved in ethanol (EtOH)) was added to normal and HoFH fibroblasts, no difference was detected in HMGCR activity, suggesting an error in acquiring and processing LDL-cholesterol (Brown, Dana and Goldstein 1974).

The LDLR was next discovered through experiments using ^{125}I-LDL, where healthy control fibroblasts had high affinity binding sites for ^{125}I-LDL where as HoFH fibroblasts did not (Goldstein and Brown 1974). This indicated that it must be a problem with LDL-cholesterol internalisation and thus a problem with the LDLR itself. The LDLR receptor was finally purified in 1982 (Schneider *et al.* 1982) and the main culprit for FH identified.

1.6.2 Prevalence and genetic causation of familial hypercholesterolaemia

FH is now a well characterized genetic disease and one of the most common genetic diseases in the world (Willard 2010). It is an autosomal dominant disorder which primarily results (~85% of cases) from a loss of function mutation in the LDLR (Al-Allaf *et al.* 2010). There have now been over 1600 different mutations in the *LDLR* gene characterized to cause FH (Wilson et al), separated into distinct classes, described in the table below.

Class of mutation	Effect on LDLR
1	Mainly in the promoter: No detectable mRNA or LDLR at the protein level
2A	Completely retard maturation of the LDLR from 120KDa to 160KDa glycosylated form
2B	Partially retard maturation of the LDLR from 120KDa to 160KDa glycosylated form
3	Defects in binding LDL
4	Defects in internalization normally due to mutations in the cytoplasmic tail
5	Error in degradation of the receptor, preventing recycling of the receptor to the cell membrane
6	Failure to direct the LDLR to the basolateral membrane of polarised cells

Table 2 - Different classes of mutations in the LDLR resulting in FH

Loss of function mutations in *ApoB* and gain of functions in the *PCSK9* genes account for most of the remaining cases of FH, at 5-10% and 5% respectively (Goldberg *et al.* 2011). Though it must be noted there are patients with no mutations in these three genes who do have hypercholesterolaemia with a polygenic origin to their phenotype (Talmud *et al.* 2013). The prevalence of FH worldwide is estimated between 1-250-500 people with heterozygous FH and 1/160000-1000000 for people with homozygous FH (Cuchel *et al.* 2014). The occurrence of FH can be much more common in certain isolated populations such as French Canadians, South African Afrikaners or Jews, due to a founder effect, where the frequency can be as low as 1:50 (Austin *et al.* 2004).

1.6.3 Clinical diagnosis and prognosis

FH is diagnosed using five criteria: family history of coronary artery disease (CAD), presence of early CAD, elevated LDL and the appearance of tendon xanthomas (deposition of LDL-cholesterol at the tendons on the knees, elbows, hands, Achilles tendon and other parts of the body) or corneal arcus (LDL-

cholesterol deposits or hyalinosis of the corneal stroma). HeFH patients typically have a serum cholesterol level of 250-450 mg/dL (6.5-11.6 mmol/L) and LDL-cholesterol of 200-400 mg/dL (5.2-10.4 mmol/L). There is an increase in developing CAD of around 20-fold for a HeFH patient, if they remain untreated, compared to a non FH patient (Goldberg *et al.* 2011). It is estimated there are ~10 million people who have HeFH worldwide, causing 200,000 deaths due to CAD per year and representing a huge health and economic burden. Of these, 85% of males and 50% of females with FH will suffer a coronary event before 65 years old if no therapeutic intervention takes place (Civeira 2004). Some estimates suggest less than 20% of HeFH patients are diagnosed, with even less than that receiving any treatment (Hopkins *et al.* 2011).

To combat this, in 2008 UK NICE released guidelines advocating DNA testing to confirm an FH diagnosis (Wierzbicki *et al.* 2008), providing unambiguous identification of affected relatives. This strategy has been successfully implemented in the Netherlands (Umans-Eckenhausen *et al.* 2001) thus allowing pharmacological treatment for all family members as well. Despite this, most HeFH patients fail to reach their LDL-cholesterol lipid goal, with different studies estimating it to only be between 10-30% (Pijlman *et al.* 2010; Perez de Isla *et al.* 2016). For HoFH the phenotype is much more severe, with patients presenting serum cholesterol levels ≥460 mg/dL (≥12 mmol/L), though this can be even higher in patients on a western diet (Marais 2004). HoFH patients very commonly present with tendon xanthomas and or corenal arcus and most individuals experience severe vascular disease even when treated, in the first two decades of life (Youngblom and Knowles 1993). In total, FH is responsible for ~5% of cardiovascular events below 60 and ~20% before the age of 45 (Goldstein *et al.* 1973; Dorsch *et al.* 2001), further treatments remain a huge unmet clinical need.

1.6.4 Current therapies for familial hypercholesterolaemia

1.6.4.1 Statins

After diagnosis of FH, all patients will be advised to undergo dramatic lifestyle changes including switching to a diet low in trans and saturated fats, refined sugars and of course cholesterol. Diets rich in plant sterols and fibre such as the Mediterranean diet have been shown to protect from cardiovascular events

(Estruch *et al.* 2013). Almost all FH patients will fail to achieve a LDL-cholesterol below 190 mg/dL (4.9 mmol/l) on diet alone and will begin with the front line pharmacotherapy, statins.

Statins, first discovered over 30 years ago (Alberts et al. 1980; Endo et al. 1977), act by inhibiting one of the rate determining enzymes in the cholesterol biosynthesis pathway, HMGCR, as detailed in Figure 6. By inhibiting HMGCR, the intracellular cholesterol concentration drops, causing the cell to upregulate the LDLR and acquire cholesterol from the extracellular environment, lowering plasma cholesterol (Yamamoto *et al.* 1980; Raasch 1991). Statins have been highly successful in reducing primary and secondary cardiovascular events in the general population. In primary studies such as the WSCOPS (West of Scotland Coronary Prevention Study) trial, 5-year treatment with a statin lead to a 26% reduction in LDL-cholesterol and a 31% decrease in cardiovascular events (Shepherd *et al.* 1995). Interestingly, a 20-year follow up of the WCOPS trial showed that participants who had been on the statin arm showed a legacy benefit and had a 21% decrease in cardiovascular death compared with the placebo group (Ford *et al.* 2016). In the JUPITER trial, patients with what is considered normal cholesterol levels (130mg/dL (3.4 mmol/l)) showed a 44% reduction in cardiovascular events when taking a statin, the trial was stopped early (median 1.9 years follow up) on ethical grounds and both groups went on a statin (Ridker *et al.* 2008).

No randomized clinical trials for statins have been done in a HeFH population, however due to the high baseline of the 4S (Scandinavian Simvastatin Survival Study) (Pedersen 1994), WOSCOPS (Shepherd *et al.* 1995), and LRC-CPPT (Lipid Research Clinics Coronary Primary Prevention Trial) (The Lipid Research Clinics Coronary Primary Prevention Trial results. I. Reduction in incidence of coronary heart disease. 1984) trials, it is likely there was an enrichment of FH patients, where they demonstrated that LDL-cholesterol lowering reduces CHD risk. Retrospective analysis of cohorts in the Netherlands have reported a reduction in all cardiovascular events by 44% in HeFH patients taking high dose statins (Besseling *et al.* 2016). High dose statins reduce cardiovascular risk greater than moderate dose statins regardless of the baseline (Collaboration

2010). Almost all HeFH patients will be on high dose stains to try and achieve the recommended <100mg/dL (Goldberg *et al.* 2011), unfortunately less than 10% of HeFH patients reach their lipid goal, due to the efficacy of current treatments or compliance with statins (Pijlman *et al.* 2010).

The side effects associated with statins mainly involve muscle symptoms but headache, sleep disorders, dyspepsia, nausea, rash, alopecia, erectile dysfunction, gynecomastia, and/or arthritis have all been reported (Banach *et al.* 2015). There has been some controversy with the rate of adverse events related to statins, with some of the large random controlled trials reporting no difference in reported side effects compared with placebo (Ridker *et al.* 2008). The rate of myopathy in these trials is usually around 3% (Bays 2006), however the rate of statin intolerance in the general population may be as high as 10-15% (Grundy 2002; Joy and Hegele 2009). This discrepancy between the two findings may be explained by the random controlled trials excluding patients with any history of statin related side effects and patients who are more at risk from developing the side effects (women, elderly or patients with other conditions (liver/kidney failure)), being underrepresented. In addition, many of the studies ignored muscle problems as a side effect and only reported serum creatine kinase levels (Bitzur *et al.* 2013a). Only very few may go on to develop serious side effects such as myopathy, myositis or rhabdomyolysis though the more minor muscle problems are still enough for patients to end their statin regime. How exactly statins cause the muscle related side effects is still a topic of hot debate. As statins inhibit one of the early steps of cholesterol biosynthesis as shown in Figure 6, they suppress the production of many other isoprenoid molecules synthesised from the intermediates of this pathway. In particular, the inhibition in synthesis of ubiquinone (Coenzyme Q10), dolichol, farnesyl pyrophosphate (FPP) and geranylgeranyl pyrophosphate (GPP) is linked with alterations in mitochondrial function, glycosylation, cell maintenance and cell growth respectively. The mechanisms behind the side effects of statins is discussed in detail in section 3.1.2.

In HoFH patients, statins are much less efficacious, due to in most cases, there not being a functional LDLR to upregulate. The efficacy will of course be dependent on the functionality of the LDLR, with HoFH patients being classified as

either receptor negative (0–2% receptor activity) or receptor defective (2–25% receptor function) (Cuchel *et al.* 2014). Under the maximally tolerated dose, statins do demonstrate modest LDL-cholesterol reductions (3-20%), by inhibiting *de novo* cholesterol synthesis, thereby decreasing further LDL particle formation. If the patient is receptor defective, further upregulating the minimally functional LDLR will provide additional efficacy (Raal *et al.* 2011). A decrease in cardiovascular events is seen with maximal dose stains in HoFH patients (Marais, Blom and Firth 2002). The reason for the efficacy of statins in HoFH patients may also be attributable to their associated pleiotropic effects. In trials comparing statin lowering and non-stain lowering therapeutics, even though a similar decrease in LDL-cholesterol was achieved, statins demonstrated other biological benefits not seen in the other treatment groups (Wang, Liu and Liao 2008). In one study, patients with heart failure showed improvements in endothelial function and reduced oxidative stress after 4-weeks of pravastatin but not ezetimibe, even though both achieved comparable lipid lowering (Landmesser *et al.* 2005).

Just as the side effects of statins are thought to be caused by the inhibition of certain isoprenoid intermediates so are the pleiotropic effects. Statins have been shown to improve vascular function, where by inhibiting GPP, they prevent RhoA geranylgeranylation and increase the production of NO in endothelial cells (Laufs *et al.* 1998). Other off target effects include anti-inflammatory properties, once again through inhibiting GPP production. GPP reduce the activation of a subset of small GTPases that regulate antigen presentation, through MHC II expression. This immunomodulatory effect could be reversed with supplementation of mevalonate or GPP but not squalene (Greenwood, Steinman and Zamvil 2006).

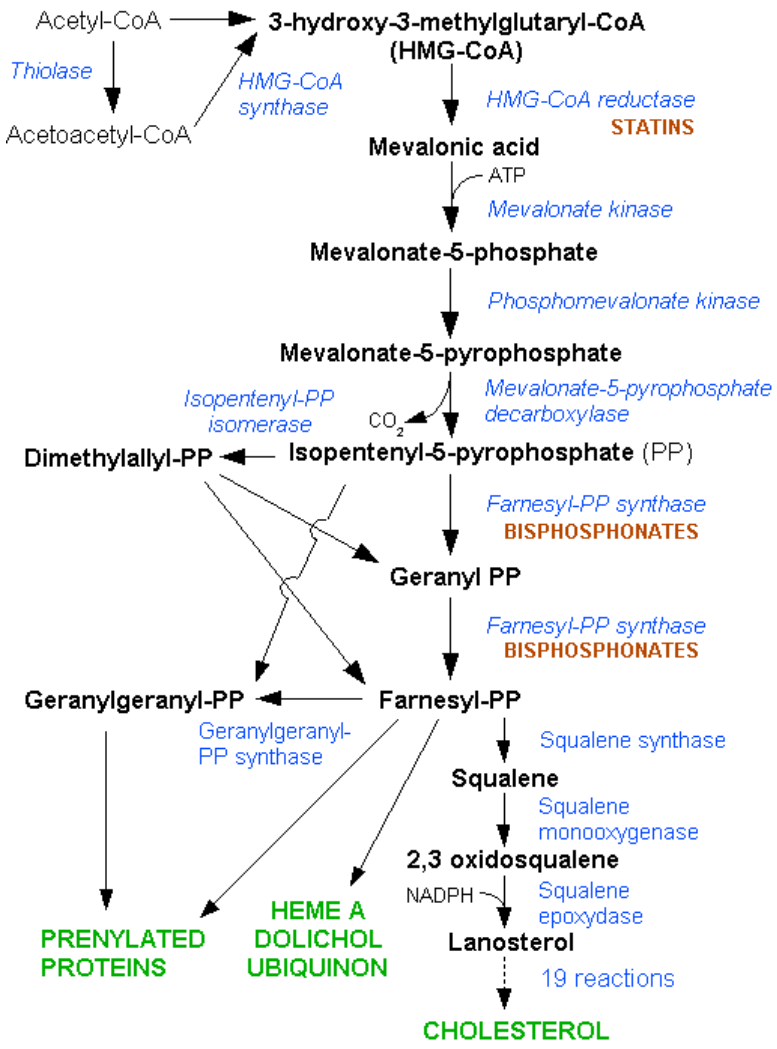


Figure 6 – Cholesterol biosynthesis pathway demonstrating where statins inhibit

1.6.4.2 Statin combination therapy

1.6.4.2.1 Ezetemibe

Ezetemibe is a cholesterol absorption inhibitor, acting by blocking the NPC1L1 protein in the jejunal brush border, integral to the uptake of intestinal lumen micelles into the enterocyte (Davis *et al.* 2011). Ezetimibe was shown to lower cholesterol and improve vascular outcomes in many pre-clinical models (van Heek, Compton and Davis 2001) (Davis *et al.* 2001). In a meta-analysis of 2700 patients receiving Ezetimibe as a monotherapy, there was on average an 18.5% decrease in LDL-cholesterol compared with placebo (Pandor *et al.* 2009). As a combination therapy with a statin, Ezetmibe has shown a further LDL-cholesterol

lowering of 16.5% when compared with statin monotherapy in HeFH patients (Kastelein *et al.* 2008). Ezetemibe failed to alter the primary end point of this study although it did cause a further reduction in carotid-artery intima-media thickness. In HoFH patients, Ezetimibe added to medium or high dose statin gave a 21% and 27% decrease in LDL-cholesterol compared with a 7% decrease when the dose of stain was doubled (Hamilton-Craig *et al.* 2010). This enhanced combinatorial effect may be explained by the fact statins have been shown to upregulate cholesterol absorption (Huff and Burnett 1997) and vice versa, Ezetimibe causes an upregulation of *de novo* cholesterol synthesis (Bays 2002).

Despite this many clinical studies failed to show added benefit of Ezetimibe when added to statins in primary out comes of atherosclerotic development or cardiovascular events (Brown and Taylor 2008; Kastelein *et al.* 2008). IMPROVE-IT was the first study to show an added benefit of adding a non-statin drug to a statin in a primary outcome of having a cardiovascular event (Cannon *et al.* 2015). Over 7 years, the addition of ezetimibe to simvastatin 40 mg reduced the risk of cardiovascular death, MI, unstable angina requiring rehospitalisation, coronary revascularization, or stroke by 6.4% when compared with patients who received simvastatin alone. Until the very recent development of PCSK9 inhibitors, Ezetemibe was the only non-statin therapy to demonstrate an enhanced effect on reducing cardiovascular events.

1.6.4.2.2 Fibrates/Niacin

The fibrate class of compounds cause an increase in HDL through increasing apoA-I and apoA-II expression in the liver. Fibrates also decrease VLDL through increased LPL activity, induction of hepatic fatty acid uptake and reduction of hepatic triglyceride production (Staels *et al.* 1998). These effects occur through the activation of PPAR transcription factors. Niacin is another compound shown in pre-clinical models to increase HDL production (Mani and Rohatgi 2015). Both classes of compounds have failed to show any added benefit on cardiovascular outcomes when added with a statin to date (Group 2010; Investigators 2011). HDL levels are correlated inversely with cardiovascular risk, however no HDL raising therapy has demonstrated benefits on cardiovascular outcomes. It is becoming increasingly apparent that it is not HDL quantity but quality where the next line of

focus must lie. One particular study demonstrated that certain posttranslational modifications on human HDL can make it defunct and even pro-inflammatory (Huang *et al.* 2014). Increased rates of myopathy have been reported when fibrates are given in combination with statins and niacin can cause flushing, leading to these classes of compounds being used less and less frequently with FH patients (Jacobson 2009; Mani and Rohatgi 2015).

1.6.4.2.3 Cholesterol absorption inhibitors

Bile acid sequestrants like cholestyramine, bind bile salts in the intestinal lumen preventing their enterohepatic recirculation. The loss of bile acids is accounted for by the liver, which uses further cholesterol ester from its intracellular pool to make more bile acid thus depleting hepatic intracellular cholesterol (Robinson and Keating 2007). Bile acid sequestrants lower LDL cholesterol by 10 to 20%, but cholestyramine is associated with significant gastrointestinal side effects such as constipation, reducing its tolerability (Tonstad *et al.* 1996).

1.6.4.3 MTP inhibitors and Mipomerson

Lomitapide, an MTP small molecule inhibitor has recently been approved by the Food and Drug Administration (FDA) and European Medicines Agency for use in HoFH pateints alongside current lipid lowering therapy and LDL apheresis (Raal *et al.* 2013). Inhibiting MTP leads to a decrease of the synthesis of chylomicron, VLDL and LDL particles and release into the circulation. In an open label trial in HoFH patients, Lomitapide gave a further ~50% lowering of LDL-cholesterol and decreased lipoprotein (a) by ~15% after 26 weeks. This effect was seen on top of maximally tolerated lipid lowering therapy and LDL-apheresis and persisted for 12 months (Cuchel *et al.* 2013).

Mipomerson is an antisense oligonucleotide targeting ApoB mRNA, thus decreasing the production of VLDL (Crooke and Geary 2013). Similar to Lomitapide, after an open label study involving Mipomersen on top of lipid lowering therapy and LDL apheresis, there was an additional 26% lowering of LDL-cholesterol and 31% decrease in lipoprotein (a), after 26 weeks (Raal *et al.* 2010). Both Lomitapide and Mipomersen demonstrate similar side effects with elevated levels of alanine aminotransaminase (ALT), greater than 3 times the upper limit of normal (ULN) were reported for 34 and 12% of patients respectively.

This elevation in liver toxicity was most likely associated with an increase in hepatic fat content, which in both studies correlated with efficacy. Due to the risk of hepatic toxicity, both agents have been restricted to use only when all other treatments do not reduce LDL-cholesterol to a safe enough level.

1.6.4.4 PCSK9 Inhibitors

Recently, three monoclonal antibodies targeting PCSK9 have been made available (evolocumab, alirocumab, and bococizumab), with evolocumab and alirocumab receiving market authorization in Europe and the US. These monoclonal antibodies are still being evaluated in large clinical trial programs; initial results demonstrate an additional ~60% decrease in LDL-cholesterol on top of what can be achieved with maximal dose stains (Robinson *et al.* 2014, 2015). Inhibiting PCSK9 has a synergistic effect with statins as it combats the concomitant upregulation of PCSK9 that accompanies upregulation of the LDLR, therefore further increasing the LDLR expression achieved with statins (Dubuc 2004). Importantly, no significant increase in adverse events has been reported using PCSK9 inhibitors compared to statins alone (Dadu and Ballantyne 2014). The OYDESSEY trials involving alirocumab, has an arm specifically for unresponsive HeFH patients, again where an additional 58% LDL-cholesterol lowering was seen in these patients (Kastelein *et al.* 2015).

In receptor defective HoFH patients, PCSK9 inhibitors have also shown efficacy, with reductions of 19 and 26% in LDL-cholesterol, depending on the frequency of dosing (Stein *et al.* 2013). There was no effect as would be expected in receptor negative HoFH patients in the same study. The PCSK9 inhibitors are given as sub-cutaneous injections every 2-4 weeks and being monoclonal antibodies are estimated to cost $14,000 per patient per year (Kazi *et al.* 2016). Assuming these prices stay as they are, PCSK9 inhibitors do not meet generally acceptable incremental cost-effectiveness thresholds and are estimated to increase US health care costs substantially (Kazi *et al.* 2016). This hurdle on cost and delivery will need to be overcome to ensure that all HeFH and receptor defective HoFH patients can benefit.

1.6.4.5 LDL apheresis

LDL apheresis is an approved therapy for HoFH or treatment resistant HeFH patients. It involves the removal of ApoB containing lipoproteins from the circulation, by passing the blood through a column containing either anti-apolipoprotein B antibodies, dextran sulphate, or heparin (Thompson 2003). LDL apheresis typically removes ~60% of the circulating LDL-cholesterol however hypercholesterolaemia normally returns to baseline levels within 12-13 days (Kroon *et al.* 2000). Few side effects are associated with LDL apheresis, with hypotension being the most common reported. LDL apheresis has actually shown regression in xanthoma size and shown to modify a number of cardiovascular markers of diseases such as lipoprotein (a) (Keller 2007). For many HoFH patients, LDL apheresis remains the only treatment to retard the development of atherosclerosis, this treatment is limited by the time it takes to complete (more than 3 hours every 1 to 2 weeks), the low availability around the world and the cost (Thompsen and Thompson 2006).

1.6.4.6 Liver transplantation

The first liver transplantation occurred in 1984 for a HoFH patient in a 6-year-old girl with severe CHD (Starzl *et al.* 1984). An additional 30 cases have been reported to date of either liver transplantation or heart and liver combined. Liver transplantation provides functional copies of the LDLR to the patient and results in an almost immediate improvement in the lipid profile of the patient (Küçükkartallar *et al.* 2011). A reduction in lipids of ~80% is reported post-transplantation, with statin therapy shown to be able to match that of the donors (Khalifeh *et al.* 2005). The longest follow up to date was a 33 year old man who remained CAD free 20 years post transplantation, although he had developed cyclosporine-induced chronic renal failure (Ibrahim *et al.* 2012). There are of course many risks with liver transplantation, coronary reperfusion procedures and death have been reported in a few of the HoFH liver transplantation cases along with hepatic artery thrombosis and acute rejection episodes. Lifelong immunosuppression from such a young age also brings the risk of diabetes and the metabolic syndrome, nephrotoxicity, osteoporosis and an increased risk of developing certain cancers (Page *et al.* 2014).

1.7 Gene therapy for familial hypercholesterolaemia

1.7.1 Gene therapy

Gene therapy is the delivery of nucleic acids into somatic cells of an individual for the treatment of a genetic or acquired disease. The unfortunate death of Jesse Gelsinger in a clinical trial for ornithine transcarbamoylase deficiency due to a large immune response against the adenoviral vector(Sibbald 2001), sobered the scientific community to the dangers of gene therapy. Later patients in a clinical trial for X-linked severe combined immuno-deficiency (X-SCID), a genetic condition resulting in a compromised immune system, initially appeared cured from the condition. Unfortunately, a proportion of them went on to develop leukaemia, again linked to the viral vector delivering the nucleic acid (Check 2002). The recent approval of Glybera, a treatment for LPL deficiency has finally started to fulfil the promise gene therapy held for so long (Scott 2015). Since Glyberas approval, other gene therapies have been licensed for various conditions including Chronic Granulomatus Disorder and X-SCID (Cicalese *et al.* 2016), with an ex-vivo approach resulting to date in a 100% survival of all the patients within the trial. This therapy, Strimvelis for X-SCID marks a turn in the tide for the development of gene therapy with many more in late stage clinical trials.

1.7.2 A liver targeted gene therapy for familial hypercholesterolaemia

The rapid resolution of hypercholesterolaemia in patients who undergo liver transplantation provides very strong evidence that a liver directed gene therapy would provide metabolic correction of FH. As most cases of FH result in a mutation within the *LDLR* and almost all the work in gene therapy for FH has focused on the *LDLR*, that will be what is discussed here. In the broadest terms, gene therapy for FH can be divided into *ex vivo* and *in vivo*. The *ex vivo* approach involves the isolation of hepatocyte cells from the patient, followed by *in vitro* modification. A virus is used to carefully select for individual clones with the most desirable characteristics, avoiding direct vector toxicity, dissemination, and genetic modification of non-liver cells (Nguyen and Ferry 2004). Although this approach offers greater safety and control over integrative mutagenesis and germline transmission of the LDLR, it is often very laborious and expensive. The studies in

clinical trials thus far have been stumped by poor engraftment of the hepatocytes back into the patient (Grossman *et al.* 1994, 1995). The *in vivo* approach involves the use of a vector to deliver the gene after administration into the circulation. The liver is an ideal target for gene therapy as it is the largest and most vascularized organ in the body with two circulation systems, the systemic and the portal. The *in vivo* approach circumvents the need for engraftment and therefore is easier to perform and likely more cost effective (Nayerossadat, Maedeh and Ali 2012). The vector chosen to deliver the gene can vary quite dramatically in transduction/transfection and safety profile as discussed below.

1.7.2.1 Viral gene therapy for familial hypercholesterolaemia

Many different viruses have been used as vectors for delivery of the LDLR in FH, their differing properties are listed below in Table 3. The *LDLR* is 45kb in length so only the herpes simplex viruses-1 (HSV-1) vector has the capacity to fit the gene in its entirety. In fact the whole LDLR locus (135kb) was cloned into a HSV-1 vector, successfully being delivered and providing functional complementation to an *Ldlr*$^{-/-}$ cell line (Wade-Martins et al. 2003.). The other vectors instead use the *LDLR* cDNA (2583bp), so that the genetic material can be successfully packaged into a virion.

Virus	Genetic material	Capacity (kb)	Retention	Pre-existing host antibodies
Retrovirus	RNA	8	Integration	Unlikely
Lentivirus	RNA	8	Integration	Unlikely
HSV-1	dsDNA	152	Episomal	Likely
AAV	ssDNA	5	<10% integration	Yes
Adenovirus	dsDNA	30	Episomal	Yes

Table 3 - General properties for the most commonly used viral vectors for FH gene therapy

How the vector is maintained when within the host cell can vary, the vector can either integrate its genome into the hosts chromosomes or remain as a circular plasmid within the nucleus, known as an episome. Present integrating vectors involve an almost random integration (certain areas of DNA are preferentially integrated into), of the transgenic DNA into the host chromosome where it can be passed down to future daughter cells (Verma and Somia 1997). The integration involving non-homologous end joining of the vector DNA is facilitated by a viral

integrase enzyme. The retro and lentiviruses are the most commonly used vectors for integration though it must be noted that integration does not always guarantee expression. Many other factors including genetic silencing, immune-elimination and physiological cell death of vector modified cells can limit the efficacy of the vector (Chen *et al.* 1997).

In clinical trials hoping to correct X-SCID using integrating retroviruses or lentiviruses, a number of patients in each trial went on to develop leukaemias (Hacein-Bey-Abina *et al.* 2003, 2008). The insertions were found to be in proto-oncogenes, *LMO2*, *BMI1* and *CCDN2*, with retroviruses appearing to favour integration into promoter regions (Mitchell *et al.* 2004) and lentiviruses into the transcription unit (Schröder *et al.* 2002). Insertional mutagenesis was also seen more recently in a clinical trial for chronic granulomatous disease and remains a real safety concern (Ott *et al.* 2006).

Adenoviruses, HSV-1 and adeno-associated viruses (AAV) remain as an episome, though it must be noted that a very small proportion of the AAV does integrate and has shown insertional mutagenesis *in vivo* (Donsante *et al.* 2001). All three of these vectors have shown persistent expression *in vivo* as an episome (Ehrhardt, Xu and Kay 2003). Adenovirus and AAV vectors can produce an immunogenic response unfortunately, resulting in a tolerance to future administrations or clearance of cells expressing the viral or delivered proteins (Aubert *et al.* 2002; Manno *et al.* 2006). Non-integrating vectors can be lost during cell division, to prevent this the Epstein-Barr Virus (EBV) expresses a gene called the EBV nuclear antigen 1 (EBNA-1), which allows the replication and transfer of the episome to the daughter cell (Tsurumi, Fujita and Kudoh 2005). To help prolong transgene expression after vector administration, EBNA-1 has been cloned into adenoviruses demonstrating long term persistence albeit in immunocompetent mice (Gil, Gallaher and Berk 2010). To combat immune responses against the AAV and AD vector systems, administration with an acute dose of an immunosuppressive drug may get around certain patients who have an already developed immunity to the vector (Parzych *et al.* 2013).

1.7.2.1.1 Retrovirus vectors for the treatment of familial hypercholesterolaemia

As retrovirus vectors are unable to transduce non-dividing cells, their application in developing treatments for FH has been confined to *ex vivo* approaches. Using retroviral vectors to provide a functional copy of the LDLR was the first gene therapy approach undertaken for FH, involving the re-infusion of autologous hepatocytes into the Watanabe heritable hyperlipidemic *(*WHHL*)* rabbit (Chowdhury *et al.* 1991). The hepatocytes were first removed from the WHHL rabbit before *in vitro* correction took place using vectors based on the Moloney murine leukemia virus MoMLV. New Zealand white rabbit LDLR cDNA was successfully delivered resulting in a 30-50% reduction in total serum cholesterol, lasting 122 days. Using the same system, canines and non-human primates also demonstrated a phenotypic correction (Grossman, Raper and Wilson 1992). This progressed on to the first ever clinical trial in a 29-year old woman. The patient underwent a 25% hepatectomy, the hepatocytes were isolated and human LDLR cDNA was delivered under the control of the cytomegalovirus (CMV) enhanced chicken β-actin promoter (Grossman *et al.* 1994). The patient achieved a 17% lowering of LDL-cholesterol measured at the end of the 18-month study. Four more HoFH patients underwent hepatectomy and subsequent reperfusion of the transformed hepatocytes (Grossman *et al.* 1995). A much wider variability in response to the treatment was seen this time and although one patient did have a 20% LDL-cholesterol lowering for the duration, presumably low gene transfer levels in many of the other patients resulted in the study being far less successful. Progressing this therapeutic approach therefore required a much higher transfection using the retrovirus and hepatocyte engraftment; pending these improvements no further patients have underwent the procedure.

1.7.2.1.2 Lentiviral vectors for the treatment of familial hypercholesterolaemia

Lentiviral vectors have only been used in a handful of pre-clinical studies for FH and so will only briefly be mentioned. Delivery of rabbit LDLR cDNA under the control of the HSP promoter resulted in a 34% decrease in total serum cholesterol after two years in the WHHL rabbit (Kankkonen *et al.* 2004). The possible risks of insertional mutagenesis where not evaluated in this study however. It has been difficult for many groups to produce infectious lentiviruses that express the human LDLR under the control of a ubiquitous promoter (Al-Allaf *et al.* 2010).

Improvements on achieving high enough viral titre and safety must be improved before this approach can progress.

1.7.2.1.3 Adenoviral vectors for the treatment of familial hypercholesterolaemia

Adenoviruses were first investigated as delivery vectors for human LDLR in 1993. Hepatocytes from HoFH patients were transduced with a replicative deficient adenovirus, demonstrating a 20-fold increase in expression of the LDLR compared with endogenous levels (Kozarsky, Grossman and Wilson 1993). Adenovirus systems expressing the human or rabbit LDLR under strong heterologous promoters were used in high fat fed $Ldlr^{-/-}$ mice or WHHL rabbits (Ishibashi *et al.* 1993; Li *et al.* 1995). Hypercholesterolaemia was corrected after a few days in each study but returned as transgene expression was found to be transient. Of greater concern, the huge transgene expression initially achieved resulted in a pathological intracellular lipid accumulation, as the rate of catabolism could not keep up with the rate of intake (Kozarsky *et al.* 1994; Heeren *et al.* 1999; Cichon *et al.* 2004). It appears that the transient nature of the expression may not only be down to cell death but host immune responses against the adenovirus itself (Dai *et al.* 1995). The severity of the immune response that could be elicited against adenoviruses was tragically found out, when as stated earlier Jesse Gelsinger died after administration in a clinical trial (Sibbald 2001). These tragic events have led scientists to try and come up with safer ways to introduce a gene using an adenovirus.

Helper-dependent adenoviruses, where almost all viral elements needed for packaging and replication are provided in trans, was one such solution. Helper-dependent adenoviruses have shown at low doses to completely halt the progression of atherosclerosis in $Ldlr^{-/-}$ mice after 60-weeks, from a single administration. These mice also demonstrated a lipid lowering effect of 108 weeks, where all control mice had died (Nomura *et al.* 2004). The application of adenovirus may be hindered however through the relatively high rate of patients who may already carry antibodies to a specific serotype (Pilankatta *et al.* 2010) or develop an immune response to the adenovirus. Reducing the immune response and potentially cytotoxic constitutive expression of the LDLR will need to be further

investigated to repurpose the adeno or helper-dependent adenoviruses as anything more than a proof of principle in the FH field.

1.7.2.1.4 Adeno-associated viruses for the treatment of familial hypercholesterolaemia

AAV vectors are non-pathogenic and replication defective, making them suitable for gene therapy. Although AAV vectors are not known to cause disease they are limited by the fact that ~85% of the population is sero-positive for antibodies against AAV capsid proteins (Berns 1990). Switching the capsid protein too other AAV serotypes can often overcome this problem however (Davidoff *et al.* 2005). AAV vectors were first used in 2000, were an AAV-2 vector delivered the VLDLR into $Ldlr^{-/-}$ mice fed a high fat diet (Chen *et al.* 2000). This was the first proof of concept study that an AAV could be used to lower total serum cholesterol for a prolonged period of time and slow the progression of atherosclerosis. Phenotypic correction in this study was incomplete however due to immune responses against the AAV vector and a low level of transduction and expression using this AAV serotype towards the liver.

The laboratories of Dr Rader and Dr Wilson have then pioneered the development of AAV for the treatment of FH. First a comparison between AAV-2, AAV-7 and AAV-8 serotypes was carried out in $Ldlr^{-/-}$ mice fed a high cholesterol diet (Lebherz *et al.* 2004). Unlike AAV-2, AAV-7 and AAV-8 completely normalised the total and LDL-cholesterol levels when the LDLR was delivered though a single injection. A switch to using a more modest liver specific promoter (thyroxin binding globulin (TBG)) resulted in no pathological intracellular lipid accumulation within the liver. The use of the AAV-8 serotype resulted in ~85% transduction of hepatocytes and 50 genome copies per cell, compared with 2 genome copies per cell seen with the AAV-2. Importantly, with the AAV-8 serotype no expression terminating immune responses were detected. The AAV-8, expressing human LDLR was able to completely correct the hyperlipidaemia in a humanized mouse model, where $Ldlr^{-/-}$ mice are also *Apobec1*$^{-/-}$ (Kassim *et al.* 2010). This mouse model is discussed in detail in section 5.1.3 but essentially causes the mice to carry most of the cholesterol in the ApoB containing LDL fraction. With high doses of the AAV-8 vector expressing human LDLR, they demonstrated complete amelioration of the

hyperlipidaemia resulting in cessation in the development of atherosclerosis. The AAV-8 vector system also showed efficacy in a humanized HeFH mouse model (Kassim *et al.* 2013).

This work has led to the first clinical trial using AAV vectors for FH, which is ongoing now with the results scheduled for released in January 2018 (https://clinicaltrials.gov/ct2/show/NCT02651675). The exact serotype to use for the human trials may be more complicated than expected, recently, Bissig-Choisat et al., demonstrated in a mouse xenograft model using hepatocytes from a HoFH patient, that in fact AAV-9 was superior in transducing human hepatocytes. Surprisingly, the AAV-9 and AAV-8 were poor transducers in primary human hepatocytes *in vitro* but when transducing the same hepatocytes repopulated in the mouse liver, AAV-8 and AAV-9 appeared superior to the other serotypes, with AAV-9 providing the highest expression of the transgene (Bissig-Choisat *et al.* 2015). It is unfortunate that antibodies to all serotypes can be found in a large proportion of individuals which may restrict this treatment to only a subset of patients and prevent repeated administration in those individuals (Mingozzi and High 2013). Despite this the AAV system remains very promising for the development of a gene therapy for FH.

1.7.2.2 Non-viral gene therapy for the treatment of familial hypercholesterolaemia

The use of modified viral gene transfer systems remains the most popular in the FH field due to the high level of transduction that can be achieved. Viral gene delivery is however still hampered by the potential toxic effects that accompany delivering a high titre of virus into the circulation (Nayak and Herzog 2010). As previously mentioned predisposed immunity may be able to be overcome with the co-administration of immunosuppressive drugs (Parzych *et al.* 2013). Just as serious, is the risk for insertional mutagenesis with some of the most commonly used viral vectors (Hacein-Bey-Abina *et al.* 2003) however as the understanding of how these processes occur the risk can be reduced.

A non-viral approach would ameliorate any of these safety concerns and in theory, is still the most attractive approach for gene therapy. Non-viral vectors are not limited by size, allowing the delivery of the whole locus of a gene. The whole

LDLR loci, containing the 45 kb human *LDLR* within a 135 kb genomic DNA insert, was successfully delivered using a HSV-1 based amplicon vector, termed an infectious bacterial artificial chromosome (iBAC) (Wade-Martins et al. 2003).

These vectors utilised the EBV retention elements to confer episomal retention of the plasmids for 3 months in Chinese hamster ovary (CHO) cells. Specifically, EBNA-1 and the oriP sequences are required for retention, where EBNA-1 is a DNA sequence binding protein which binds to multiple sites throughout the oriP sequence to facilitate this. A dyad symmetry (DS) sequence made up of inverted EBNA-1 binding sites at one end of oriP functions as an origin of DNA replication. EBNA-1 bound to the DS then binds to the replication machinery within the host cell ensuring that as the host genome is replicated so is the EBNA-1 bound episome (Lindner and Sugden 2007). Another region of the oriP is made up of 21-30 bp imperfect repeats, termed the family of repeats (FR). EBNA-1 also binds to the FR, forming a bridge with the episome and metaphase chromosomes, effectively tethering daughter episomes generated during S phase to host daughter chromosomes (Lindner and Sugden 2007). Plasmids containing both these elements can persist in human or primate cells with around 95% retention per cell cycle, however episomal retention only occurs in mouse cells in the presence of a large fragment of human DNA around 10kb or larger (Krysan and Calos 1993).

Scaffold/matrix attachment regions (S/MARs) are 70% AT-rich sequences which are believed to play many important roles in chromatin function. The human genome is organized in a complex structure within the nucleus, where DNA interacts with histones and chromatin proteins to form a 30-nm fibre, which appears to be organized into loops by interaction of S/MARs with the nuclear matrix (Heng *et al.* 2004). In 1999 Piechaczek et al., described the construction of a new vector, named pEPI, containing an S/MAR isolated from the human interferon β-gene (Piechaczek *et al.* 1999). It appears incorporating an S/MAR tethers the plasmid to the nuclear matrix machinery needed for replication and expression of the transgene, as well as aiding episomal retention (Alvarez *et al.* 2000). A second iBAC-*LDLR* vector was generated again containing the native promoter of the LDLR and all regulatory sequences but this time with an S/MAR

episomal retention element (Lufino, Manservigi and Wade-Martins 2007a). Delivery of this iBAC-*LDLR*-S/MAR amplicon was able to provide complete restoration of LDLR function in a *Ldlr* deficient CHO cell line. The LDLR could be detected for at least 240 cell generations and most importantly was responsive to the cholesterol content within the cell, as LDLR expression increased and decreased in the presence of statins and sterols respectively. By delivering the whole *LDLR* gene not only are the protein coding exons delivered but the entire promoter region as well, allowing for physiological regulation. As has been discussed this may be essential for long term efficacy, due to the dire consequences cholesterol imbalance can have on the health of a cell (Cichon *et al.* 2004).

The BAC-*LDLR* plasmid containing the EBV episomal retention elements (pEHZ-*LDLR*), was delivered to MF-1 mice via a hydrodynamic injection (discussed in section 4.1.3) (Hibbitt *et al.* 2007a). This non-viral method gave expression up to 4 months of the LDLR and β-Gal transgenes, which were co-locally expressed in the liver. The pEHZ-*LDLR* plasmid was reduced in size to increase the level of transfection following hydrodynamic delivery. The second generation of non-viral plasmids (p*LDLR-LDLR,* Figure 28B), contained the *LDLR* promoter driving the *LDLR* cDNA. These plasmids expressed the LDLR 9-months post-delivery in MF-1 mice and the plasmid promoter responded to statins in a physiological manner *in vivo* (Hibbitt *et al.* 2010). Delivery of the p*LDLR-LDLR* plasmid to Ldlr$^{-/-}$ mice resulted in a significant decrease in LDL-cholesterol levels which was then enhanced by co-delivery with a miRNA sequence targeting *Hmgcr* (Hibbitt *et al.* 2012). This non-viral gene therapy approach edged closer to an ideal therapy where by not only was the dysfunctional gene replaced but regulation of the gene was restored to the native system. Recently the p*LDLR-LDLR* plasmids were used to transfect induced pluripotent stem cells (IPSCs) derived from FH patient fibroblasts (Ramakrishnan *et al.* 2015). After six months of culture the plasmids could be recovered from the IPSCs and transfected into a CHO cell line lacking the Ldlr receptor where again similar to what was seen with Hibbitt et al., 2010, they responded in a physiological manner to statin and sterol stimuli.

Another recent non-viral approach has been the use of a sleeping beauty transposon to integrate the Ldlr or Vldlr into hepatocytes of $Ldlr^{-/-}$ mice. Only sleeping beauty vectors containing mouse Vldlr reduced total cholesterol in this study up to 26-weeks post-delivery (Turunen *et al.* 2015). Atherosclerosis however was significantly reduced throughout the aorta in mice delivered with Ldlr and Vldlr vectors after 6-months. The efficacy seen with this integrating system would need to be improved as unfortunately only a very modest level of transgene expression could be detected post study. Insertional mutagenesis is again still a risk due to the random integration of the vector and so further refinement and additional safety for this method to progress into larger pre-clinical models is still needed.

1.8 Aims of thesis

The unmet clinical need of most HeFH and all HoFH patients requires the development of future therapeutics, which one day may better help the management of hypercholesterolaemia within this patient population. Within this project we set out to identify, develop and characterise two novel therapies which act by modulating expression of the LDLR, a small molecule approach and a gene therapy approach. The three aims, each consisting of a chapter, are given below.

1. **Identify and characterise a novel set of small molecules that are able to upregulate the LDLR via a mechanism distinct to statins.**

2. **Progress the lead compound *in vivo,* evaluating the pharmacokinetics and efficacy of the compound within a mammalian system.**

3. **Characterize a novel combinatorial non-viral vector in a mouse model of familial hypercholesterolaemia**

Chapter 2: Materials and Methods

2.1 Cell culture of immortalised cell lines

2.1.1 Cell Culture

All cell cultures were maintained in a saturated humidity incubator at 37°C with 5% CO_2. All cell culture work was carried out in a Class II laminar flow cabinet under aseptic conditions. Wildtype (WT) CHO cells (CHO-WT) and CHO cells stably transfected with p*LDLR-Luc* (Figure 28D) (CHO-p*LDLR-Luc*) were grown in Hams F-12 media (Sigma) supplemented with 10% fetal bovine serum (FBS), 1% penicillin/ streptomycin, 1% L-glutamine (Life Technologies). For luciferase experiments CHO cells were seeded in 24-well plates at $1.5x10^5$ cells per well. After 24 hours, cells were changed to HamsF-12 media supplemented with 5% lipoprotein deficient serum (LDPS), 1% penicillin/ streptomycin, 1% L-glutamine.

Human Hep3B cells were a kind gift from Dr Zoe Holloway. Mouse hepatoma Hepa 1–6 cells were a kind gift from Dr Natalia Sacilotto. Both cell lines were grown in Dulbecco's modified Eagle's medium (DMEM, Sigma) supplemented with 10% FBS, 1% penicillin/ streptomycin, 1% L-glutamine. For mRNA analysis Hep3B cells were seeded in 24-well plates at $1.5x10^5$ cells per well. For Western blot analysis Hepa1-6 cells were seeded in 6-well plates at $2.5x10^5$ cells per well. After 24 hours, cells were changed to Dulbecco's modified Eagle's medium (DMEM, Sigma) supplemented with 5% lipoprotein deficient serum (LDPS), 1% penicillin/ streptomycin, 1% L-glutamine.

2.1.2 Drug treatment

Compounds and simvastatin (Sigma) were dissolved in Dimethyl Sulfoxide (DMSO, Sigma) and Cholesterol (Sigma) and 25-Hydroxycholesterol (Sigma) were dissolved in ethanol, before being added 24 hours after switching to LDPS supplemented media for all cell culture experiments. 0.1% DMSO was used as a control for all drug treated cells.

2.1.3 Cryopreservation of cells

Cells grown in a 75cm^2 conical flask were trypsinized using 2 mL trypsin-EDTA (Sigma) at 37 °C for 5 minutes. Trypsinization was halted using the cell media used to culture that cell line in, as stated above. The cell suspension was spun at 1000 rpm for 5 minutes and resuspended in an appropriate volume of media. 1 mL of 2x freeze mix (60% DMEM, 30% FBS, 10% DMSO) was added to every 1 mL of cells and then was transferred to a cryovial (Nunc). Cells were frozen over night at -80^{o}C and then transferred to a liquid nitrogen store the next day.

2.1.4 Thawing of frozen cell stocks

Cells were rapidly thawed in a 37^{o}C water bath. Cells were added to 13mLs of the cell media used to culture that cell line as stated above. Cell suspension was centrifuged at 1000rpm for 5 minutes to pellet cells and resuspended in 8mL of cell culture media. Cells were plated in a 25cm^2 conical flask ready for culture.

2.2 Plasmid transfection

Hep3B cells were plated as described above before being transfected with p*LDLR-Luc or* p*CMV-Luc* plasmid. Briefly Lipofectamine 2000 (Life Technologies) and plasmid were added to separate aliquots of Opti-MEM media (Thermofisher) and left to sit for 5 minutes, before being pulled together and left to sit for a further 25 minutes. Cells were then treated with the Lipofectamine 2000 containing the plasmid for 6 hours and then switched back to DMEM supplemented with 5% lipoprotein deficient serum (LDPS), 1% penicillin/ streptomycin, 1% L-glutamine. Cells were left for 24 hours before any compound treatments.

2.3 *In vitro* luciferase activity assay

Cellular media was aspirated and cells were lysed 48 hours after compound treatment using a lysis buffer (1% Triton X-100, 25mM TrisPO_4 (pH 7.8), 2mM CDTA, 10% Glycerol in H_2O). Cells were shaken for 20 minutes, spun down at 4500rpm for 5 minutes and 75 µL of lysate was loaded into a clear bottom 96-well plate. Luciferase assay buffer (15mM $MgSO_4$, 15mM KPO_4 (pH7.8), 4mM EGTA (pH7.8), 2mM ATP (Sigma) and 2mM DTT (Life technologies) in H_2O) and 1mM $_D$-Luciferin (Cambridge Bioscience) were loaded into separate injectors of a Dynex Technologies MLX 96 well plate luminometer (Dynex). 100 µL of luciferase assay

buffer and 50 µL of D-Luciferin were injected into the lysate and luminescence was read immediately.

2.4 Protein quantification

Protein concentration from cell lysates and tissue homogenates were quantified using the bicinchoninic acid (BCA, Sigma) assay. Protein standards were made up using bovine serum albumin (BSA, Sigma) of increasing concentrations (0-2000 µg/mL) in appropriate lysate buffer and samples were diluted to fall within this range. 10 µL of sample was added to 200 µL of a 50:1 solution of BCA:Copper Sulphate. Samples were incubated at 37oC for 30 minutes before being read on a Synergy HT microplate reader (Biotek) at an absorbance of 562nm.

2.5 Cytotoxicity assay

Cell media was collected from wells of cells treated with compounds for 48 hours. Adenylate kinase concentration present in the media was quantified as a measure of cytotoxicity using a Bioluminescence Cytotoxicity Assay Kit (Biovision). 100 µL of cell media was added to a 96-well clear bottom plate along with 100 µL of the AK working reagent solution supplied by the manufactures. Luciferase activity was quantified on a Dynex Technologies MLX 96 well plate luminometer after 5 min incubation.

2.6 Analysis of mRNA expression

2.6.1 RNA isolation

Cell media was aspirated 24h after compound treatment and cells were washed in 500 µL of phosphate buffered saline (PBS). Cells were lysed in 350 µL of TRIzol (Life Technologies) before 200 µL of chloroform was added to each sample and shaken vigorously for 20-30 seconds for phase separation. Samples were spun at 13,000 rpm for 60 seconds before the upper aqueous phase was transferred to an RNase free Eppendorf. An equal volume of 70% EtOH was added to each sample. An RNeasy kit (Qiagen) was used to purify the RNA with all centrifugation steps at 13,000rpm for 60 seconds unless stated. The resulting solution was loaded onto an RNeasy spin column, centrifuged and the flow through discarded. 350 µL of

RW1 buffer was added onto each column and centrifuged. 80 µL of 1:8 DNase I:RDD buffer (Qiagen) was loaded on each column membrane and left to incubate for 10 minutes. Each column was washed in 350 µL RW1 buffer, centrifuged and the flow through discarded. Two further wash steps of 500 µL of RPE buffer then followed before the column was centrifuged at 10,000rpm for two minutes to dry the membrane. All samples were transferred to a 1.5mL collection tube, 30 µL of RNase free H_2O was pipetted onto the membrane and left to stand for 2 minutes. After centrifugation to elute the RNA all samples were stored at -80^oC.

2.6.2 cDNA synthesis

RNA was quantified on a Nanodrop-1000 Spectrophotometer (Nanodrop) and each sample diluted with RNase free H_2O, making all samples the same concentration. 1 µL of Random primers (150ng, Life Technologies) and 1 µL of dNTP mix (10mM, Life Technologies) were added to 11 µL of RNA and heated to 65^oC for 5 minutes followed by 1 minute on ice. RNA was then transcribed into complementary DNA (cDNA) using a Superscript III Reverse Transcriptase Kit (Life Technologies) as per manufactures instructions. Briefly 4µL of 5X first strand buffer, and 1µL of 0.1M DTT, RNaseOUT recombinant RNase inhibitor and SuperScript™ III RT were added to each sample and run on a Tetrad 2 Thermal Cycler (Biorad) under the following conditions:

-25^oC for 5 minutes

-55^oC for 60 minutes

-70^oC for 15 minutes

cDNA was then diluted 1:10 with DNase free H_2O and stored at -20^oC or proceeded to qRT-PCR anlaysis.

2.6.3 Quantitative real time polymerase chain reaction (qRT-PCR)

qRT-PCR was used to analyse cDNA expression and therefore indirectly mRNA expression. Each reaction was set up as follows: 12.5 µL SYBR green master mix (Applied Biosystems), 1µL of cDNA, 3 µL DNase free H_2O and 3.5 µL of forward and reverse primer (1 µM). Primers used are listed in table below.

Gene target	Species	Primer Sequence 5'>3'
LDLR_F	Human	GACAGATGCGAAAGAAACGA
LDLR_R	Human	ACAGACAAGCACGTCTCCTG
β-Actin_F	Human	AGCGCGGCTACAGCTTCA
β-Actin_R	Human	CGTAGCACAGCTTCTCCTTAATGTC

Table 4 - Primer sequences

Each primer was first optimized with pulled cDNA from multiple samples of the same cell line to produce a standard curve. Only primers which had a primer efficiency between 90-110% were used for qRT-PCR analysis.

Samples were then run on a Step One Plus Real Time PCR System (Applied Biosystems) as follows:

Stage	Time (seconds)	Temperature (ºC)
Holding	20	95
Cycling (x40 cycles)	3	95
	30	60
Melt Curve	15	95
	60	60
	15	95

Table 5 - qRT-PCR run conditions

A melt curve was run at the end of each run to assess homogeneity of the PCR products.

2.6.4 qRT-PCR expression analysis

Ct (cycles till threshold reached) obtained from each gene was normalized to the Ct values of control genes, in this case β-Actin. The normalized values (ΔCt) were subtracted from the specific control groups ΔCt value to calculate ΔΔCt. This value is a log value and is inversely proportional to the amount of DNA/RNA. Therefore, calculation of 2-ΔΔCt provides the fold change as an expression ratio. This method was used in all normalization throughout this project.

2.7 Western blot analysis of protein expression

2.7.1 Protein extraction

Cell media was aspirated and cells were washed in 1 mL of PBS. 250 µL of lysis buffer (50mM Tris pH 7.5, 150mM NaCl, 1% NP40, 0.5mM EDTA, 0.1% SDS, 1 cOmplete EDTA-free protease inhibitor tablet (Roche) and dH20) was added to each well, cells were scraped and pipetted into Eppendorf's. For liver tissue samples the right median lobe was removed from the mouse and homogenised in the lysis buffer using a tissue tearer (Biospec Products) before being sonicated for 5-10 seconds. To remove cell debris the samples were centrifuged at 13,000rpm for 15 mins at 4^{o}C and the supernatant removed and pipetted into a new Eppendorf. The protein concentration was determined using the BCA assay as previously described in section 2.4.

2.7.2 Western blot

Proteins in cell or tissue lysates were reduced and denatured by boiling samples for 5 minutes at 95^{o}C in Laemmli buffer (60 mM Tris pH 6.8, 2% SDS, 10% glycerol, 5% β-mercaptoethanol, 0.01% bromophenol blue). A 10% Acrylamide gel was made up as shown below.

Reagent	Volume
Distilled Water	4.00mL
1.5M Tris-HCl pH 8.8	2.5mL
30% Acrylamide/bis (Biorad)	3.3mL
10% SDS (Biorad)	100µL
10% Ammonium persulfate (Sigma)	100µL
TEMED (Sigma)	4µL
Total Volume	10mL

Table 6 - Western blot running gel

Reagent	Volume
Distilled water	6.8mL
0.5M Tris-HCl pH 6.8	1.7mL
Acrylamide/Bis 30%	1.25mL
10% SDS	100µL
Ammonium persulfate (10%)	100µL
TEMED	10µL
Total Volume	10mL

Table 7 - Western blot stacking gel

Samples were loaded into the gel and protein was separated by size by running at 100V for 20 minutes followed by 140V for an hour in running buffer (3.03 g Tris base, 14.4g glycine, 1 g SDS and Mili-Q H_20 up to 1 L). A Spectra Broadrange protein ladder molecular weight marker (Biorad) was loaded alongside the samples. Protein was transferred from the gel onto a methanol activated PVDF membrane (Merck-Milipore) in transfer buffer (Glycine 14.4g, Tris base 3.03g and Mili-Q H_20 up to 1 L) at 100 V for 70 minutes on a Criterion Blotter (Biorad). The membrane was blocked with 5% skimmed milk powder in tris buffered saline (TBS) (20mL 1M Tris pH 7.5, 8g NaCl and Mili-Q H_20 up to 1 L) Tween-20 (0.075%) for 1 hour. Primary antibody for LDLR (ab30532, Abcam) or HMGCR (ab98018) was diluted in 5% skimmed milk in TBS-Tween 20 at 1.5 µg/mL and incubated with the membrane overnight at 4^{o}C. β-Actin (ab8227, Abcam) was used as a housekeeper and incubated with the membrane using the same conditions as the LDLR antibody. Membrane was washed in TBS-Tween 20 before 1 hour incubation with a horseradish peroxidase (HRP) -conjugated goat anti-rabbit secondary antibody (Biorad). Membrane was washed again in TBS-Tween 20 and then developed using Immobilon Western chemiluminescent HRP substrate onto film. Quantification was performed using Image J software.

2.8 HMG-CoA Reductase activity assay

HMG-CoA Reductase activity was assessed using a HMG-CoA Reductase Assay Kit (Sigma) as per manufactures instructions. The assay measures the activity of HMG-CoA Reductase indirectly by a spectrophotometric measurement of the decrease in absorbance at 340nm, which represents the oxidation of the cofactor NADPH by the catalytic subunit of HMG-CoA Reductase in the presence of HMG-CoA, as detailed in the figure below.



Figure 7- Enzymatic reaction involving HMG-CoA Reductase

NADPH, HMG-CoA and HMG-CoA Reductase were all added to the provided assay buffer along with the compounds to be tested. Pravastatin is provided as a positive control. Absorbance at 340nm was read on a Synergy HT microplate reader at 37ºC every 20 seconds for 15 minutes.

2.9 Squalene Synthase activity assay

Squalene synthase activity was assessed as first described by (Amin *et al.* 1992). Each assay was in 1 mL assay buffer (50mM phosphate buffer, pH 7.4 containing 10mM $MgCl_2$) containing 0.5mM NADPH, 12 µg of human liver microsomes and compound or vehicle (DMSO) alone in 16x100mm glass screw cap tubes. All components were allowed to equilibrate for 10 minutes at 37ºC before addition of radiolabelled [^{3}H]-FPP (50nM 0.045 Ci/mmol, Perkin Elmer). The reaction was left for 10 minutes and then halted with 1 mL of 15% KOH dissolved in EtOH. Tubes were incubated at 65ºC for 30 minutes before addition of 5 mL of petroleum ether and shaken for 10 minutes. The lower aqueous phase was frozen and the upper organic phase containing squalene was transferred to clean glass tubes containing 2mL distilled water. 1.5mL of the upper organic phase was removed and counted with 3mL of scintillation liquid on a Tri-Carb 2800 TR Liquid Scintillation Analyzer.

2.10 Animal husbandry, breeding and experimental procedures

Maintenance of animals and animal experiments were carried out in accordance with the UK Home Office regulations under the Animals (Scientific Procedures) Act (ASPA) of 1986. Animals had access to food and water ad libitum unless required otherwise for testing conditions. All mice were fed a chow diet unless stated otherwise (Global 16% Protein Rodent Diet, TD.2016, Harlan-Teklad). Mouse holding rooms were constantly maintained at 22°C and 60 – 70% humidity, with a regular 12 h light-dark cycle. Animals were sacrificed using terminal anaesthesia and death was confirmed by perfusion fixation or terminal withdrawal of blood from the vena cava. $Ldlr^{-/-}$ mice (on a mixed C57BL/6 and 129 genetics background, stock number: 2077) were obtained from Jackson Laboratories (Bar Harbor, ME), and maintained as a homozygous knockout colony. Male MF-1 and CD-1 mice were ordered in from Charles River between 21-25g. Four studies using diet intervention are presented here. In study I, male $Ldlr^{-/-}$ mice (8-10 weeks old, n = 5-6/group) or C57BL/6J mice were fed either a 1% (TD.02127) high cholesterol (HC) or regular chow (RC) diet for 12-weeks. Plasma was collected 0, 4, 8 and 12 weeks after diet intervention for plasma lipid analysis of diet intervention and mice were euthanized at 12-weeks for atherosclerotic analysis. In study II male $Ldlr^{-/-}$ mice (8-10 weeks old, n = 5-6/group) were fed either 0.5% (TD.140399) or 0.25% (TD.140633) HC-diet or RC-diet for 8 weeks. Plasma was collected at 0, 2 and 8 weeks of diet intervention and mice were euthanized at 8-weeks for atherosclerotic analysis. In Study III, the effect of pLDLR-LDLR-miR82 was evaluated in male $Ldlr^{-/-}$ mice (8-10 weeks old, n = 6/group) fed a 1% HC diet described above. Male $Ldlr^{-/-}$ mice were fed the 1% HC-diet for 2 weeks prior to initiation of plasmid treatment. 50 µg of pLDLR-LDLR, pLDLR-LDLR-miR82 or pLDLR-LDLR-miRNT were then administered hydrodynamically via the tail-vein. Plasma was obtained 0, 2 and 4 weeks post-injection and analysed for lipid levels. All mice were euthanized 4 weeks post-injection for protein expression analysis. In Study IV, male $Ldlr^{-/-}$ mice (8-10 weeks old, n = 8-12/group) had 50 µg (a dose determined previously8) of either pEHZ, pLDLR-LDLR, pLDLR-LDLR-miR82 or pLDLR-LDLR-miRNT delivered hydrodynamically via the tail-vein. On the same

day the mice were switched onto a 0.25% HC-diet for 12-weeks. Plasma was taken at day 2 and 2, 6 and 12 weeks post vector delivery, before animals were euthanized and tissue harvested for subsequent analysis.

2.11 Pharmacokinetic measurement of compounds in mouse plasma

2.11.1 Preparation of compounds for delivery

Pharmacokinetic properties of Compound 40 were assessed with different vehicles. Compound 40 was first dissolved in DMSO and then diluted down in the following vehicles as listed in the table below. Rounds of heating and vortexing were often needed for complete solubilisation.

Vehicle	Components
1. β-Cyclodextrin	60% 2-Hydroxypropyl-β-Cyclodextrin (Sigma)
	PBS
2. PEG-400	40% PEG-400 (Sigma)
	10% Solutol (Sigma)
	5% EtOH
	PBS
3. PEG-400 (2)	30% PEG-400
	20% Solutol
	10% Kolliphor EL
	PBS
4. PEG-400 (3)	15% PEG-400
	Corn Oil
5. Kolliphor EL	15% Kolliphor EL
	Corn Oil

Table 8 - List of vehicles used to dissolve Compound 40

Compound 15a was first dissolved in DMSO then diluted in PBS for all dosing studies.

2.11.2 Dosing and collection of samples

MF-1 male mice were administered with Compound 40, Compound 15a or vehicle via the intraperitoneal route. Mice were then euthanized at 5, 10, 30, 180 and 360 minutes post compound delivery and whole blood was taken via the Vena Cava. Blood was stored on ice until being spun at 3000xg for 15 minutes at 4^{o}C to remove red blood cells. Plasma layer was then removed and stored at -80^{o}C for HPLC analysis.

2.11.3 HPLC analysis of compounds in plasma

For each run a standard curve was made up whereby known concentrations of Compound 40/15a where spiked into untreated mouse plasma for preparation alongside the unknown samples. Acetonitrile (Sigma) was added to each sample in a 1:8 ratio, samples were shaken for 15 minutes, before being spun at 13,000rpm for 15 minutes at 4^{o}C. 200 µL of the supernatant was run on a Waters 600 controller HPLC machine (Waters) with a C18 reverse phase column (Waters). A linear gradient mobile phase of 20:1 H2O with 0.1% TFA: Acetonitrile with 0.1% TFA rising to 1:20 H2O with 0.1% TFA: Acetonitrile with 0.1% TFA over 10 minutes at a flow rate of 1.5mL/min was used to elute the compounds. A standard curve was generated and concentrations were determined based on the area under the curve (AUC) of the peak.

2.12 Vector cloning

2.12.1 Miniprep

Kanamycin (15 µg/mL) and Ampicillin (100 µg/mL) were added to 1.5mL of LB broth. A DMSO stock of the required plasmid was inoculated into the culture and grown overnight in a shaker at 37^{o}C. A QIAprep miniprep kit (Qiagen) was used to purify plasmid DNA from the bacterial prep. Bacteria were pelleted with centrifugation at 8000rpm for 3 min, all steps carried out at room temperature. The pellet was resuspended in 250 µL of buffer P1. To lyse the cells 250 µL of buffer P2 was added, tubes inverted and the reaction stopped by addition of 350 µL of buffer N3. The resulting solution was centrifuged for 10 minutes at 13,000rpm and the supernatant added to a QIAprep spin column. All resultant centrifuge steps were carried out at 13000rpm for 1 minute. Column was spun, flow through

discarded and 500 µL of buffer PB was added to the column. This process was repeated with the addition of 750 µL of buffer PE, flow through discarded and column re-spun to air dry. Spin column was placed in a DNase free 1.5mL Eppendorf, 30 µL of buffer EB (Pre-heated to 70ºC) was pipetted onto column membrane and left to stand for 2 minutes. DNA was eluted by centrifugation and quantified on a Nanodrop Spectrophotmeter-1000.

2.12.2 Endotoxin free megaprep

Large amounts of endotoxin free plasmid were prepared using the EndoFree Plasmid Mega Kit (Qiagen). 500mL LB broth cultures containing Kanamycin (15 µg/mL) and Ampicillin (100 µg/mL) were inoculated with a DMSO stock of the required plasmid. and cultured overnight in a shaker at 37ºC. Bacteria were harvested by centrifugation at 6000xg for 15 minutes at 4ºC. Pellet was resuspended in 50 mL buffer P1 and lysed with 50 mL buffer P2 for 5 minutes. The reaction was halted by addition of 50 mL buffer P3 and poured onto a QIAfilter cartridge for a 10 minute incubation. Lysate was pulled through the filter by vacuum, followed by 50 mL of buffer FWB2. 12.5 mL Buffer ER was added to the filtered lysate, inverted and left on ice for 30 minutes. Qiagen-tip 2500 was equilibrated with 35 mL buffer QBT before the lysate was added. The membrane was washed with 200 mL buffer QC and the DNA eluted with 35 mL buffer QN into endotoxin free 50 mL falcon tubes (Corning). DNA was precipitated through addition of 24.5 mL isopropanol and spun at 4665xg for 1 hour at 4ºC. The supernatant was decanted and the DNA pellet washed in 7 mL endotoxin-free 70% EtOH. The DNA was spun at 4665xg for 1 hour at 4ºC and once more the supernatant decanted. The pellet was air-dried for 30 minutes before being resuspended in 500 mL of dH_2O. DNA was quantified on a Nanodrop Spectrophotmeter-1000.

2.12.3 Restriction digest of plasmids

To confirm plasmid identity before transfection or hydrodynamic delivery a restriction digest was performed. A reaction made up of restriction enzyme (NEB) 1 µL, appropriate NEB buffer 5 µL, 10 µL of plasmid and DNA and 34 µL of dH_2O was incubated at 37ºC for 1 hour.

2.12.4 Agarose gel electrophoresis

Agarose gels were prepared in 1x Tris-borate EDTA (TBE) (Sigma) at a concentration of 0.7 (w/v). The mix was heated in a microwave until the agarose was dissolved. Ethidium bromide (Sigma) was added at a concentration of 5 mg/mL and the gel was set. Sample 6x loading buffer (1.5 g Ficoll 400, Orange G dye and dH_2O up to 10 mL) was added to each sample from the restriction digest and loaded into the set gel. Gene ruler 1kb plus (Thermofisher) was loaded alongside samples for size quantification. Electrophoresis was performed using a Sub-Cell GT gel electrophoresis system (Bio-Rad) with a covering volume of 1x TBE. Gels were imaged on a GelDoc XR system (Biorad).

2.13 *In vivo* luciferase activity assay

2.13.1 Hydrodynamic delivery

Mice weighing between 18-35 g received hydrodynamic tail-vein injections of plasmid DNA as described(Liu, Song and Liu 1999). Animals were anaesthetized with isoflurane and body temperature was maintained using a heating pad. 50 µg of plasmid DNA was resuspended in TransIT-EE Hydrodynamic Delivery Solution (Mirus), to a total volume equivalent to 10% of the mouse's total body weight. Delivery of the plasmid was administered via the tail-vein with an injection time between 8-11 seconds depending on the weight of the mouse. Animals were allowed to recover and left for the appropriate amount of time before sacrifice.

2.13.2 Luciferase imaging

Mice 5 days post hydrodynamic delivery had 150 µL of a 15mg/mL $_D$-Luciferin solution delivered via the intraperitoneal (I.P) route, before being anaesthetized using Isoflurane. Following a 5 minute incubation period, mice were placed inside the chamber of an IVIS-100 luciferase imaging camera (Caliper Life Sciences) and imaged with a 2 minute exposure time. Mice were dosed 8, 24 and 32 hours after acquiring the baseline image with either Compound 40 (40mg/kg), vehicle alone or Pravastatin (600mg/kg), an uninjected group was also included as a control. 48 hours on from the first image the mice were imaged under the exact same conditions as before. Images were analysed using LivingImage software (Caliper Life Sciences).

2.14 Plasma analysis of lipids and proteins

Blood was collected via the tail-vein in studies I, II and III and via the saphenous vein in study IV using Microvette 300 capillary tubes (Sarstedt) at designated time points. Capillary tubes were spun at 2,500g for 5 minutes for plasma collection. Plasma concentrations of total cholesterol, HDL-cholesterol, LDL-cholesterol, triglycerides (TG) and liver enzyme (ALT, alanine aminotransferase, AST, aspartate aminotransferase) were measured with an Olympus AU400 automated clinical chemistry analyser equipped with an ion selective electrode by Harwell, MRC, Oxford, UK.

2.15 Immunohistochemistry

2.15.1 Fixation and processing of heart and liver samples

Mice were perfused with PBS and the right median liver lobe sections and whole heart were excised. Mouse heart and liver were fixed in 4% paraformaldehyde (PFA) and kept at 4^{o}C. For paraffin embedding, hearts were cut parallel to and below the atria. Tissue was processed through a series of dehydration steps overnight as indicated by the table below using a Leica TP1020 tissue processor (Leica). Paraffin wax was heated to 58^{o}C.

Solution	Time (hours)
70% EtOH	1
95% EtOH	1
100% EtOH	1.5
100% EtOH	1.5
100% EtOH	2
Histoclear	1
Histoclear	1
Paraffin wax	1
Paraffin wax	1

Table 9 - Dehydration of tissue samples for paraffin embedding

Heart and liver samples were paraffin embedded in 40.1 x 28.5 x 6.5 mm cassettes using a EG1150 (Leica) tissue embedder and left to set. 7 µm sections were cut serially throughout the liver section on a Leica RM2155 (Leica). The

heart was cut parallel to the atria, starting nearest the apex going towards the aorta. Sections were collected once all three cusps of the aortic valve were present. All tissue sections were mounted on Polysine slides (Thermo Scientific).

2.15.2 Immunofluorescent detection of LDLR

Samples were rehydrated as listed in the table below

Solution	Time (minutes)
Histoclear	5
Histoclear	5
100% EtOH	1
100% EtOH	1
96% EtOH	1
96% EtOH	1
70% EtOH	1
70% EtOH	1

Table 10 - Rehydration of paraffin embedded samples for immunofluorescence

Samples were submersed in PBS-Tween 20 (0.075%) ready for antigen retrieval. Antigen retrieval was performed using antigen retrieval buffer (ab93678) and slides were heated in a steamer for 20 minutes. Endogenous peroxidase was quenched by incubating slides in peroxidase blocking solution (3% H_2O_2 in PBS) for 5 minutes. All steps where now carried out in a humidity chamber. Sections were washed twice in PBS, outlined using a hydrophobic pap-pen and blocked in 1% blocking solution (10mg/mL BSA in PBS/Tween 20 (0.075%)) for 2 hours at room temperature. LDLR primary antibody (ab134998) at 1µg/mL in 1% BSA blocking solution was pipetted on with one section on each slide used as a control receiving 1% blocking solution. Primary antibody was incubated for overnight at 4ºC in a humidity chamber. Sections were washed in PBS-Tween 20 (0.075%) three times and HRP-conjugated goat anti-rabbit secondary antibody (1 µg/mL in 1% blocking solution) (T20922, Thermofisher) was incubated on the slides for 1 hour at room temperature. Slides were washed in PBS-Tween 20 (0.075%) three times. Tyramide (T20922, Thermofisher) was prepared as per manufactures instructions, diluting tyramide 1:100 in tyramide amplification buffer (0.0015%

H_2O_2) and added to slides for 5-10 minutes. The sections were further washed in PBS-Tween 20 (0.075%) and counterstained with 4',6-diamidino-2-phenylindole (DAPI) nuclei stain. A stock vial of DAPI containing 0.025mg at 5mg/mL was spiked into a staining chamber and left on a rocker for 5 minutes. The slides were washed in PBS-Tween 20 (0.075%) three times and mounted using Floursave mounting media (Calbiochem). All samples were protected from light until imaged using a EVOS™ FL auto, fluorescence microscope.

2.15.3 Immunohistochemical detection of Galectin-3

Aortic root sections containing all three cuspids of the aortic valve were rehydrated as shown in Table 7. Sections were outlined using a hydrophobic pap-pen and all steps were carried out in a humidity chamber. Serum free protein block (DAKO) was used to block samples for an hour at room temperature. Galectin-3 primary antibody (1 µg/mL in PBS) (AF1197, R&D Systems) was used to stain sections for 2 hours at room temperature. Sections were then washed in PBS three times and a biotinylated rabbit anti-goat secondary antibody (1:200 in PBS) (Vector BA-5000) was applied for 1 hour at room temperature. After secondary incubation all slides were washed in PBS three times and incubated in ABC-AP solution (Vector AK-5000) prepared according to the manufacturer's instructions for 30 minutes at room temperature. Solution was tapped off and slides washed in PBS followed by Tris- HCL 100 mM (pH 8.2). Vector red alkaline phosphatase substrate in Tris-HCL 100 mM pH 8.2 (Vector laboratories SK-5100) was added to each sample, colorimetric development was monitored and substrate was removed 5-15 minutes after application. Slides were washed once more in Tris- HCL 100 mM (pH 8.2) followed by distilled H_2O. All samples were dehydrated in reverse order to rehydration as outlined in table 7. Slides were mounted with Neo-Mount (Merck) and imaged using a coolSNAP-pro camera, Leica DMRBE microscope (Leica). Image Pro-Plus was used for quantification.

2.16 Aortic root plaque size analysis

Three aortic root sections containing all three cuspids of the aortic valve and at least 80 µm apart were rehydrated as shown in Table 7. Samples were then stained as indicated in the table below.

Solution	Time (minutes)
Weigert's iron hematoxylin	10
Running tap water	10
1% Acetic acid (in dH_2O)	0.5
Biebrich scarlet acid fuchsin	5
1% Acetic acid (in dH_2O)	0.5
Phosphotungstic acid	10
1% Acetic acid (in dH_2O)	0.5
Light Green SF	2
1% Acetic acid (in dH_2O)	0.5

Table 11 - Masson trichrome staining

Samples were dehydrated by following the reverse order to rehydration as outlined in table 7 and mounted using Neo-Mount (Merck) and imaged using a coolSNAP-pro camera, Leica DMRBE microscope. Image Pro-Plus was used for quantification.

2.17 Oil red-O lipid staining

2.17.1 En face aorta plaque analysis

The entire aorta from the aortic root to the femoral bifurcation was dissected from the mouse and fixed in 4% PFA and kept at 4^{o}C. The outer fat and adventitia was removed before staining and the aorta was rinsed briefly in 60% aqueous tri-ethyl phosphate. Oil red-O (0.5% Oil red O in 60% aqueous tri-ethyl phosphate) was filtered before use and used to stain whole aorta for 10 minutes. Aortas were washed in 60% aqueous tri-ethyl phosphate 1-2 times before being washed in dH_2O. Each aorta was cut along the arch on one side and along the total aorta on the other side and pinned out on paraffin. Aortas were photographed on a coolSNAP-pro camera, Leica DMRBE microscope and lesion size quantified using Image Pro Plus.

2.17.2 Fixation and processing frozen liver samples

Mice were perfused with PBS and the caudate liver lobe section was excised. Liver was washed in PBS and sequentially submerged in 10, 20 and 30% sucrose solutions. Tissue was suspended in specimen blocks with OCT solution (Tissue

Tek) and snap frozen using liquid nitrogen. Frozen tissue was sectioned on a CM 1900 Cryostat (Leica) at a 12 µm thickness and collected on Polysine slides.

2.17.3 Oil red-O staining on frozen liver sections

Sections were fixed in ice cold 4% PFA for 10 minutes and rinsed in dH2O. The slides were left to air dry and placed in 100% propylene glycol for 5 minutes. Samples were stained with Oil red-O (0.5% Oil red O in 60% aqueous tri-ethyl phosphate) for 1 hour at room temperature. Slides were washed in 85% propylene glycol for 5 minutes and rinsed twice in dH_2O. Liver sections were co-stained with Mayer's Heamatoxylin (DAKO), dunking the slides in for 2-3 seconds twice before washing them thoroughly in running tap water for 3 minutes. Slides were placed in dH_2O and mounted with Fluorsave mounting media.

2.18 Plasmid rescue assay

2.18.1 Isolation of total DNA from liver

Frozen caudate liver lobe tissue was isolated from the mouse and snap frozen in liquid nitrogen. Total DNA was isolated using a GenElute Mammalian Genomic DNA Purification Kit (Sigma) as per manufactures instructions. Liver tissue was lysed in 200 µl of Lysis Solution T with Proteinase K (2mg/mL) at 55ºC. RNase A solution was added after lysis and incubated for a further 2 minutes. 200 µL of Lysis Solution C was added to complete the lysis and samples were vortexed thoroughly and left to incubate at 70ºC for 10 minutes. 500 µL of the Column Preparation Solution was added to each GenElute Miniprep Binding Column and centrifuged at 12,000 x g for 1 minute. To prepare DNA to bind to column, 200 µL of 100% EtOH was added to the lysate before it was added to the column and centrifuged at 6500 x g for 1 minute. 500 µL of Wash Solution was added to the binding column and centrifuged for 1 minute at ≥6,500 × *g*. A further 500 µL of Wash Solution was loaded onto the column and centrifuged for 3 minutes at 12,000 x g. DNA was eluted with 400 µL of the Elution Solution, first incubated on the membrane of the column for 5 minutes and then spun for 1 minute at 6,500 × *g.* DNA was quantified on a Nanodrop Spectrophotmeter-1000. In some cases lysate was put through a QIAprep spin column and plasmid DNA was further isolated as described in section 2.12.1.

2.18.2 Electrocompetent cells

10-beta Electrocompetent E. coli (New England Biolabs) were grown overnight in 1.5 mL bacterial cultures at 37ºC in a shaker. Cultures were diluted in 100 mL of LB broth and grown further until an optical density at 600nm had reached 0.3 – 0.5. After a 20 minute incubation on ice each culture was pelleted by centrifugation at 4,500 x g for 15 minutes at 4°C. The pellet was washed three times with 100 ml ice-cold autoclaved 10% glycerol with centrifugation at 6,750 x g for 15 minutes at 4°C between each wash. The pellet was resuspended in the residual 10% glycerol left over in the tube from the last wash. The cells were divided into 50 µl aliquots and snap-frozen on dry ice then stored at - 80°C.

2.18.3 Electroporation of DNA into electrocompetent cells

10-beta Electrocompetent E. coli, cuvettes and DNA were thawed and kept on ice. 50 µL of bacteria and 5 µL of DNA were mixed and pulsed under the following conditions using a Bio-rad Gene Pulser (Bio-rad)..

Cuvette electrode gap – 0.1cm

Voltage – 1,800 Volts

Capacitance – 25 µFaradays

Internal resistance – 200 Ohms

Immediately after applying the electroporation pulse 380 µL of S.O.C medium (New England Biolabs) was added and all transferred to a mini-prep growth tube. The bacteria were incubated for 1 hour at 37ºC in a shacking incubator. After incubation the entire volume was plated out on a 14cm LB agar dish containing Kanamycin (15 µg/mL) and Ampicillin (100 µg/mL).

2.18.4 Plasmid rescue

Bacterial colonies were picked from culture plates and plasmid DNA was isolated as described in section 2.12.1. Isolated DNA was then digested as described in section 2.12.3 using the restriction enzyme AfeI (New England Biolabs). DNA was then visualized on an agarose gel as described in section 2.12.4.

2.19 **Statistical analysis**

All experimental data presented in this study are expressed as mean values ± standard deviation (SD) for experiments with an n<5 and standard error of the mean (SEM) for experiments with an n≥5. Each n number equals a biological replicate which has been carried out as two technical replicates for each *in vitro* assay or as a single animal for all *in vivo* studies. Paired student-t-test, One-Way Anova analysis, followed by Dunnetts post-test comparison and Two-Way Anova analysis, followed by Dunnetts post-test comparison were calculated using GraphPad Prism version 5.02 (Graphpad Software, San Diego, CA). Differences were considered statistically significant at $P \leq 0.05$ and each statistical test used is indicated in each figure legend.

Chapter 3: Identification of a novel series of small molecules able to upregulate the low-density lipoprotein receptor

3.1 Introduction

3.1.1 The need for further small molecules able to upregulate the low-density lipoprotein receptor

Since the approval of statins in the 1980s (Endo 2010), many other therapeutic approaches have been worked on to upregulate the LDLR through alternative mechanisms. These include interacting with SCAP and the transcription factor regulating the LDLR, SREBP-2 (Ochiai *et al.* 2015), extending the half-life of the LDLR mRNA (Kong *et al.* 2004), inhibiting proteasome degradation of the LDLR (Yan *et al.* 2014) or inhibiting other enzymes in the cholesterol biosynthesis pathway (Ness, Zhao and Lopez 1996). The drive to discover agents to further upregulate the LDLR comes from the success of statins, which remain the primary therapeutic used to decrease cardiovascular events. In fact, only therapeutics which lower LDL-cholesterol have shown any efficacy in lowering cardiovascular incidents and so remain the only sure strategy to produce a therapeutic which will have a real clinical benefit.

The PCSK9 inhibitor trials demonstrated that additional LDLR upregulation, on top of what can be achieved under maximal statin dose had clear benefits in terms of LDL-cholesterol lowering and cardiovascular outcomes (Robinson *et al.* 2015). There are, of course, many hurdles posed by delivery of monoclonal antibodies to a large population of patients (discussed in section 1.6.4.4), with a small molecule that can be easily taken daily alongside the patient's statin still an ideal combinatorial therapy. HeFH patients will take high doses of statins and other lipid lowering medication to reach their strict LDL-cholesterol goals. By having additional small molecules or biologics included in a treatment plan, lower doses of each therapeutic can be used to reach the same lipid goal, helping to reduce side-effects and increase compliance.

3.1.2 Potential mechanisms underlying the side effects of statins

The rate of side effects seen in statin treated patients is a fiercely debated topic and can depend on what is classed as a side-effect (discussed in section 1.6.4.1). Many large random controlled trials reported myopathy, only if it was muscle pain accompanied by an elevation in creatine kinase plasma elevations greater than 10 times the upper limit of normal (ULN) (Collins *et al.* 2007). These studies reported the incidence of side effects to be around 1.5-5%, however other trials reporting compliance to statins due to any kind of muscle pain, reported the adherence to be within 50% after 5 years (Avorn *et al.* 1998) and even lower in elderly patient populations (Benner et al. 2002). The precise mechanisms behind statin induced myopathy are unknown but prominent theories will be discussed.

3.1.2.1 Genetic causes of statin side effects

Polymorphisms in the gene *SOLC1B1* have been associated with simvastatin induced myopathy (SEARCH Collaborative Group *et al.* 2008), with an odds ratio for increased risk of 4.5 for heterozygous and 16.9 for homozygous carriers. *SOLC1B1* codes for the protein, organic anion transporting polypeptide 1B1, a transporter shown to be responsible for the hepatic uptake of simvastatin. Lipophilic statins such as Atorvastatin which diffuse into hepatocytes are not associated with the muscle side effects in patients carrying these polymorphisms (Santos *et al.* 2012). The polymorphisms most likely result in an imbalance of the hepatic uptake of the hydrophilic statins and increased accumulation in muscle tissue (Neuvonen, Niemi and Backman 2006). In fact, a recent study overexpressed organic anion transporting polypeptide 1B1 in muscle cells *in vitro*, which caused an increase in accumulation of the statin in the cells and cytotoxicity (Knauer *et al.* 2010). The genetic findings here provide evidence that the statins themselves cause the side effects with alterations in uptake resulting in increased incidence of side effects, however the exact mechanism is probably not down to a single genetic disposition.

3.1.2.2 Metabolic causes of statin side effects

3.1.2.2.1 Depletion of ubiquinone leading to mitochondrial dysfunction

Statins not only inhibit the production of cholesterol, but as seen in Figure 6, the production of other isoprenoid molecules produced from the mevalonate pathway

including Ubiquinone (Coenzyme Q10). Ubiquinone is a component of the mitochondrial electron transport chain during oxidative phosphorylation, thus a lowering of Ubiquinone could theoretically cause a disruption of mitochondrial respiration. A study where muscle biopsies were taken from patients on high dose statins which presented with muscle related pain unveiled findings consistent with mitochondrial dysfunction, including increased intramuscular lipid, diminished cytochrome oxidase staining, and ragged red fibres (Phillips *et al.* 2002). Discontinuation with the statin resulted in reversal of the muscle phenotype in future biopsies. Other studies have not found a link between elevated creatine kinase levels and mitochondrial dysfunction (Lamperti *et al.* 2005) though decreased mitochondrial DNA in skeletal muscle has been reported with statin use (Schick *et al.* 2007). Supplementing with Ubiquinone has produced mixed results, with one study showing a 40% decrease in pain severity and interference (Caso *et al.* 2007) with another finding no difference (Young *et al.* 2007). As no muscle biopsies were performed in these studies, no quantification of whether the Ubiquinone supplementation actually increased muscle concentrations can be determined. Therefore, it is difficult to conclusively determine the impact of Ubiquinone on muscle related side effects, though it does appear it may play a role.

3.1.2.2.2 Depletion of farnesyl pyrophosphate and geranylgeranyl pyrophosphate.

FPP and GPP are lipid attachment molecules that constitute key intermediates for post-translational events of several cell signalling proteins, including the small GTPase family members Ras, Rac, and Rho (Gazzerro *et al.* 2012). These GTPases play a diverse role in many cellular processes including maintenance of cell shape, motility, factor secretion, differentiation, proliferation and apoptosis. Activation of these GTPases is dependent on the attachment of FPP or GPP known as isoprenylation. The application of statins to human muscle cells has been shown to induce apoptosis, an effect which could not be seen with the addition of squalene synthase or epoxidase inhibitors (Sirvent, Mercier and Lacampagne 2008). Squalene synthase and epoxidase are downstream of the synthesis of FPP and GPP in the cholesterol biosynthesis pathway (Figure 6), suggesting that the effect was not due to blocking of cholesterol biosynthesis itself but the synthesis of isoprenoid intermediates. *In vitro* studies have demonstrated

that the addition of statins can cause increased autophagy, with the increase paralleled by the degree of HMGCR inhibition (Araki, Maeda and Motojima 2012). The increase in autophagy progressed to an increase in cell death which and could be reversed by the addition of mevalonate, polyisoprenoid diphosphates or GPP.

Other studies in rat skeletal muscle cells showed inhibition of protein synthesis and morphologic changes when a statin was added to the culture, with no such changes occurring when a squalene synthase inhibitor was used. Once again, the cellular phenotype could be rescued by the supplementation of FPP and GPP to the cells (Flint *et al.* 1997). The Ubiquitin proteasome pathway is a major governor of skeletal muscle architecture. Statins cause an upregulation of proteins in this pathway, namely atrogin-1 which is associated with muscle atrophy and wasting (Di Stasi *et al.* 2010). Just as the beneficial pleiotropic effects of statins are thought to arise from decreases in these molecules, so are the side-effects, as these molecules play a diverse role in many cellular processes, it is unsurprising that this is the case.

3.1.3 Squalene synthase

Squalene synthase (SQS) is an enzyme in the cholesterol biosynthesis pathway and is the first committed step in cholesterol synthesis (Figure 6). Squalene synthase is a 416 amino acid, 47 kDa protein that resides on the endoplasmic reticulum, anchored by its C-terminus (Pandit *et al.* 2000). The catalytic N-terminus faces out into the cytosol, where it can accept two water soluble FPP molecules and release lipophilic squalene to the membrane of the endoplasmic reticulum (Stamellos *et al.* 1993). The reaction involves the conversion of two molecules of FPP, which bind sequentially with different affinities to two binding sites in the active site of SQS to from pre-squalene diphosphate (Tansey and Shechter 2000a). It is thought the pre-squalene diphosphate remains bound to SQS, where a conformational change in SQS then allows NADPH to reduce pre-squalene diphosphate and release squalene (Radisky and Poulter 2000). This reaction is a key regulatory step in cholesterol biosynthesis as FPP is the substrate for at least five other enzymes, SQS therefore controls the fate of FPP

either directing for sterol or non-sterol isoprenoid synthesis (Goldstein and Brown 1990).

Like many of the enzymes in the cholesterol biosynthesis pathway, SQS is regulated by the intracellular sterol concentration through the SREBP transcription family. Unlike HMGCR, SQS has binding sites for SREBP-1a, a transcription factor involved in triglyceride production (Tansey and Shechter 2000b), as well as SREBP-2.

3.1.4 Squalene synthase inhibitors as hypocholesterolaemic agents

SQS has been an attractive drug target for hypercholesterolaemia for a number of years (Poulter *et al.* 1989), as inhibition causes an upregulation of the LDLR, without inhibiting other isoprenoid intermediates of the mevalonate pathway. The first line of SQS inhibitors (SSIs) were the bisphosphonates, which were shown to be able to inhibit purified SQS and cholesterol biosynthesis in rat hepatocytes (Amin *et al.* 1992). Since then, many academic groups and private pharmaceutical companies have published SSIs that upregulate the LDLR and cause lipid lowering in many different animal species, including canines, non-human primates, rabbits and hamsters (Harwood *et al.* 1997; Ugawa *et al.* 2000; Nishimoto *et al.* 2003a). The SSIs have shown equal or greater lipid lowering in these models compared with statins and were able to reduce atherosclerotic progression in a cholesterol fed rabbit model (Tavridou *et al.* 2007). Interestingly, SSIs have been shown not only to inhibit cholesterol biosynthesis but also triglyceride production, giving an added benefit over statins (Ugawa *et al.* 2002). The complexity of inhibiting this pathway at two separate points was unveiled through a microarray study looking at orthalogs gene expression on hepatocellular physiology after addition of either a statin or SSI (Rondini *et al.* 2016). The study found SSIs independently influence 90 orthalogs, with many involved in lipid metabolism driven by PPARα, providing evidence to explain why SSIs may have a dual therapeutic effect in reducing triglycerides.

SSIs result in an accumulation of FPP, which was thought to be safer than the accumulation of other metabolites seen with statins, due to FPP being water soluble and the substrate for other metabolic pathways (Do *et al.* 2009). Humans that were given a squalene synthase inhibitor for 4 weeks had an increase in doic

acid (a metabolite of FPP) in their urine, providing evidence the body could cope with a build-up of FPP (Sharma *et al.* 1998). Atorvastatin induced myotoxicity in human muscle skeletal cells was actually reduced with the addition of a squalene synthase inhibitor, hypothesised to be due to an increase in FPP and GPP (Nishimoto *et al.* 2003b). Addition of either a squalene synthase inhibitor or FPP and GPP to rat skeletal cells is able to ameliorate statin induced changes in protein synthesis ([3H]leucine incorporation), total cellular protein (a measure of cell loss), intra and extracellular lactate dehydrogenase activity (a measure of membrane integrity), and cell morphology (Flint *et al.* 1997).

The most promising SSI to date has been TAK-475 which demonstrated significant lipid lowering in animal models of hypercholesterolaemia, including the $Ldlr^{-/-}$ mouse, alluding to an additional LDLR independent mechanism of action (Amano *et al.* 2003). TAK-475, called Lapaquistat acetate when delivered in man was taken through to Phase II/III clinical trials (n=6151 study participants) (Stein *et al.* 2011). Lapaquistat gave a dose dependent decrease in LDL-cholesterol of 18.3 (50mg) and 23.4% (100mg) when administered as a monotherapy and 13.9 (50mg) and 19.1% (100mg) in additional lipid lowering when administered with a statin. An HeFH patient population also received Lapaquistat, these patients were on maximum dose statins, with Lapaquistat delivering an additional 16.4% LDL-cholesterol lowering compared with placebo. Lapaquistat consistently reduced mean non–HDL-cholesterol, total cholesterol, ApoB, and VLDL-cholesterol levels and median triglycerides relative to placebo, in all study arms.

No difference in muscle related side effects associated with creatine kinase increases were reported with Lapaquistat, compared with placebo or a statin. The incidence of adverse events leading to withdrawal was fairly similar for all treatment groups, with the statin monotherapy group being slightly lower overall. The statin dose of 10mg Atorvastatin is lower than doses reported to cause an increase of adverse events, which may explain this finding (Illingworth *et al.* 2001). Lapaquistat was withdrawn from clinical trial due to 2 out of 5100 patients experiencing hepatotoxicity. It was never investigated whether the hepatotoxicity was a result of Lapaquistat acetate itself or the inhibition of squalene synthase.

To try and address this a squalene synthase knockout mouse has been generated (Nagashima *et al.* 2015). A modest transient liver injury was seen in this mouse with a 100% decrease in squalene synthase activity, thought to be a build-up of the squalene synthase substrate farnesyl diphosphate (FPP). Treatment with a statin should alleviate this build up, similar to what was seen using this combination to prevent non-sterol isoprenoid depletion associated with statins (Wasko *et al.* 2011).

3.1.5 A compound screen to identify novel molecules which upregulate the low-density lipoprotein receptor

Previously, a stable CHO clonal cell line containing 10 kb of genomic DNA including the human LDLR promoter (described in section 2.1.1) driving expression of the *Luc* gene (CHO-p*LDLR-Luc*), was used to screen for small molecules (Work carried out by Dr S Agkatser). The 10 kb promoter region has been shown to include all elements necessary for physiological regulation of the *LDLR*, which should yield more physiologically relevant information than more traditional assay systems using truncated promoter fragments. In a pilot screen 216 compounds, selected on the basis of their similarity to known modulators of gene transcription, e.g. sterols, were screened at a single concentration (20 µM) in the CHO-pLDLR-Luc cell line. Compounds 49 (15a), 50 and 51 from the screen appearing to give an increase in luciferase expression compared with vehicle treated cells (Figure 8A). These particular compounds were included in the screen due to their similarities in structure to sterol molecules themselves, as can be seen in the overlay of compound 15a with cholesterol (Figure 8C). From these three, compound 15a was determined to be the most potent, a stilbene with a *N,N*-dimethylaminopropyloxy chain at the para position (Figure 8B)

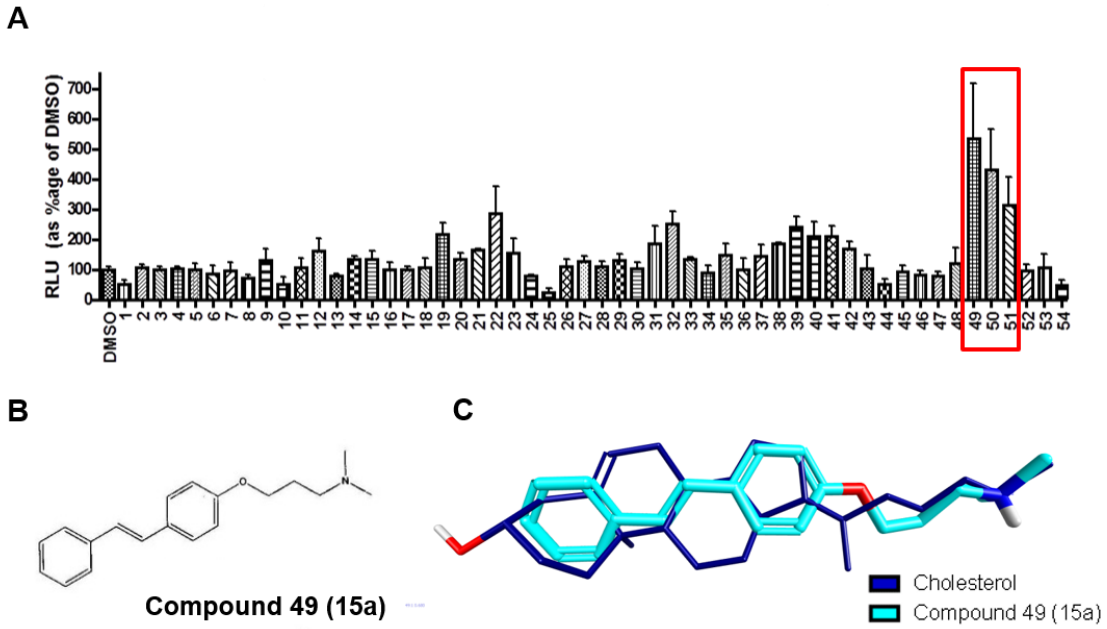


Figure 8 - Identification of three novel small molecules which upregulate LDLR promoter activity.

A compound library of 216 small molecules were screened at a single concentration(20µM) in a CHO-p*LDLR-Luc* cell line. Luciferase is under the control of 10 kb of genomic DNA upstream of the LDLR, including the promoter and all elements essential for physiological regulation. (**A**) Three initial hits appeared to give an increase in luciferase expression compared to DMSO (0.1%) control treated cells. (**B**) Of the three initial hits compound 49 (15a) was the most potent. (**C**) Overlay of compound 49 (15a) and cholesterol showing their similarity in structure.

3.2 Results

3.2.1 Identification of a novel set of small molecules which drive expression through the LDLR promoter

Authentic samples of compound 15a (Figure 9A) alongside two derivatives of compound 15a, compound 65 and 90 were synthesised. Compound 65 offers a chain contraction compared with compound 15a, with the amine chain being replaced by a shorter methyl chain (Figure 9B). Compound 90 involved a modification to compound 65, tightening the conformational constraints and synthesising an alkyne linker to the two benzene rings (Figure 9C). The substitution of the amine would uncover if this was the pharmacophore of the molecule, whilst the alkyne linker would establish if altering the three-dimensional shape of the molecule had any effect on potency. All three compounds gave a dose-dependent increase in luciferase expression compared to vehicle treated cells (Figure 9A-C). With all three EC_{50} values in the nanomolar range (Compound 15a: 39nM, Compound 65: 50nM and Compound 90: 250nM).

To assess the toxicity of these compounds *in vitro* we quantified adenylate kinase release in the media alongside luciferase expression. Adenylate kinase is a ubiquitous plasma membrane protein, which is released into the media when the plasma membrane is damaged under conditions of cell stress or toxicity (Jacobs *et al.* 2013). All three compounds did not show any increased release of adenylate kinase in the media compared to the untreated cells, at the concentrations required to increase luciferase expression (Figure 9D-E). Interestingly at the highest doses of Compound 15a and 65, there was a drop off in luciferase expression which at the same concentration gave an increase in adenylate kinase release, indicating the drop off in expression may be due to cytotoxicity.

To confirm that the three compounds were acting via increasing *LDLR* promoter activity and not by interacting or stabilising D-Luciferin or luciferase, Hep3B cells were transfected with a p*CMV-Luc* plasmid (A plasmid identical to p*LDLR-Luc* with a CMV promoter replacing the 10 kb LDLR promoter (Hibbitt *et al.* 2010)). Concentrations known to cause a large increase in luciferase expression were used to treat the cells, with no difference in luciferase expression detected

between any of the treatment groups (Figure 10A). Finally, to ensure that the compounds themselves did not fluoresce, Hep3B cells were treated with the compounds with no differences between any of the treatment groups detected (Figure 10B).

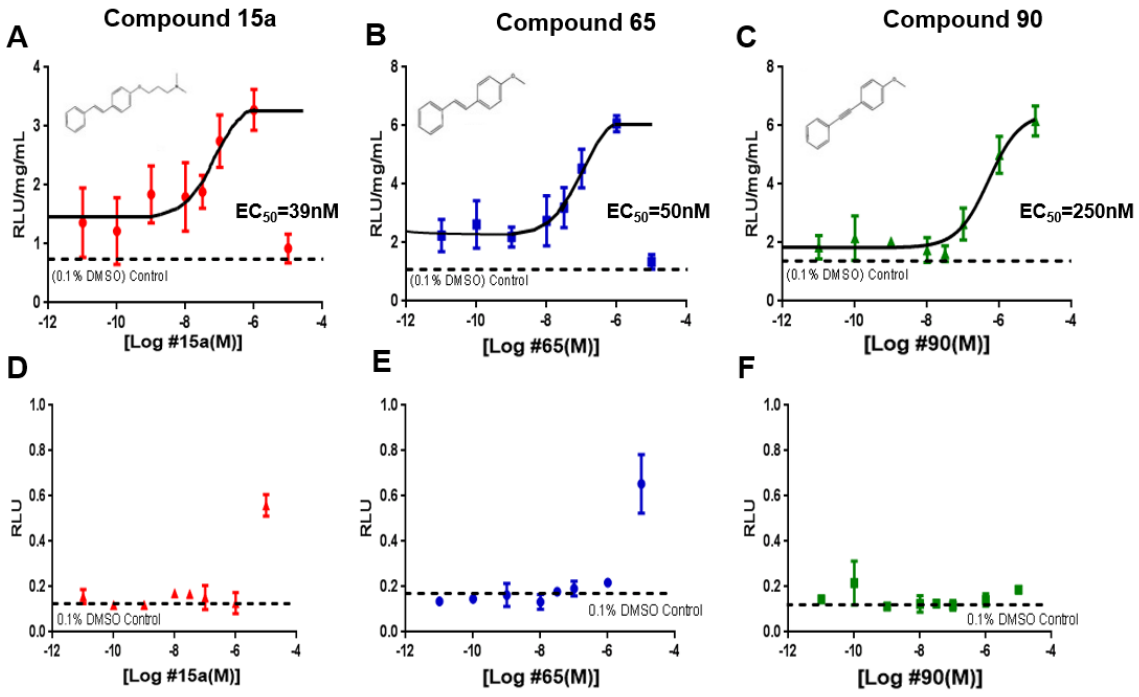


Figure 9 - Compounds 15a, 65 and 90 dose dependently increase luciferase expression in the CHO-p*LDLR-Luc* cell line

(**A-C**) CHO-p*LDLR-Luc* cells were treated with either Compounds 15a, 65, 90 or a vehicle control (0.1% DMSO) for 48 hours before luciferase expression was measured. All three compounds gave a dose dependent increase in luciferase expression compared with vehicle treated cells. Luciferase expression was normalised to total protein. Each compound had an EC_{50} in the nanomolar range with the structure of each compound given within the appropriate graph. (**D-F**) Adenylate kinase release into the media was used to quantify cytotoxicity profiles of each compound, with all three demonstrating favourable toxicity properties. n=4. Error bars denote standard deviation (SD).

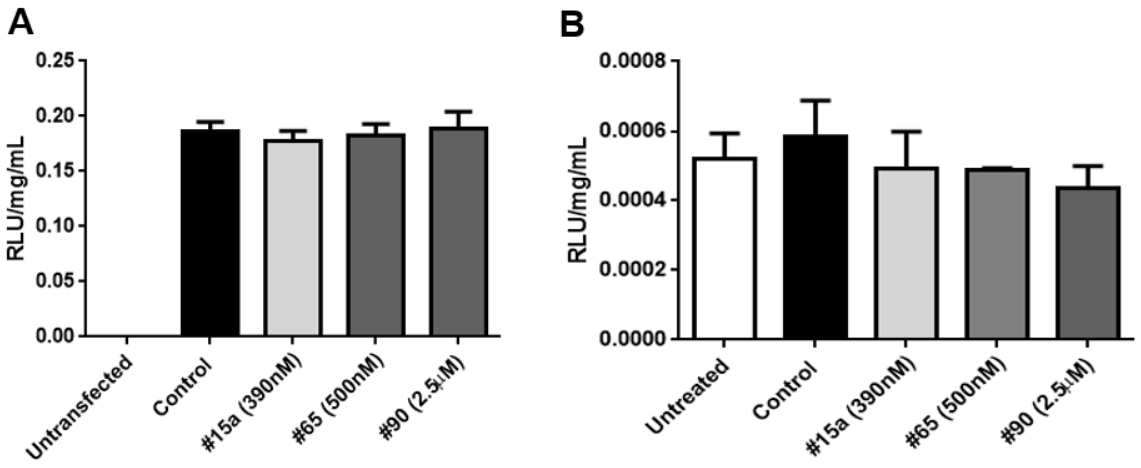


Figure 10 – Compounds 15a, 65 or 90 do not stabilise or interact with D-Luciferin or luciferase nor do they fluoresce themselves.
(**A**) Hep3B cells were transfected with a p*CMV-Luc* plasmid 24 hours prior to compound treatment of 15a, 65, 90 or vehicle control. An untransfected well was left to control for transfection. 48 hours after compound treatment luciferase expression was analysed with no differences detected between vehicle and compound treated cells. (**B**) Untransfected Hep3B cells were treated with either compounds 15a, 65, 90 or vehicle control. 48 hours after compound treatment no significant differences could be detected between any group. Luciferase expression was normalised to total protein. n=2. Error bars denote SD.

3.2.2 Compounds 15a, 65 and 90 do not inhibit HMG-CoA reductase

Compounds 15, 65 and 90 were tested to see if they caused an increase in *LDLR* promoter activity through inhibition of HMGCR (Figure 11). The activity of purified HMGCR is measured indirectly through measuring the absorption of NADPH at 340 nm over time. As HMGCR converts HMG-CoA to mevalonate, NADPH, a co-substrate in the reaction is oxidised to $NADP^+$ (Figure 11), leading to a decrease in the absorption at 340 nm. The activity of the enzyme was confirmed, as there is a significant decrease in absorption between blank (no enzyme added) and vehicle treated samples (enzyme added). As a positive control pravastatin was used which significantly inhibits the decrease in absorption compared to a vehicle treated sample after 15 minutes. No significant difference was observed between vehicle treated and compound 15a, 65 or 90 treated samples. Importantly, no difference was seen between vehicle treated and activity (enzyme alone) samples. This assay confirms that the three compounds are able to increase *LDLR* promoter activity via a mechanism distinct from statins.

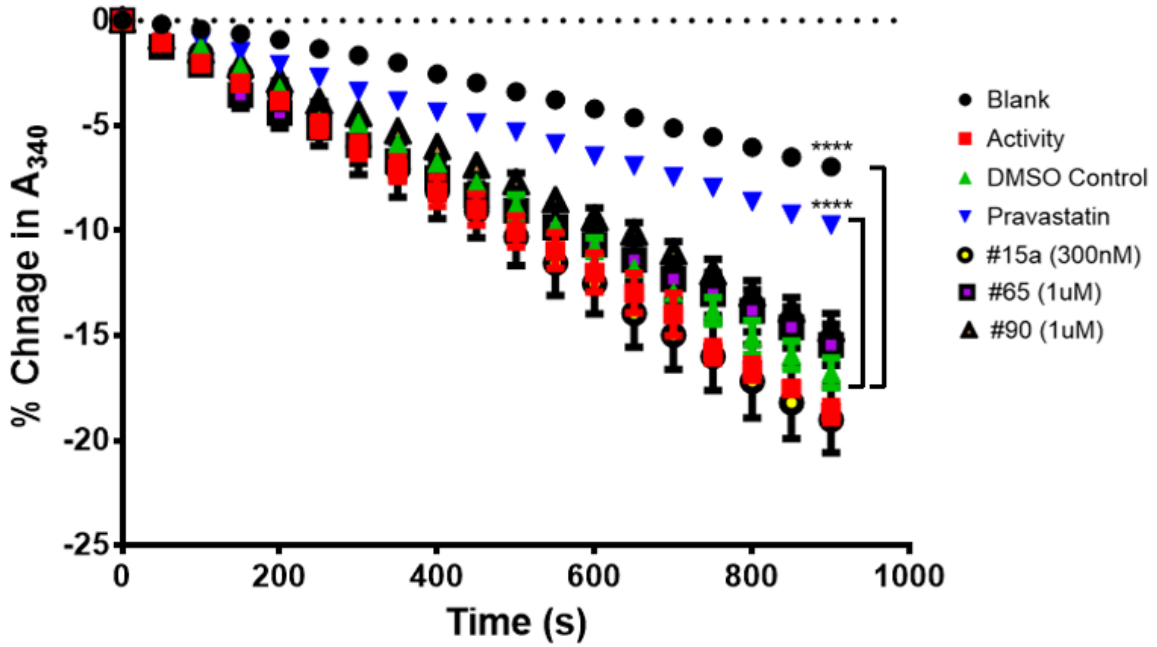


Figure 11 - Compounds 15a, 65 or 90 do not inhibit HMG-CoA reductase activity.

Purified HMGCR was added to samples containing either vehicle, pravastatin, compounds 15a, 65 or 90 alongside all substrates necessary for the reaction to process. A set of samples had no enzyme added (Blank) and another just contained all components for the reaction with nothing additional added (Activity), which acted as negative controls. Absorbance was measured at 50 second intervals, Pravastatin significantly inhibited the decrease in absorbance at 340 nm representing of NADPH being oxidised to $NADP^+$ and indicative of HMGCR activity. None of the other three compounds inhibited this decrease, demonstrating that they do not inhibit HMGCR. ****P<0.0001. n=3. Error bars denote SD. One-way ANOVA with Dunnetts post hoc analysis

3.2.3 Compounds 15a and 65 are able to increase the LDLR at the mRNA and protein level in hepatocyte cell lines

The EC_{50} dose from the primary assay and 10-fold above and below this concentration were selected to see if they could cause an upregulation of the LDLR in hepatocyte cell lines. Compounds were treated to a human hepatocyte cell line for 24 hours and LDLR mRNA expression was analysed alongside a housekeeping gene to control for total mRNA (Figure 12). Simvastatin, a known upregulator of LDLR mRNA expression, was used as a positive control and cholesterol used as a negative control. All three compounds appeared to give a dose dependent increase in LDLR mRNA expression, with the highest doses of compound 15a and 65 giving a significant increase compared to vehicle treated control cells. The same concentration of compounds 15a and 65 were then added to mouse hepatocyte cells where they both again significantly increased the Ldlr at the highest dose compared with vehicle treated cells after 48 hours (Figure 13). The increase with the novel compounds seemed to be equal to that seen with a statin in both cell lines.

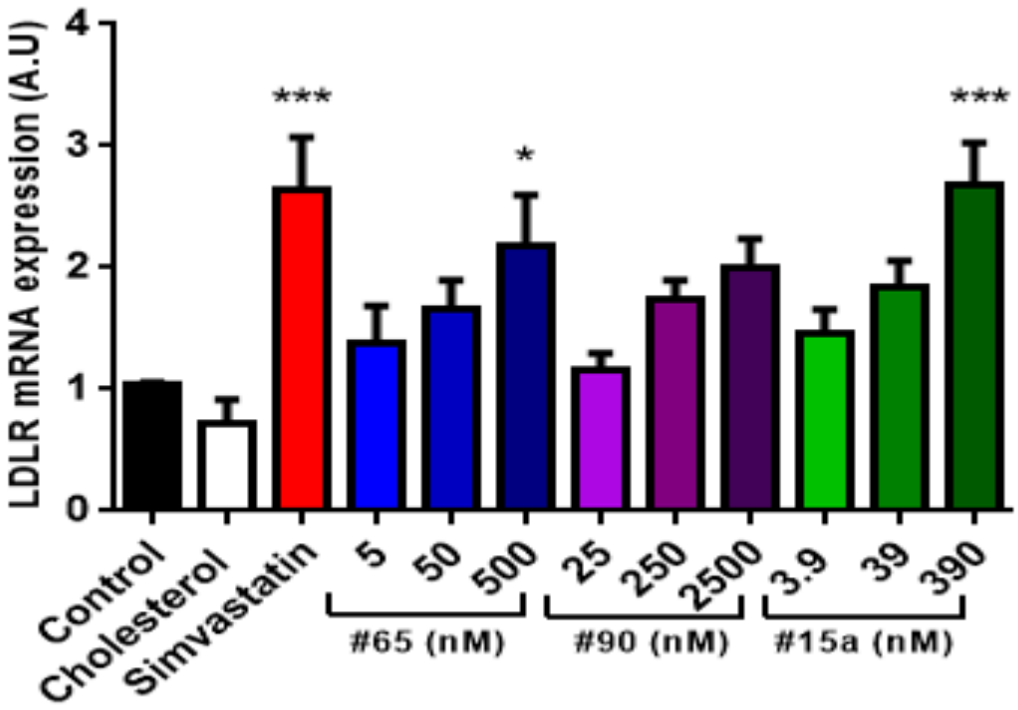


Figure 12 – Compounds 15a and 65 significantly upregulate LDLR mRNA expression in a human hepatocyte cell line

Hep3B cells were treated with increasing doses of compounds 15a, 65 or 90 for 24 hours before mRNA expression was analysed. Cholesterol treated (25.8µM) and Simvastatin treated (500nM) cells acted as a negative and positive controls respectively. Compounds 15a and 65 gave a significant increase in LDLR mRNA expression compared with vehicle treated cells. LDLR mRNA expression was normalised using β-actin housekeeping control and expressed using ΔΔCt compared with vehicle treated control (0.1% DMSO). Significance represents treatment compared to vehicle treated control *P<0.05, ***P<0.001. n=5. Error bars denote SD. One-way ANOVA with Dunnetts post hoc analysis.

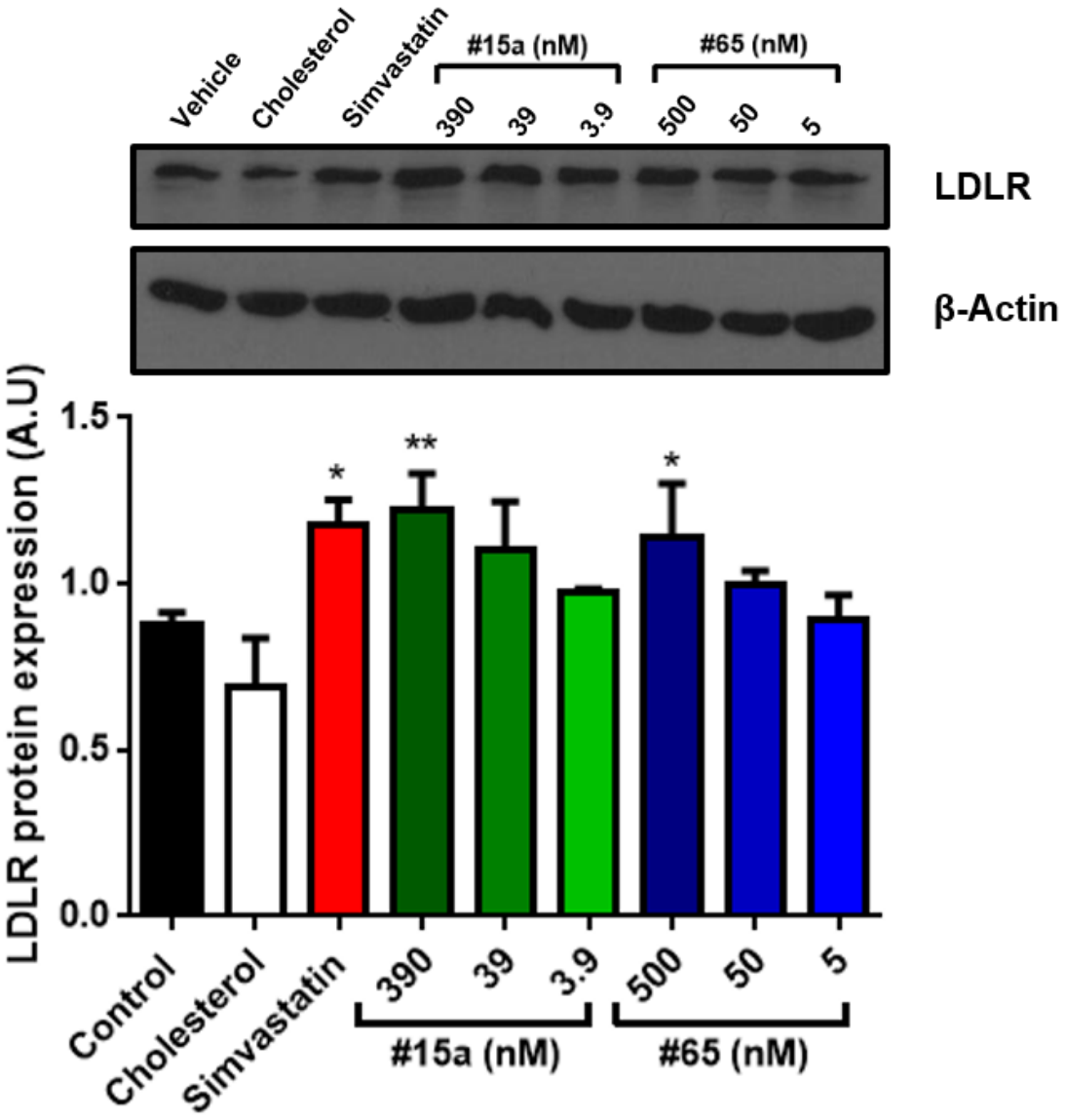


Figure 13 – Compounds 15a and 65 both increase Ldlr protein expression in a mouse hepatocyte cell line

Mouse Hepa1-6 cells were treated with increasing concentrations of compound 15a or 65 for 48 hours before Ldlr protein expression was analysed using western blot analysis. Cholesterol (25.8µM) and Simvastatin (500nM) were used as negative and positive controls respectively. Compounds 15a and 65 gave a significant increase in Ldlr protein expression compared with control (vehicle treated 0.1% DMSO) cells. Ldlr protein expression was normalised using β-actin housekeeping control. A representative immunoblot is shown with quantification displayed below. Significance represents treatment compared to vehicle treated control. *P<0.05, **P<0.01. n=3. Error bars denote SD. One-way ANOVA with Dunnetts post hoc analysis.

3.2.1 Compound 40 and Compound 15a inhibit squalene synthase

Through an extensive literature search, molecules strikingly similar to compound 15a were shown to inhibit SQS (Figure 14A) (Harwood *et al.* 1997). In the reaction SQS converts two molecules of FPP first into an intermediate, pre-squalene diphosphate (Figure 14B) and then to a single molecule of squalene. Upon examination, it appeared as if compound 15a could mimic this intermediate if present in its ammonium form (Figure 14C) as shown by the overlay in Figure 14D.

SQS activity was measured in human liver microsomes, in the presence of Compounds 40 and 15a. Compound 40 was identified through structure-activity relationship studies to improve the potency and pharmacokinetics of compound 15a described in detail in section 4.2.2. The compounds were pre-incubated with the microsomes for 10 minutes before the reaction was started by adding [^{3}H]-FPP. The reaction went on for 10 minutes before inhibition was assessed. The EC_{50} values for Compound 40 (26nM) and Compound 15a (39nM) established in the CHO-p*LDLR-Luc* assay and concentrations 10 fold above and below this were used. Compounds 40 and 15a both dose dependently inhibited the conversion of FPP to squalene both showing ~60% inhibition at the higher dose (Figure 15A). The IC_{50} value for compound 15a was 121nM and for compound 40, 182nM. YM-53601 a known SSI was used as a positive control in this assay (Ugawa *et al.* 2000).

In silico modelling was carried out on these compounds to determine how they may inhibit squalene synthase. MOE software was used with the available human squalene synthase crystal structure (PDB: 1EZF), which had been co-crystallised with the ligand CP-320473 (Pandit *et al.* 2000). Compound 15a was docked in its neutral state as compounds which would not be protonated had shown comparable activity (Figure 19). Compound 15a was predicted to bind in a similar manner to the co-ligand CP-320473 in the active site, with the hydrophobic aryl group sitting deep in the pocket, while the chain, bearing hydrogen bond acceptors protrudes out to interact with Arg-52 (Figure 15B). To further validate this possible mechanism of binding, Compound 15b was docked into the active site, a molecule

which demonstrated no activity in the CHO-p*LDLR-Luc* assay (Figure 15C). As with 15a, the nitrogen atom of 15b is predicted to interact with Arg-52, however the molecule sits in an alternative conformation in the active site, slightly further out. It is proposed that this leads to greater instability of the complex, which could explain the lack of activity observed for this compound. This helps to show that the regiochemistry of the stilbene core at the para position may be crucial for activity. Compound 40 was predicted to bind slightly different to Compound 15a (Figure 15D). As with the previous molecules the hydrophobic aryl group sat deep in the active site pocket, however in a slightly different conformation with the end hydroxyl group interacting with Arg77 and Tyr 72 to stabilize the complex. The squalene synthase activity assay coupled with the *in silico* modelling confirms Compound 40 and 15a as inhibitors of squalene synthase.

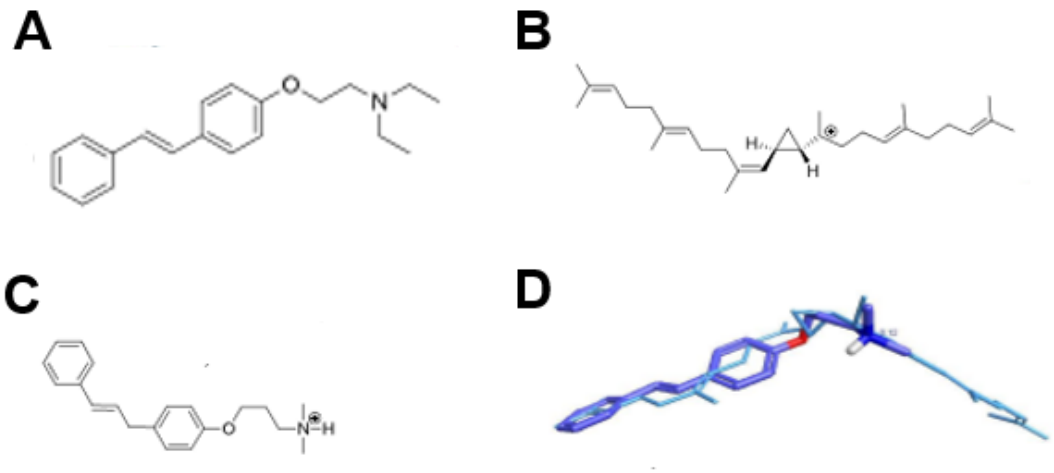


Figure 14 – Compound 15a structure could mimic pre-squalene diphosphate and inhibit squalene synthase

(**A**) 4-(diethylamino-ethoxy) stilbene, developed by Pfizer (Harwood *et al.* 1997), (**B**) Pre-squalene diphosphate an intermediate in the conversion of farnesyl pyrophosphate to squalene. (**C**) The protonated form of compound 15a, in a provocative orientation that could mimic the intermediate in (**B**). (**D**) An overlay of the pre-squalene diphosphate and the protonated ammonium form of compound 15a demonstrating homology in their conformational shape.

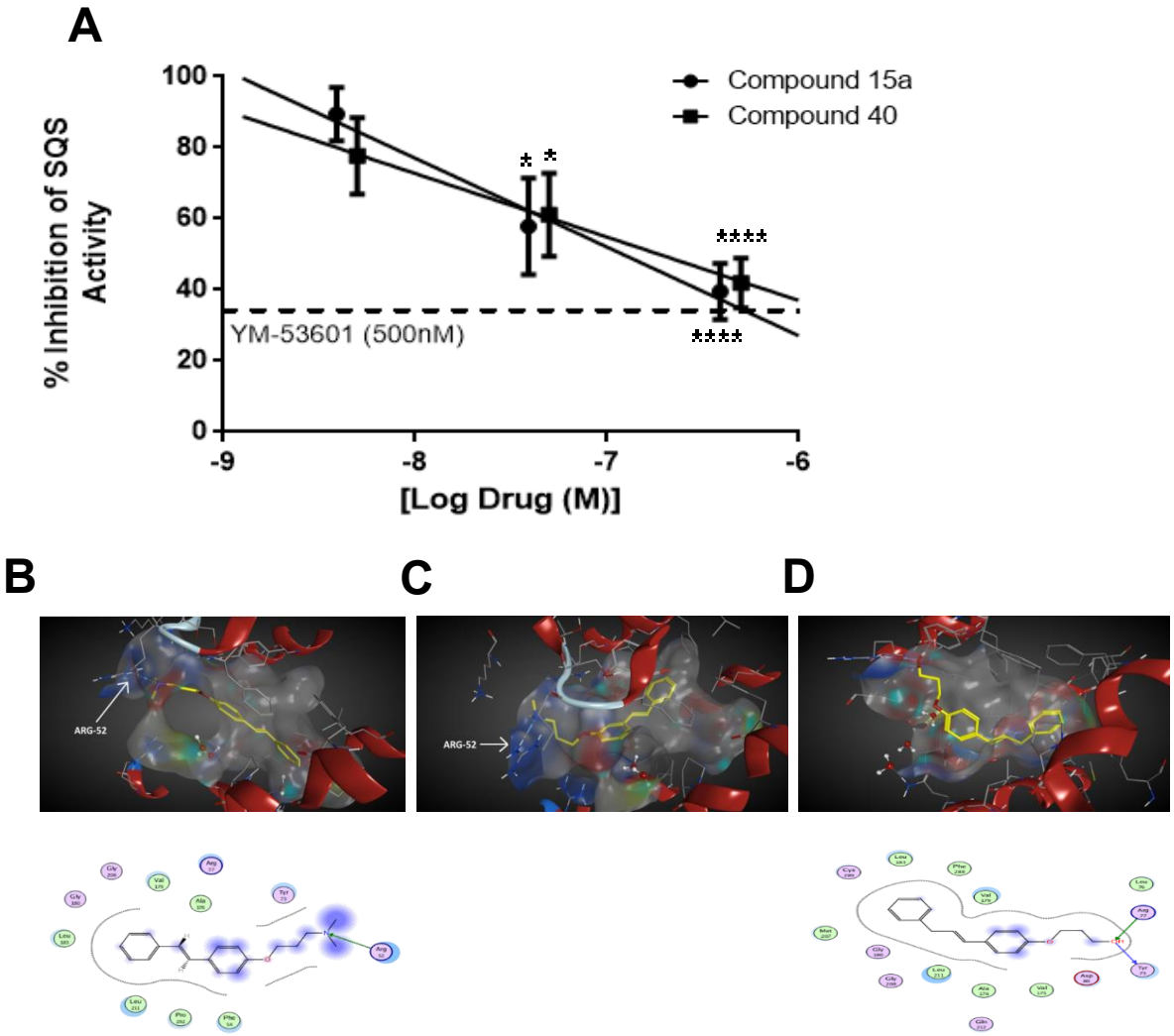


Figure 15 - Compounds 15a and 40 competitively inhibit squalene synthase through binding in the active site.

(**A**) Purified human liver microsomes were incubated with radiolabelled FPP and all necessary co-substrates in the presence of compounds 15a, 40 or vehicle. YM-53601 was used as a positive control. Both compounds 15a and 40 dose dependently inhibited SQS activity at nanomolar concentrations. *In silico* modelling of (**B**) compound 15a, (**C**) compound 15b and compound 40 (**D**) using MOE software. The stilbene of compound 15a and 40 is able to sit within the active site as seen with the graphical representation below each respective compound and stabilize with the indicated amino acids. Compound 15b a molecule shown to have no activity in our CHO-p*LDLR-Luc* screening assay is predicted to sit in an alternative confirmation in the active site, potentially unable to bind into the active site. *P<0.05, ****P<0.0001. n=4-7. Error bars denote standard error of the mean (SEM). One-way ANOVA with Dunnetts post hoc analysis

3.2.1 A squalene synthase inhibitor and statin used in combination causes a synergistic drive in expression from the *LDLR* promoter

We set out to determine if a squalene synthase inhibitor and statin combined is able to drive human LDLR promoter expression greater than what can be achieved with either class of drug alone. As before, compounds were treated for 48 hours in the CHO-p*LDLR-Luc* cell line to measure the effect of these molecules in driving the human *LDLR* promoter. A dose-response curve was generated for Compound 40 (Figure 16A) and Simvastatin (Figure 16B) alone, giving EC_{50} values of 26 and 128nM respectively. A dose-response of Compound 15a was carried out in the presence of the EC_{50} of Compound 40 (Figure 16C). There was no enhancement in luciferase expression using two squalene synthase inhibitors (E_{max}: 2.43 RLU/mg/mL) compared to the dose response of Compound 15a alone (E_{max}: 3.28 RLU/mg/mL) (Figure 9A). The same was seen when two statins were dosed together, a dose response of pravastatin was carried out in the presence of the EC_{50} of Simvastatin (Figure 16D). No increases in the luciferase expression were seen using two statins (E_{max}: 2.04 RLU/mg/mL) compared to Simvastatin alone (E_{max}: 2.76 RLU/mg/mL).

Dose-response curves for Simvastatin in the presence of the EC_{50} and EC_{80} of Compound 40 (Figure 16E-F) gave a much greater increase in luciferase expression, with E_{max} values of 6.35 and 11.77 RLU/mg/mL respectively. The same was true for the reverse experiment where a dose-response of Compound 40 was carried out in the presence of the EC_{50} of Simvastatin (Figure 16G). The E_{max} value was 16.77 RLU/mg/mL, a much larger increase in luciferase expression than was seen using two squalene synthase inhibitors. The fold increases in expression given when two squalene synthase inhibitors or two statins were dosed compared to vehicle treated cells was 3.9 and 1.1 respectively. In comparison the fold increase when a statin was dosed alongside a EC_{50} or EC_{80} dose of a squalene synthase inhibitor was 10- and 16.1-fold respectively, compared to vehicle treated cells. This work clearly demonstrates a synergistic effect of inhibiting the cholesterol biosynthesis pathway at two distinct parts of the pathway can greatly enhance the drive in expression of the human *LDLR*.

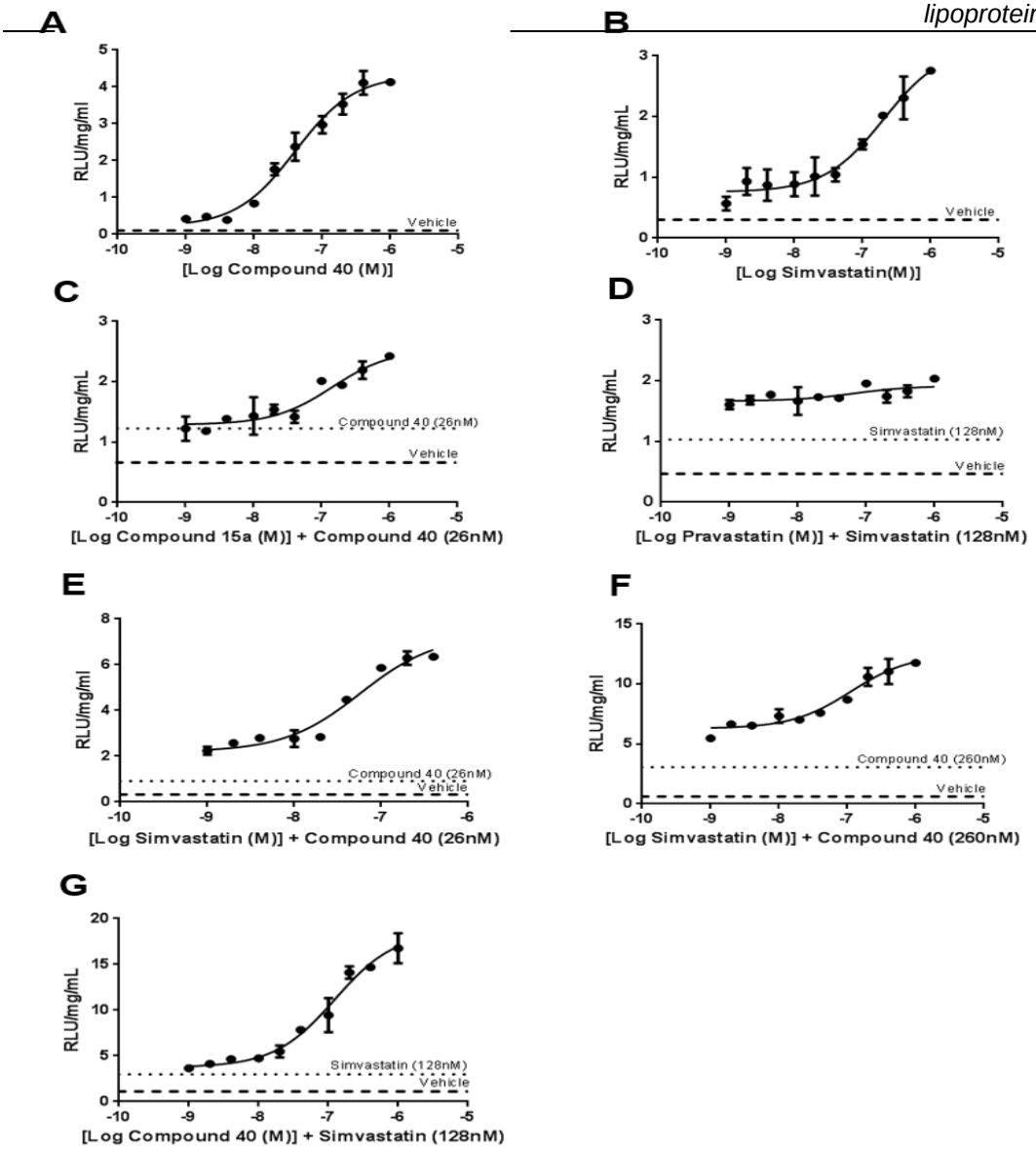


Figure 16 – A statin and squalene synthase inhibitor produce a synergistic effect further upregulating LDLR promoter activity

To determine if a statin and squalene synthase inhibitor produced a greater upregulation of the *LDLR* promoter compared to either class alone, dose response experiments in the CHO-p*LDLR-Luc* cell line were carried out. (**A**) A dose response of compound 40 and (**B**) simvastatin established the EC_{50} and EC_{80} values to be used in the combination treatments. (**C**) A dose response of compound 15a in the presence of the EC_{50} of compound 40, looking at the effect of two squalene synthase inhibitors. (**D**) A dose response of pravastatin in the presence of the EC_{50} of simvastatin, looking at the effect of two statins. (**E**) the EC_{50} and (**F**) EC_{80} of compound 40 treated alongside a dose response of simvastatin. (**G**) the EC_{50} of simvastatin treated alongside a dose response of compound 40. The dashed line represents vehicle (0.1% DMSO) treated cells and the dotted line is the single concentration of the EC_{50} or EC_{80} used alone. In combination using a statin with a squalene synthase inhibitor leads to a much larger increase in luciferase expression than can be seen with using two classes of the same inhibitor. n=4. Error bars denote SD.

3.3 Discussion

The present body of work details the identification of a novel series of small molecules able to upregulate the LDLR through a mechanism distinct from the current clinically used medication, statins, *in vitro*. We confirm the activity in different hepatocyte cell lines and elucidate their mechanism of action as SSIs. Encouragingly, we demonstrate that these molecules can act in synergy with stains to drive expression of the human *LDLR* promoter to a far larger degree than can be done with either class of compound alone. This work provides further evidence that a second class of inhibitors may be of great therapeutic use to patients who struggle to meet their lipid goal, particularly HeFH patients where this a common occurrence.

Through a compound screen of 216 molecules in a reporter cell line, previously made within this laboratory (CHO-p*LDLR-Luc*), three compounds were identified, 49 (15a), 50 (15b) and 51 as initial hits. Re-synthesising and testing authentic samples of each of these three compounds determined that only compound 15a was a true hit. Derivatives of compound 15a were synthesised (compound 65 and 90) and dose response curves carried out generating EC_{50} values for each compound. In the secondary assays, significant increases in LDLR mRNA and protein were only achieved with compounds 15a and 65. It is possible that 90 is a less potent compound at inhibiting mouse or human SQS compared with Chinese hamster SQS. Almost all mammalian SQS has a highly conserved catalytic domain (Gu *et al.* 1998) so it would be unlikely that efficacy would be achieved in only certain mammalian species. Many other competitive SSIs have also demonstrated similar efficacies across mammalian species (Ugawa *et al.* 2000). No cytotoxicity was detected at any of the concentrations used with compound 90, so if necessary higher concentrations could be used to determine its efficacy in the secondary assays, as it showed the lowest potency this was not carried out.

We identified compound 40 and 15a as SSIs, with each molecule showing a dose-dependent inhibition of the human SQS at nanomolar potencies. A literature search found molecules similar in structure to compound 15a (Figure 14A) that were able to inhibit SQS (Harwood *et al.* 1997). Harwood et al., reasoned that the stilbene moiety could mimic the donor FPP molecule and fit into the active site

where the ammonium group would stabilise the conformation, the mechanism they hypothesised was occurring with the pre-squalene diphosphate intermediate. In this study however, no molecules lacking the amine functionality were tried. Our work demonstrates that an ammonium cation is not required for activity, as we show compound 40 (Figure 20) which has the amine group replaced with a hydroxyl, is able to dose dependently inhibit SQS activity to the same degree as a compound with the protonatable amine group. This finding is contrary to previous literature findings (Ishihara *et al.* 2004), although it opens up a lot more modifications which could be made to this series of molecules, if necessary to improve other chemical or pharmacological properties.

The weakened potency with compound 90 starts to tease apart how our novel series of small molecules interact with SQS, with decreases in the stilbene moieties conformational flexibility reducing efficacy. Our *in silico* modelling suggests that it is the stilbene that sits in the active site of the SQS catalytic site and so any modifications on it should rightly affect potency. Compound 65, which has had the whole amine chain removed and replaced with a shorter methyl chain, was not docked in the active site for *in silico* modelling. It does show similar EC_{50} values to compound 15a (50 and 39nM), which throws into doubt the importance of the SSIs interaction with Arg72, a factor hypothesised as essential in the SQS crystal structure with the SSI CP-320473 (Pandit *et al.* 2000) and deemed to interact with compound 15a by the *in silico* modelling.

As compound 15a and 40 is similar to the structure of FPP, it would be a concern that these molecules also inhibit other enzymes which accept FPP as a substrate, notably enzymes which synthesise ubiquinone and dolichol. Other similar squalene synthase inhibitors have been shown to inhibit other FPP accepting enzymes (Harwood *et al.* 1997), albeit at 100-500 fold higher IC_{50} values than for SQS. It was again hypothesised that the amine was essential for the specificity of these compounds for SQS and no other FPP accepting enzymes. To further progress these compounds, it would be important to assess their activity on the prenyltransferases involved in dolichol and ubiquinone production (Beytia and Porter 1976).

Another compound which shares homology with our two SSIs, compound 40 and 15a, is tamoxifen (Figure 17A). Tamoxifen is used to treat breast cancer but has also been shown to lower LDL-cholesterol in the clinic (Morales *et al.* 1996) and prevent atherosclerotic build up in non-human primates (Williams *et al.* 1997). I found in the CHO-p*LDLR-Luc* assay, tamoxifen increased human *LDLR* promoter activity (Figure 17B). Previous work has shown tamoxifen is able to inhibit enzymes downstream of SQS, namely sterol Δ'8-isomerase, sterol Δ'24-reductase and sterol Δ'14-reductase, all involved in the conversion of lanosterol to cholesterol (Cho, Kim and Paik 1998). Interestingly, the authors conclude that the inhibition is non-competitive but hypothesise that the formation of the protonated form of tamoxifen may be able to interact where the carbocationic intermediates produced in all three of these cholesterol biosynthesis reactions bind, a similar proposed mechanism to the competitive inhibition suggested by Harwood et al.,. Harwood et al., also investigated whether their SSIs cause a build-up of other metabolites within the cholesterol biosynthesis pathway. They detected a build-up of other non-saponifiable lipids such as squalene epoxidase and squalene dioxide, indicating additional enzyme inhibition along this pathway. It is possible that our compounds would also have inhibitory effects at the enzymes just downstream of SQS, such as squalene epoxidase, another enzyme which has been targeted for lipid lowering therapy (Sawada *et al.* 2001), giving our compounds a dual beneficial therapeutic affect over other SSIs. Carrying out the SQS activity assay in the presence of digitonin, a compound which disrupts the activity of all the other enzymes downstream of SQS (Eilenberg *et al.* 1989), may provide a quick answer to this.

Resveratrol (Figure 17C) is a phenolic compound with a stilbene core, notably found in red wine (Frémont 2001). Resveratrol is similar in structure to our compound series in particular compound 65, with the stilbene core and hydroxyl group at the para position. Resveratrol has been shown to inhibit squalene monooxygenase, the next enzyme downstream of SQS, converting squalene to 2'3'–oxidosqualene (Laden and Porter 2001). Resveratrol was shown to non-competitively inhibit squalene monooxygenase at micro-molar concentrations. The potency of resveratrol fits compounds we have tested in our CHO-p*LDLR-Luc* assay, whereby modifications with electron-donating or electron-withdrawing

groups onto the stilbene benzene ring decreased the EC_{50} into the micro-molar range (Figure 19). This provides further evidence that our compounds may also inhibit multiple enzymes on the cholesterol biosynthesis pathway. Interestingly, resveratrol and other very similar compounds including pterostilbene (phenolic compound found in blueberries) have shown anti-oxidant properties, including protection against the formation of oxidised-LDL (Frankel, Waterhouse and Kinsella 1993; Zhang *et al.* 2012b). In addition, resveratrol and similar compounds demonstrate PPARα agonism *in vivo* (Inoue *et al.* 2003; Rimando *et al.* 2005). PPARα is a known regulator of fatty acid oxidation and triglyceride metabolism, (Varga, Czimmerer and Nagy 2011) it is possible are series of small molecules may also interact with this family of transcription factors, potentially modulating plasma triglycerides, as has been seen with other SSIs (Ugawa *et al.* 2000).

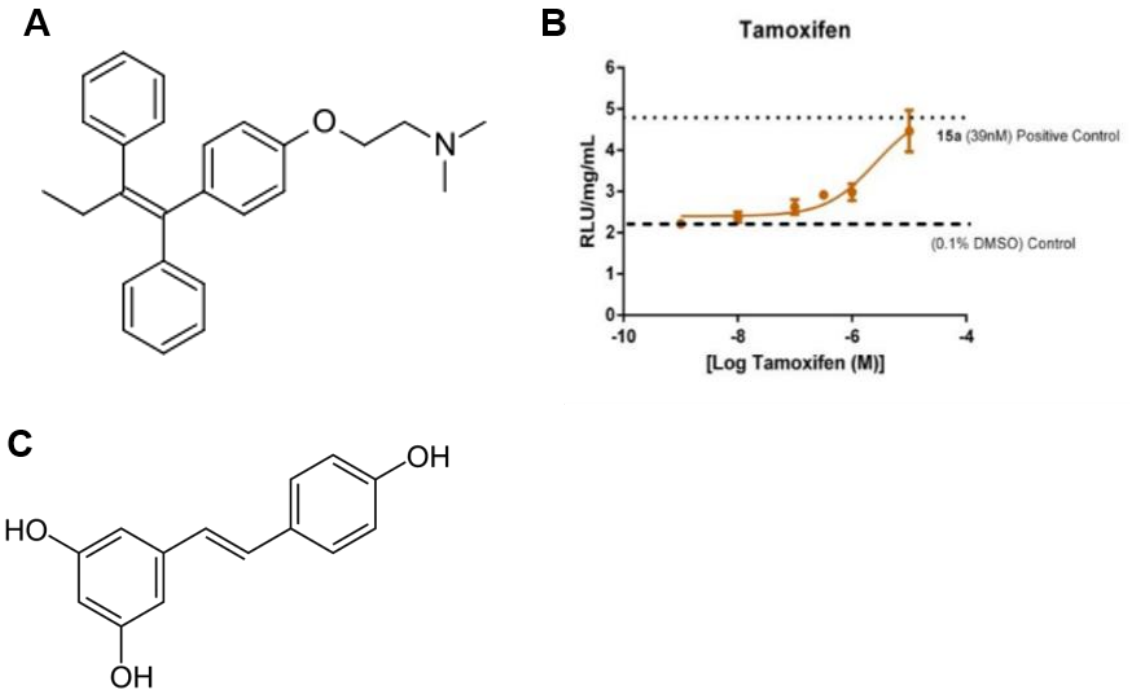


Figure 17 – Tamoxifen increases LDLR promoter activity in the CHO-p*LDLR-Luc* cell line.

(**A**) Chemical structure of tamoxifen. (**B**) CHO-p*LDLR-Luc* cells treated with tamoxifen show a dose dependent increase in luciferase expression compared with vehicle (0.1% DMSO) treated cells. Compound 15a was used as a positive control. (**C**) Chemical structure of resveratrol n=2. Error bars denote SD.

Chapter 4: Demonstration of *in vivo* efficacy of a novel squalene synthase inhibitor

4.1 Introduction

4.1.1 Squalene synthase and other cholesterol biosynthesis inhibitors in animal models

The first cholesterol biosynthesis inhibitors tested in animal models were the HMGCR inhibitors, statins (Endo *et al.* 1977b). In most cases, once the efficacy of the statin had been established *in vitro*, the molecules were first tested in smaller mammalian species such as the mouse or rat (Alberts *et al.* 1980; Tsujita *et al.* 1986). In these experiments the effect on cholesterogenesis was evaluated using radiolabelled acetate, injected into the mouse or rat after delivery with a statin. These studies failed to detect the hypocholesterolaemic effects of statins in mice and rats, except in rats injected with Triton WR-1339 (Endo *et al.* 1979; Tsujita *et al.* 1986). The Triton WR-1339 model of acute hypercholesterolaemia, results from the detergent associating with triglycerides in the plasma and therefore inhibiting their hydrolysis by LPL (Otway and Robinson 1967). This is a very artificial hypercholesterolaemic model however and its use and relevance to in particular FH drug discovery, have led to its decline in use.

The lipid profiles of a number of rodent strains, non-primate and non-human primates were compared to a human lipid profile, alongside the efficacy of a statin in each model (Yin *et al.* 2012). A statin had no effect in lowering any parameters in any of the 8 rodent models looked at by Yin et al., including the Ldlr$^{-/-}$ mouse. As described in section 5.1.3, this is most likely due to the differences in the lipid profile between humans and rodents, with most of the cholesterol in rodents carried in the HDL fraction. One study has shown efficacy of atorvastatin in Ldlr$^{-/-}$ mice, showing decreases up to 30% in LDL-cholesterol levels after one week of dosing, however this decrease in plasma cholesterol is lost after three weeks due to large increases in VLDL production. The authors demonstrate that the statins inhibit ApoB-100 secretion, forcing hepatocytes to upregulate ApoB-48 production,

forming lipoproteins which can be cleared through non-LDLR dependent pathways (Ishibashi *et al.* 1994). As ApoB-48 is not expressed in human hepatocytes, this work further highlights the discrepancies between rodent and human lipid metabolism and handling. In larger mammalian species such as rabbit, dog and non-human primates, statins have consistently shown decreases in plasma cholesterol (Berkhout *et al.* 1997; Pecoraro *et al.* 2014). All three of these models carry the majority of their cholesterol in the LDL-fraction just like in humans. In particular the rabbit, canine and non-human primate species express CETP, and though not inherently prone to atherosclerosis, undergo atherogenesis with a relatively low amount of dietary cholesterol (Kolodgie *et al.* 1996; Yin *et al.* 2012). A stark difference from mouse models where often genetic manipulation and extreme high cholesterol (HC)-diets are needed to cause an atherosclerotic pathology.

Similar to statins, squalene synthase inhibitors (SSIs) have shown cholesterol biosynthesis inhibition in rodent models (Griebenow *et al.* 2011; Ichikawa *et al.* 2013) and lipid lowering in canine, rabbit, guinea pig and non-human primate models (Ugawa *et al.* 2000; Amano *et al.* 2003). SSIs have shown more consistent cholesterol lowering in rats than has been seen with statins (Harwood *et al.* 1997; Ishihara *et al.* 2004). This in part may be explained by SSIs exerting a much lower compensatory upregulation of Hmgcr expression (Flint *et al.* 1997). Squalene synthase (SQS) is a lot less prone to negative feedback regulation than HMGCR, as it is not one of the major regulatory enzymes of cholesterol synthesis, (Ugawa *et al.* 2002). This important feature limits the induction of upstream and downstream enzymes of the cholesterol biosynthetic pathway, that would increase the rate of LDL production. In animal models of HoFH, SSIs have also demonstrated lipid lowering, due to a decrease in lipoprotein secretion (Amano *et al.* 2003). SSIs demonstrated an additional decrease in ApoB and VLDL and unlike statins, decreases in triglyceride levels, indicating a dual hypotriglyceridaemic, hypocholesterolaemic function (Rondini *et al.* 2016).

Other inhibitors of the cholesterol biosynthesis pathway have also been tested in *in vivo* models, examining their effect on cholesterol biosynthesis and plasma lipid levels. Squalene epoxidase and oxidosqualene cyclase inhibitors have been

developed, targeting these two enzymes which are downstream of SQS. Both classes were able to show inhibition of cholesterol biosynthesis and lipid lowering in rodent and canine models (Nakayama *et al.* 1997; Fouchet *et al.* 2008). Unfortunately both these classes of compounds caused the development of skin ulcerations and cataracts and so work on these classes was discontinued (Rozman and Monostory 2010).

4.1.2 Development of a functional in vivo reporter assay for the determination of compound efficacy

Previously in this laboratory, we developed a plasmid (p*LDLR-Luc*) which contatins 10 kb of the human *LDLR* promoter, with all elements necessary for physiological regulation driving luciferase expression (5.1.1). The p*LDLR-Luc* plasmid can be delivered to mouse liver via a hydrodynamic injection (discussed in section 4.1.3). The level of luciferase expression is sensitive to known modulators of intracellular cholesterol levels, and can be measured at multiple time points through non-invasive optical imaging. In our hands, administration of pravastatin and siRNAs targeting *Hmgcr* after delivery of the p*LDLR-Luc* plasmid led to an increase in luciferase expression compared to vehicle or scrambled siRNA controls respectively (Hibbitt *et al.* 2010, 2012). This assay provides an excellent first look at determining whether the efficacy of a molecule *in vitro* translates into a mammalian system *in vivo*, eliminating the use of radiolabelled isotopes or having to deal with the discrepancies between the mouse and human lipid profile. Even more so, it is the full 10 kb human *LDLR* promoter, comprising of the three sterol response elements (SREs), the 5′-untranslated region, and ~8 kb of upstream sequence, which may contain unknown further elements essential for expression, which is driving the luciferase expression.

4.1.3 Hydrodynamic delivery of a non-viral plasmid to the liver

Non-viral methods of DNA transfection to the liver involve either chemical carriers, namely inorganic nanoparticles, cationic polymers or cationic lipids, or physical methods involving electroporation or sonoporation (Al-Dosari and Gao 2009). All present non-viral delivery methods to date suffer from poor transfection efficiency. Hydrodynamic delivery remains the most efficient way to deliver naked DNA to rodent liver. Hydrodynamic delivery involves an intravenous injection of 0.9%

saline containing the plasmid, equivalent in volume to 10% of the mouse's body weight (Liu, Song and Liu 1999). The injection is not just dependent on the volume but also the speed, which depending on the size of the mouse will need to occur between 4-7 seconds in smaller mice and 6-11 seconds in larger mice. Both the high speed and large volume act to create high pressure as the bolus of the fluid pools in the inferior vena cava halting venous return. The fluid then flows retrograde, into the hepatic vein and central veins of the liver lobes causing a huge increase in pressure (Crespo *et al.* 2005). Pores form in the hepatocyte cell membrane due to the pressure overload allowing the naked DNA to pass into the cell, as the pressure declines the pores re-seal and homeostasis is restored. Increase in liver transaminases is transient and persistence and expression of vectors delivered via this method has been reported up to over a year after delivery (Bonamassa, Hai and Liu 2011).

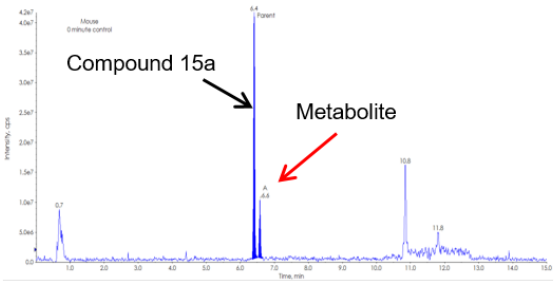
4.2 Results

4.2.1 Compound 15a has a low half-life when spiked into mouse liver microsomes

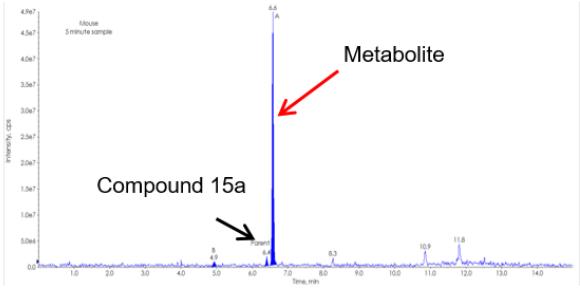
To progress the newly identified SSIs characterized *in vitro* in Chapter 3, we first assessed the metabolic stability of our lead compound 15a. An authentic sample of compound 15a was sent to Cyprotex™ who spiked the sample into mouse liver microsomes. Samples were then taken at different time points to analyse the amount remaining of compound 15a and any metabolites through LC/MS. Compound 15a was spiked into the microsomes and immediately sampled, already a large amount of it had been modified, leading to the appearance of a second peak with a slightly longer retention time (Figure 18A). After 5 minutes, less than 3% of compound 15a remained (Figure 18B). The half-life of compound 15a in this assay was less than five minutes, with five metabolites detected (Figure 18C). The five metabolites were all attributed to a single (+16 m/z) or double (+32 m/z) oxidation, as quantified using multiple ion monitoring data. The oxidation could have occurred at three points along the molecule, the aryl carbon-hydrogen bond (Dharwadkar 2016), the tertiary amine group (Lim *et al.* 1994) or across the double bond on the stilbene group (Zbaida & Kariv 1989.). Despite several attempts, none of the theoretical metabolites could be synthesised and so their

activity on driving the *LDLR* promoter could not be determined, therefore structure-activity relationship (SAR) studies were carried out to try and improve the pharmacokinetic profile.

A



B



C

	Absolute area in Sample		Area percentage in sample	
	0 minute control	5 minute control	0 minute control	5 minute control
Parent	$3.21e^{7}$	$2.10e^{6}$	70.7	2.20
A	$1.33e^{7}$	$9.15e^{7}$	29.3	95.9
B	ND	$1.25e^{6}$	NA	1.31
C	ND	$7.33e^{4}$	NA	0.0768
D	ND	$9.32e^{4}$	NA	0.0977
E	ND	$4.18e^{5}$	NA	0.439

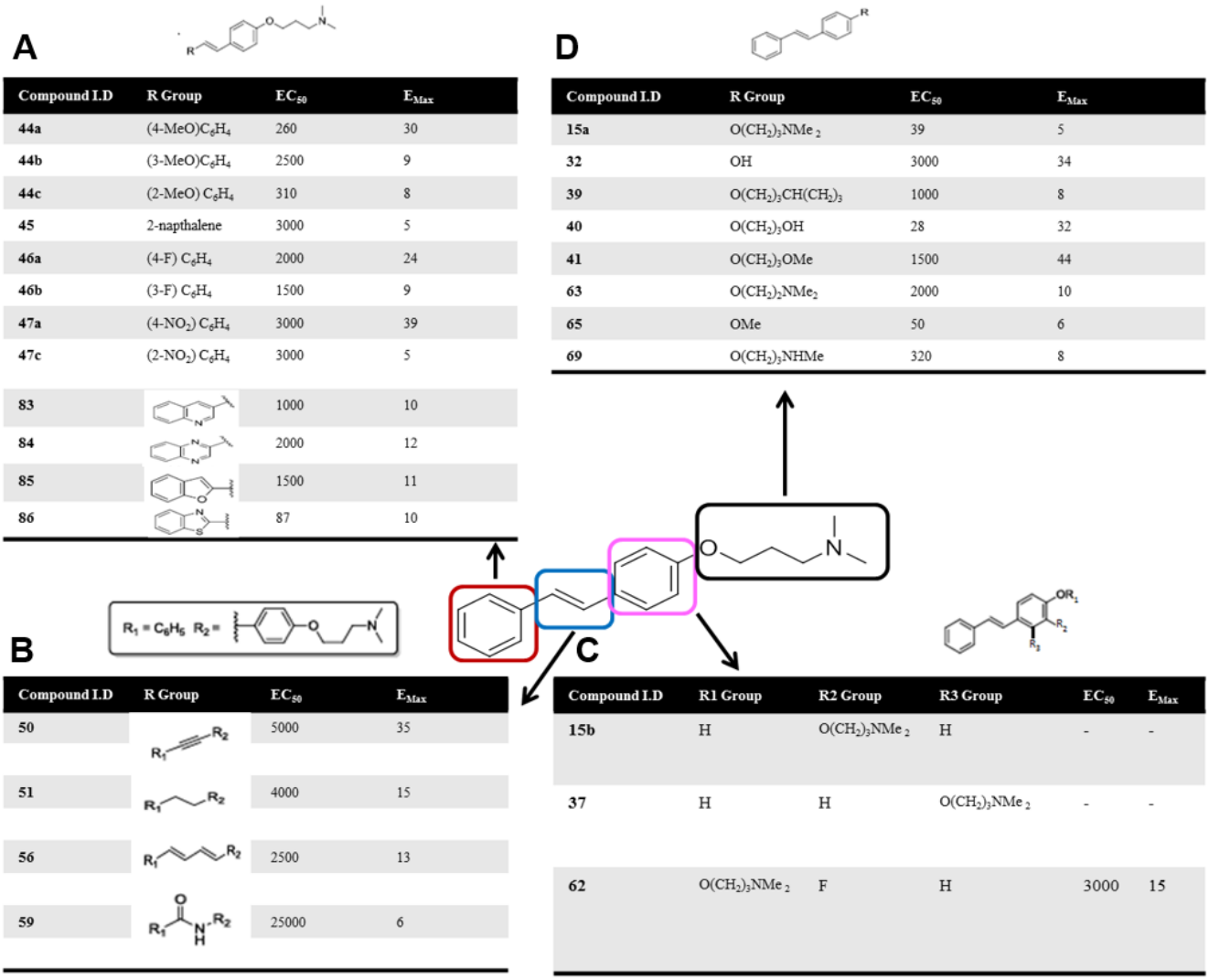
Figure 18 – Compound 15a has a half-life of less than 5 minutes in mouse liver microsomes.

Representative LC/MS trace of compound 15a (black arrow) and the detection of a potential metabolite (red arrow), (**A**) 0 and (**B**) 5 minutes after being spiked into mouse liver microsomes. (**C**) A table showing the percentage of compound 15a remaining at the given time points, and detection of potential metabolites with different retention times. Only 2.2% of compound 15a remained after 5 minutes incubation with mouse liver microsomes.

4.2.2 Compound 40 is a more potent analogue of Compound 15a with improved pharmacokinetics

To improve the efficacy and pharmacokinetics of Compound 15a, analogues were made and their efficacy tested in the CHO-p*LDLR-Luc* clonal cell line. Compound 15a was conceptually split into four key sections (Figure 19), the two aromatic rings in the stilbene (Red(A) and Pink (C) square) the carbon double bond linker (Blue (B) square) and the N,N-dimethylaminopropyloxy chain (Black (D) rectangle) (All chemistry carried out by Joe Mason and Dr Carole Bataille). Each of the four components was modified individually in order to gain a robust array of information concerning how the structure of the molecule impacts upon its activity, measured through EC_{50} and E_{max} values. All modifications to the unesterified benzene ring (Figure 19A), which increased the electron density of the stilbene core resulted in poorer activity than Compound 15a (EC_{50}: 39 nM, E_{max}: 5). Compound 86, a heterobiaryl gave a nanomolar EC_{50} value and high E_{max} though it appeared to be cytotoxic at concentrations of 1 µM and above, seen with a complete drop off in luciferase activity, so was not considered for further development. To alter the conformational three-dimensional shape of the molecule the alkane, cis-alkene, alkyne and 1,3-butadiene linker analogues were synthesised (Figure 19B), increasing the compounds conformational flexibility. Compound 51 resulted in lower potency suggesting that the olefin is key. Other alterations in the geometry (Compound 50, 56 and 59) also resulted in reduced potency, highlighting the importance of the (E)-alkene to the molecules effect. Shifting the N,N-dimethylaminopropyloxy chain to the ortha and meta positions (Figure 19C) resulted in a complete loss of activity. Compound 62 confirmed that any alterations to the electron density of the esterified benzene ring resulted in reduced activity. Finally the N,N-dimethylaminopropyloxy chain was modified as shown in Figure 19D. Compound 40 which has a propyl alcohol chain gave a lower EC_{50}, 26nM compared to 39nM and a six times higher E_{max}. Potency was lost with compound 63, where its tertiary amine would be predicted to lie further away from the Arg-52 residue, shown to interact with the amine group in the *in silico* binding studies (Figure 15). Apart from compound 40, all other compounds gave no improvement on the EC_{50} compared with the original compound 15a.

Compound 40 was selected alongside other analogues which contained heterobiaryl groups, commonly used to improve metabolic stability (Taylor, MacCoss and Lawson 2014) and spiked into mouse liver microsomes (Figure 20A). Of these Compound 40 demonstrated the greatest stability, having a half-life greater than 45 minutes. All the other compounds tested had dropped below 5% of their starting amount after 45 minutes, indicating that it may be the tertiary amino group leading to the metabolic instability. With the greatest potency and pharmacokinetics, Compound 40 (Figure 20B) was taken forward as the lead molecule.



A

Compound I.D	R Group	EC_{50}	E_{Max}
44a	(4-MeO)C_6H_4	260	30
44b	(3-MeO)C_6H_4	2500	9
44c	(2-MeO) C_6H_4	310	8
45	2-napthalene	3000	5
46a	(4-F) C_6H_4	2000	24
46b	(3-F) C_6H_4	1500	9
47a	(4-NO_2) C_6H_4	3000	39
47c	(2-NO_2) C_6H_4	3000	5
83		1000	10
84		2000	12
85		1500	11
86		87	10

B

Compound I.D	R Group	EC_{50}	E_{Max}
50		5000	35
51		4000	15
56		2500	13
59		25000	6

C

Compound I.D	R1 Group	R2 Group	R3 Group	EC_{50}	E_{Max}
15b	H	$O(CH_2)_3NMe_2$	H	-	-
37	H	H	$O(CH_2)_3NMe_2$	-	-
62	$O(CH_2)_3NMe_2$	F	H	3000	15

D

Compound I.D	R Group	EC_{50}	E_{Max}
15a	$O(CH_2)_3NMe_2$	39	5
32	OH	3000	34
39	$O(CH_2)_3CH(CH_2)_3$	1000	8
40	$O(CH_2)_3OH$	28	32
41	$O(CH_2)_3OMe$	1500	44
63	$O(CH_2)_2NMe_2$	2000	10
65	OMe	50	6
69	$O(CH_2)_3NHMe$	320	8

Figure 19 – Identification of compound 40 a more potent analogue of compound 15a

Extensive SAR studies were carried out on compound 15a, whereby each component of the molecule was altered individually and screened in the CHO-p*LDLR-Luc* at 1,10,30,100,300,1000, 10000 nM concentrations. The EC_{50} and E_{max} values for each modification made on the (**A**) red squared aromatic ring, (**B**) blue squared double bond linker, (**C**) pink squared aromatic ring and (**D**) N,N-dimethylaminopropyloxy chain are detailed in the corresponding tables. Modifications on the N,N-dimethylaminopropyloxy chain lead to the identification of compound 40, a compound with improved potency. All compounds were screened at n = 2.

A

Compound I.D	Compound Remaining (% of 0 minute)				
	0 minute	5 minute	15 minute	30 minute	45 minute
15a	100	4.83	0.497	0.359	0.322
83	100	114	49.9	9.03	2.58
84	100	104	61.5	17.4	4.82
85	100	98.7	48.4	10.1	4.19
40	100	102	77.4	67.5	64.8

B

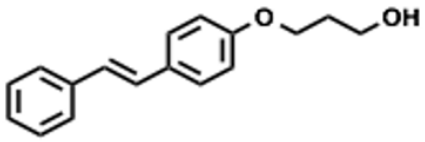


Figure 20 – Compound 40 has superior metabolic stability compared to compound 15a and other heterobiaryl derivatives.

(**A**) Listed compounds were spiked into mouse liver microsomes and after given time points the remaining amounts were quantified through LC/MS. The amount is given in the table as a percentage in comparison with the amount detected at the 0-minute time point. Of these compound 40 was the most stable, with over half still present after 45 minutes. (**B**) Compound 40 chemical structure.

4.2.3 Compound 40 can be detected in mouse plasma 6 hours post administration

To assess the pharmacokinetic profile of compound 40 in a mammalian system, we developed a HPLC protocol to measure the compound in mouse plasma. Compound 40 was spiked into isolated mouse plasma at known concentrations before extraction using acetonitrile and centrifugation to deplete the plasma protein content. The resulting supernatant was loaded onto the HPLC column, where a prominent peak in absorbance at 300 nm could be detected (Figure 21B). A vehicle spiked control gave no such peak at the retention time seen with the compound 40 samples (Figure 21A). A standard curve for compound 40 could be constructed, where there was a liner decrease in the peak area with decreasing concentrations (Figure 21C). Compound 40 could be detected as low as 10 nM in mouse plasma using this method.

Compound 40 was dissolved in β-cyclodextrin and dosed preliminarily at 0.75 mg/kg via intraperitoneal (I.P) injection, demonstrating first order elimination

kinetics (Figure 22A). No signs of discomfort, distress or toxicity where seen in the mice with the 0.75 mg/kg dose or any subsequent higher doses. The 0.75 mg/kg dose showed similar metabolic stability to that seen in the mouse liver microsomes assay, with a half-life of 59 minutes. The pharmacokinetic profile of compound 40 was then established at increasing doses, first at 5, then 25 and finally 40 mg/kg, with the level of compound present in the plasma measured up to 6 hours post dosing (Figure 22B). Each dose again appeared to demonstrate first order elimination kinetics, with a liner decrease when the log concentration was plotted against time. An example of the HPLC trace for the 40mg/kg dose is shown in Figure 23. As previously seen, no peaks were detected in uninjected (Figure 23A) or vehicle injected (Figure 23B) mice. A standard curve was run prior to each study for calculation of concentration in each sample. Compound 40 can be detected at all time points up to 6 hours (black arrow) (Figure 23C-F), with its peak concentration at 30 minutes. It appears as though a metabolite of compound 40 can also be detected (red arrow), with a slightly shorter retention time, however this metabolite was never quantified using mass spectroscopy. As the doses of compound 40 escalate, the T_{max} (time to reach maximal concentration) increases from 10 (5mg/kg) to 30 minutes (25,40mg/kg), driven by the rate of absorption of the compound from the I.P cavity (Figure 22C). The C_{max} (maximum concentration achieved systemically) increases proportionally to the amount of drug administered to the mouse as would be expected. The relative bioavailability can be calculated as the area under the curve and is ~8% for each concentration apart from the 40mg/kg, which is 11%. The percentage of β-cyclodextrin was higher at the 40mg/kg dose in order to solubilise compound 40 completely before delivery, it may be however that without the higher percentage of β-cyclodextrin, that some of the compound comes out of solution once injected *in vivo*.

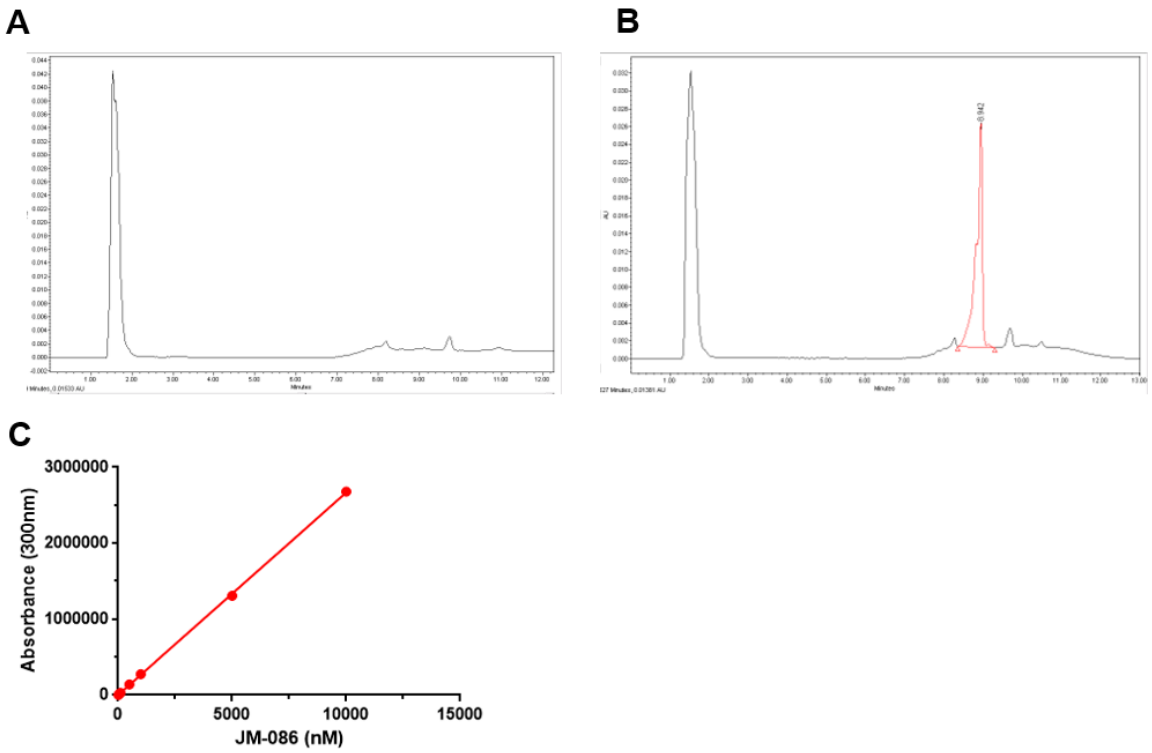
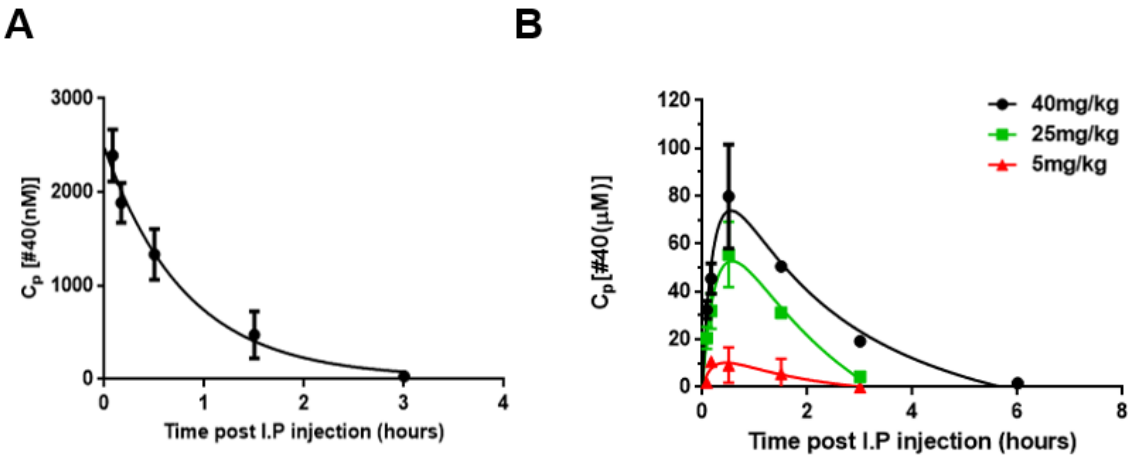


Figure 21 – Compound 40 can be detected in mouse plasma up to 10nM using HPLC

Compound 40 was spiked into isolated mouse plasma and extracted using acetonitrile. Representative trace for (**A**) vehicle and (**B**) compound 40 (1 µM) spiked into mouse plasma. (**C**) The area under the curve is quantified and a standard curve can be constructed for determination of unknown concentrations.



C

Dose (mg/kg)	5	25	40
$t_{½}$ (minutes)	76	91	90
C_{max} (µM)	10.7	55.54	82.11
T_{max} (minutes)	10	30	30
AUC (Equating to relative bioavailability) (%)	8.17	8.82	11

Figure 22 - A 40mg/kg dose of compound 40 in β-cyclodextrin produces high plasma concentrations of the drug.

CD-1 male mice received an I.P injection of compound 40 in β-cyclodextrin at (**A**) 0.75 (**B**) 5, 25 or 40mg/kg with plasma harvested at given time points up to 6 hours post injection. Concentration of compound 40 in plasma was confirmed through HPLC analysis of the area of the peak compared with known spiked in standards. (**C**) The pharmacokinetic properties of compound 40 in β-cyclodextrin was calculated from the resultant plasma concentration-time profiles. n=2 per time point. Error bars denote SD

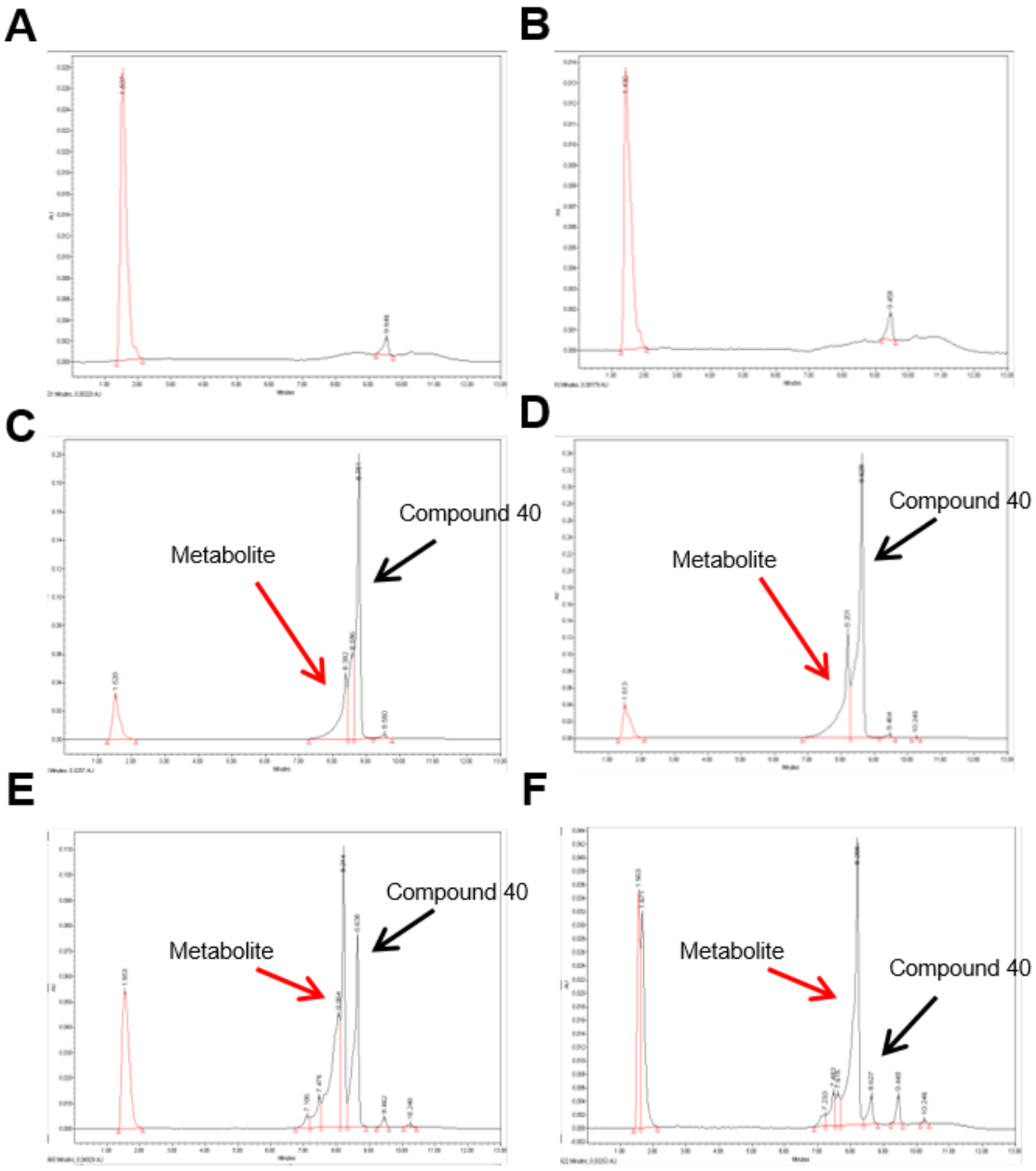


Figure 23 – Compound 40 can be detected up to 6 hours post I.P injection in CD-1 male mice.

Compound 40 (40mg/kg) was injected I.P into CD-1 male mice and plasma concentration was analysed using HPLC. Representative traces of (**A**) uninjected or (**B**) vehicle injected mice give no peak at 8.2 minutes, where as a peak at this time can be seen in all compound injected mice. Traces showing mouse plasma after (**C**) 10, (**D**) 30, (**E**) 180 and (**F**) 360 minutes post compound 40 delivery. Compound 40 is indicated with a black arrow and a metabolite with a red arrow.

4.2.4 After hydrodynamic delivery the right median lobe shows the highest level of transgene expression.

For future *in vivo* studies looking at determining the efficacy of our lead compound, and in the next chapter our non-viral gene therapy vectors, we would require delivering a non-viral plasmid to the liver via hydrodynamic delivery. For our compound studies, we decided to use male MF-1 mice for the hydrodynamic delivery over 28 grams, as this outbred strain has been shown previously to tolerate the procedure and express the transgene after injection (Hibbitt *et al.* 2007a). In studies involving the hydrodynamic injection, it is shown that the speed and percentage of body weight injected are the variables which will determine expression level (Liu, Song and Liu 1999). As we had not performed hydrodynamic delivery on this exact mouse gender and size before, we carried out a volume and speed escalation study, to determine the best parameters for expression and tolerability. In the MF-1 mice, we found a 10% injection volume necessary for maximal expression (Figure 24A) and that the injection speed had to be under 11 seconds for robust luciferase detection (Figure 24B). Previously Nakamura and colleagues demonstrated that it is the right median lobe which gives the strongest transgene expression after hydrodynamic delivery (Nakamura *et al.* 2013). We confirmed that it was indeed the right median lobe in MF-1 mice which gave the highest luciferase expression in our hands as well (Figure 24C) The right median lobe was therefore used for all expression studies throughout this thesis. Finally, the responsiveness of the *LDLR* promoter in the p*LDLR-Luc* plasmid to the intracellular cholesterol content was once again confirmed in a CHO-WT cell line, ready for all future *in vivo* experiments using the plasmid (Figure 24D). As would be expected an increase in luciferase expression was observed with 48-hour treatment of either a statin (pravastatin) or SSI (compound 40).

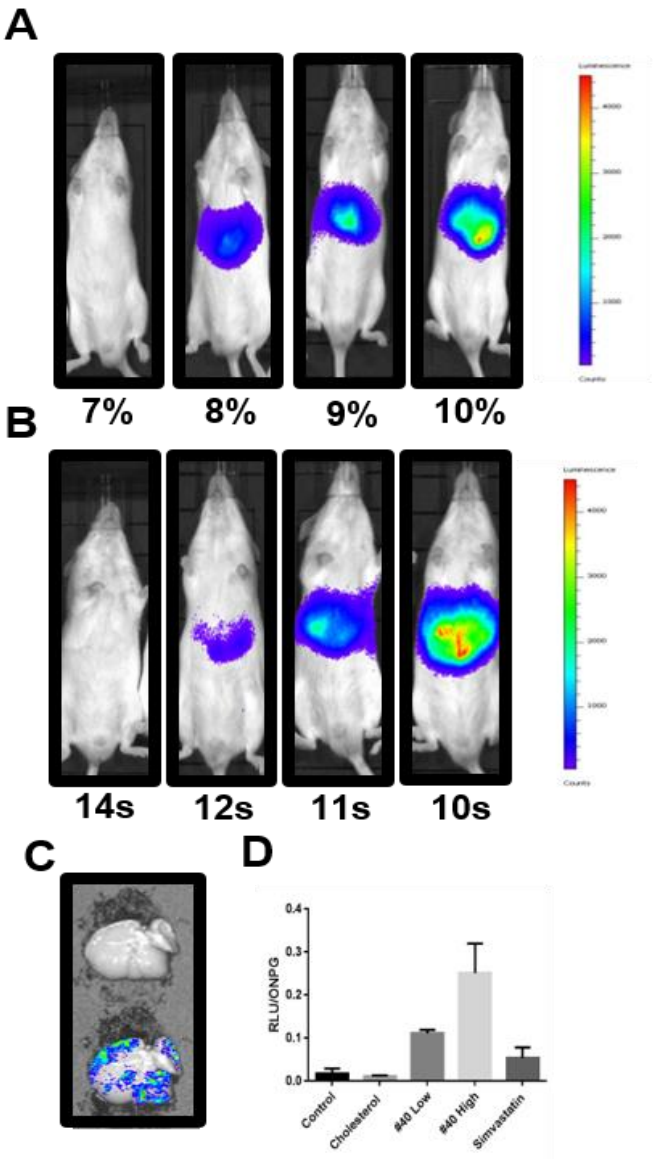


Figure 24 – Volume and speed of hydrodynamic injection is essential for expression in MF-1 male mice

MF-1 male mice received a hydrodynamic injection of p*LDLR-Luc* plasmid with a different (**A**) percentage body weight volume or (**B**) injection speed before luciferase expression was analysed, 5 days post-delivery. Injection volumes of 10% body weight and speeds under 10 seconds produced the largest luciferase expression. (**C**) Liver from a MF-1 mouse which received a hydrodynamic delivery of 10% body weight over 11 seconds. Top panel is a light photograph of the liver and bottom panel after a 4 second exposure. (**D**) CHO-WT cells transfected with the p*LDLR-Luc* plasmid 24 hours prior to 48-hour compound treatment. Luciferase expression was quantified and normalised to Lac Z expression to control for level of transfection. Pravastatin and compound 40 increased luciferase expression compared to control (vehicle treated) cells. n=2. Error bars denote SD

4.2.5 β-cyclodextrin causes increased expression of the human *LDLR* promoter *in vivo*

We have previously shown that the p*LDLR-Luc* plasmid luciferase expression is responsive to statins after hydrodynamic delivery in mouse liver (Hibbitt *et al.* 2010). To test if our lead compound maintains *in vivo* the efficacy seen *in vitro,* we employed a similar experiment, to analyse luciferase expression, driven by the 10 kb human *LDLR* promoter before and after compound administration. MF-1 male mice had a hydrodynamic injection of the p*LDLR-Luc* plasmid before being left to recover for 5-days. Baseline luciferase images were taken prior to any compound administration (Figure 25A) and 6 hours later, mice received either vehicle alone (β-cyclodextrin in PBS), compound 40 (40mg/kg), pravastatin (300mg/kg) or pravastatin (600mg/kg), an uninjected group acted as a negative control. Liver luciferase was quantified again, 18 hours post compound dosing (Figure 25B) and compared to the baseline image from the same mouse. The 18-hour time point was chosen based on the half-life of compound 40 and relative half-life of luciferase (Thompson, Hayes and Lloyd 1991). Vehicle treated mice demonstrated an increased luciferase expression compared with uninjected mice, making it hard to interpret the increase in luciferase expression also seen with compound 40 (Figure 25C). Pravastatin at the lower 300mg/kg dose seemed to have no effect on luciferase expression at this time point. A switch was made to a higher dose of pravastatin (600mg/kg) after it was apparent that the lower dose was not having an effect in this assay. Unfortunately, the experiment was stopped early after it appeared the vehicle was having an effect on luciferase expression and so an adequate sample size for each group was not completed to draw any further conclusions.

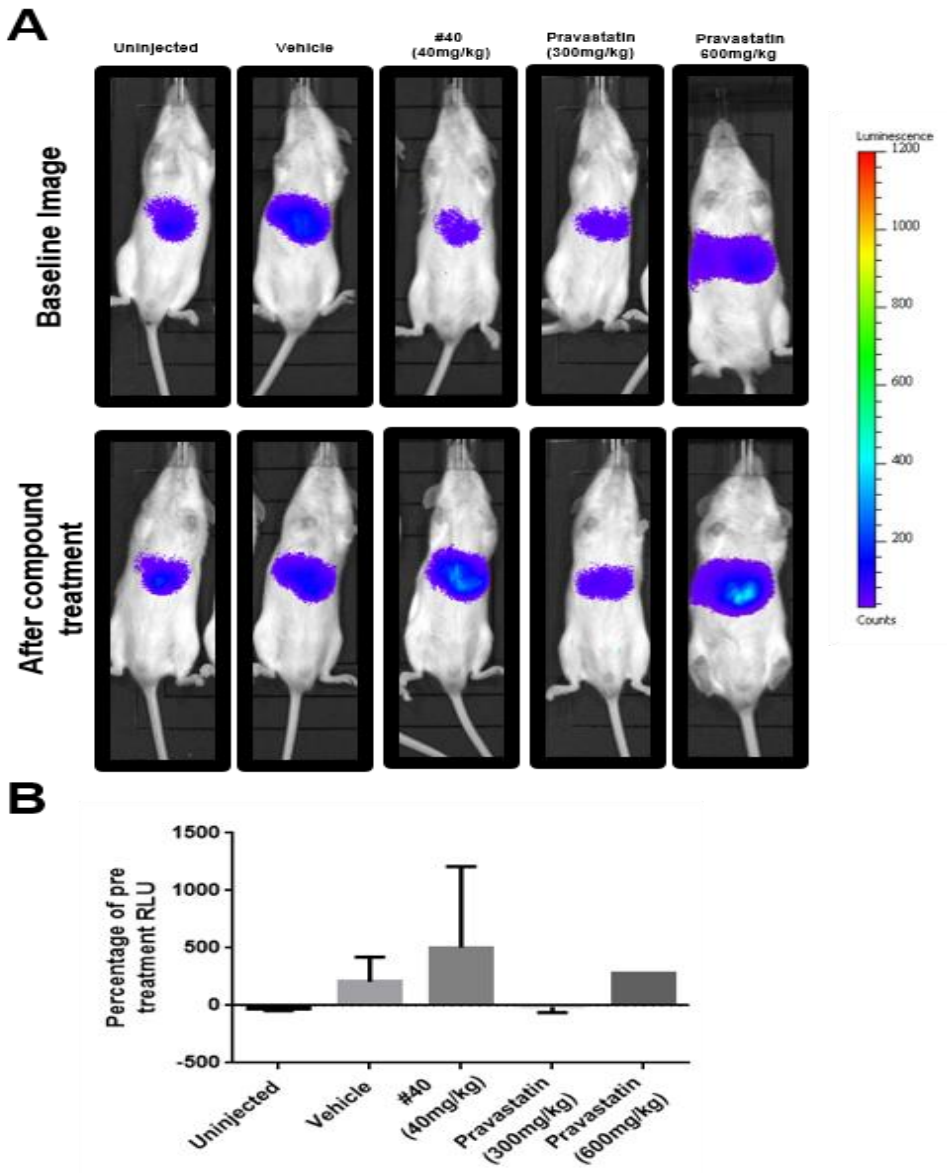
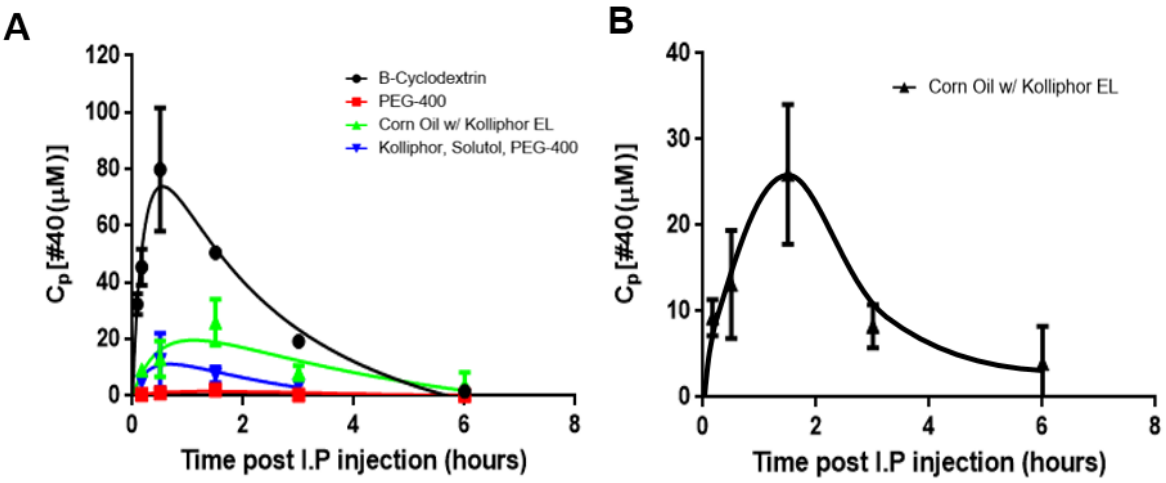


Figure 25 – β-cyclodextrin causes an increase in human LDLR promoter activity in vivo

Male MF-1 mice received a hydrodynamic injection of the p*LDLR-Luc* plasmid. After 5 days (**A**) a baseline image of luciferase expression was taken before compound administration. An uninjected control group which received hydrodynamic delivery but no I.P injections of compound or vehicle acted as a negative control. 18 hours post compound administration (**B**) a second luciferase image was taken. (**C**) Groups injected with vehicle alone (β-cyclodextrin), compound 40 (40mg/kg) or pravastatin (600mg/kg) appeared to give an increase in luciferase expression. The experiment was cut short due to the effect β-cyclodextrin appeared to be having on luciferase, making it not possible to determine the efficacy of compound 40 *in vivo*. Animal numbers for each group are as follows: Uninjected (3), vehicle (4), compound 40 (4), pravastatin-300mg/kg (3), pravastatin-600mg/kg (1). Error bars denote SD

4.2.6 Corn oil with Kolliphor EL can act as a vehicle for compound 40

Given that β-cyclodextrin had such a profound effect on the luciferase expression, other vehicles were trialled to see if they could achieve a reasonable plasma concentration of compound 40 once dosed I.P. A number of vehicles were tried with PEG-400 in PBS, PEG-400 with Solutol and Kolliphor EL in PBS and Kolliphor EL in corn oil all able to resuspend a 40/mg/kg concentration of compound 40 (section 2.11.1). CD-1 male mice were dosed with compound 40 in the different vehicles, and plasma was isolated at various time points up to 6 hours. The plasma concentration for compound 40 was determined as described in section 4.2.3. With all three vehicles, compound 40 could be detected up to 3 hours post administration but only with Kolliphor EL in corn oil and PEG-400 in PBS at the 6-hour time point (Figure 26A). None of the vehicles tested here gave a higher plasma concentration compared with β-cyclodextrin. Compound 40 dissolved in corn oil with Kolliphor EL achieved the highest plasma concentration (Figure 26B) after β-cyclodextrin with a C_{max} of 25.95 μM. The T_{max} for all three new vehicles was shifted from 30 minutes, seen with β-cyclodextrin, to 90 minutes, which may be down to the higher viscosity of the other vehicles and their rate of absorption (Figure 26C). Corn oil with Kolliphor EL had the highest bioavailability of the newly tested vehicles and was physically easier to resuspend compound 40 in, compared with PEG-400 alone or in combination with Solutol and Kolliphor EL.



C

Vehicle (40mg/kg)	β-Cyclodextrin	PEG-400	Corn Oil w/ Kolliphor EL	Kolliphor EL w/ Solutol + PEG-400
$t_{½}$ (minutes)	101	123	84	187
C_{max} (µM)	82.11	2.13	25.95	6.73
T_{max} (minutes)	30	90	90	90
AUC (Equating to relative bioavailability) (%)	11	0.3	4.3	1.7

Figure 26 – Corn oil with Kolliphor EL will be the vehicle used for future compound 40 dosing studies

Compound 40 was resuspended at 40mg/kg in PEG-400 in PBS, PEG-400 with Solutol and Kolliphor EL in PBS and Kolliphor EL in corn oil and administered I.P to CD-1 male mice. Mice were sacrificed at certain time points up to 6 hours and plasma was isolated. (**A**) Compound 40 plasma concentration was determined for the three vehicles, with β-cyclodextrin plotted on the graph as a reference. (**B**) Kolliphor EL in corn oil provided the better pharmacokinetic profile compared to PEG-400 formulations and could be detected up to 6-hours post administration. (**C**) The pharmacokinetic parameters of compound 40 in the given vehicles were calculated from the resultant plasma concentration-time profile. n=2 per time point. Error bars denote SD

4.2.7 Compound 40 is able to upregulate the human LDLR promoter in vivo

Using the alternate vehicle of Kolliphor EL in corn oil, the *in vivo* efficacy of compound 40 was tested for its ability to cause an increase in expression of the luciferase transgene, by increasing human *LDLR* promoter activity. MF-1 male mice had a hydrodynamic injection of the p*LDLR-Luc* plasmid before being left to recover for 5-days. Baseline luciferase images (Figure 27A) were taken prior to any compound administration. Mice then received three doses of vehicle (Kolliphor EL in corn oil), compound 40 (40mg/kg) or pravastatin (600mg/kg) spaced over 48 hours before final luciferase imaging (Figure 27A). An uninjected group which received the p*LDLR-Luc* plasmid but no I.P injections were used as a negative control. Compound 40 injected mice had significantly higher luciferase expression post compound delivery compared with vehicle treated mice (Figure 27B). Pravastatin injected mice also had significantly higher luciferase expression than vehicle injected mice, as would be expected and has previously been shown (Hibbitt *et al.* 2010). No difference was observed between uninjected mice and mice receiving the vehicle treatment. Here we demonstrate that our lead SSI is able to drive expression of the human *LDLR* promoter *in vivo*.

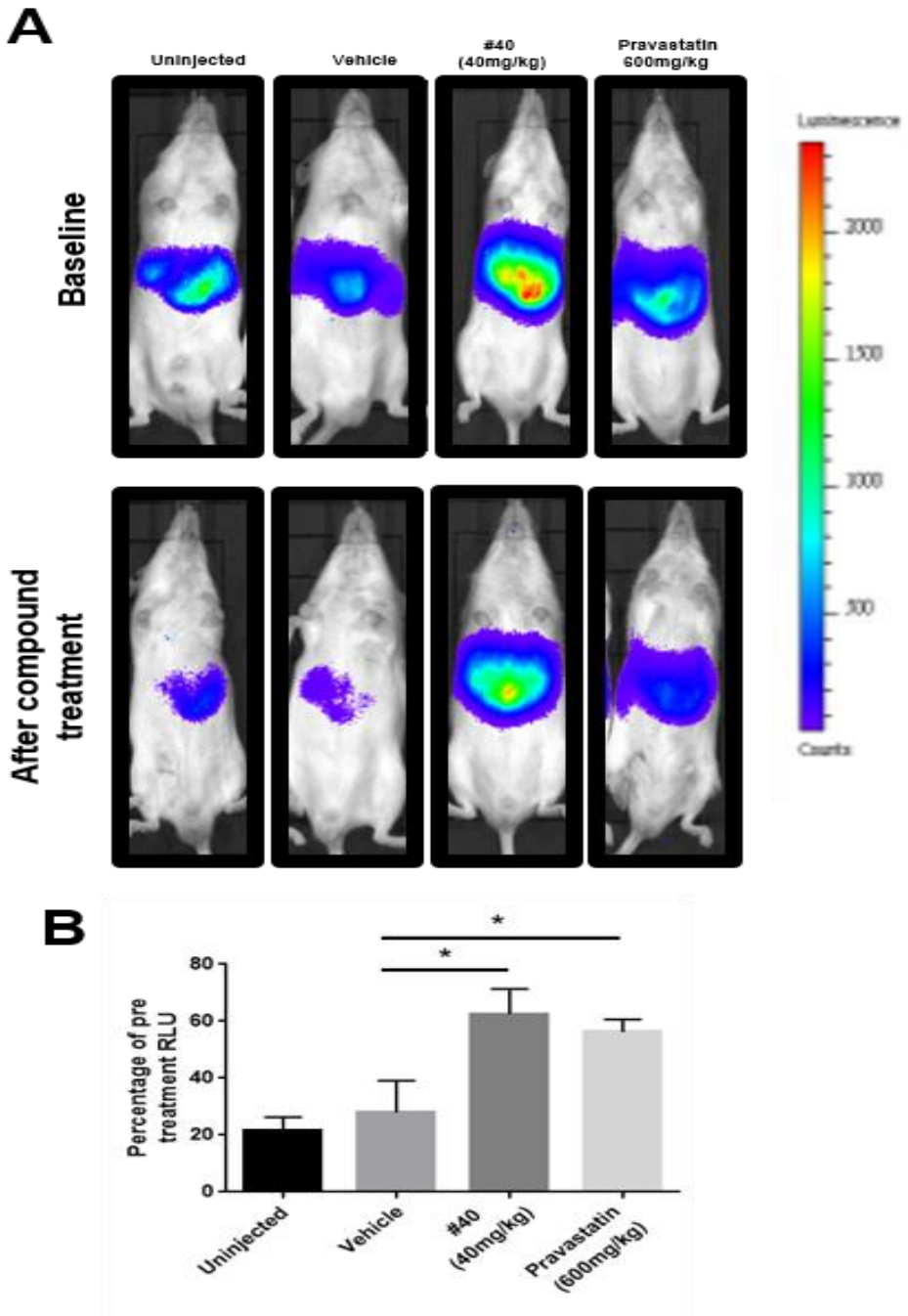


Figure 27- Compound 40 is able to drive expression of the human *LDLR* promoter in a mammalian system

p*LDLR-Luc* plasmid was delivered to MF-1 male mice via hydrodynamic injection. (**A**) Baseline luciferase images were taken before three doses of either vehicle (Kolliphor EL in corn oil), compound 40 (40mg/kg) or pravastatin (600mg/kg) were administered over 48 hours. An uninjected group where the plasmid was delivered but no compound was administered, was used as a negative control. (**B**) Compound 40 and pravastatin gave a significant increase in luciferase expression compared to vehicle treated mice. *P<0.05 n=5-6 per group, Error bars denote SEM. One-way ANOVA with Dunnetts post hoc analysis.

4.3 Discussion

Here we present a novel small molecule able to drive expression of the human *LDLR* promoter *in vivo*, through inhibition of SQS. From an *in vitro* screen we identified compound 15a as a molecule able upregulate the LDLR in primary and secondary *in vitro* assays, however a short half-life meant it was not the right candidate to progress into animal model efficacy studies. To address the pharmacokinetic properties of the molecule we carried out extensive SAR work on compound 15a, individually altering components of the molecule, leading to the identification of compound 40. Compound 40 was found to be more potent than the parent compound 15a, and had a much longer half-life when dosed into mouse liver microsomes and mouse. Finally, we were able to show that compound 40 is able to carry its biological efficacy into a mammalian system, where we demonstrated its ability to drive LDLR promoter activity after being dosed in mouse.

Compound 15a was found to be metabolized into five different metabolites, all with the addition of one or two oxygen groups to the molecule. The three most likely areas of the compound were thought to be the tertiary amine on the chain, the central double bond and the aryl C-H bond. Unfortunately, the metabolites could not be synthesised in this project's timeframe, to determine if they also upregulated the LDLR. Any modifications to the stilbene group in the SAR work resulted in a decrease in potency of the compound, so it is plausible that if the oxidation had occurred across the stilbene, the metabolites would also demonstrate a blunted potency.

The other potential site of oxidation is the tertiary amine group, which is the site of oxidation in tamoxifen, a similar compound in structure to 15a (Lim *et al.* 1994). Further evidence that the amine group is the site of liver enzyme modification came from our own work, where all changes in functionality of the stilbene to a more stable heterobiaryl failed to extend the half-life beyond 30 minutes. A change of the amine group to a hydroxyl in compound 40 lead to the greatest increase in half-life, extending it by over 40 times. Since compound 15a demonstrated upregulation of the Ldlr in a hepatocyte cell line after a 48-hour treatment (Figure 13), one might assume if the compound is metabolised by the hepatocyte

microsomes in under 5 minutes then the metabolite must retain some level of activity. Many studies have demonstrated however, that hepatocyte immortalised cell lines lack a substantial set of liver-specific functions, especially major cytochrome P450 and cytochrome P450-related enzyme activities (Aninat *et al.* 2006) and therefore the half-life seen in primary mouse liver microsomes and in an immortalised cell line may vary. Harwood et al., dosed a compound in rat, very similar in structure to compound 15a, demonstrating cholesterol lowering after 6-days of daily oral dosing (Harwood *et al.* 1997). As the compound only differs by ethyl groups instead of methyl groups on the tertiary amine, it is possible this compound also has a very short half-life, however it was never analysed in their study. The fact the compound used by Harwood et al., does have a cholesterol lowering effect, would suggest if it did share a similar pharmacokinetic profile, its metabolites are active, of course this requires further investigation to confirm this. As their 4-(diethylaminoethoxy) stilbene demonstrated efficacy *in vivo* at 40mg/kg, this was the dose chosen as the starting point for our *in vivo* studies.

Previously in our hands, we saw that pravastatin was able to cause an increase in human *LDLR* promoter activity when dosed in mouse (Hibbitt *et al.* 2010). Pravastatin, which, unlike other statins is the biologically active form, has a half-life of 1-3 hours (Lennernäs and Fager 1997) and almost half is recovered unmodified in the urine. Our compound displayed a similar half-life between 1.5-3 hours depending on the vehicle, with a certain metabolite seemingly present much longer (Figure 23C-F). Thus the SSIs pharmacokinetic profile seems comparable to currently approved cholesterol biosynthesis inhibitors. Future work will involve purifying the metabolite and trying to identify whether it also has LDLR modulating activity.

In our first *in vivo* study we found that β-cyclodextrin alone gave an increase in luciferase expression. Cyclodextrins are naturally occurring cyclic oligosaccharides derived from the enzymatic conversion of starch. They contain a hydrophilic outer shell and a hydrophobic inner core, allowing them to solubilise very lipophilic compounds into aqueous solutions (Thompson 1997). In particular, cyclodextrins solubilise cholesterol and other sterol molecules and have routinely been shown to modulate cholesterol content within a cell, as they are able to

transport cholesterol across membranes (Christian *et al.* 1997). Recently, 2-hydroxy-propyl β-cyclodextrin has been shown to have efficacy in a Niemann–Pick type C disease mouse model (Liu *et al.* 2009). In this disease, cholesterol builds up in the lysosomes as mutations in Niemann–Pick type C1 protein, hinder it from transporting cholesterol across the lysosomal membrane and into the cytosol. 2-hydroxy-propyl β-cyclodextrin at concentrations similar to what we used in our study, transported the cholesterol out of the lysosomes relieving the cholesterol burden. 2-hydroxy-propyl β-cyclodextrin has gone on to be approved for compassionate-use treatment in a small number of children with NPC disease (Fomby and Cherlin 2011). As 2-hydroxy-propyl β-cyclodextrin is able to modulate the cholesterol content of a hepatocyte (Liu *et al.* 2010), and the human *LDLR* promoter is regulated by intracellular cholesterol content, it is entirely possible that it was the β-cyclodextrin itself that caused the increase in luciferase expression.

In the future, our *in vivo* reporter model could be used to screen an array of small molecules for their ability to drive the human *LDLR* promoter in a mammalian system. This platform provides a quick and effective method to eliminate any compounds that do not carry their *in vitro* efficacy over to an *in vivo* system. It is well known that statins do not have the same effect in rodents as they show in man, with some studies actually showing a decrease in Ldlr expression and no change in total cholesterol (Rashid *et al.* 2005) after statin administration. Similar findings have also been reported in rats, where administration of different statins resulted in a decrease in Ldlr expression (Ness, Zhao and Lopez 1996). Other studies have reported statin administration even in hypercholesterolaemic mice has failed to lower LDL-cholesterol (Aprahamian *et al.* 2006). This is not what is seen in humans, where administration of pravastatin has been shown to increase LDLR expression up to 180% (Shulman and et al 2016). This in part could be attributed to the differences in how rodents and humans carry their cholesterol (Camus *et al.* 1983) (discussed in detail in section 4.1.1), with mice carrying most of their cholesterol in the high-density lipoprotein (HDL) fraction. Other differences due to the lack of certain proteins such as Cholesteryl Ester Transfer Protein (Guyard-Dangremont *et al.* 1998) in mouse or inclusion of Apolipoprotein-48 (Greeve *et al.* 1993) into LDL particles result in a decreased shuttling of cholesterol ester to the LDL particles and enhanced clearance of LDL particles

respectively. Inhibitors of cholesterol biosynthesis show efficacy in larger mammals such as guinea pig (Matsunaga *et al.* 1991) or rabbit (Krause and Newton 1995; Bocan *et al.* 1998), Our reporter system could provide a more economical and higher throughput system, to quickly assess *in vivo* efficacy, before embarking on a longer term study in a larger mammalian species.

Chapter 5: Characterisation of a novel non-viral combinatorial vector in an animal model of familial hypercholesterolaemia

5.1 Introduction

5.1.1 Development of the p*LDLR-LDLR* 2nd generation mini-gene vector

Earlier work in this laboratory had cloned out from a BAC library the whole 135 kb genomic DNA *LDLR* locus, containing the 45 kb *LDLR,* along with all promoter and regulatory elements required for complete physiological regulation and processing (Wade-Martins et al. 2003). These studies demonstrated that *in vitro* delivery of the whole genomic locus of the *LDLR*, leads to full and long-term physiological complementation of the LDLR deficit in *Ldlr* knockout cell lines and primary FH patient fibroblasts. The locus was delivered in the only viral vector system able to accommodate the 154 kb genomic locus, the gutless HSV-1 amplicon. Previous studies have shown that i*n vivo* delivery to the liver using HSV-1 amplicons results in poor transduction, with less than 2% of hepatocytes expressing the transgene after systemic administration (Fraefel *et al.* 1997).

A non-viral gene delivery approach was then adopted using hydrodynamic delivery (section 4.1.3), which transfects between 25-40% of hepatocytes after a single administration (Zhang, Budker and Wolff 1999; Suda *et al.* 2007). The 135 kb genomic insert was cloned into a pEHZ plasmid (Figure 28A) containing the EBV retention elements (discussed in section 1.7.2.2) and delivered to MF-1 mouse liver. Expression of the *LDLR* transgene was detected up to 4 months post-delivery whilst Lac Z expression under the control of a CMV promoter from the same plasmid could only be detected up to 30 days. Expression from strong heterologous promoters is known to be silenced and highlights the use of large genomic DNA vectors for prolonged expression. Unfortunately, due to the very large size of the BAC vector, not enough hepatocytes could be transfected to provide functional complementation in the *Ldlr*$^{-/-}$ mouse.

To increase the delivery efficiency of the vector a second generation mini gene vector was developed termed p*LDLR-LDLR* (Figure 28B) (Hibbitt *et al.* 2010). A 10 kb piece of genomic DNA 5′ to the *LDLR* gene which includes: all three of the SREs needed for physiological control, a portion of the first coding exon (exon 2), the previous noncoding (exon 1), the 5'-untranslated region and ~8 kb of upstream sequence that also may or may not be essential for physiological control. 10 kb is also a large enough size of genomic DNA to allow the episomal retention elements to function, aiding retention and expression as discussed previously (section 1.7.2.2).

The 10 kb promoter element was cloned in to drive expression of the *LDLR* cDNA, thus reducing the size of the new plasmid to 30 kb. A second plasmid was generated where by the same excised 10 kb promoter element was used to drive expression of the luciferase gene (p*LDLR-Luc*, Figure 28C). The 10 kb promoter element conferred physiological regulation *in vitro*, demonstrating sterol and statin responsive internalisation of Dil-LDL in primary FH patient fibroblasts. *In vivo* luciferase expression, under the control of the 10 kb promoter confirmed the physiological regulation was maintained in mouse liver, after delivery of the p*LDLR-Luc*. Finally, co-localized LDLR and Lac Z expression could be detected up to 9 months post-delivery in mouse liver cells after p*LDLR-LDLR* delivery.

5.1.2 Development of the p*LDLR-LDLR*-miR82 3rd generation mini-gene vector

To further enhance the expression of the *LDLR* from the p*LDLR-LDLR* plasmid and take advantage of having the native transcription factors driving expression of the *LDLR*, an siRNA targeting *Hmgcr* was used. The siRNA, co-delivered with the p*LDLR-Luc* plasmid was able to drive expression of the 10 kb *LDLR* promoter, 300-fold greater than when the plasmid was delivered alone (Hibbitt *et al.* 2012). Four different siRNA sequences targeting *Hmgcr* were cloned into a BlockIT polII miRNA expression system (Invitrogen), as miRNA expression systems are a safer option for RNAi *in vivo* (Boudreau, Martins and Davidson 2009). The miRNA expression vectors were co-delivered with the p*LDLR-Luc* plasmid to MF-1 mice and again luciferase expression in mice receiving both miRNA and p*LDLR-Luc* plasmid was 12-fold higher, when compared to mice receiving p*LDLR-Luc* plasmid

alone. The effect translated to a phenotypic effect, with *Ldlr*$^{-/-}$ mice having significantly lower LDL-cholesterol levels after delivery of the p*LDLR-LDLR* plasmid after two weeks. Lowering of LDL-cholesterol was further enhanced with the co-delivery of the four miRNA expression vectors, indicating that a combinatorial therapy involving targeted knockdown of *Hmgcr,* coupled with physiologically functioning gene replacement may result in greater therapeutic efficacy.

Dr Lawrence Tam combined both arms of the gene therapy, by annealing and embedding the most potent of the siRNA sequences (si82) in an artificial miRNA scaffold within the pBlockit-miR vector (Invitrogen) to generate pmiR82. The siRNA sequence targeted the 3' untranslated region of the *Hmgcr* transcript. A non-targeting miR control containing scrambled sequence was also generated (pmiRNT). Delivery of the pmiR82 into mice resulted in a significant knockdown of Hmgcr transcripts in C57/BL6 mice and a subsequent significant upregulation of the Ldlr, when compared to pmiRNT control mice. Following validation of the pmiR82 knock-down vector, a combinatorial vector was developed where by the pmiR82 elements were cloned into the original p*LDLR-LDLR* plasmid, generating the vector p*LDLR-LDLR*-miR82 (*LDLR*-Hmgcr-RNAi) (Figure 28D). Similarly, a control vector expressing a scrambled non-targeting (NT) miRNA sequence was also generated (p*LDLR-LDLR*-miRNT). Transfection of p*LDLR-LDLR*-miR82 into mouse Hepa1-6 cells led to significantly higher levels of human LDLR transgene expression compared to p*LDLR-LDLR* using species-specific qRT-PCR analysis (Figure 29A). p*LDLR-LDLR*-miR82 delivery in mice resulted in significantly reduced levels of Hmgcr protein as compared to control mice injected with the p*LDLR-LDLR*-miRNT plasmid (Figure 29B). Furthermore, LDLR protein levels were found to be significantly increased in p*LDLR-LDLR*-miR82 injected animals compared with controls (Figure 29C). This data confirmed the ability of the combined vector to efficiently suppress endogenous mouse Hmgcr expression, driving induction of the *LDLR* promoter (Work carried out by Dr Lawrence Tam).

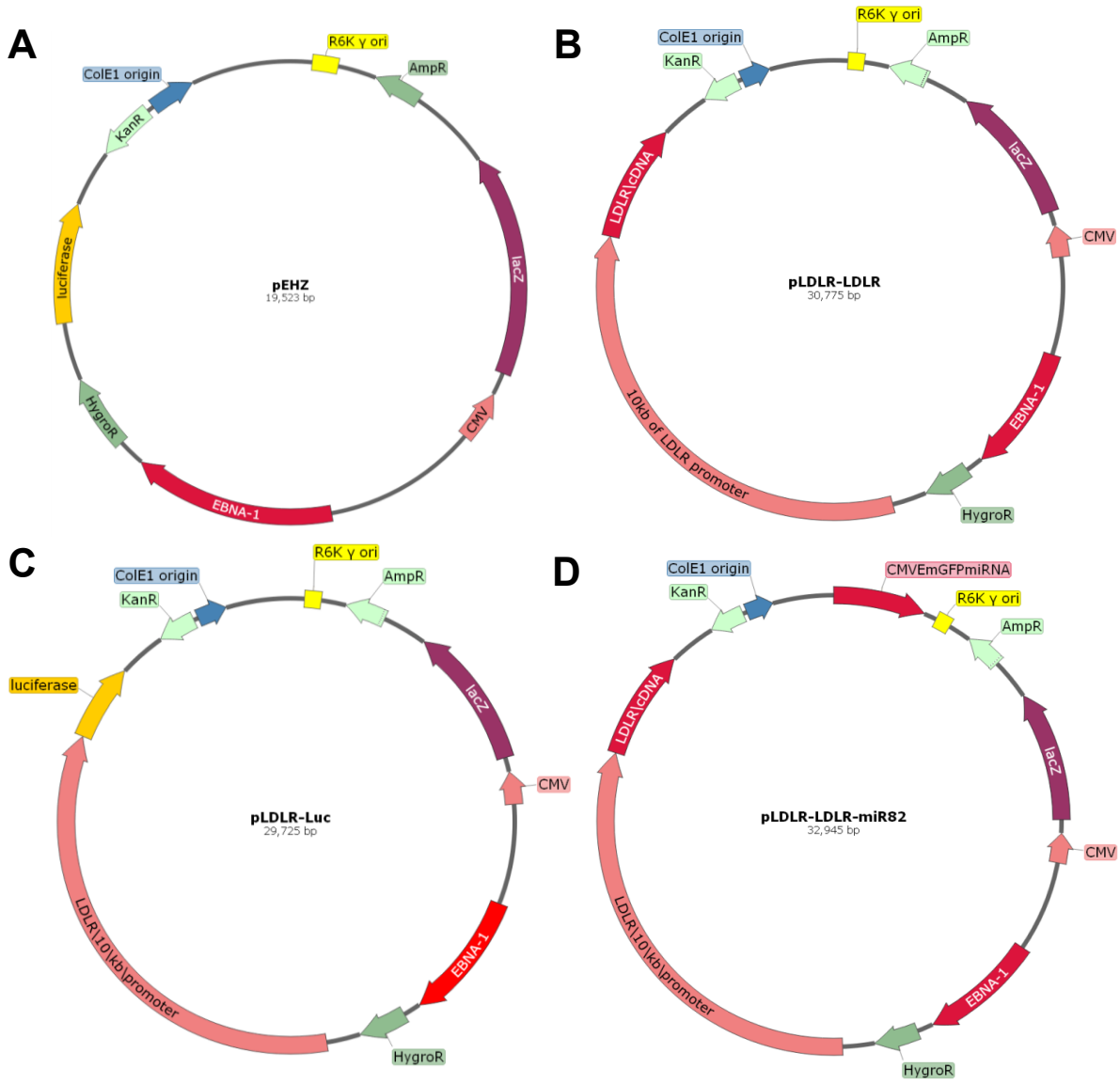


Figure 28 - Vector maps for pEHZ (**A**), p*LDLR-LDLR* (**B**), p*LDLR-Luc* (**C**) and p*LDLR-LDLR*-miR82 (**D**)

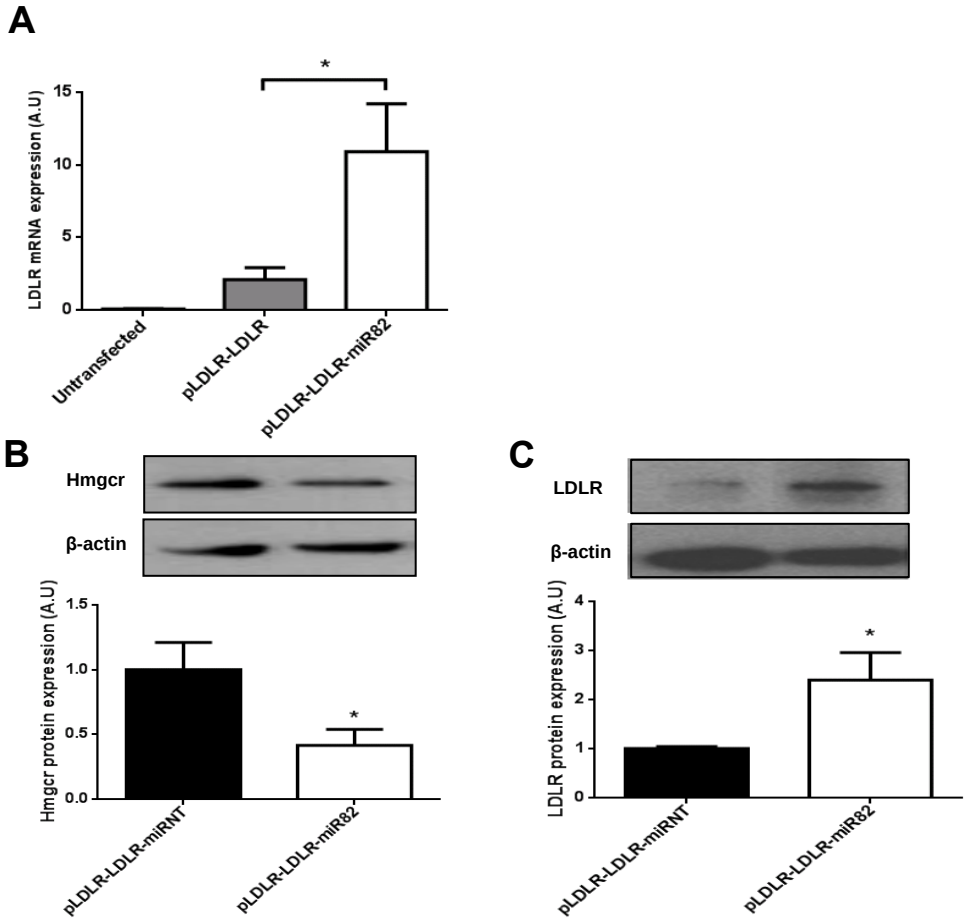


Figure 29 - **The p*LDLR-LDLR*-miR82 vector reduces *Hmgcr* and elevates LDLR expression *in vitro* and *in vivo.***

Evaluation of gene expression in Hepa1-6 liver cells *in vitro* and gene and protein expression in *Ldlr*$^{-/-}$ mice *in vivo* after p*LDLR-LDLR*-miR82 vector delivery. (A) Hepa1-6 cells transfected with p*LDLR-LDLR*-miR82 show significantly higher levels of human *LDLR* mRNA expression as compared to p*LDLR-LDLR* vector alone. *Ldlr*$^{-/-}$ mice injected with p*LDLR-LDLR*-miR82 show (B) decreased Hmgcr protein expression, and (C) increased LDLR protein expression, as compared to control. Error bars denote SEM. n=3 *$P < 0.05$ (One-way ANOVA with Bonferroni post hoc analysis (A) Student's *t*-test (B,C). (All work carried out by Dr Lawrence Tam)

5.1.3 Animal models of familial hypercholesterolaemia

The larger animal models of FH much closer resemble the phenotype seen in humans. Of these the most commonly used is the Watanabe heritable hyperlipidemic (WHHL) rabbit, which exhibits a natural in-born mutation in four amino acids in the ligand binding domain of the LDLR (Watanabe 1980; Yamamoto *et al.* 1986). The mutation results in improper trafficking of the LDLR to the cell surface and renders it almost unable to bind LDLR. The WHHL rabbit develops severe hypercholesterolaemia, through elevated levels of LDL and atherosclerotic plaques rich in foam cells and xanthomas. Another larger animal model which is used with an ever increasing frequency is the porcine model. Which has a natural in-born mutation in the ApoB protein resulting in delayed LDL clearance (Prescott *et al.* 1991). Recently, as genome editing of larger species has progressed, the *Ldlr*$^{-/-}$ Yucatan miniature pig has been developed (Davis *et al.* 2014). Both models present severe hypercholesterolemia resulting in atherosclerotic lesions in the coronary arteries and abdominal aorta that resemble human atherosclerosis.

In contrast to the mouse, it is expensive to feed and maintain conditions for modern day animal husbandry and often there is a much longer process for disease to develop in the larger animal models. For this reason, much of the early, pre-clinical therapy development is carried out in the *Ldlr*$^{-/-}$ mouse. The *Ldlr*$^{-/-}$ mouse was developed in 1993 through homologous recombination of a neomycin cassette into exon 4, a non-functional truncated form of the protein is produced (Ishibashi *et al.* 1993). The *Ldlr*$^{-/-}$ mouse does not develop atherosclerosis without diet modification until very late in life however (Teupser, Persky and Breslow 2003). This is due to a few differences between how mice and humans carry and process the different lipoprotein fractions. Mice carry most of their cholesterol in the HDL fraction and unlike humans do not show anywhere near the heterogeneity in different subclasses of HDL particle (Kapourchali *et al.* 2014). Mice also do not express CETP, which may go part of the way to explain why they express a lot more cholesterol in the HDL fraction (Barter *et al.* 2003b). Additionally, in the mouse liver ApoB mRNA is extensively edited by Apobec-1

generating ApoB-48-containing lipoproteins (Greeve *et al.* 1993). ApoB-48 lipoproteins are rich in ApoE and much more rapidly cleared from the circulation. Humans only express apobec-1 in the intestine so only lipoproteins formed in the intestine express ApoB-48. To try and humanize the lipoprotein profile of the mouse a *Ldlr*$^{-/-}$*apobec-1*$^{-/-}$ mouse was developed (Powell-Braxton *et al.* 1998). This reverts the mouse to carrying most of its cholesterol in the ApoB-100 carrying lipoproteins and makes it susceptible to developing atherosclerosis with no diet intervention. Other groups have taken this further knocking in a human ApoB$^{100/100}$ transgene (Kassim *et al.* 2013) resulting in an even more aggressive development of atherosclerosis.

In the *Ldlr*$^{-/-}$ mouse different modified diets have been used to induce atherosclerosis. The most common diet is the western type diet (WTD) which consists of 21% milk fat and 0.2% total cholesterol (Getz and Reardon 2012), though quite a few variations on this are used so not all experiments are standardised or comparable between laboratories. In the scheme of FH however these diets do not just induce hypercholesterolaemia but other co-commitant metabolic disorders such as hypertriglyceridaemia and hyperinsulinaemia. They will independently drive atherosclerosis in the mouse and importantly in regard to FH, are not found phenotypes present in HoFH patients. A modified high cholesterol (HC) diet was used in *Ldlr*$^{-/-}$ mice by Hartvisgen et al., in comparison to the most commonly used WTD. The HC-diet was able to independently drive atherogenesis and induce a comparable hypercholesterolaemia, producing a mouse model with a closer lipid profile to an FH patient (Hartvigsen *et al.* 2007). For these studies, we investigated the use of the HC-diet to develop a more representative model of FH, for which we could then test the efficacy of our combinatorial vector in its ability to maintain LDLR expression, knockdown *Hmgcr*, lower plasma cholesterol and slow the progression of atherosclerosis.

5.2 Results

5.2.1 Characterisation of a 1% high cholesterol diet as a model of familial hypercholesterolaemia

We implemented a HC-diet to induce hypercholesterolaemia in *Ldlr*$^{-/-}$ mice to provide a better FH model in which to test our gene therapy approach. We compared *Ldlr*$^{-/-}$ and wild-type C57BL/6J mice fed either a regular chow (RC) or a HC-diet for 12 weeks to assess the impact of high cholesterol feeding on plasma lipid levels. We chose a 1% cholesterol-enriched chow diet previously described (Hartvigsen *et al.* 2007) which showed predominant elevation of LDL cholesterol in *Ldlr*$^{-/-}$ mice. Blood was collected from mice maintained on a regular or HC-diet for 0, 4, 8 and 12 weeks for plasma lipid analysis. Figure 30A shows that total plasma cholesterol level increased by up to 5 fold in *Ldlr*$^{-/-}$ mice after only 4 weeks of HC feeding, and were maintained at the same elevated level up to 12 weeks. Similarly, LDL-C levels were elevated by up to 6-fold after 4 weeks of HC-feeding in *Ldlr*$^{-/-}$ mice (Figure 30B), which persisted until the end of experiment. The average total and LDL cholesterol level induced by the HC-diet was significantly higher than the regular chow fed *Ldlr*$^{-/-}$ mice and the C57BL/6J mice fed either a regular chow or a HC-diet. The *Ldlr*$^{-/-}$ mice also had significantly higher LDL-cholesterol than the C57BL/6J mice fed either diet. We did not observe any differences in HDL-cholesterol, triglyceride or glucose levels between all groups of animals after 12 weeks of HC-feeding (Figure 30C-E), illustrating that the HC-diet has minimal side-effects on other metabolic parameters. *Ldlr*$^{-/-}$ mice fed a HC-diet for 12-weeks developed atherosclerotic plaques, in the aortic root when stained by Masson's Trichrome (Figure 30F-G). There was a significant increase in the size of the atherosclerotic plaques between Ldlr$^{-/-}$ mice fed a HC and RC-diet in the aortic root, demonstrating this model displays an accelerated atherogenic phenotype.

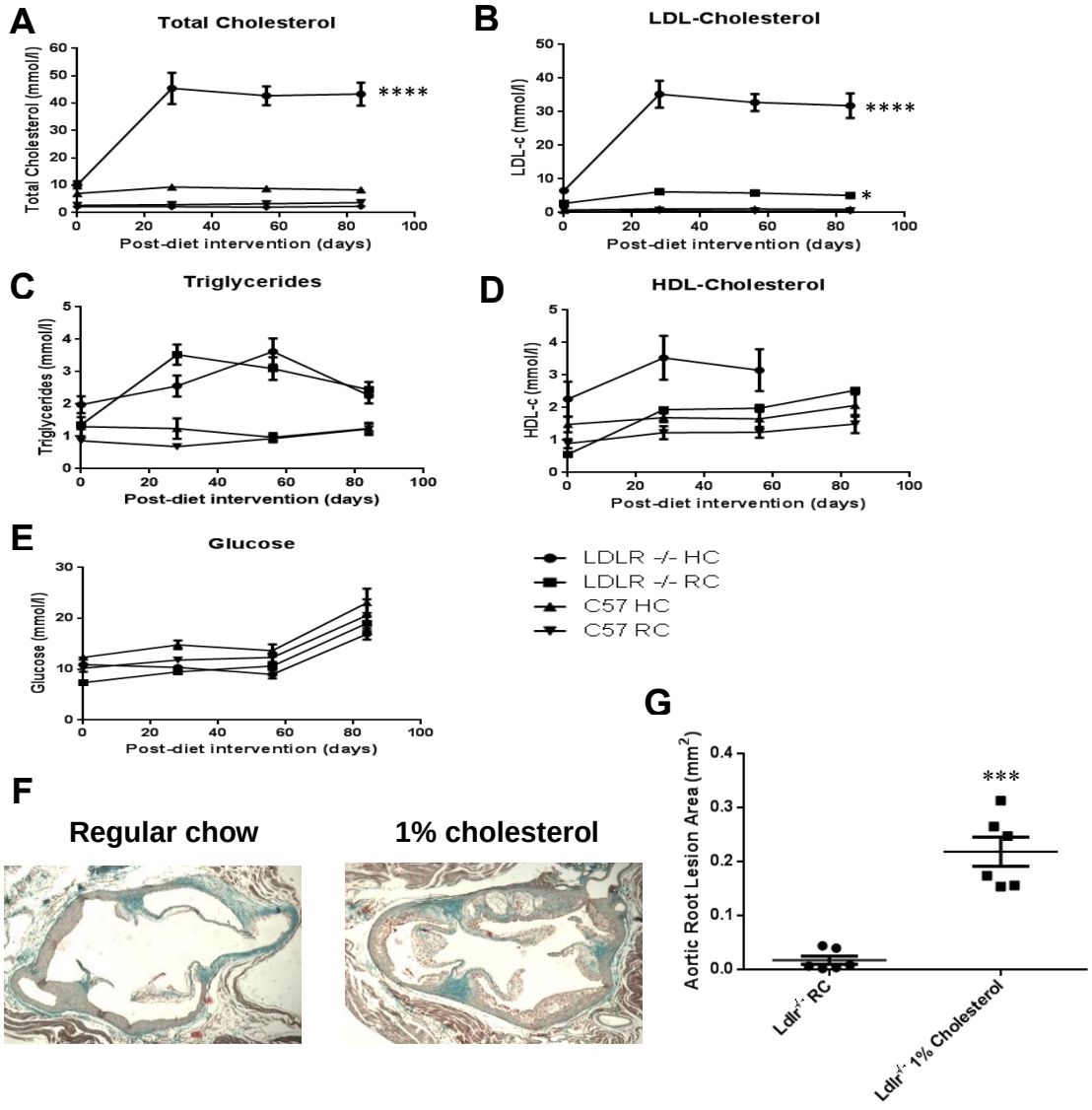


Figure 30 - A 1% cholesterol diet causes hypercholesterolaemia and atherogenesis in a *Ldlr*$^{-/-}$ male mice after 12- weeks diet intervention.

Total (**A**) and LDL (**B**) cholesterol levels are significantly elevated in *Ldlr*$^{-/-}$ mice fed a 1% HC-diet for 12-weeks compared to *Ldlr*$^{-/-}$ mice fed a RC-diet or C57/BL6 mice fed a HC-diet or RC-diet. No significant difference was detected in other metabolic parameters including triglycerides (**C**), HDL cholesterol (**D**) or glucose (**E**). Significance represents the average total or LDL-cholesterol level obtained throughout the study compared between groups. Representative images of Masson Trichrome staining, showing aortic root atherosclerosis after 12-week 1% HC-diet or RC feeding in *Ldlr*$^{-/-}$ mice (**F**). 1% HC feeding significantly increased atherosclerotic plaque development in the aortic root compared to RC-fed mice (**G**). *P<0.05 **P<0.01, ***P<0.001, ****P<0.0001. Error bars denote SEM. n=5-6 per group. One-way ANOVA with Dunnetts post hoc analysis (**A,B**) Students *t*-test (**G**). (Work carried out in collaboration with Dr Lawrence Tam)

5.2.2 *LDLR*-Hmgcr-RNAi results in lipid lowering and sustained LDLR upregulation in 1% HC-fed *Ldlr*$^{-/-}$ mice

We conducted a short-term proof of principle experiment to determine the lipid lowering property of p*LDLR-LDLR*-miR82 in mice fed a 1% HC-diet. Eight week old *Ldlr*$^{-/-}$ mice were switched from regular chow to the HC-diet 2 weeks prior to vector administration to induce hypercholesterolaemia. Two-weeks after diet-switch, blood was collected from all *Ldlr*$^{-/-}$ mice for plasma analysis, and 72 hours later, all animals received hydrodynamic injection of 50 µg of either p*LDLR-LDLR*, p*LDLR-LDLR*-miRNT or p*LDLR-LDLR*-miR82 (n=6 per group). An uninjected group was also included as a negative control. 2 weeks post-injection animals were bled for plasma analysis and four weeks post-injection animals were sacrificed for tissue and plasma lipid analysis. Western blot analysis performed on liver lysates from p*LDLR-LDLR*-miR82 injected animals showed a significant reduction in Hmgcr protein expression, as compared to uninjected animals, and groups injected with p*LDLR-LDLR*-miRNT and p*LDLR-LDLR* vector alone (Figure 31A). Furthermore, LDLR protein levels were found to be markedly increased in liver lysates of animals injected with p*LDLR-LDLR*-miR82 as compared to uninjected animals, as well as cohorts injected with p*LDLR-LDLR*-miRNT and p*LDLR-LDLR* vector alone (Figure 31B) (Tissue harvesting and processing was carried out by Mr Alastair Kerr, Western blot analysis was carried out by Dr Lawrence Tam).

The impact of *LDLR* vectors on lipid parameters in HC-fed *Ldlr*$^{-/-}$ mice was examined by plasma lipid analysis. *Ldlr*$^{-/-}$ mice developed a hypercholesterolaemic phenotype after two weeks of HC-feeding. This was attenuated by the administration of p*LDLR-LDLR*-miR82 which resulted in a progressive decline of both total cholesterol and LDL-cholesterol over a 4-week period compared to uninjected animals (Figure 32A). In animals treated with p*LDLR-LDLR*-miR82, there was a significant lipid lowering of ~50% as compared to uninjected animals (Figure 32A). We did not observe any marked changes in HDL-cholesterol and triglyceride levels between all experimental groups (Figure 32B). Potential liver injury caused by the hydrodynamic procedure on animals was assessed by analysing plasma levels of alanine aminotransferase (ALT) and aspartate aminotransferase (AST) (Figure 32C). There were no significant differences in

ALT or AST levels between treatment groups at 2 and 4-weeks post-delivery. Overall, these data demonstrate that a single injection of the p*LDLR-LDLR*-miR82 vector can lead to profound reduction of plasma lipid through induction of the LDLR promoter via targeted knockdown of Hmgcr

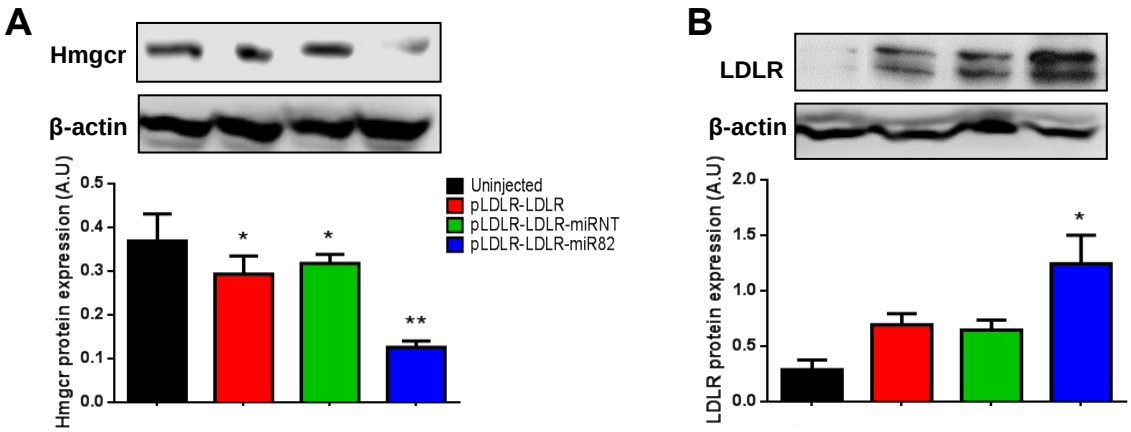


Figure 31 – p*LDLR-LDLR*-miR82 decreases Hmgcr and subsequently increases LDLR expression 4 weeks post delivery

Representative immunoblots showing vector mediated effects on Hmgcr and LDLR protein in livers of 1% HC-fed *Ldlr*$^{-/-}$ mice. Hmgcr expression was downregulated in mice treated with all three therapeutic vectors (**A**). LDLR protein expression was subsequently significantly increased in liver tissues that had had the additional miR82 suppression of endogenous *Hmgcr* four weeks post-delivery of vectors (**B**). Significance represents each treatment group compared to uninjected control group. *P<0.05 **P<0.01. Error bars denote SEM. n=5-6 per group One-way ANOVA with Dunnetts post hoc analysis. (Liver tissue harvested and stored by Alastair Kerr, western blot analysis carried out by Dr Lawrence Tam)

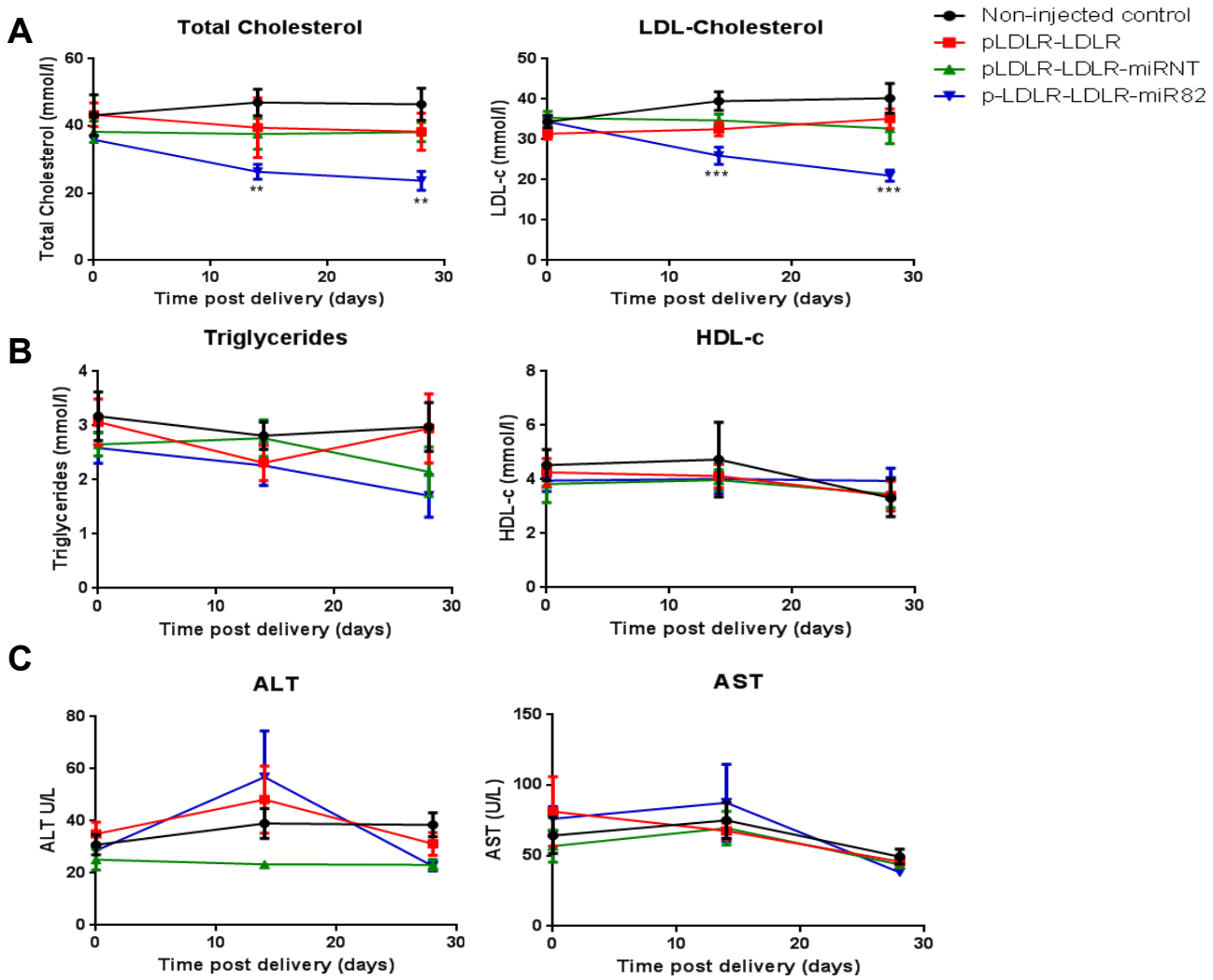


Figure 32 - p*LDLR-LDLR*-miR82 significantly reduces total and LDL cholesterol in a mouse model of FH.

Lipid and hepatic safety profiles were analysed in *Ldlr*$^{-/-}$ mice fed a 1% HC-diet, for two weeks prior to vector delivery, measurements were made 72 hours prior and two and four weeks post-delivery. Total and LDL-cholesterol were significantly decreased by p*LDLR-LDLR*-miR82 administration for the duration of the four-week study (**A**). No significant differences between any of the groups were detected in other metabolic parameters (**B**) or liver transaminases (**C**). *P<0.05 **P<0.01. Error bars denote SEM. n=5-6 per group. One-way ANOVA with Dunnetts post hoc analysis.

Atherosclerotic plaque development was assessed in the whole aorta using *en face* analysis and in the aortic root using Masson's trichrome staining. In addition, Galectin-3 a marker of macrophage infiltration into the plaque was also assessed, as this has been suggested to be an early marker of atherosclerotic plaque progression (Arar *et al.* 1998; Douglas *et al.* 2012). After 6-weeks of HC-diet feeding, only a small amount of atherosclerotic plaque formation had occurred in the aortic arch and root. There were no detectable differences between the uninjected and vector treated groups in the aortic arch (Figure 33) or aortic root (Figure 34A/C). There was a trend to a slowing in the progression of atherosclerosis in the p*LDLR-LDLR*-miR82 group, however this study was underpowered to be able to confirm any difference. Galectin-3 within the aortic arch also failed to detect any significant differences between any of the groups (Figure 34B/D). 6-weeks of HC-diet feeding and 4-weeks of therapeutic intervention is a relatively short amount of time to have a therapeutic effect on atherosclerotic development and so longer term studies were carried out to assess the effect of vectors on atherogenesis.

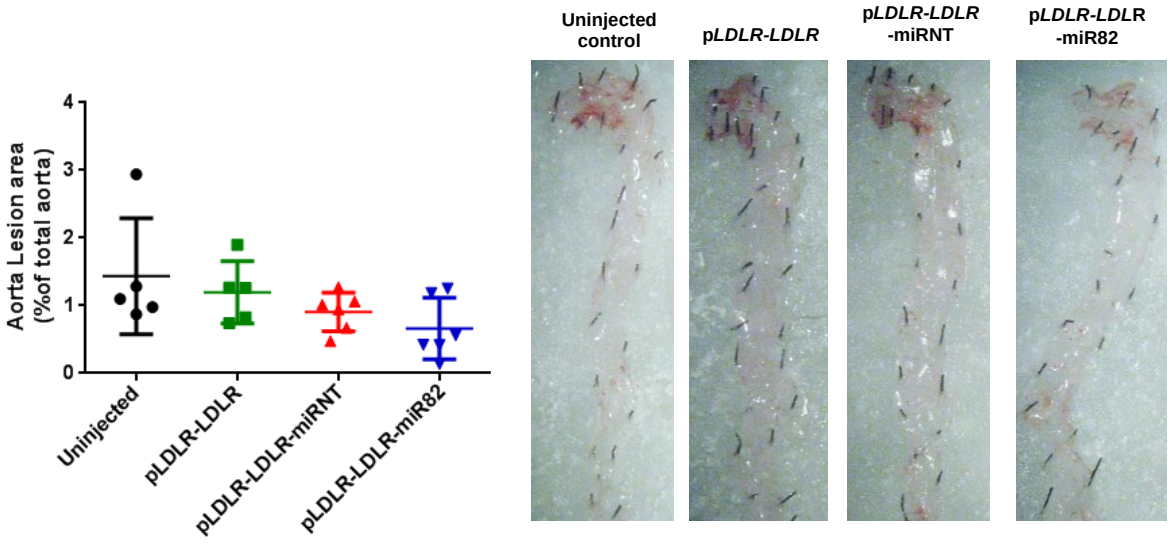


Figure 33 - LDLR mini-gene vectors had no significant effect on atherosclerotic plaque progression in the aortic arch after 4-weeks therapeutic intervention.

Atherosclerotic plaque size was assessed in the arotic arch of *Ldlr*$^{-/-}$ mice fed a 1% HC-diet and treated with either p*LDLR-LDLR,* p*LDLR-LDLR*-miRNT or p*LDLR-LDLR*-mir82 for 4-weeks. A representative image from each group depicts only a small amount of atherogenesis occurring with the arotic arch. Quantitation of the atherosclerotic plaque development demonstrates no detectable difference between any of the treatment groups.

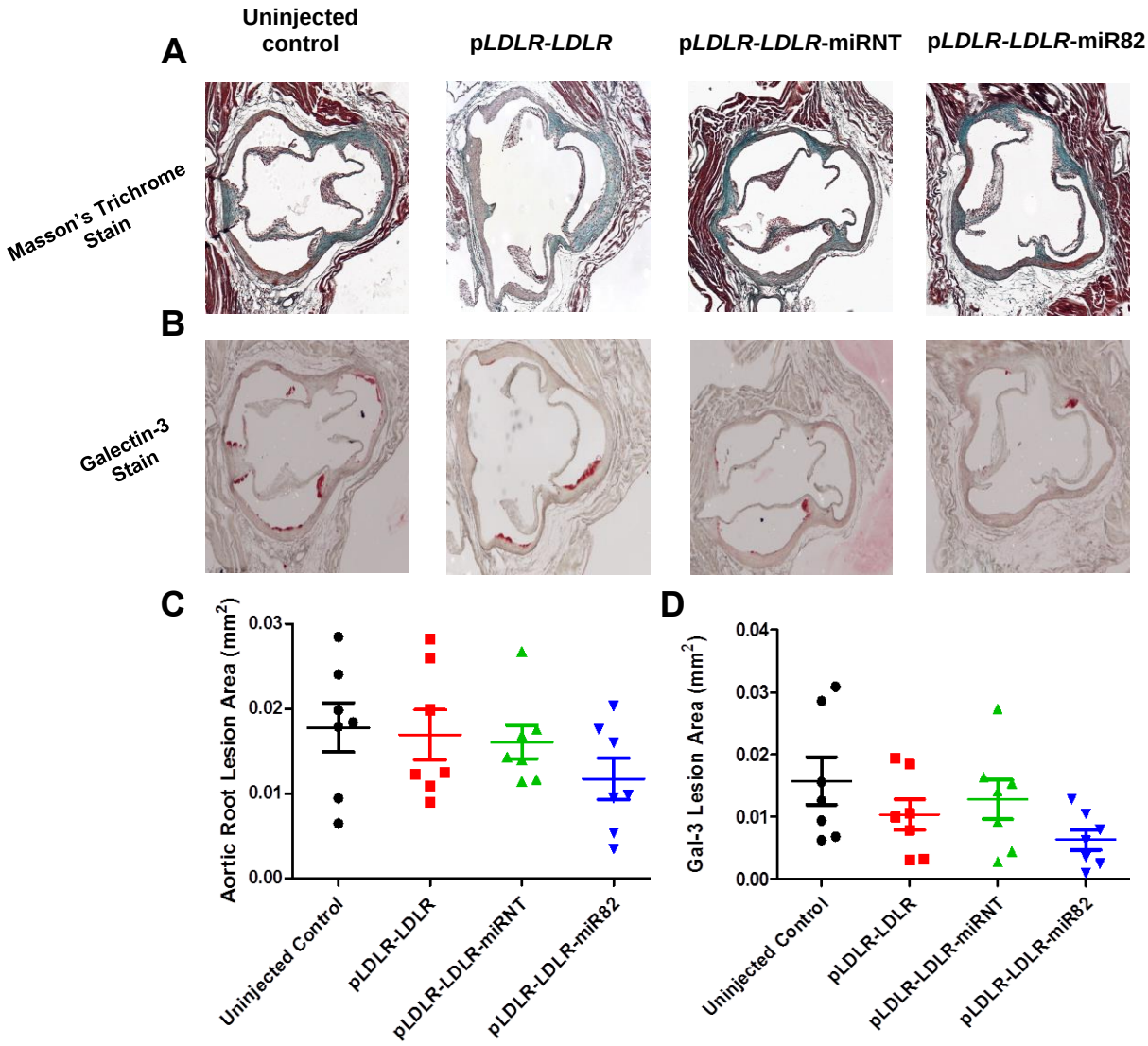


Figure 34 - *LDLR* mini-gene vectors had no significant effect on atherosclerotic plaque progression in the aortic root or macrophage infiltration after 4-weeks therapeutic intervention.

Atherosclerotic plaque progression and macrophage recruitment was assessed in the aortic root of *Ldlr*$^{-/-}$ mice treated for 4-weeks with the therapeutic vectors p*LDLR-LDLR,* p*LDLR-LDLR*-miRNT or p*LDLR-LDLR*-mir82. Representative images from each group after Masson's trichrome (**A**) and galectin-3 staining (**B**) demonstrate the little plaque formation which had occurred over this time period. Quantitation of the size of plaque formation (C) and galectin-3 infiltration (D) resulted in no significantly detectable differences between either group. Error bars denote SEM. n=5-6 per group

5.2.3 A meta-analysis of diet intervention in the *Ldlr*$^{-/-}$ mouse

To ensure any future long term studies carried out were powered towards detecting changes in atherosclerotic development in a physiologically relevant hypercholesterolaemic model, a meta-analysis of current literature involving male *Ldlr*$^{-/-}$ mice was carried out. Studies were selected by a PubMed search using the terms 'male *Ldlr*$^{-/-}$ mice' and 'cholesterol'. All recent studies which incorporated 6-14 week old male *Ldlr*$^{-/-}$ mice fed an atherogenic diet, with no pharmacological, surgical or biological intervention were included (A table of all the references used is provided below (Table 12)). Each study was binned by the average total cholesterol level achieved by the atherogenic diet throughout its duration to the nearest 10mmol/L. With each study in a category for cholesterol level experienced by the mouse, the duration of the study was plotted against the average aortic root lesion area (Figure 35). Our previous two studies were added to the meta-analysis, with no real difference observed between any cholesterol level in terms of atherosclerosis development at 6 weeks, indicating it would have been very difficult for us to detect a change at this time point. At 8-weeks diet intervention the atherosclerosis becomes accelerated in mice with the higher cholesterol levels. By 12-weeks there is discernible differences between each cholesterol banded group and the amount of atherosclerotic plaque development. Interestingly *Ldlr*$^{-/-}$ mice with cholesterol of 14.9mmol/L of cholesterol and lower seem to have a much slower atherosclerotic development than either of the other groups. In our previous study our therapeutic vector was able to reduce total cholesterol by ~45%. A future experiment would be best powered to detect a change in atherosclerotic progression by achieving a total cholesterol level between 15-29.9 mmol/L, for a duration of 12-weeks.

Paper	Title
Joven et al., 2007	The results in rodent models of atherosclerosis are not interchangeable: The influence of diet and strain
Bu et al., 2011	Impairment of the Programmed Cell Death-1 Pathway Increases Atherosclerotic Lesion Development and Inflammation
Kappus et al., 2014	Activation of Liver X Receptor Decreases Atherosclerosis in *Ldlr*$^{-/-}$ Mice in the Absence of ATP-Binding Cassette Transporters A1 and G1 in Myeloid Cells

Choi et al., 2011	5-(4-Hydroxy-2,3,5-trimethylbenzylidene) thiazolidine-2,4-dione attenuates atherosclerosis possibly by reducing monocyte recruitment to the lesion
Choi et al., 2010	Anti-atherogenic effect of BHB-TZD having inhibitory activities on cyclooxygenase and 5-lipoxygenase in hyperlipidemic mice
Caravaggio et al., 2013	Insulin-degrading enzyme deficiency in bone marrow cells increases atherosclerosis in LDL receptor-deficient mice
Han et al., 2009	Antiatherosclerotic effects of Artemisia princeps Pampanini cv. Sajabal in LDL receptor deficient mice.
Foks et al., 2011	Differential effects of regulatory T cells on the initiation and regression of atherosclerosis
Lammers et al., 2011	Macrophage Adipose Triglyceride Lipase Deficiency Attenuates Atherosclerotic Lesion Development in Low-Density Lipoprotein Receptor Knockout Mice
Choi et al., 2005	Trichostatin A exacerbates atherosclerosis in low density lipoprotein receptor-deficient mice
Netherland et al., 2010	Cannabinoid receptor type 2 (CB2) deficiency alters atherosclerotic lesion formation in hyperlipidemic *Ldlr*-null mice
Klindenberg et al., 2013	Depletion of FOXP3+ regulatory T cells promotes hypercholesterolemia and atherosclerosis
Dong et al., 1998	The combined role of P- and E-selectins in atherosclerosis.
Peng et al., 2011	A novel potent synthetic steroidal liver X receptor agonist lowers plasma cholesterol and triglycerides and reduces atherosclerosis in LDLR(-/-) mice
Methia et al., 2001	Localized reduction of atherosclerosis in von Willebrand factor-deficient mice
Tardy et al ., 2013	CER-001, a HDL-mimetic, stimulates the reverse lipid transport and atherosclerosis regression in high cholesterol diet-fed LDL-receptor deficient mice
Bu et al., 2011	Impairment of the Programmed Cell Death-1 Pathway Increases Atherosclerotic Lesion Development and Inflammation
Karasawa et al., 2011	Sterol regulatory element-binding protein-1 determines plasma remnant lipoproteins and accelerates atherosclerosis in low-density lipoprotein receptor-deficient mice.
Parks et al., 2006	Loss of the lysophosphatidylcholine effector, G2A, ameliorates aortic atherosclerosis in low-density lipoprotein receptor knockout

	mice.
Aslanian et al., 2006	Targeted disruption of the scavenger receptor and chemokine CXCL16 accelerates atherosclerosis.
Ishibashi et al., 2013	TLR3 deficiency protects against collagen degradation and medial destruction in murine atherosclerotic plaques
Foks et al., 2013	Interruption of the OX40-OX40 ligand pathway in LDL receptor-deficient mice causes regression of atherosclerosis.
Curtiss et al., 2012	Atherosclerosis induced by endogenous and exogenous toll-like receptor (TLR)1 or TLR6 agonists
Li et al., 2000	Peroxisome proliferator–activated receptor γ ligands inhibit development of atherosclerosis in LDL receptor–deficient mice
Lee et al., 2005	Cilostazol Reduces Atherosclerosis by Inhibition of Superoxide and Tumor Necrosis Factor-α Formation in Low-Density Lipoprotein Receptor-Null Mice Fed High Cholesterol
Miyazaki et al., 2011	m-Calpain induction in vascular endothelial cells on human and mouse atheromas and its roles in VE-cadherin disorganization and atherosclerosis
Teupser et al., 2004	Major reduction of atherosclerosis in fractalkine (CX3CL1)-deficient mice is at the brachiocephalic artery, not the aortic root
Ryu et al., 2012	Effect of an oral astaxanthin prodrug (CDX-085) on lipoprotein levels and progression of atherosclerosis in LDLR−/− and ApoE−/− mice
Sehayek et al .,2001	Hyodeoxycholic acid efficiently suppresses atherosclerosis formation and plasma cholesterol levels in mic
Zampolli et al., 2005	Contrasting effect of fish oil supplementation on the development of atherosclerosis in murine models
Nawrocki et al., 2010	Lack of association between adiponectin levels and atherosclerosis in mice
Ma et al., 2012	Hyperlipidemia and Atherosclerotic Lesion Development in Ldlr-Deficient Mice on a Long-Term High-Fat Diet
Zhou et al., 2012	Enhanced expression of salusin-β contributes to progression of atherosclerosis in LDL receptor deficient mice
Ketonen et al., 2008	Effects of dietary sodium on reactive oxygen species formation and endothelial dysfunction in low-density lipoprotein receptor-deficient mice on high-fat diet
Rotlan et al., 2014	Hematopoietic Akt2 deficiency attenuates the progression of atherosclerosis.

Han et al., 2009	Hepatic insulin signaling regulates VLDL secretion and atherogenesis in mice.
Meissner et al., 2011	Voluntary wheel running increases bile acid as well as cholesterol excretion and decreases atherosclerosis in hypercholesterolemic mice
Meissner et al., 2013	Bile acid sequestration normalizes plasma cholesterol and reduces atherosclerosis in hypercholesterolemic mice. No additional effect of physical activity
Joseph et al ., 2002	Synthetic LXR ligand inhibits the development of atherosclerosis in mice
Marquart et al., 2013	Anti-miR-33 Therapy Does Not Alter the Progression of Atherosclerosis in Low-Density Lipoprotein Receptor-Deficient Mice
Wang et al., 2014	Cathepsin G activity lowers plasma LDL and reduces atherosclerosis
Lian et al., 2012	Ces3/TGH deficiency improves dyslipidemia and reduces atherosclerosis in Ldlr(-/-) mice.
Miyazaki et al., 2011	m-Calpain induction in vascular endothelial cells on human and mouse atheromas and its roles in VE-cadherin disorganization and atherosclerosis
VanderLaan et al., 2009	VLDL best predicts aortic root atherosclerosis in LDL receptor deficient mice
Netherland et al., 2010	Cannabinoid receptor type 2 (CB2) deficiency alters atherosclerotic lesion formation in hyperlipidemic Ldlr-null mice
Kappus et al., 2014	Activation of Liver X Receptor Decreases Atherosclerosis in Ldlr−/− Mice in the Absence of ATP-Binding Cassette Transporters A1 and G1 in Myeloid Cells
Peng et al., 2008	Differential anti-atherosclerotic effects in the innominate artery and aortic sinus by the liver X receptor agonist T0901317

Table 12 – Reference list of all studies included in meta-analysis of diet-intervention induced atherosclerotic lesion development.

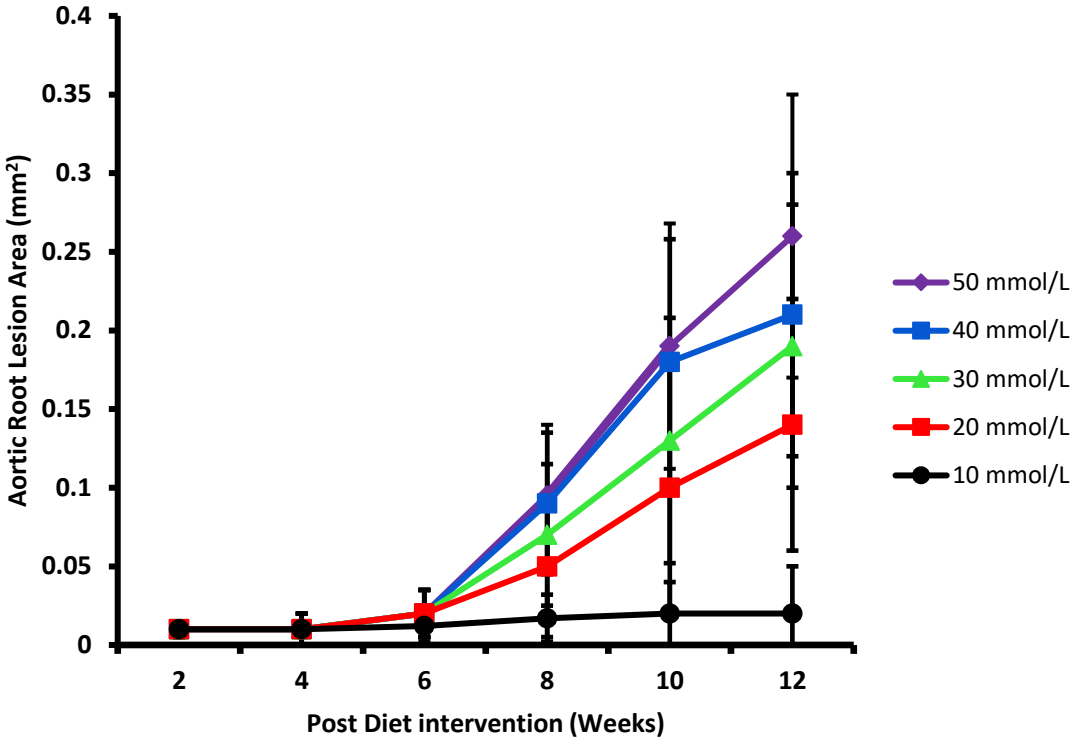


Figure 35 – A meta-analysis of aortic root atherosclerotic development, demonstrates the biggest difference in progression occurs between mice of total cholesterol levels between 10 and 20 mmol/L.

Each study involving male *Ldlr*$^{-/-}$ mice fed an atherogenic diet was separated into the average total cholesterol level achieved. Aortic root lesion area was plotted against the duration of the study. No detectable differences between the different cholesterol levels exists until 8-10 weeks of diet intervention, with 12-weeks giving the largest differences. The largest difference in lesion size between total cholesterol levels occurs in groups with 10 and 20mmol/L.

5.2.4 Characterisation of a more moderate hypercholesterolaemic diet as a model for familial hypercholesterolaemia

Two other HC-diets of 0.5% and 0.25% cholesterol were fed to *Ldlr*$^{-/-}$ male mice for 8-weeks alongside the 1% HC and RC-diet control group. Mouse weights were monitored and plasma was taken for lipid analysis at day 0, 14 and 56. At the end of the study the mice were sacrificed and aortic root lesion development was assessed. All three HC-diets produced a hypercholesterolaemic phenotype in the mice, with all three diets leading to a significantly higher level of total and LDL cholesterol experienced throughout the study compared to RC fed mice (Figure 36A-B). As the percentage of cholesterol within the diet was titrated down in

parallel was the total and LDL-cholesterol levels. No significant differences were observed in any other metabolic parameters measured such as HDL-cholesterol, triglycerides, and glucose (Figure 36C-F). Once again highlighting the fact that no other metabolic disorders such as hypertriglyceridemia or hyperinsulinemia are induced. There were no significant differences in the weights of the mice as a result of the atherogenic diets. Atherosclerotic lesion size in mice fed the 0.25 and 0.5% HC-diet was significantly increased in both groups compared to the RC-fed mice (Figure 37). As a result, the 0.25% HC-diet was chosen to be used for a future long term study as it produced a more physiological hypercholesterolaemia that was still able to drive atherogenesis.

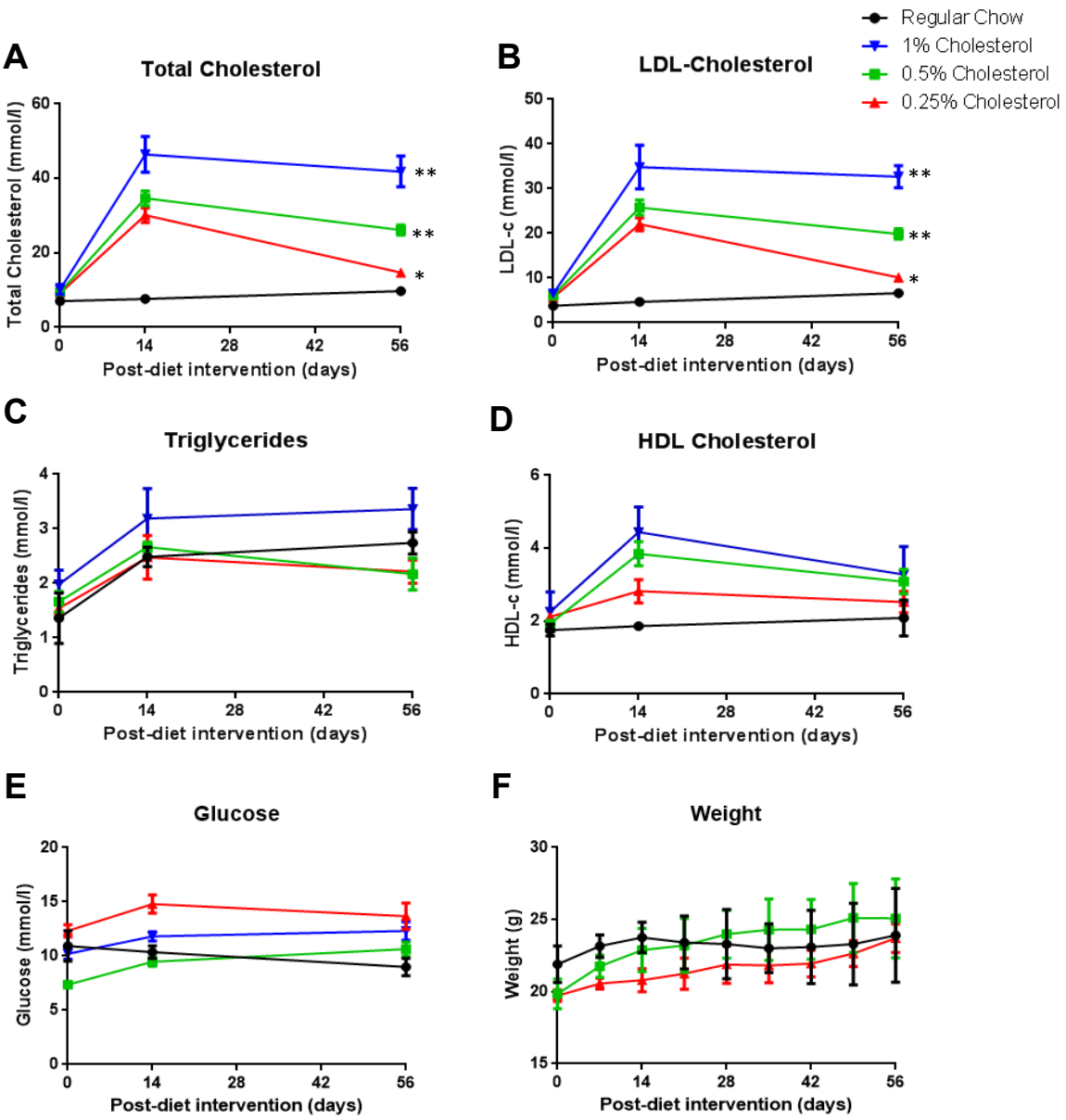


Figure 36 - A 0.25 and 0.5% cholesterol diet causes hypercholesterolaemia in *Ldlr*$^{-/-}$ male mice after 8- weeks diet intervention.

Ldlr$^{-/-}$ mice fed a 0.25, 0.5 or 1% cholesterol diet demonstrate elevated total (**A**) and LDL (**B**) cholesterol levels compared to RC-fed mice. No other metabolic parameter was elevated by the high cholesterol diets, including HDL-cholesterol (**C**), triglycerides (**D**), glucose (**E**) or weight (**F**). Significance represents the average total or LDL-cholesterol level obtained throughout the study compared between groups. *P<0.05 **P<0.01, ***P<0.001, Error bars denote SEM. n=5-6 per group. One-way ANOVA with Dunnetts post hoc analysis.

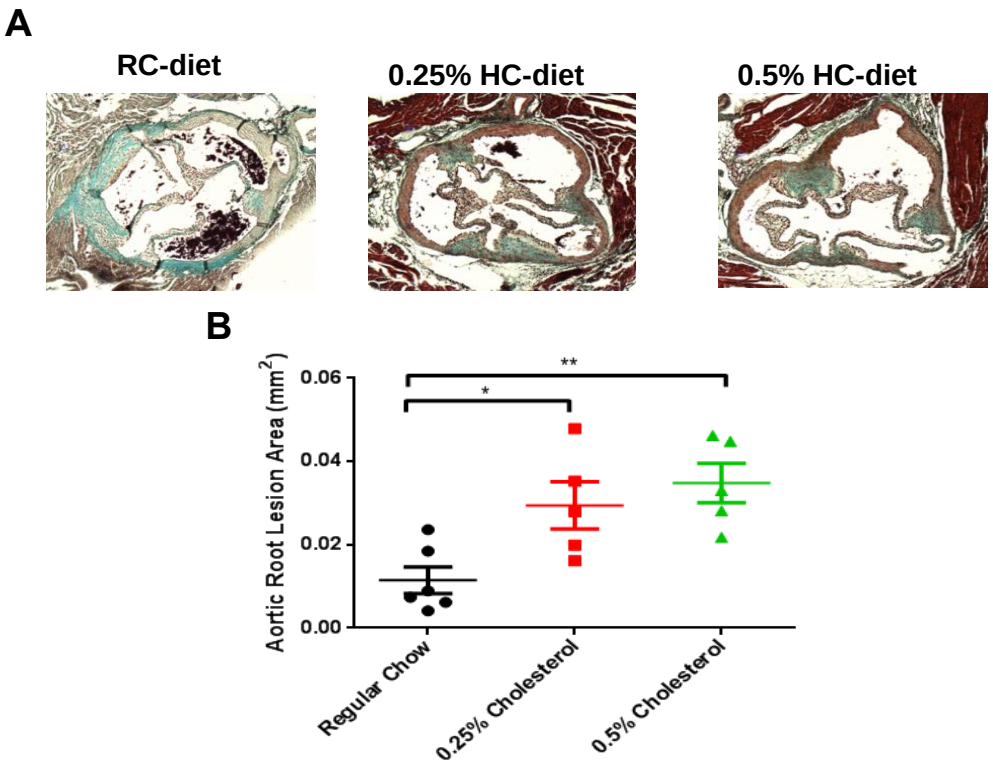


Figure 37 – A 0.25 and 0.5% high cholesterol (HC) diet is able to induce atherogenesis after 8-weeks

Effect of 0.5 and 0.25% HC-diets on atherosclerosis in *Ldlr*$^{-/-}$ mice, eight weeks post diet intervention. Representative aortic root lesions from the 0.5 and 0.25% HC-diet and RC-fed mice after eight weeks, stained using Masson Trichrome (**A**). Quantification of lesion size found that both HC-diets increase atherogenesis compared to RC-diet (**B**). *P<0.05; **P<0.01, Error bars denote SEM. n=5-6 per group. One-way ANOVA with Dunnetts post hoc analysis.

5.2.5 *LDLR-Hmgcr*-RNAi vector treatment results in long term lipid lowering and reduced atherosclerosis

To determine whether the pLDLR-LDLR-miR82 vector confers long-term lipid lowering and a subsequent reduction in atherogenesis, we conducted a 12-week study in *Ldlr*$^{-/-}$ mice. The study timeline is shown in Figure 38, where *Ldlr*$^{-/-}$ mice were hydrodynamically injected with 50 µg of either p*LDLR-LDLR*-miR82 (n=8), p*LDLR-LDLR*-miRNT (n=12), or p*LDLR-LDLR* (n=12), or an empty vector backbone, (pEHZ, lacking the *LDLR* or miRNA expression elements) (n=10). Animal numbers were calculated based on the standard deviation of the aortic lesion analysis seen using the 0.25% HC-diet in our pilot study and assuming a similar ~50% reduction in total and LDL-cholesterol with the p*LDLR-LDLR*-miR82 vector. Mice were placed on the 0.25% HC-diet on the day of hydrodynamic delivery. Each group aimed to include an n of 12 but unfortunately during the study not every mouse received a full 10% body weight injection. The transient rise in ALT and AST as shown in Figure 40 E-F with mice that received a full hydrodynamic injection was not seen in mice that did not receive the full 10% and they were therefore excluded from the study. A non-injected group of *Ldlr*$^{-/-}$ mice was maintained on a RC-diet to provide baseline lipid levels (n=3). At 2 days and at 2, 6 and 12 weeks post-injection blood samples were collected for lipid analysis. At 12 weeks, all mice were sacrificed and tissues harvested for analysis. Immunohistochemical analysis of paraffin embedded liver sections from each group revealed that the LDLR transgene expression was sustained at 12 weeks post-administration (Figure 39A top panel). No LDLR immunofluorescence signal was detected in pEHZ-injected or non-injected *Ldlr*$^{-/-}$ mice. Lipid accumulation was assessed using Oil Red O staining on frozen liver sections (Figure 39A bottom panel). None of the livers appeared steatotic from any of the treatment groups after 12-weeks, demonstrating that the expression of the LDLR did not cause pathological lipid deposits in the hepatocytes, representative images from each group are shown. To determine whether the plasmids had remained intact and as non-integrating episomes, plasmid rescue into bacteria was performed from liver tissue. Intact plasmid was recovered from ~80% of mice injected with vectors with each lane representing plasmid recovered from an individual mouse (Figure 39B).

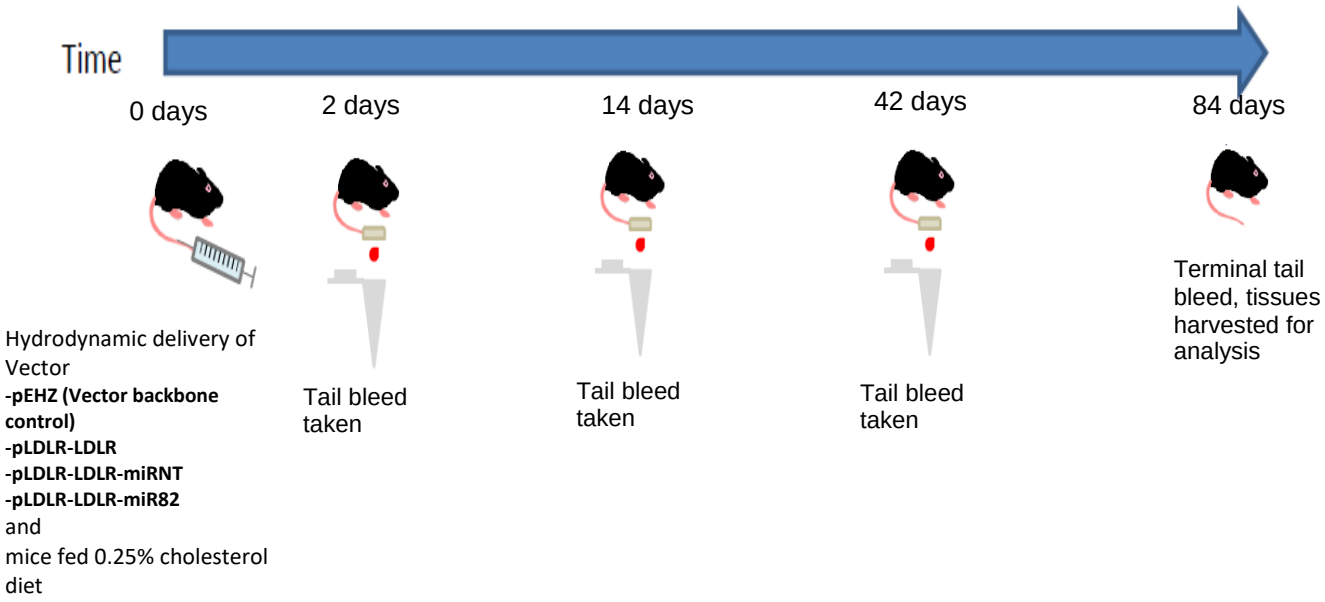


Figure 38 - Graphical representation of the long term efficacy study

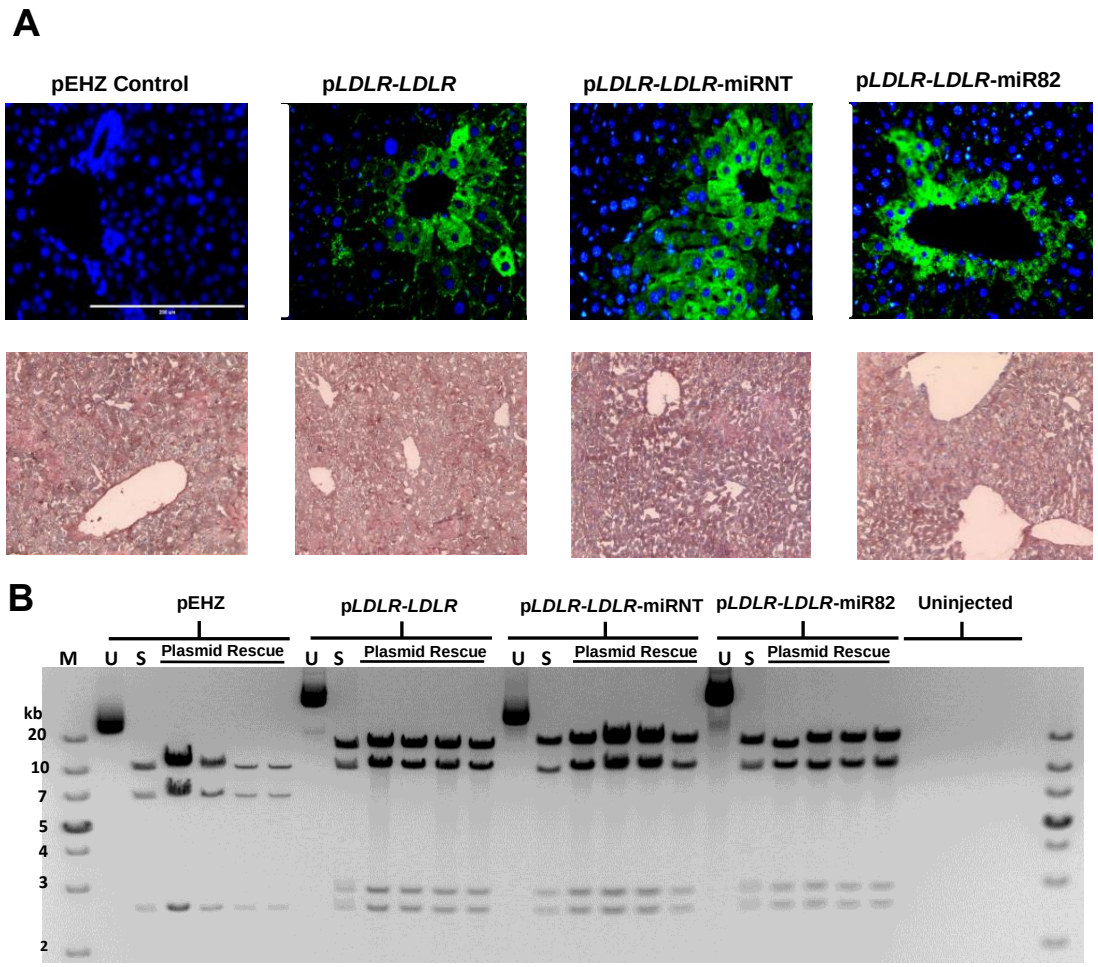


Figure 39 – *LDLR* mini-gene vectors result in prolonged LDLR transgene expression without causing lipid accumulation within *Ldlr*$^{-/-}$ mouse liver

Ldlr$^{-/-}$ mice were fed a 0.25% HC-diet and administered with the therapeutic or control vectors by hydrodynamic delivery. Immunofluorescence, lipid staining and plasmid rescue was carried out 12 weeks post vector delivery. (**A**) Top panel: Immunofluorescence images of liver tissue, showing LDLR protein expression twelve weeks post-delivery. Scale bar = 200 µm. LDLR signals are detected in transfected hepatocytes. Blue=DAPI; Green=LDLR. Bottom panel: Oil Red-O staining of frozen liver sections counterstained with haematoxylin, no lipid accumulation could be seen in any of the liver sections stained. (**B)** Episomal plasmid could be rescued from *Ldlr*$^{-/-}$ mouse liver, intact into bacteria, with high efficiency 12 weeks post-delivery. Each lane represents individual mice from the four treatment groups. Mouse liver without plasmid delivery was used as a negative control. M: DNA marker, U: Undigested stock plasmid, S: AfeI digested stock plasmid.

Lipid analysis of plasma samples from the pEHZ control group indicated that after two weeks the *Ldlr*$^{-/-}$ mice reached peak total and LDL-cholesterol levels, which then plateaued for the remainder of the study (Figure 40A-B). There were no significant differences in HDL-cholesterol, triglycerides or weight between all the treatment groups ((Figure 40C-E). Transient increases in ALT and AST were observed 2 days after hydrodynamic delivery, which fell to levels within the safe reference range (ALT 17-77 and AST 54-226 U/L) for the remainder of the study ((Figure 40F-G), demonstrating the plasmids themselves did not induce any liver damage over the twelve weeks. p*LDLR-LDLR*-miR82 injected mice had significantly reduced total and LDL-cholesterol at each time point analysed when compared with pEHZ injected mice (Figure 40A-B). Significant reductions were also detected for the p*LDLR-LDLR* and p*LDLR-LDLR*-miRNT plasmids in total and LDL-cholesterol levels at various time points throughout the study. No difference in Hmgcr mRNA expression in the liver was detected at the end of the study, suggesting that the miR was likely silenced at this time point (Figure 40H). The long-term efficacy of the vectors is demonstrated both by prolonged LDLR expression, and prolonged reduction in total and LDL-cholesterol levels.

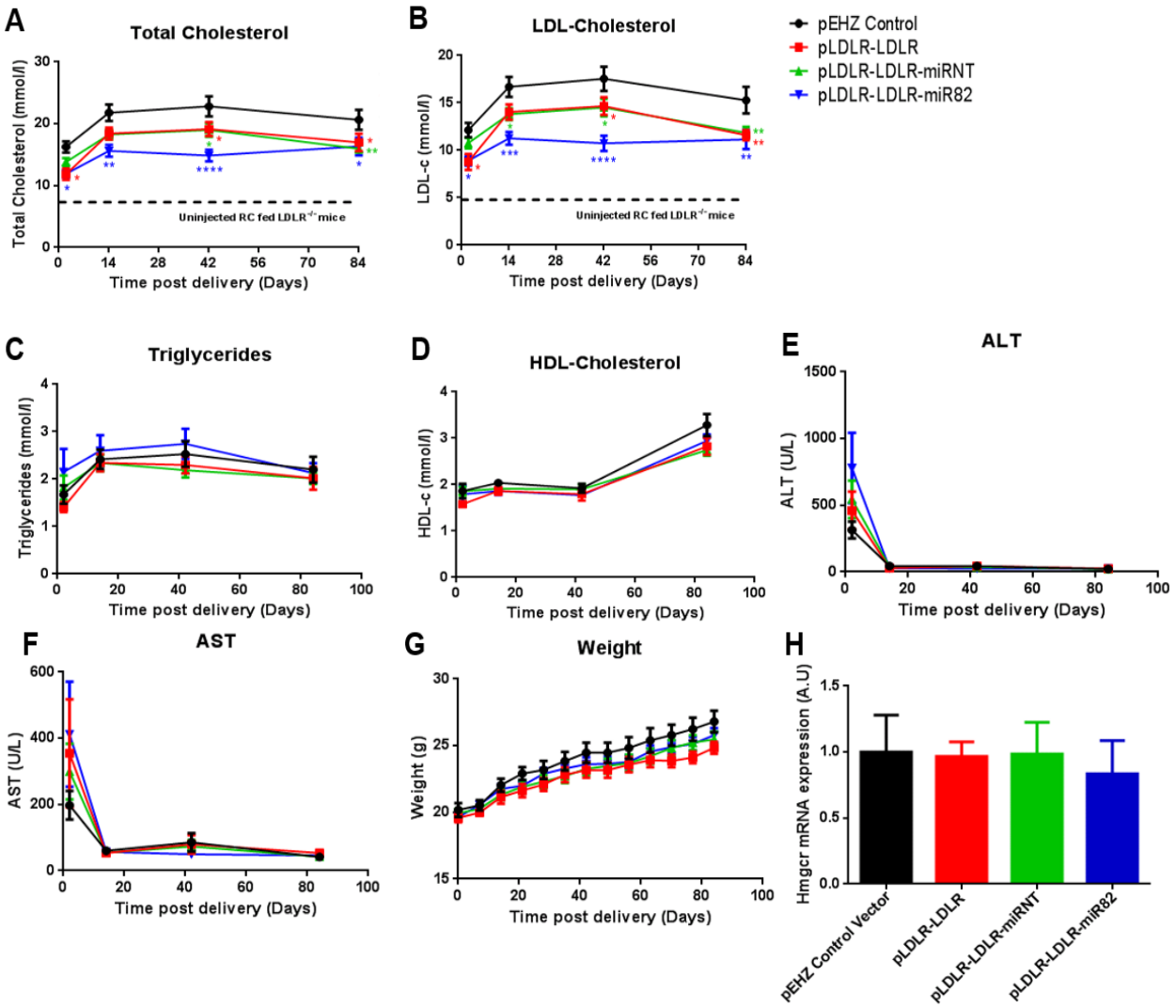


Figure 40 - Delivery of LDLR vectors results in long-term cholesterol lowering

Ldlr$^{-/-}$ mice were fed a 0.25% HC-diet for 12 weeks and the therapeutic or control vectors were hydrodynamically delivered on the day of diet intervention. Plasma lipid levels were assessed throughout the study. (**A**) Total and (**B**) LDL-cholesterol levels were lowered using the p*LDLR-LDLR*-miR82 at two days and two, six and twelve weeks post-delivery. p*LDLR-LDLR*-miRNT and p*LDLR-LDLR* also significantly reduced total and LDL-cholesterol. No detectable differences were observed in (**C**) HDL-cholesterol, (**D**) triglycerides, (**E**) or weight (of the mice throughout the study. A transient increase in (**F**) AST (**G**) and ALT levels in the plasma were seen in all groups accounted for by the hydrodynamic delivery. AST and ALT remained within the reference values for the remainder of the study. No difference in liver Hmgcr mRNA expression was detected between any of the groups, indicating miR82 may have been silenced. Significance is displayed as the colour of the treatment group versus pEHZ control plasmid. *P<0.05 **P<0.01, ***P<0.001, ****P<0.0001 Error bars denote SEM. n=8-12 per group. Two-way ANOVA with Dunnetts post hoc analysis.

We analysed the development of atherosclerosis in the aortic root at 12 weeks, to measure the therapeutic impact of long term cholesterol lowering (Figure 41A). Aortic root lesion area was significantly reduced in the p*LDLR-LDLR*-miR82 and p*LDLR-LDLR* groups compared to the pEHZ control mice (Figure 41B). We analysed the correlation between the average LDL-cholesterol level and atherosclerotic lesion area for each mouse in the 12 week study (Figure 41C). We observed a positive correlation between the two variables (Pearson correlation coefficient p=0.01), indicating the lower the LDL-cholesterol level achieved with the vector, the greater the reduction of atherogenesis. Galectin-3 staining (Figure 42A) did not show any significant differences between the groups but did show a similar trend to what was seen with the Masson's trichrome stain (Figure 42C). Sirius red staining of collagen in the aortic root (Figure 42B) showed no difference between the groups but, given that almost all of the lesions did not display hallmarks of advanced atherosclerotic plaques, this may be expected (Figure 42D). Oil Red-O staining of the whole aorta showed very little plaque development had occurred (Figure 43A-B), with no significant difference between any of the vector treated groups. Taken together, these data show that an episomal non-viral vector, is able to significantly lower total and LDL-cholesterol and slow the progression of atherosclerosis in a model of FH after a single administration.

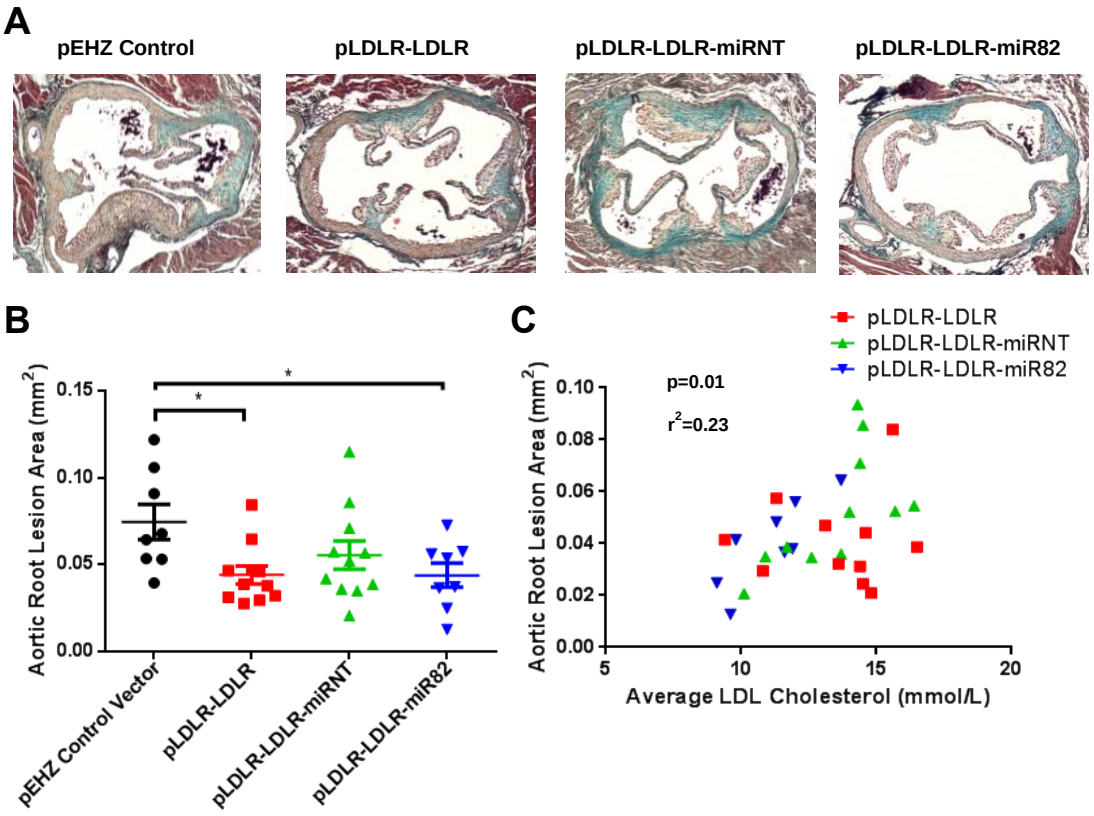


Figure 41 – *LDLR* mini-gene vectors slow the progression of atherosclerosis in a mouse model of familial hypercholesterolaemia

Ldlr$^{-/-}$ mice were fed a 0.25% HC-diet for 12 weeks and the therapeutic or control vectors were hydrodynamically delivered on the day of diet intervention. At the end of the study the aortic root was dissected and stained for plaque analysis. (**A**) Representative images of Masson Trichrome staining, showing aortic root atherosclerosis. p*LDLR-LDLR*-miR82 halted the progression of atherosclerosis as did p*LDLR-LDLR* compared to pEHZ vector control mice (**B**). There was a significant correlation (Pearson correlation coefficient p=0.0002) between the average LDL-cholesterol level of each mouse throughout the study, with the extent of atherogenesis in the aortic root (**C**). *P<0.05 **P<0.01, ***P<0.001, ****P<0.0001. Error bars denote SEM. n=8-12 per group. One-way ANOVA with Dunnetts post hoc analysis.

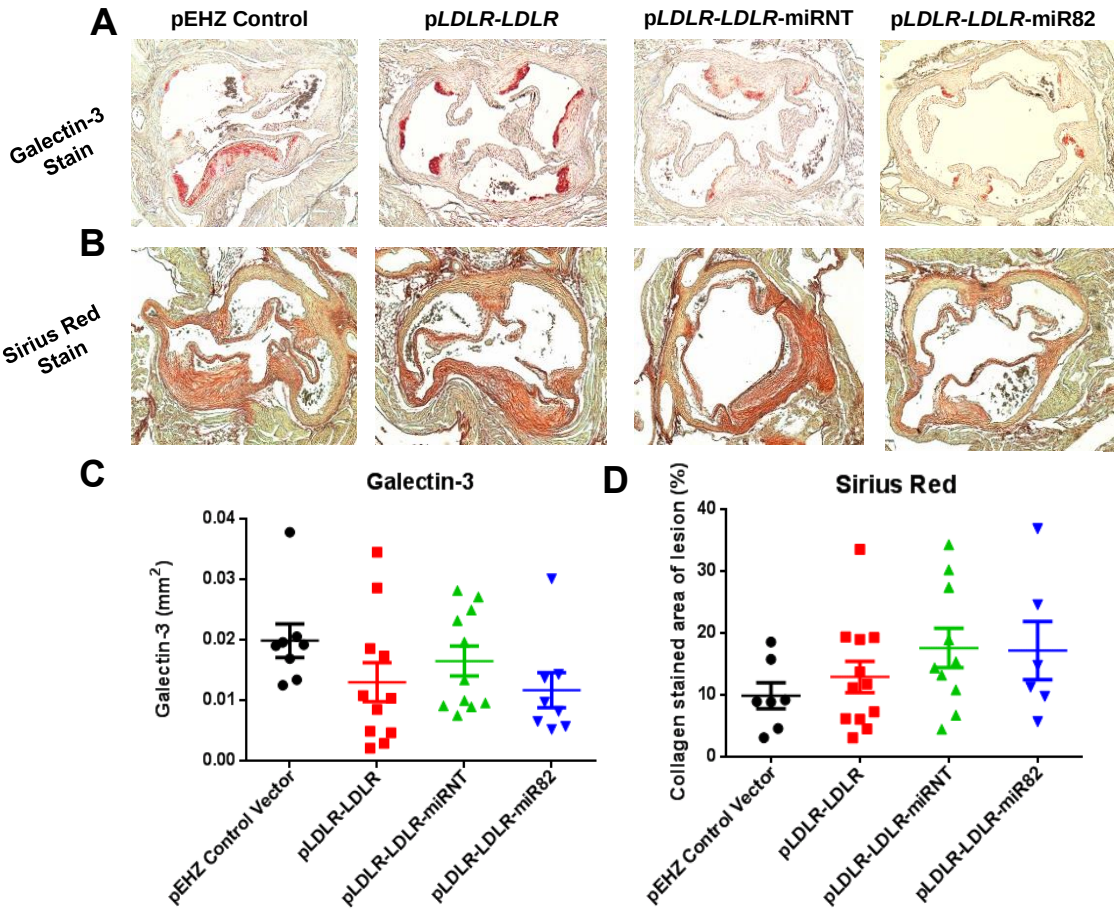


Figure 42 – *LDLR* mini-gene vectors had no significant effect on galectin-3 or collagen content of atherosclerotic plaques

Ldlr$^{-/-}$ mice were fed a 0.25% HC-diet for 12 weeks and the therapeutic or control vectors were hydrodynamically delivered on the day of diet intervention. At the end of the study the aortic root was dissected and stained for plaque analysis. Representative images of aortic root galectin-3 (**A**) and Sirius red staining (**B**) showing macrophage recruitment and collagen content respectively. Quantification of galectin-3 (**C**) and Sirius red staining (**D**) demonstrated a trend to lower macrophage recruitment and higher collagen content within the aortic root although no significance was reached. Error bars denote SEM. n=8-12 per group.

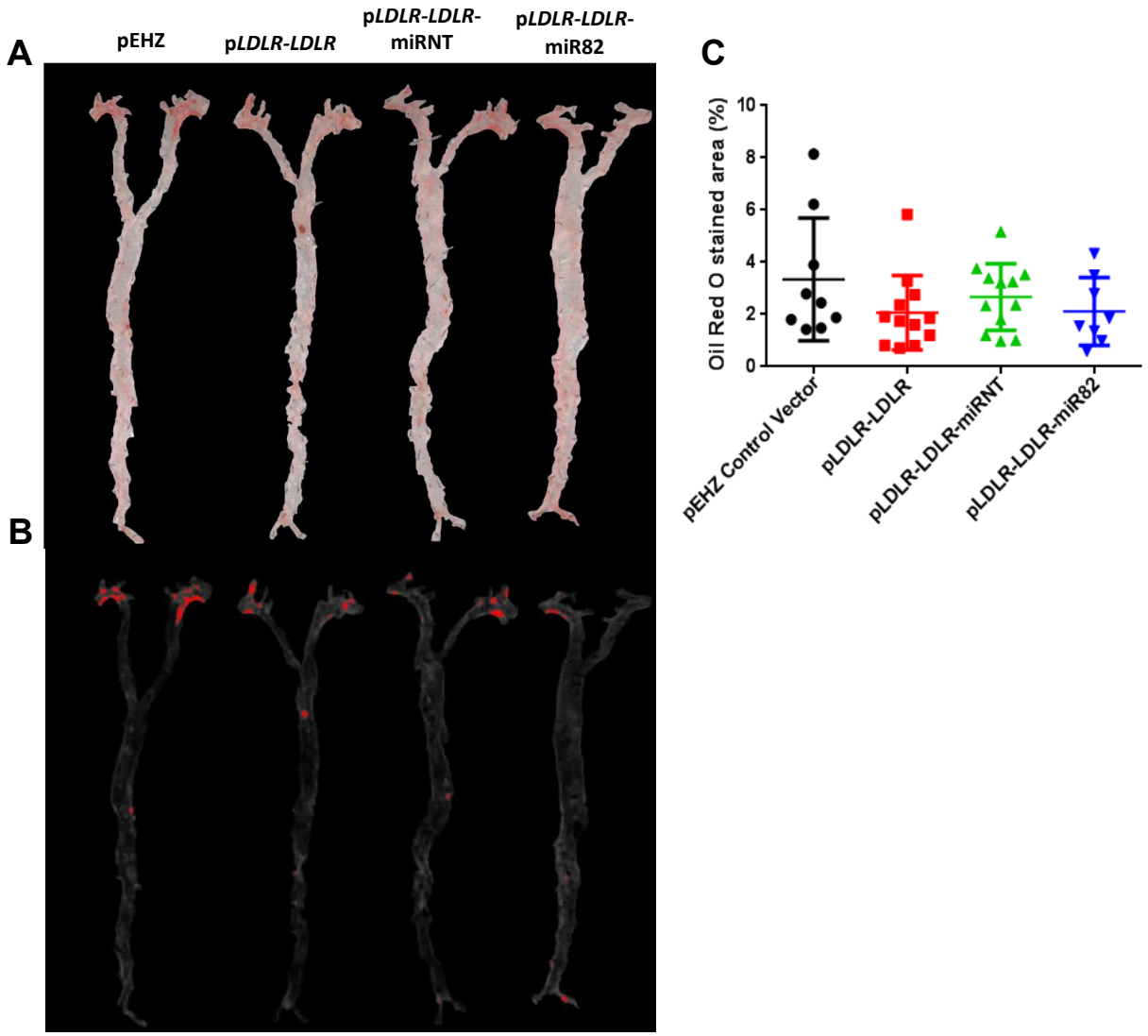


Figure 43 – *LDLR*-mini gene vectors had no significant effect on atherosclerotic plaque development in the whole aorta

Ldlr$^{-/-}$ mice were fed a 0.25% HC-diet for 12 weeks and the therapeutic or control vectors were hydrodynamically delivered on the day of diet intervention. At the end of the study the aorta was dissected and stained for plaque analysis. Representative images of the whole aorta from each group, as an original photo (**A**) and false coloured to better illustrate the plaque which was quantified (**B**). No significant differences could be detected between pEHZ control treated mice any of the LDLR mini-gene vector groups. Error bars represent SEM. n=8-12

5.3 Discussion

We report here the first use of an episomal non-viral vector to both lower total and LDL-cholesterol, and reduce the progression of atherosclerosis long term *in vivo* in a model of FH. Our work brings us closer towards effective gene therapy for HoFH by delivery of functional copies of the *LDLR* to hepatocytes, resulting in long term phenotypic correction.

A combinatorial vector was generated that allowed both the delivery of a functional copy of the LDLR, under the control of its native promoter and a miRNA targeting *Hmgcr* to further enhance the expression of the LDLR. To circumvent any issues with co-delivery of two separate plasmids, a validated siRNA sequence was cloned into an artificial miRNA scaffold driven by a polymerase II promoter. Short hairpin RNAs (shRNAs) can oversaturate the natural endogenous shRNA/miRNA pathway leading to liver toxicity and mortality in mice (Grimm *et al.* 2006), By embedding the siRNA sequence into an artificial miRNA scaffold, driven by weaker polymerase II promoters, shRNA-associated toxicity is avoided, preventing any disruption of the endogenous RNAi (McBride *et al.* 2008). *LDLR* transgene expression was improved through knockdown of endogenous Hmgcr, which induced the *LDLR* promoter leading to significant upregulation of the LDLR.

To test our therapeutic vectors, we first validated a more accurate model of HoFH. In our hands a 1, 0.5 or 0.25% HC-diet produced a hypercholesterolaemic phenotype even after two days feeding which plateaued after two weeks. Importantly, as has been reported previously with this diet (Hartvigsen *et al.* 2007) no other co-commitant metabolic disorders (hypertriglyceridemia, hyperinsulinemia, accelerated weight gain) which are known to independently drive atherogenesis result, providing a metabolic profile much more representative of an HoFH patient. In addition, it has been reported that the HC-diet, unlike the WTD does not cause fatty infiltration of livers, which would allow us to directly determine if our therapeutic vectors caused steatosis, without any confounding factors. It has been previously shown that the LDL particles formed through WTD and HC-diet intervention differ. LDL particles associated with the WTD are alot richer in triglyceride, less atherogenic and less human like, unlike the cholesterol richer LDL particles found after HC-diet feeding (Véniant *et al.* 2000). As the diet

had originally been characterized in males, with other variations of HC-diets also using males (Teupser, Persky and Breslow 2003) and the known sex differences in atherogenesis between genders (Caligiuri *et al.* 1999), all work was carried out in male mice. We first characterised a 1% HC-diet, which produced an extreme hypercholesterolaemic phenotype in our male *Ldlr*$^{-/-}$ mice with total cholesterol levels of 46mmol/L. 46mmol/L is around as high a total cholesterol level that is seen in Ldlr$^{-/-}$ mice (some studies using WTD report plasma levels >50mmol/L (Methia *et al.* 2001; Peng *et al.* 2011)) and much greater than is ever seen in a HoFH patient.

We conducted a meta-analysis of the current literature to determine at which total cholesterol levels do differences in atherosclerotic lesion development occur in the aortic root of male *Ldlr*$^{-/-}$ mice. The age of the mice included in the study (8-14 weeks old), the variation in atherogenic diet (mainly WTD), housing densities (Paigen *et al.* 2012) and litter to litter variation will most likely account for the large error seen within each group. It was our initial thinking and appeared to be confirmed by the data in the literature, that even halving the cholesterol levels in these extreme unphysiological HC-diets would still be high enough to drive the development of atherosclerosis. A more clinically relevant model of HoFH was characterised by titrating down the percentage cholesterol in the diet to 0.25%.

In two separate studies, we demonstrated significant total and LDL-cholesterol lowering with our p*LDLR-LDLR*-miR82 combinatorial vector. In the first study using the 1% HC-diet the p*LDLR-LDLR*-miR82 plasmid lowered total and LDL-cholesterol by ~50% and in the second longer term study total and LDL-cholesterol by 28% and 32%, respectively. In the second study using the 0.25% HC-diet the p*LDLR-LDLR* and p*LDLR-LDLR*-miRNT vectors also significantly lowered total and LDL-cholesterol at various time points throughout. The p*LDLR-LDLR* and p*LDLR-LDLR*-miRNT vectors did not significantly lower total or LDL-cholesterol in the more extreme hypercholesteroleamic environment seen in the first study. This could be due to the lack of power in the first proof of principle study, as not all time points in the second study were significant indicating the power was on the cusp of detection. Another explanation could be that the LDLR mini-gene vectors are not able to lower LDL-cholesterol in the more extreme

hypercholesteroleamic environment and it is necessary to additionally block intracellular cholesterol biosynthesis to have a therapeutic effect in this model. Lowering of cholesterol in hypercholesterolaemic mouse models by greater than 25% has shown decreased atherosclerotic progression previously (Ason *et al.* 2014). Critically, decreases in LDL-cholesterol of 20% or greater, have routinely shown a reduction in cardiovascular events and mortality in the clinic (Pedersen 1994).

Total and LDL-cholesterol levels, measured at the end of the 12-week study were comparable between all three therapeutic vectors and it appeared that the miR82 was providing no added effect on lowering lipid levels at this time point. It is possible that the miR was silenced, which has been reported previously, over a similar time period for constructs driven by CMV (Everett *et al.* 2004). In fact previously in our laboratory it was shown that CMV driven Lac Z expression could no longer be detected although the LDLR was being expressed from the same plasmid (Hibbitt *et al.* 2007b). This hypothesis is further backed up by the fact we detected no lowering of Hmgcr at the mRNA level at the end of this study.

In the 12-week study we observed a slowing in the progression of atherosclerosis after delivery of the p*LDLR-LDLR* and p*LDLR-LDLR*-miR82 vectors. Even though the lipid lowering was initially lower in the p*LDLR-LDLR*-miR82 group the impact on atherogenesis was comparable. This has been seen before in other non-viral gene therapy studies, where a vector carrying the LDLR cDNA did not result in a significant cholesterol lowering but did show comparable slowing of atherosclerotic progression to one that did achieve significant plasma cholesterol lowering (Turunen *et al.* 2015). It would be expected that the p*LDLR-LDLR* and p*LDLR-LDLR*-miRNT vector would have a similar impact on atherogenesis as cholesterol lowering was very similar throughout the study. This further highlights the heterogeneity of the atherosclerotic process, where it is more than just cholesterol driving the pathology but also a large immune component as well.

We did not detect any significant changes between the treatment groups in macrophage content in the aortic root or using *en face* analysis of the whole aorta. In our current study we did not observe extensive atherogenesis and so it is perhaps unsurprising that we were only able to detect a significant change in total

plaque size at the aortic root, as it is the first location to develop atherosclerosis in the mouse (Nakashima *et al.* 1994a, 1994b). Similar to the *en face* analysis, sirius red staining of collagen did not show any significant differences between any of the treatment groups. An increase in collagen within the plaque is usually found in advanced type V lesions (Stary *et al.* 1995), the lesions produced with the 0.25% cholesterol diet did not show characteristics of advanced lesions and so may explain why no difference was detected in collagen content.

We highlight the safety aspects of our treatment by demonstrating that the combined vector does not cause changes in metabolic parameters, and only transient elevation was observed in liver transaminases. Transient mild liver injury following hydrodynamic injection has previously been observed by other groups(Crespo *et al.* 2005). This transient effect may be the result of elevated intravascular pressure caused by the sheer force of injection, which expands the liver fenestrae to generate transient pores in the plasma membrane of hepatocytes (Suda *et al.* 2007). In this study, the rise in ALT and AST actually provided confirmation that the hydrodynamic delivery had been successful, a group of mice were excluded from this study based on this parameter. When LDLR expression was looked for in these mice no detectable levels were present and no vector could be detected using plasmid rescue.

No steatosis was visible from Oil Red O staining of liver sections from *Ldlr*$^{-/-}$ mice delivered with the therapeutic plasmids after 3 months post-delivery. As our vectors contain the necessary SRE for physiological regulation of the LDLR, once the hepatocytes reach a certain cholesterol concentration intracellularly, expression of the LDLR can be switched off. This control should prevent pathological intracellular lipid accumulation; hence why we did not detect any during this study.

Importantly, the therapeutic vector remained episomal throughout the study, as shown through plasmid rescue of the vectors 12 weeks post-delivery. The plasmid is retained as an episome within the cell due to the presence of the oriP and EBNA-1 episomal retention elements. These elements have previously been shown to provide episomal vector retention and persistence of gene expression (Wade-Martins *et al.* 2000), avoiding the risk of insertional mutagenesis seen with

integrating vector systems (Hacein-Bey-Abina *et al.* 2003). The EBNA-1 has been linked to aiding nuclear import of EBNA-1/oriP containing plasmids, whereby EBNA-1 is able to bind to the oriP and target the plasmid to the nucleus (Längle-Rouault *et al.* 1998). The SV40 sequences have also been linked to nuclear trafficking of the plasmid (Graessmann *et al.* 1989) and may play a role alongside the EBNA-1 retention elements, in ensuring after the plasmid has reached the cytoplasm, it can efficiently reach the nuclear matrix.

Chapter 6: Discussion

At the start of this thesis, we set out three aims in order to progress the development of two novel molecular therapies for the treatment of FH. The aims involved the identification and characterisation of a set of small molecules able to regulate the LDLR and the progression of a non-viral vector into an FH relevant animal model. Listed below is a summary for the outcome for each aim.

Aim 1: Identify and characterise a novel set of small molecules that are able to upregulate the LDLR via a mechanism distinct to statins.

We identified and confirmed the lead molecule from the initial compound screen as compound 15a, which was re-tested through the primary assay to develop a dose-response curve and establish the EC_{50}. Compound 15a and a derivative were shown to upregulate the LDLR at the mRNA and protein level in hepatocyte cell lines, through a mechanism distinct from statins. The mechanism of action was elucidated for this compound series as inhibition of squalene synthase (SQS). Importantly these compounds were found to cause a much greater upregulation of human *LDLR* promoter activity than could be achieved with statins alone, indicating these compounds could be used in addition to statins to further help heFH patients reach their lipid goals.

Aim 2: Progress the lead compound *in vivo,* evaluating the pharmacokinetics and efficacy of the compound within a mammalian system.

The lead compound, compound 15a, demonstrated a very unfavourable pharmacokinetic profile once dosed in liver microsomes, so extensive structure-activity relationship studies were carried out. Through individual alteration of the four different elements of the compound, we discovered compound 40, a more potent analogue with a much greater half-life. We developed a HPLC protocol to measure our compound *in vivo* and characterised the pharmacokinetic profile of compound 40 in mouse. Finally, we demonstrated that our lead compound was able to drive the human *LDLR* promoter in mouse liver.

Aim 3: Characterize a novel combinatorial non-viral vector in a mouse model of familial hypercholesterolaemia

We validated a high cholesterol (HC)-diet in Ldlr$^{-/-}$ mice as a diet able to induce an FH lipid profile and drive atherogenesis. Using a combinatorial non-viral vector, containing 10 kb of the human *LDLR* promoter driving expression of the LDLR, with expression further increased using RNAi (*LDLR*-Hmgcr-RNAi), we demonstrated efficacy in two *in vivo* studies. In a short term study, in an extreme hypercholesterolaemic model our *LDLR*-*Hmgcr*-RNAi lowered plasma and total cholesterol two and four weeks post-delivery, through expression of the LDLR, further upregulated by Hmgcr knockdown. In a second long term twelve week-study, our *LDLR*-*Hmgcr*-RNAi vector significantly lowered total and LDL-cholesterol at every time point measured, with the LDLR still able to be detected at the end of the study. Most importantly, we show for the first time an episomal non-viral vector is able to slow the progression of atherosclerosis in an animal model of FH, further progressing non-viral viral gene therapy for FH and the capabilities of using larger genomic DNA constructs.

6.1 Small molecule squalene synthase inhibitor

Squalene synthase inhibition has been an attractive target for developing a hypocholesterolaemic agent for many decades (Poulter *et al.* 1989). Where a long standing hypothesis of inhibiting cholesterol biosynthesis at the first cholesterol committed step within the pathway (SQS), would reduce some of the side-effects associated with statins. The difficulties of producing another cholesterol biosynthesis inhibitor was realised with the withdrawal and termination of the squalene synthase inhibitor (SSI) Lapaquistat from phase II/III clinical trials in 2007 (Stein *et al.* 2011). The withdrawal was due to a very modest difference in alanine aminotransaminase (ALT) and aspartate aminotransferase (AST) levels in patients receiving Lapaquistat compared to placebo. The incidence for ALT levels ≥ 3 times the upper limit of normal (ULN) was 0.8% in Lapaquistat versus 0.2% in the placebo group, for ≥ 5 times the ULN it was 0.8% in Lapaquistat versus 0.1% in the placebo and for ≥ 10 times the ULN it was 0.2% in Lapaquistat versus 0% in the placebo. Two incidences of hepatotoxicity from 5107 patients exposed to the

SSI were central to the discontinuation of Lapaquistat, with each patient meeting the Food and Drug Administration–defined Hy-Law criteria of ALT elevation accompanied by increases in total bilirubin (Reuben 2004). Both cases resolved after discontinuation of the drug, although only one case was investigated to see if there were any other underlying pathologies which may have led to the hepatitis, such as any autoimmune disorder or viral hepatitis.

The hepatic safety profile of Lapaquistat was in fact very similar to what was seen in the clinic with Atorvastatin, where treatment for 24-weeks (same duration as the Lapaquistat study) at 80 mg, showed ALT levels ≥ 3 times the ULN at a rate of 3.8%, ≥ 5 times the ULN at a rate of 2.1% and ≥ 10 times the ULN at a rate of 1.2% (Illingworth *et al.* 2001). One subject in this study out of 826 patients given Atorvastatin 80 mg met the Hy Law criteria, a rate of 0.25% which is five times higher than with Lapaquistat at 0.05%. Atorvastatin and the other classes of statins are known to be safe with cases of liver toxicity found in only a handful of case reports or reports in clinical trials (Bays 2006). Larger and longer clinical trials would need to be undertaken to see if Lapaquistat, just like with Atorvastatin (Cannon *et al.* 2004), turns out to be safe, despite initial liver toxicity concerns.

Despite the liver safety profile, Lapaquistat proved that a squalene synthase inhibitor (SSI) could provide long term lipid lowering. As a monotherapy, Lapaquistat lowered LDL-cholesterol by 23% and in combination with the highest dose of the 3 most commonly used statins gave an additional 19% LDL-cholesterol lowering(Stein *et al.* 2011). In HoFH patients, there was an 11% lowering of LDL-cholesterol and in clinically defined and genetically confirmed HeFH pateints, an additional 16.4% lowering in LDL-cholesterol on top of maximal dose statins. There was also significant decreases in C-reactive protein, ApoB, HDL-cholesterol and as seen in the pre-clinical studies (Amano *et al.* 2003) in triglycerides. A doubling of the statin dose equates to a further 5-7% decrease in LDL-cholesterol (Wierzbicki, Hardman and Viljoen 2012), so for statin treatment to reach the lowering achieved by Lapaquistat a further 8-fold increase in the dose would be required, greatly enhancing the chance of side effects (Bitzur *et al.* 2013b).

Our SSI, compound 40 had an IC_{50} of 182 nM in the human liver microsomes assay. This nanomolar potency is very similar to some of the most published SSIs, including YM-53601 (Ugawa *et al.* 2000) and Lapaquistat (Miki *et al.* 2002), with our inhibition calculated from primary human liver microsomes as apposed from HepG2 cell lines. Work has continued on the development of SSIs since the discontinuation of Lapaquistat, with many other groups publishing SSIs, again with nanomolar potencies (Wasko *et al.* 2011; Ichikawa *et al.* 2013; Ladopoulou *et al.* 2015). To progress compound 40 through pre-clinical development not only would efficacy in different larger mammalian species be required but due to the results of Lapaquistat, extensive models of toxicity as well. Lapaquistat did show hepatocellular changes at high concentrations in a multiple dose canine model(Stein *et al.* 2011), and so a comparison with compound 40 against Lapaquistat in this model may be a good starting point. The recent development of 3D primary human hepatocyte spheroid *in vitro* models, may also prove useful in the evaluation of the hepatotoxicity of compounds in man (Bell *et al.* 2016). These hepatocyte structures have been shown to be sensitive to a number of known hepatotoxins, including fialuridin, a compound which was found to be non-toxic in all 2D *in vitro* and pre-clinical models but resulted in severe hepatotoxicity in the clinic for 7/15 patients (McKenzie *et al.* 1995). If the hepatotoxicity of high dose Lapaquistat could be recapitulated within these models, more confidence could be given progressing a future SSI into the clinic. It was never shown if the toxicity of Lapaquistat resulted directly from SQS inhibiton or an off target effect of the compound itself.

Many different enzymes have been targeted within the cholesterol biosynthesis pathway and it is apparent that the different intermediates that then accumulate can have potentially grave consequences. Triparanol was the first cholesterol biosynthesis inhibitor used and was found to lower plasma cholesterol in man (Steinberg, Avigan and Feigelson 1961). Unfortunately inhibiting at the very last step of cholesterol synthesis also caused the development of cataracts and the compound was withdrawn (Kirby 1967).Other compounds inhibiting downstream of SQS have also shown the development of cataracts (Rozman and Monostory 2010). We demonstrated in our work, that inhibiting the cholesterol biosynthesis pathway at two distinct points caused a much greater upregulation of the human

LDLR promoter activity then with either compound class alone and lower doses of either drug could be given to elicit a much larger response. Recently Wasko et al., also demonstrated that multiple enzyme inhibition in this pathway may limit off-target effects due to depletion of isoprenoid intermediates (Wasko *et al.* 2011). In the clinic the low dose of Lapaquistat in combination with a statin also resulted in a lower report of adverse events (Stein *et al.* 2011).

Although the primary development of SSIs has been for the treatment of hypercholesterolaemia, they also show great potential as chemotherapeutic agents against trypanosomatids and fungi. Ergosterol and other 24-alkyl sterols produced through a SQS pathway are essential for the growth of trypanosomatids and fungi (de Macedo-Silva, de Souza and Rodrigues 2015). SQS is the first committed enzyme in the synthesis of erogsterol and inhibition has shown anti-proliferative effects in *L. amazonensis* and *Trypanosoma cruzi* at nanomolar potencies (Urbina *et al.* 2004; Rodrigues, Urbina and de Souza 2005). Interestingly, SSIs were shown to block proliferation of a *Candida tropicalis* strain resistant to fluconazole, itraconazole, and amphotericin B (Ishida *et al.* 2011). It is beyond the scope of this current work to evaluate our SSIs in models of these infectious diseases but it represents another interesting potential use for this novel set of small molecules.

As lipid goals become stricter for patients who have dyslipidaemia especially in high risk patients, such as heFH patients, high dose statins may become intolerable and as previously stated only a small percentage of heFH patients reach their lipid goal (Pijlman et al. 2010). The emergence of the proprotein convertase subtilisin/kexin type 9 (PCSK9) inhibitors are a welcome addition to try and further lower the LDL-cholesterol of heFH patients (Robinson et al. 2015) and a recent reminder of the benefits of additional lipid lowering. Evolocumab demonstrated that lowering LDL-cholesterol on top of maximal statin therapy caused regression of coronary atherosclerotic plaque (results from GLAGOV trial to be announced at this coming American Heart Association meeting November 2016). The excellent lipid lowering of these class of biologics are surely promising, however as they need to be administered via a subcutaneous injection every two weeks and are expected to have a high cost (Zimmerman 2015) there may still be

room for an oral medication which can be taken alongside lower dose statins. To really lower the incidence of coronary heart disease, lipid lowering medication may have to be initiated at a younger age, coronary atherosclerosis was seen in 78% of soldiers under 35 returning from the Korean war who had died from noncardiac trauma (Joseph *et al.* 1993). If longer and more aggressive lipid lowering therapy is to be undertaken, then additional therapies which can lessen side effects or provide alternatives if particular medication is intolerable in a certain individual will be of use.

6.2 Combinatorial non-viral gene therapy

Gene therapy remains the theoretical gold standard for HoFH, with the belief that a liver directed gene therapy could achieve phenotypic correction in a patient just as liver transplantation has (Starzl *et al.* 1984). There has been much effort previously to develop gene replacement therapy for FH, based on the use of recombinant virus-based vectors, coupled with strong constitutive viral promoters(Kozarsky *et al.* 1994; Li *et al.* 1995). In these early studies, unfortunately transgene expression was often transient possibly due to immune responses against viral proteins (Yang, Ertl and Wilson 1994). In addition, continuous overexpression of the LDLR was shown to cause pathological intracellular lipid accumulation, which is cytotoxic to hepatocytes (Heeren *et al.* 1999; Cichon *et al.* 2004).

To address these issues, more recent viral gene therapy approaches have used hepatocyte specific promoters, such as the thyroid binding globulin (TBG), which did not result in pathological lipid accumulation (Kassim *et al.* 2013). Unlike in man, mice are able to turn off cholesterol absorption and so it is possible they are better equipped to deal with continual expression of the LDLR (Dawson and Rudel 1999). Given the stringent regulation of the LDLR in hepatocytes, the long term effects of unregulated constitutive expression of the LDLR in man, remain unclear.

Theoretically, using the native promoter as we have is the ideal therapy, as it restores the native system lost through FH gene mutation. Only a few vector systems are able to deliver such a large promoter region and apart from the HSV-

1 vectors, which show limited expression in hepatocytes (Fraefel *et al.* 1997), non-viral delivery appears the most efficient option. The efficacy of non-viral vectors is still dependent on the delivery methods available at present. The lipid lowering demonstrated in this study may have been limited by hydrodynamic delivery of this size plasmid, only transfecting ~25% of hepatocytes (Hibbitt *et al.* 2010). Viral vectors such as helper dependent-adenovirus or adeno-associated virus (Nomura *et al.* 2004) typically show 60-70% hepatocyte transduction, which may explain their increased lipid lowering when compared to our system. Hydrodynamic delivery was originally scaled up and trialled in pig and in human (Khorsandi *et al.* 2008). The procedure was well tolerated but a low-level of transfection and expression was achieved. To improve the procedure, a computer controlled injection system has been used to administer the hydrodynamic injection directly to each lobe within the liver in swine and canine (Kamimura *et al.* 2013, 2014). A balloon catheter is guided using X-ray and used to obstruct the local blood flow from the liver, allowing enough pressure to build up using the computer assisted injection, to cause the transfection of the hepatocytes. Transfection of the plasmid using this system in pig has shown similar expression levels to that seen in the mouse (Kamimura *et al.* 2013), although no expression persisted after two months, most probably due to the use of viral promoters (CMV), which are known to be silenced (Everett *et al.* 2004). A large pre-clinical trial is underway using the new liver-targeted computer-controlled hydrodynamic gene-delivery in large pigs, roughly same weight as humans, with the procedure seemingly well tolerated (Kamimura *et al.* 2015). To date hydrodynamic delivery remains the most efficient delivery method for non-viral liver directed gene therapy.

Once the plasmid has been delivered into the cell, the next goal for a gene therapeutic is persistence of expression. It has long been known that viral and bacterial elements within a plasmid can lead to methylation of those regions and silencing of expression (Everett *et al.* 2004; Herbst *et al.* 2012). *In vivo* studies have shown that short-lived transgene expression can occur even when plasmid DNA is readily detectable in transfected cells (Gill, Pringle and Hyde 2009). To improve expression, a mini-circle vector system was developed where the bacterial elements needed for production of the plasmid, are excised after large amounts of the plasmid are made in the bacterial cells (Kay, He and Chen 2010).

Delivery of mini-circle plasmids to the liver via hydrodynamic injection show greater persistence and level of transgene expression compared to the parent plasmid (Argyros *et al.* 2011a). The transgene expression can be further improved with the addition of S/MAR mammalian episomal retention elements. Hou et al., recently cloned a 2 kb *LDLR* promoter element containing the sterol response elements (SREs) into a mini-circle vector driving expression of the *LDLR* cDNA (Hou *et al.* 2016). The mini-circle vector is able to reduce total cholesterol in Ldlr$^{-/-}$ mice on a normal diet up to 19-weeks post-delivery. It would be very interesting to compare the 10 kb promoter element used in our p*LDLR-LDLR* vector against the 2 kb shortened element used by Hou et al., in terms of expression and degree of physiological regulation *in vivo*. Combining our large genomic 10 kb promoter system and episomal retention elements, shown to further enhance and prolong expression in the mini-circle system (Argyros *et al.* 2011b) would be an exciting progression of the gene therapy to next evaluate.

The use of the miR targeting Hmgcr provided a proof of principle that our vectors would be amenable to current lipid lowering therapies which reduce intracellular cholesterol, such as statins. To further develop our therapy, a switch from using a CMV promoter to drive the expression of the miR would be required. CMV is known to be silenced *in vivo*, in the liver(Nguyen *et al.* 2008) and it appeared to be in our current study as well. The use of mammalian liver specific promoters such as α1-antitrypsin or TBG have been shown to provide a much more stable level of expression compared to viral promoters (Nguyen *et al.* 2008). Once again reducing the amount of non-mammalian elements within the vector may prevent silencing of the vector system (Chen *et al.* 2008). Targeted knockdown of Hmgcr using the miR, may help to reduce the muscle related side effects from statins as only cholesterol biosynthesis in the hepatocytes would be affected.

It has been reported that use of the human LDLR is less efficient in clearing mouse apolipoprotein B containing lipoproteins (Kassim *et al.* 2013), due to the mouse and human LDLR only having 74% amino acid sequence homology in the ligand binding domain. It is well known that mice express both isoforms of Apolipoprotein B (Apo-B48 and Apo-B100)(Greeve *et al.* 1993), the major lipoprotein found on LDL-particles. Apo-B48 containing lipoproteins are able to be

internalized by alternative receptors to the LDLR (Veniant *et al.* 1998), which can dampen the effect seen by introducing the LDLR transgene in this model. The use of mouse LDLR, may have resulted in an even greater lipid-lowering effect, of course this would have to be tested. An LDLR variant which has been genetically engineered through point mutations in order to avoid post-translational modification has recently been developed, which is resistant to IDOL and PCSK9 downregulation (Somanathan *et al.* 2014). If the hepatocyte has no physiological control over expression of the LDLR, this system may be more likely to result in a pathological accumulation of cholesterol within the cell. With our vectors however, where expression can be turned off if cholesterol levels reach a certain concentration, addition of this LDLR cDNA may improve efficacy without increasing safety concern.

Taken together, these data indicate that patients with homozygous FH, who are receptor negative (express no detectable functional receptors), may be the most suitable candidates for our new combined gene therapy vector, as there are few other therapeutic options for this group of patients. These patients are most likely to show the greatest benefit, as they have no initial receptor function and genotype-to-phenotype correlation in FH patients suggests that even a modest increase in receptor function should be highly therapeutic. In principle, the p*LDLR-LDLR*-miR82 or p*LDLR-LDLR* vectors could be used in conjunction with statins or PCSK9 inhibitors (Yadav *et al.* 2016) for an even greater therapeutic effect if required. Furthermore, long term persistence of the vector in the liver may greatly reduce administration intervals required to maintain therapeutic efficacy. Considering FH patients with severe risk for premature coronary heart disease would require treatments to be initiated at an early stage, the economic burden of repeated treatments such as LDL apheresis is rather substantial compared to a single or infrequent gene therapy.

In regard to clinical translation of our approach, the *LDLR-Hmgcr*-RNAi vector contains the oriP/EBNA-1 long-term retention elements from EBV. Replacement with mammalian DNA episomal retention systems, such as those that utilise Scaffold Matrix Attachment Region (S/MAR) suitable for ensuring long-term LDLR expression (Lufino, Manservigi and Wade-Martins 2007b) may increase efficacy.

To improve expression of the miR82, replacing the CMV promoter with a liver specific promoter has previously shown to prolong expression in hepatocytes which may further enhance the therapeutic effect (Nguyen *et al.* 2008). The evaluation of our vector as a mini-circle, which may lead to enhanced and prolonged LDLR expression, due to a decrease in size and bacterial and viral elements (Chen *et al.* 2003) would be an exciting option, as well as using the newly described 'gain of function LDLR mutant' (Somanathan *et al.* 2014). An important step before clinical application would be to investigate the anti-atherogenic property of the *LDLR-Hmgcr*-RNAi vector in larger pre-clinical animal models of FH such as the Watanabe Heritable Hyperlipidaemic (WHHL) rabbit. The WHHL being the most relevant large pre-clinical animal model for FH, having a similar lipoprotein metabolism to that of humans(Watanabe 1980). In summary, our work showing that an episomal non-viral combinatorial gene therapy vector is able to slow atherogenesis in a model of FH represents an important new approach in the application of gene therapy for FH.

References

Adams CM, Reitz J, De Brabander JK *et al.* Cholesterol and 25-hydroxycholesterol inhibit activation of SREBPs by different mechanisms, both involving SCAP and Insigs. *J Biol Chem* 2004;**279**:52772–80.

Al-Allaf FA, Coutelle C, Waddington SN *et al.* LDLR-Gene therapy for familial hypercholesterolaemia: problems, progress, and perspectives. *Int Arch Med* 2010;**3**:36.

Al-Dosari MS, Gao X. Nonviral Gene Delivery: Principle, Limitations, and Recent Progress. *AAPS J* 2009;**11**:671–81.

Alberts AW, Chen J, Kuron G *et al.* Mevinolin: a highly potent competitive inhibitor of hydroxymethylglutaryl-coenzyme A reductase and a cholesterol-lowering agent. *Proc Natl Acad Sci U S A* 1980;**77**:3957–61.

Alonso R, Andres E, Mata N *et al.* Lipoprotein(a) levels in familial hypercholesterolemia: An important predictor of cardiovascular disease independent of the type of LDL receptor mutation. *J Am Coll Cardiol* 2014;**63**:1982–9.

Alvarez JD, Yasui DH, Niida H *et al.* The MAR-binding protein SATB1 orchestrates temporal and spatial expression of multiple genes during T-cell development. *Genes Dev* 2000;**14**:521–35.

Amano Y, Nishimoto T, Tozawa R ichi *et al.* Lipid-lowering effects of TAK-475, a squalene synthase inhibitor, in animal models of familial hypercholesterolemia. *Eur J Pharmacol* 2003;**466**:155–61.

Amin D, Cornell S a, Gustafson SK *et al.* Bisphosphonates used for the treatment of bone disorders inhibit squalene synthase and cholesterol biosynthesis. *J Lipid Res* 1992;**33**:1657–63.

Aninat C, Piton A, Glaise D *et al.* Expression of cytochromes P450, conjugating enzymes and nuclear receptors in human hepatoma HepaRG cells. *Drug Metab Dispos* 2006;**34**:75–83.

Anitschkow N. Über die veränderungen der kaninchenaorta bei experimenteller cholesterinsteatose. *Beitr Pathol Anat* 1913:379–404.

Anuurad E, Boffa MB, Koschinsky ML *et al.* Lipoprotein(a): A Unique Risk Factor for Cardiovascular Disease. *Clin Lab Med* 2006;**26**:751–72.

Aprahamian T, Bonegio R, Rizzo J *et al.* Simvastatin treatment ameliorates autoimmune disease associated with accelerated atherosclerosis in a murine lupus model. *J Immunol* 2006;**177**:3028–34.

Araki M, Maeda M, Motojima K. Hydrophobic statins induce autophagy and cell death in human rhabdomyosarcoma cells by depleting geranylgeranyl diphosphate. *Eur J Pharmacol* 2012;**674**:95–103.

Arar C, Gaudin JC, Capron L *et al.* Galectin-3 gene (LGALS3) expression in experimental atherosclerosis and cultured smooth muscle cells. *FEBS Lett* 1998;**430**:307–11.

Argyros O, Wong SP, Fedonidis C *et al.* Development of S / MAR minicircles for enhanced and persistent transgene expression in the mouse liver. *J Mol Med* 2011a;**89**:515–29.

Argyros O, Wong SP, Fedonidis C *et al.* Development of S/MAR minicircles for enhanced and persistent transgene expression in the mouse liver. *J Mol Med* 2011b;**89**:515–29.

Ason B, van der Hoorn JWA, Chan J *et al.* PCSK9 inhibition fails to alter hepatic LDLR, circulating cholesterol, and atherosclerosis in the absence of ApoE. *J Lipid Res* 2014;**55**:2370–9.

Aubert D, Ménoret S, Chiari E *et al.* Cytotoxic Immune Response Blunts Long-Term Transgene Expression after Efficient Retroviral-Mediated Hepatic Gene Transfer in Rat. *Mol Ther* 2002;**5**, DOI: 10.1006.

Austin MA, Hutter CM, Zimmern RL *et al.* Genetic Causes of Monogenic Heterozygous Familial Hypercholesterolemia : A HuGE. *Am J Epidemiol* 2004;**160**:407–20.

Avorn J, Monette J, Lacour A *et al.* Persistence of use of lipid-lowering medications: a cross-national study. *JAMA* 1998;**279**:1458–62.

Banach M, Rizzo M, Toth PP *et al.* Statin intolerance - An attempt at a unified definition. Position paper from an International Lipid Expert Panel. *Arch Med Sci* 2015;**11**:1–23.

Barter PJ, Brewer HB, Chapman MJ *et al.* Cholesteryl Ester Transfer Protein: A Novel Target for Raising HDL and Inhibiting Atherosclerosis. *Arterioscler Thromb Vasc Biol* 2003a;**23**:160–7.

Barter PJ, Brewer HB, Chapman MJ *et al.* Cholesteryl ester transfer protein: a novel target for raising HDL and inhibiting atherosclerosis. *Arterioscler Thromb Vasc Biol* 2003b;**23**:160–7.

Bays H. Ezetimibe. *Expert Opin Investig Drugs* 2002;**11**:1587–604.

Bays H. Statin safety: an overview and assessment of the data--2005. *Am J Cardiol* 2006;**97**:6C–26C.

Bell CC, Hendriks DF, Moro SM *et al.* Characterization of primary human hepatocyte spheroids as a model system for drug-induced liver injury, liver function and disease. *Sci Rep* 2016;**6**:25187.

Benner JS, Glynn RJ, Mogun H *et al.* Long-term persistence in use of statin therapy in elderly patients. *JAMA* **288**:455–61.

Berkhout TA, Simon HM, Jackson B *et al.* SR-12813 lowers plasma cholesterol in beagle dogs by decreasing cholesterol biosynthesis. *Atherosclerosis* 1997;**133**:203–12.

Berns KI. Parvovirus replication. *Microbiol Rev* 1990;**54**:316–29.

Besseling J, Hovingh GK, Huijgen R *et al.* Statins in Familial Hypercholesterolemia: Consequences for Coronary Artery Disease and All-Cause Mortality. *J Am Coll Cardiol* 2016;**68**:252–60.

Beytia ED, Porter JW. Biochemistry of Polyisoprenoid Biosynthesis. *Annu Rev Biochem* 1976;**45**:113–42.

Bissig-Choisat B, Wang L, Legras X *et al.* Development and rescue of human familial hypercholesterolaemia in a xenograft mouse model. *Nat Commun* 2015;**6**:7339.

Bitzur R, Cohen H, Kamari Y *et al.* Intolerance to statins: mechanisms and management. *Diabetes Care* 2013a;**36 Suppl 2**:S325-30.

Bitzur R, Cohen H, Kamari Y *et al.* Intolerance to Statins: Mechanisms and Management. *Diabetes Care* 2013b;**36**:S325–30.

Bloch K. The biological synthesis of cholesterol. *Science* 1965;**150**:19–28.

Bocan TM, Mueller SB, Brown EQ *et al.* HMG-CoA reductase and ACAT inhibitors act synergistically to lower plasma cholesterol and limit atherosclerotic lesion development in the cholesterol-fed rabbit. *Atherosclerosis* 1998;**139**:21–30.

Bonamassa B, Hai L, Liu D. Hydrodynamic gene delivery and its applications in pharmaceutical research. *Pharm Res* 2011;**28**:694–701.

Borén J, Olin K, Lee I *et al.* Identification of the principal proteoglycan-binding site in LDL. A single-point mutation in apo-B100 severely affects proteoglycan interaction without affecting LDL receptor binding. *J Clin Invest* 1998;**101**:2658–64.

Boudreau RL, Martins I, Davidson BL. Artificial microRNAs as siRNA shuttles: improved safety as compared to shRNAs in vitro and in vivo. *Mol Ther* 2009;**17**:169–75.

Briggs MR, Yokoyama C, Wang X *et al.* Nuclear protein that binds sterol regulatory element of low density lipoprotein receptor promoter. I. Identification of the protein and delineation of its target nucleotide sequence. *J Biol Chem* 1993;**268**:14490–6.

Brown BG, Taylor AJ. Does ENHANCE diminish confidence in lowering LDL or in ezetimibe? *N Engl J Med* 2008;**358**:1504–7.

Brown MS, Anderson RG, Goldstein JL. Recycling receptors: the round-trip itinerary of migrant membrane proteins. *Cell* 1983;**32**:663–7.

Brown MS, Dana SE, Goldstein JL. Regulation of 3-hydroxy-3-methylglutaryl coenzyme A reductase activity in human fibroblasts by lipoproteins. *Proc Natl Acad Sci U S A* 1973;**70**:2162–6.

Brown MS, Dana SE, Goldstein JL. Regulation of 3-hydroxy-3-methylglutaryl coenzyme A reductase activity in cultured human fibroblasts. Comparison of cells from a normal subject and from a patient with homozygous familial hypercholesterolemia. *J Biol Chem* 1974;**249**:789–96.

Brown MS, Goldstein JL. A receptor-mediated pathway for cholesterol homeostasis. *Science* 1986;**232**:34–47.

Brown MS, Goldstein JL. Cholesterol feedback: from Schoenheimer's bottle to Scap's MELADL. *J Lipid Res* 2009;**50 Suppl**:S15-27.

Caligiuri G, Nicoletti A, Zhou X *et al.* Effects of sex and age on atherosclerosis and autoimmunity in apoE-deficient mice. *Atherosclerosis* 1999;**145**:301–8.

Camus M, Chapman MJ, Forgez P *et al.* Lipoproteins and Apoproteins in the Mouse ,. 1983;**24**.

Cannon CP, Blazing MA, Giugliano RP *et al.* Ezetimibe Added to Statin Therapy after Acute Coronary Syndromes. *N Engl J Med* 2015;**372**:2387–97.

Cannon CP, Braunwald E, McCabe CH *et al.* Intensive versus Moderate Lipid Lowering with Statins after Acute Coronary Syndromes. *N Engl J Med* 2004;**350**:1495–504.

Caso G, Kelly P, McNurlan MA *et al.* Effect of coenzyme q10 on myopathic symptoms in patients treated with statins. *Am J Cardiol* 2007;**99**:1409–12.

Check E. Gene therapy: A tragic setback. *Nature* 2002;**420**:116–8.

Chen SJ, Rader DJ, Tazelaar J *et al.* Prolonged Correction of Hyperlipidemia in Mice with Familial Hypercholesterolemia Using an Adeno-Associated Viral Vector Expressing Very-Low-Density Lipoprotein Receptor. *Mol Ther* 2000;**2**, DOI: 10.1006.

Chen WY, Bailey EC, McCune SL *et al.* Reactivation of silenced, virally

transduced genes by inhibitors of histone deacetylase. *Proc Natl Acad Sci U S A* 1997;**94**:5798–803.

Chen Z-Y, He C-Y, Ehrhardt A *et al.* Minicircle DNA vectors devoid of bacterial DNA result in persistent and high-level transgene expression in vivo. *Mol Ther* 2003;**8**:495–500.

Chen Z-Y, Riu E, He C-Y *et al.* Silencing of episomal transgene expression in liver by plasmid bacterial backbone DNA is independent of CpG methylation. *Mol Ther* 2008;**16**:548–56.

Cho SY, Kim JH, Paik YK. Cholesterol biosynthesis from lanosterol: differential inhibition of sterol delta 8-isomerase and other lanosterol-converting enzymes by tamoxifen. *Mol Cells* 1998;**8**:233–9.

Chowdhury JR, Grossman M, Gupta S *et al.* Long-term improvement of hypercholesterolemia after ex vivo gene therapy in LDLR-deficient rabbits. *Science* 1991;**254**:1802–5.

Christian AE, Haynes MP, Phillips MC *et al.* Use of cyclodextrins for manipulating cellular cholesterol content. *J Lipid Res* 1997;**38**:2264–72.

Cicalese MP, Ferrua F, Castagnaro L *et al.* Update on the safety and efficacy of retroviral gene therapy for immunodeficiency due to adenosine deaminase deficiency. *Blood* 2016;**128**:45–54.

Cichon G, Willnow T, Herwig S *et al.* Non-physiological overexpression of thelow density lipoprotein receptor(LDLr) gene in the liver induces pathological intracellular lipid and cholesterol storage. *J Gene Med* 2004;**6**:166–75.

CIOCCO A. Measuring the risk of coronary heart disease in adult population groups. Discussion; implications to the biostatistician. *Am J Public Health Nations Health* 1957;**47**:58–9.

Civeira F. Guidelines for the diagnosis and management of heterozygous familial hypercholesterolemia. *Atherosclerosis* 2004;**173**:55–68.

Collaboration CTT (CTT). Efficacy and safety of more intensive lowering of LDL

cholesterol: A meta-analysis of data from 170 000 participants in 26 randomised trials. *Lancet* 2010;**376**:1670–81.

Collins R, Reith C, Emberson J *et al.* Interpretation of the evidence for the efficacy and safety of statin therapy. *Lancet* 2007;**0**:2152–61.

Crespo A, Peydró A, Dasí F *et al.* Hydrodynamic liver gene transfer mechanism involves transient sinusoidal blood stasis and massive hepatocyte endocytic vesicles. *Gene Ther* 2005;**12**:927–35.

Crooke ST, Geary RS. Clinical pharmacological properties of mipomersen (Kynamro), a second generation antisense inhibitor of apolipoprotein B. *Br J Clin Pharmacol* 2013;**76**:269–76.

Cuchel M, Bruckert E, Ginsberg HN *et al.* Homozygous familial hypercholesterolaemia: new insights and guidance for clinicians to improve detection and clinical management. A position paper from the Consensus Panel on Familial Hypercholesterolaemia of the European Atherosclerosis Society. *Eur Heart J* 2014;**35**:2146–57.

Cuchel M, Meagher EA, du Toit Theron H *et al.* Efficacy and safety of a microsomal triglyceride transfer protein inhibitor in patients with homozygous familial hypercholesterolaemia: a single-arm, open-label, phase 3 study. *Lancet (London, England)* 2013;**381**:40–6.

Dadu RT, Ballantyne CM. Lipid lowering with PCSK9 inhibitors. *Nat Rev Cardiol* 2014;**11**:563–75.

Dai Y, Schwarz EM, Gu D *et al.* Cellular and humoral immune responses to adenoviral vectors containing factor IX gene: tolerization of factor IX and vector antigens allows for long-term expression. *Proc Natl Acad Sci U S A* 1995;**92**:1401–5.

Davidoff AM, Gray JT, Ng CYC *et al.* Comparison of the ability of adeno-associated viral vectors pseudotyped with serotype 2, 5, and 8 capsid proteins to mediate efficient transduction of the liver in murine and nonhuman primate models. *Mol Ther* 2005;**11**:875–88.

Davidsson P, Hulthe J, Fagerberg B *et al.* Proteomics of apolipoproteins and associated proteins from plasma high-density lipoproteins. *Arterioscler Thromb Vasc Biol* 2010;**30**:156–63.

Davis BT, Wang X-J, Rohret JA *et al.* Targeted disruption of LDLR causes hypercholesterolemia and atherosclerosis in Yucatan miniature pigs. Zhang Y (ed.). *PLoS One* 2014;**9**:e93457.

Davis HR, Pula KK, Alton KB *et al.* The synergistic hypocholesterolemic activity of the potent cholesterol absorption inhibitor, ezetimibe, in combination with 3-hydroxy-3-methylglutaryl coenzyme a reductase inhibitors in dogs. *Metabolism* 2001;**50**:1234–41.

Davis HR, Tershakovec AM, Tomassini JE *et al.* Intestinal sterol transporters and cholesterol absorption inhibition. *Curr Opin Lipidol* 2011;**22**:467–78.

Dawson PA, Rudel LL. Intestinal cholesterol absorption. *Curr Opin Lipidol* 1999;**10**:315–20.

Dharwadkar SS. Review Implications of Drug Metabolizing Enz Chemistry & Biology Interface. 2016.

Do R, Kiss R, Gaudet D *et al.* Squalene synthase: a critical enzyme in the cholesterol biosynthesis pathway. *Clin Genet* 2009;**75**:19–29.

Donsante A, Vogler C, Muzyczka N *et al.* Observed incidence of tumorigenesis in long-term rodent studies of rAAV vectors. *Gene Ther* 2001;**8**:1343–6.

Dorsch MF, Lawrance RA, Durham NP *et al.* Familial hypercholesterolaemia is underdiagnosed after AMI. *BMJ* 2001;**322**:111.

Douglas G, Bendall JK, Crabtree MJ *et al.* Endothelial-specific Nox2 overexpression increases vascular superoxide and macrophage recruitment in ApoE$^{-/-}$ mice. *Cardiovasc Res* 2012;**94**:20–9.

Dubuc G. Statins Upregulate PCSK9, the Gene Encoding the Proprotein Convertase Neural Apoptosis-Regulated Convertase-1 Implicated in Familial Hypercholesterolemia. *Arterioscler Thromb Vasc Biol* 2004;**24**:1454–9.

Ehrhardt A, Xu H, Kay MA. Episomal persistence of recombinant adenoviral vector genomes during the cell cycle in vivo. *J Virol* 2003;**77**:7689–95.

Eilenberg H, Klinger E, Przedecki F *et al.* Inactivation and activation of various membranal enzymes of the cholesterol biosynthetic pathway by digitonin. *J Lipid Res* 1989;**30**:1127–35.

Endo A. A historical perspective on the discovery of statins. *Proc Jpn Acad Ser B Phys Biol Sci* 2010;**86**:484–93.

Endo A, Tsujita Y, Kuroda M *et al.* Inhibition of Cholesterol Synthesis in vitro and in vivo by ML-236A and ML-236B, Competitive Inhibitors of 3-Hydroxy-3-methylglutaryl-Coenzyme A Reductase. *Eur J Biochem* 1977a;**77**:31–6.

Endo A, Tsujita Y, Kuroda M *et al.* Inhibition of cholesterol synthesis in vitro and in vivo by ML-236A and ML-236B, competitive inhibitors of 3-hydroxy-3-methylglutaryl-coenzyme A reductase. *Eur J Biochem* 1977b;**77**:31–6.

Endo A, Tsujita Y, Kuroda M *et al.* Effects of ML-236B on cholesterol metabolism in mice and rats: lack of hypocholesterolemic activity in normal animals. *Biochim Biophys Acta* 1979;**575**:266–76.

Epstein FH, Ross R. Atherosclerosis — An Inflammatory Disease. *N Engl J Med* 1999;**340**:115–26.

Estruch R, Ros E, Salas-Salvadó J *et al.* Primary Prevention of Cardiovascular Disease with a Mediterranean Diet. *N Engl J Med* 2013;**368**:1279–90.

Everett RS, Evans HK, Hodges BL *et al.* Strain-specific rate of shutdown of CMV enhancer activity in murine liver confirmed by use of persistent [E1(-), E2b(-)] adenoviral vectors. *Virology* 2004;**325**:96–105.

Fisher C, Abdul-Aziz D, Blacklow SC. A two-module region of the low-density lipoprotein receptor sufficient for formation of complexes with apolipoprotein E ligands. *Biochemistry* 2004;**43**:1037–44.

Flint OP, Masters BA, Gregg RE *et al.* Inhibition of cholesterol synthesis by squalene synthase inhibitors does not induce myotoxicity in vitro. *Toxicol Appl*

Pharmacol 1997;**145**:91–8.

Fomby P, Cherlin AJ. NIH Public Access. 2011;**72**:181–204.

Ford I, Murray H, McCowan C *et al.* Long-Term Safety and Efficacy of Lowering Low-Density Lipoprotein Cholesterol With Statin Therapy: 20-Year Follow-Up of West of Scotland Coronary Prevention Study. *Circulation* 2016;**133**:1073–80.

Fouchet MH, Donche F, Martin C *et al.* Design and evaluation of a novel series of 2,3-oxidosqualene cyclase inhibitors with low systemic exposure, relationship between pharmacokinetic properties and ocular toxicity. *Bioorganic Med Chem* 2008;**16**:6218–32.

Fraefel C, Jacoby DR, Lage C *et al.* Gene transfer into hepatocytes mediated by helper virus-free HSV/AAV hybrid vectors. *Mol Med* 1997;**3**:813–25.

Frankel EN, Waterhouse AL, Kinsella JE. Inhibition of human LDL oxidation by resveratrol. *Lancet* 1993;**341**:1103–4.

Frémont L. Biological effects of resveratrol. *Antioxid Redox Signal* 2001;**3**:1041–64.

Fuchs M, Agellon L, Drover V *et al.* Bile acid regulation of hepatic physiology: III. Regulation of bile acid synthesis: past progress and future challenges. *Am J Physiol Gastrointest Liver Physiol* 2003;**284**:G551-7.

Gazzerro P, Proto MC, Gangemi G *et al.* Pharmacological Actions of Statins: A Critical Appraisal in the Management of Cancer. *Pharmacol Rev* 2012;**64**:102–46.

Getz GS, Reardon CA. Animal Models of Atherosclerosis. *Arterioscler Thromb Vasc Biol* 2012;**32**:1104–15.

Gil J, Gallaher S, Berk A. Delivery of an EBV episome by a self-circularizing helper-dependent adenovirus: long-term transgene expression in immunocompetent mice. *Gene Ther* 2010;**17**:1288–129375.

Gill D, Pringle I, Hyde S. Progress and Prospects: The design and production of

plasmid vectors. *Gene Ther* 2009;**16183**:165–71.

Glomset JA. The plasma lecithins:cholesterol acyltransferase reaction. *J Lipid Res* 1968;**9**:155–67.

Goldberg AC, Hopkins PN, Toth PP *et al.* Familial hypercholesterolemia: screening, diagnosis and management of pediatric and adult patients: clinical guidance from the National Lipid Association Expert Panel on Familial Hypercholesterolemia. *J Clin Lipidol* 2011;**5**:133–40.

Goldstein JL, Brown MS. Binding and degradation of low density lipoproteins by cultured human fibroblasts. Comparison of cells from a normal subject and from a patient with homozygous familial hypercholesterolemia. *J Biol Chem* 1974;**249**:5153–62.

Goldstein JL, Brown MS. Regulation of the mevalonate pathway. *Nature* 1990;**343**:425–30.

Goldstein JL, Brown MS. History of Discovery : The LDL Receptor. *Arterioscler Thromb* 2010;**29**:431–8.

Goldstein JL, Hazzard WR, Schrott HG *et al.* Hyperlipidemia in coronary heart disease. I. Lipid levels in 500 survivors of myocardial infarction. *J Clin Invest* 1973;**52**:1533–43.

Graessmann M, Menne J, Liebler M *et al.* Helper activity for gene expression, a novel function of the SV40 enhancer. *Nucleic Acids Res* 1989;**17**:6603–12.

Greenwood J, Steinman L, Zamvil SS. Statin therapy and autoimmune disease: from protein prenylation to immunomodulation. *Nat Rev Immunol* 2006;**6**:358–70.

Greeve J, Altkemper I, Dieterich JH *et al.* Apolipoprotein B mRNA editing in 12 different mammalian species: hepatic expression is reflected in low concentrations of apoB-containing plasma lipoproteins. *J Lipid Res* 1993;**34**:1367–83.

Griebenow N, Flessner T, Buchmueller A *et al.* Identification and optimization of

tetrahydro-2H-3-benzazepin-2-ones as squalene synthase inhibitors. *Bioorg Med Chem Lett* 2011;**21**:2554–8.

Grimm D, Streetz KL, Jopling CL *et al.* Fatality in mice due to oversaturation of cellular microRNA/short hairpin RNA pathways. *Nature* 2006;**441**:537–41.

Grossman M, Rader DJ, Muller DWM *et al.* A pilot study of ex vivo gene therapy for homozygous familial hypercholesterolaemia. *Nat Med* 1995;**1**:1148–54.

Grossman M, Raper SE, Kozarsky K *et al.* Successful ex vivo gene therapy directed to liver in a patient with familial hypercholesterolaemia. *Nat Genet* 1994;**6**:335–41.

Grossman M, Raper SE, Wilson JM. Transplantation of genetically modified autologous hepatocytes into nonhuman primates: feasibility and short-term toxicity. *Hum Gene Ther* 1992;**3**:501–10.

Group TAS. Effects of Combination Lipid Therapy in Type 2 Diabetes Mellitus. *N Engl J Med* 2010;**362**:1563–74.

Grundy SM. Can statins cause chronic low-grade myopathy? *Ann Intern Med* 2002;**137**:617–8.

Gu P, Ishii Y, Spencer TA *et al.* Function-structure studies and identification of three enzyme domains involved in the catalytic activity in rat hepatic squalene synthase. *J Biol Chem* 1998;**273**:12515–25.

Guyard-Dangremont V, Desrumaux C, Gambert P *et al.* Phospholipid and cholesteryl ester transfer activities in plasma from 14 vertebrate species. Relation to atherogenesis susceptibility. *Comp Biochem Physiol - B Biochem Mol Biol* 1998;**120**:517–25.

Hacein-Bey-Abina S, Garrigue A, Wang GP *et al.* Insertional oncogenesis in 4 patients after retrovirus-mediated gene therapy of SCID-X1. *J Clin Invest* 2008;**118**:3132–42.

Hacein-Bey-Abina S, Von Kalle C, Schmidt M *et al.* LMO2-associated clonal T cell proliferation in two patients after gene therapy for SCID-X1. *Science*

2003;**302**:415–9.

Hamilton-Craig I, Kostner K, Colquhoun D *et al.* Combination therapy of statin and ezetimibe for the treatment of familial hypercholesterolemia. *Vasc Health Risk Manag* 2010;**6**:1023–37.

Hanukoglu I. Steroidogenic enzymes: Structure, function, and role in regulation of steroid hormone biosynthesis. *J Steroid Biochem Mol Biol* 1992;**43**:779–804.

Hartvigsen K, Binder CJ, Hansen LF *et al.* A Diet-Induced Hypercholesterolemic Murine Model to Study Atherogenesis Without Obesity and Metabolic Syndrome. *Arterioscler Thromb Vasc Biol* 2007;**27**:878–85.

Harwood HJ, Barbacci-Tobin EG, Petras SF *et al.* 3-(4-chlorophenyl)-2-(4-diethylaminoethoxyphenyl)-A-pentenonitrile monohydrogen citrate and related analogs. Reversible, competitive, first half-reaction squalene synthetase inhibitors. *Biochem Pharmacol* 1997;**53**:839–64.

van Heek M, Compton DS, Davis HR. The cholesterol absorption inhibitor, ezetimibe, decreases diet-induced hypercholesterolemia in monkeys. *Eur J Pharmacol* 2001;**415**:79–84.

Heeren J, Steinwaerder DS, Schnieders F *et al.* Nonphysiological overexpression of low-density lipoprotein receptors causes pathological intracellular lipid accumulation and the formation of cholesterol and cholesteryl ester crystals in vitro. *J Mol Med (Berl)* 1999;**77**:735–43.

Heng HHQ, Goetze S, Ye CJ *et al.* Chromatin loops are selectively anchored using scaffold/matrix-attachment regions. *J Cell Sci* 2004;**117**:999–1008.

Herbst F, Ball CR, Tuorto F *et al.* Extensive Methylation of Promoter Sequences Silences Lentiviral Transgene Expression During Stem Cell Differentiation In Vivo. *Mol Ther* 2012;**20**:1014–21.

Hibbitt O, Agkatsev S, Owen C *et al.* RNAi-mediated knockdown of HMG CoA reductase enhances gene expression from physiologically regulated low-density lipoprotein receptor therapeutic vectors in vivo. *Gene Ther* 2012;**19**:463–7.

Hibbitt OC, Harbottle RP, Waddington SN *et al.* Delivery and long-term expression of a 135 kbLDLR genomic DNA locusin vivo by hydrodynamic tail vein injection. *J Gene Med* 2007a;**9**:488–97.

Hibbitt OC, Harbottle RP, Waddington SN *et al.* Delivery and long-term expression of a 135 kbLDLR genomic DNA locusin vivo by hydrodynamic tail vein injection. *J Gene Med* 2007b;**9**:488–97.

Hibbitt OC, McNeil E, Lufino MM *et al.* Long-term physiologically regulated expression of the low-density lipoprotein receptor in vivo using genomic DNA mini-gene constructs. *Mol Ther* 2010;**18**:317–26.

Hobbs HH, Russell DW, Brown MS *et al.* The LDL receptor locus in familial hypercholesterolemia: mutational analysis of a membrane protein. *Annu Rev Genet* 1990;**24**:133–70.

Hopkins PN, Toth PP, Ballantyne CM *et al.* Familial Hypercholesterolemias: Prevalence, genetics, diagnosis and screening recommendations from the National Lipid Association Expert Panel on Familial Hypercholesterolemia. *J Clin Lipidol* 2011;**5**:S9–17.

Horton JD, Shah NA, Warrington JA *et al.* Combined analysis of oligonucleotide microarray data from transgenic and knockout mice identifies direct SREBP target genes. *Proc Natl Acad Sci* 2003;**100**:12027–32.

Hou X, Jiao R, Guo X *et al.* Construction of minicircle DNA vectors capable of correcting familial hypercholesterolemia phenotype in a LDLR deficient mouse model. *Gene Ther* 2016:657–63.

Hua X, Nohturfft A, Goldstein JL *et al.* Sterol resistance in CHO cells traced to point mutation in SREBP cleavage-activating protein. *Cell* 1996;**87**:415–26.

Huang Y, DiDonato JA, Levison BS *et al.* An abundant dysfunctional apolipoprotein A1 in human atheroma. *Nat Med* 2014;**20**:193–203.

Huff MW, Burnett JR. 3-Hydroxy-3-methylglutaryl coenzyme A reductase inhibitors and hepatic apolipoprotein B secretion. *Curr Opin Lipidol* 1997;**8**:138–45.

Hussain MM. Intestinal lipid absorption and lipoprotein formation. *Curr Opin Lipidol* 2014;**25**:200–6.

Hussain MM, Kancha RK, Zhou Z *et al.* Chylomicron assembly and catabolism: role of apolipoproteins and receptors. *Biochim Biophys Acta* 1996;**1300**:151–70.

Hussain MM, Rava P, Walsh M *et al.* Multiple functions of microsomal triglyceride transfer protein. *Nutr Metab (Lond)* 2012;**9**:14.

Hussain MM, Shi J, Dreizen P. Microsomal triglyceride transfer protein and its role in apoB-lipoprotein assembly. *J Lipid Res* 2003;**44**:22–32.

Ibrahim M, El-Hamamsy I, Barbir M *et al.* Translational lessons from a case of combined heart and liver transplantation for familial hypercholesterolemia 20 years post-operatively. *J Cardiovasc Transl Res* 2012;**5**:351–8.

Ichikawa M, Ohtsuka M, Ohki H *et al.* Discovery of DF-461, a potent squalene synthase inhibitor. *ACS Med Chem Lett* 2013;**4**:932–6.

Illingworth DR, Crouse JR, Hunninghake DB *et al.* A comparison of simvastatin and atorvastatin up to maximal recommended doses in a large multicenter randomized clinical trial. *Curr Med Res Opin* 2001;**17**:43–50.

Inoue H, Jiang XF, Katayama T *et al.* Brain protection by resveratrol and fenofibrate against stroke requires peroxisome proliferator-activated receptor ?? in mice. *Neurosci Lett* 2003;**352**:203–6.

Investigators TA-H. Niacin in Patients with Low HDL Cholesterol Levels Receiving Intensive Statin Therapy. *N Engl J Med* 2011;**365**:2255–67.

Ishibashi S, Brown MS, Goldstein JL *et al.* Hypercholesterolemia in low density lipoprotein receptor knockout mice and its reversal by adenovirus-mediated gene delivery. *J Clin Invest* 1993;**92**:883–93.

Ishibashi S, Herz J, Maeda N *et al.* The two-receptor model of lipoprotein clearance: tests of the hypothesis in knockout mice lacking the low density lipoprotein receptor, apolipoprotein E, or both proteins. *Proc Natl Acad Sci U*

S A 1994;**91**:4431–5.

Ishida K, Visbal G, Cola J *et al.* Two squalene synthase inhibitors, E 28500 and ER-119884, interfere with cellular proliferation and induce ultrastructural and lipid profile alterations in a Candida tropicalis strain resistant to fluconazole, itraconazole, and amphotericin B. *J Infect Chemother* 2011;**17**:563–70.

Ishihara T, Kakuta H, Moritani H *et al.* Synthesis and biological evaluation of novel propylamine derivatives as orally active squalene synthase inhibitors. *Bioorg Med Chem* 2004;**12**:5899–908.

Jacobs AC, Didone L, Jobson J *et al.* Adenylate kinase release as a high-throughput-screening-compatible reporter of bacterial lysis for identification of antibacterial agents. *Antimicrob Agents Chemother* 2013;**57**:26–36.

Jacobson TA. Myopathy with statin–fibrate combination therapy: clinical considerations. *Nat Rev Endocrinol* 2009;**5**:507–18.

Janowski BA, Grogan MJ, Jones SA *et al.* Structural requirements of ligands for the oxysterol liver X receptors LXR and LXR. *Proc Natl Acad Sci* 1999;**96**:266–71.

Jeon H, Meng W, Takagi J *et al.* Implications for familial hypercholesterolemia from the structure of the LDL receptor YWTD-EGF domain pair. *Nat Struct Biol* 2001;**8**:499–504.

Jeong HJ, Lee H-S, Kim K-S *et al.* Sterol-dependent regulation of proprotein convertase subtilisin/kexin type 9 expression by sterol-regulatory element binding protein-2. *J Lipid Res* 2008;**49**:399–409.

Jeong JH, Cho S, Pak YK. Sterol-independent repression of low density lipoprotein receptor promoter by peroxisome proliferator activated receptor gamma coactivator-1alpha (PGC-1alpha). *Exp Mol Med* 2009;**41**:406–16.

Joseph A, Ackerman D, Talley JD *et al.* Manifestations of coronary atherosclerosis in young trauma victims--an autopsy study. *J Am Coll Cardiol* 1993;**22**:459–67.

Joy TR, Hegele RA. Narrative review: statin-related myopathy. *Ann Intern Med* 2009;**150**:858–68.

Kamimura K, Kanefuji T, Yokoo T *et al.* Safety assessment of liver-targeted hydrodynamic gene delivery in dogs. *PLoS One* 2014;**9**.

Kamimura K, Suda T, Zhang G *et al.* Parameters Affecting Image-guided, Hydrodynamic Gene Delivery to Swine Liver. *Mol Ther Acids* 2013;**2**:e128.

Kamimura K, Yokoo T, Abe H *et al.* Image-Guided Hydrodynamic Gene Delivery: Current Status and Future Directions. *Pharmaceutics* 2015;**7**:213–23.

Kankkonen HM, Vähäkangas E, Marr RA *et al.* Long-term lowering of plasma cholesterol levels in LDL-receptor-deficient WHHL rabbits by gene therapy. *Mol Ther* 2004;**9**:548–56.

Kapourchali FR, Surendiran G, Chen L *et al.* Animal models of atherosclerosis. *World J Clin cases* 2014;**2**:126–32.

Kassim SH, Li H, Bell P *et al.* Adeno-associated virus serotype 8 gene therapy leads to significant lowering of plasma cholesterol levels in humanized mouse models of homozygous and heterozygous familial hypercholesterolemia. *Hum Gene Ther* 2013;**24**:19–26.

Kassim SH, Li H, Vandenberghe LH *et al.* Gene therapy in a humanized mouse model of familial hypercholesterolemia leads to marked regression of atherosclerosis. *PLoS One* 2010;**5**:e13424.

Kastelein JJP, Akdim F, Stroes ESG *et al.* Simvastatin with or without ezetimibe in familial hypercholesterolemia. *N Engl J Med* 2008;**358**:1431–43.

Kastelein JJP, Ginsberg HN, Langslet G *et al.* ODYSSEY FH I and FH II: 78 week results with alirocumab treatment in 735 patients with heterozygous familial hypercholesterolaemia. *Eur Heart J* 2015;**36**:2996–3003.

Kay MA, He C-Y, Chen Z-Y. A robust system for production of minicircle DNA vectors. *Nat Biotechnol* 2010;**28**:1287–9.

Kazi DS, Moran AE, Coxson PG *et al.* Cost-effectiveness of PCSK9 Inhibitor

Therapy in Patients With Heterozygous Familial Hypercholesterolemia or Atherosclerotic Cardiovascular Disease. *JAMA* 2016;**316**:743.

Keller C. Apheresis in coronary heart disease with elevated Lp (a): a review of Lp (a) as a risk factor and its management. *Ther Apher Dial* 2007;**11**:2–8.

Khachadurian AK. The inheritance of essential familial hypercholesterolemia. *Am J Med* 1964;**37**:402–7.

Khalifeh M, Faraj W, Heaton N *et al.* Successful living-related liver transplantation for familial hypercholesterolemia in the Middle East. *Transpl Int* 2005;**17**:735–9.

Khalil MF, Wagner WD, Goldberg IJ. Molecular Interactions Leading to Lipoprotein Retention and the Initiation of Atherosclerosis. *Arterioscler Thromb Vasc Biol* 2004;**24**:2211–8.

Khorsandi S, Bachellier P, Weber J *et al.* Minimally invasive and selective hydrodynamic gene therapy of liver segments in the pig and human. *Cancer Gene Ther* 2008;**15**:225–30.

Kirby TJ. Cataracts produced by triparanol. (MER-29). *Trans Am Ophthalmol Soc* 1967;**65**:494–543.

Knauer MJ, Urquhart BL, Meyer zu Schwabedissen HE *et al.* Human skeletal muscle drug transporters determine local exposure and toxicity of statins. *Circ Res* 2010;**106**:297–306.

Kolodgie FD, Katocs AS, Largis EE *et al.* Hypercholesterolemia in the Rabbit Induced by Feeding Graded Amounts of Low-Level Cholesterol. *Arterioscler Thromb Vasc Biol* 1996;**16**.

Kong W, Wei J, Abidi P *et al.* Berberine is a novel cholesterol-lowering drug working through a unique mechanism distinct from statins. *Nat Med* 2004;**10**:1344–51.

Kozarsky K, Grossman M, Wilson JM. Adenovirus-mediated correction of the genetic defect in hepatocytes from patients with familial hypercholesterolemia.

Somat Cell Mol Genet 1993;**19**:449–58.

Kozarsky KF, McKinley DR, Austin LL *et al.* In vivo correction of low density lipoprotein receptor deficiency in the Watanabe heritable hyperlipidemic rabbit with recombinant adenoviruses. *J Biol Chem* 1994;**269**:13695–702.

Krause BR, Newton RS. Lipid-lowering activity of atorvastatin and lovastatin in rodent species: triglyceride-lowering in rats correlates with efficacy in LDL animal models. *Atherosclerosis* 1995;**117**:237–44.

Kroon AA, van't Hof MA, Demacker PN *et al.* The rebound of lipoproteins after LDL-apheresis. Kinetics and estimation of mean lipoprotein levels. *Atherosclerosis* 2000;**152**:519–26.

Krysan PJ, Calos MP. Epstein-Barr virus-based vectors that replicate in rodent cells. *Gene* 1993;**136**:137–43.

Küçükkartallar T, Yankol Y, Kanmaz T *et al.* Liver transplantation as a treatment option for three siblings with homozygous familial hypercholesterolemia. *Pediatr Transplant* 2011;**15**:281–4.

Kwiterovich PO. The metabolic pathways of high-density lipoprotein, low-density lipoprotein, and triglycerides: a current review. *Am J Cardiol* 2000;**86**:5–10.

Laden BP, Porter TD. Resveratrol inhibits human squalene monooxygenase. *Nutr Res* 2001;**21**:747–53.

Ladopoulou EM, Matralis AN, Nikitakis A *et al.* Antihyperlipidemic morpholine derivatives with antioxidant activity: An investigation of the aromatic substitution. *Bioorg Med Chem* 2015;**23**:7015–23.

Lagace TA. PCSK9 and LDLR degradation: regulatory mechanisms in circulation and in cells. *Curr Opin Lipidol* 2014;**25**:387–93.

Lamperti C, Naini AB, Lucchini V *et al.* Muscle coenzyme Q10 level in statin-related myopathy. *Arch Neurol* 2005;**62**:1709–12.

Landmesser U, Bahlmann F, Mueller M *et al.* Simvastatin versus ezetimibe: pleiotropic and lipid-lowering effects on endothelial function in humans.

Circulation 2005;**111**:2356–63.

Längle-Rouault F, Patzel V, Benavente A *et al.* Up to 100-fold increase of apparent gene expression in the presence of Epstein-Barr virus oriP sequences and EBNA1: implications of the nuclear import of plasmids. *J Virol* 1998;**72**:6181–5.

Larsson SL, Skogsberg J, Björkegren J. The low density lipoprotein receptor prevents secretion of dense apoB100-containing lipoproteins from the liver. *J Biol Chem* 2004;**279**:831–6.

Laufs U, La Fata V, Plutzky J *et al.* Upregulation of endothelial nitric oxide synthase by HMG CoA reductase inhibitors. *Circulation* 1998;**97**:1129–35.

Lebherz C, Gao G, Louboutin J-P *et al.* Gene therapy with novel adeno-associated virus vectors substantially diminishes atherosclerosis in a murine model of familial hypercholesterolemia. *J Gene Med* 2004;**6**:663–72.

Lecerf J-M, de Lorgeril M. Dietary cholesterol: from physiology to cardiovascular risk. *Br J Nutr* 2011;**106**:6–14.

Lennernäs H, Fager G. Pharmacodynamics and pharmacokinetics of the HMG-CoA reductase inhibitors. Similarities and differences. *Clin Pharmacokinet* 1997;**32**:403–25.

Li J, Fang B, Eisensmith RC *et al.* In vivo gene therapy for hyperlipidemia: phenotypic correction in Watanabe rabbits by hepatic delivery of the rabbit LDL receptor gene. *J Clin Invest* 1995;**95**:768–73.

Li S, Brown MS, Goldstein JL. Bifurcation of insulin signaling pathway in rat liver: mTORC1 required for stimulation of lipogenesis, but not inhibition of gluconeogenesis. *Proc Natl Acad Sci U S A* 2010;**107**:3441–6.

Lim CK, Yuan ZX, Lamb JH *et al.* A comparative study of tamoxifen metabolism in female rat, mouse and human liver microsomes. *Carcinogenesis* 1994;**15**:589–93.

Lindgren V, Luskey KL, Russell DW *et al.* Human genes involved in cholesterol

metabolism: chromosomal mapping of the loci for the low density lipoprotein receptor and 3-hydroxy-3-methylglutaryl-coenzyme A reductase with cDNA probes. *Proc Natl Acad Sci U S A* 1985;**82**:8567–71.

Lindner SE, Sugden B. The plasmid replicon of Epstein–Barr virus: Mechanistic insights into efficient, licensed, extrachromosomal replication in human cells. *Plasmid* 2007;**58**:1–12.

Liscum L. CHAPTER 14 – Cholesterol biosynthesis. *Biochemistry of Lipids, Lipoproteins and Membranes*. 2008, 399–421.

Liu B, Ramirez CM, Miller AM *et al.* Cyclodextrin overcomes the transport defect in nearly every organ of NPC1 mice leading to excretion of sequestered cholesterol as bile acid. *J Lipid Res* 2010;**51**:933–44.

Liu B, Turley SD, Burns DK *et al.* Reversal of defective lysosomal transport in NPC disease ameliorates liver dysfunction and neurodegeneration in the npc1-/- mouse. *Proc Natl Acad Sci U S A* 2009;**106**:2377–82.

Liu F, Song Y, Liu D. Hydrodynamics-based transfection in animals by systemic administration of plasmid DNA. *Gene Ther* 1999;**6**:1258–66.

Lo C-M, Nordskog BK, Nauli AM *et al.* Why does the gut choose apolipoprotein B48 but not B100 for chylomicron formation? *Am J Physiol Gastrointest Liver Physiol* 2008;**294**:G344-52.

Lufino MMP, Manservigi R, Wade-Martins R. An S/MAR-based infectious episomal genomic DNA expression vector provides long-term regulated functional complementation of LDLR deficiency. *Nucleic Acids Res* 2007a;**35**:e98.

Lufino MMP, Manservigi R, Wade-Martins R. An S/MAR-based infectious episomal genomic DNA expression vector provides long-term regulated functional complementation of LDLR deficiency. *Nucleic Acids Res* 2007b;**35**:e98.

Lundstam U, Hurt-Camejo E, Olsson G *et al.* Proteoglycans Contribution to Association of Lp(a) and LDL With Smooth Muscle Cell Extracellular Matrix.

Arterioscler Thromb Vasc Biol 1999;**19**:1162–7.

MacArthur JM, Bishop JR, Stanford KI *et al.* Liver heparan sulfate proteoglycans mediate clearance of triglyceride-rich lipoproteins independently of LDL receptor family members. *J Clin Invest* 2007;**117**:153–64.

de Macedo-Silva ST, de Souza W, Rodrigues JCF. Sterol Biosynthesis Pathway as an Alternative for the Anti-Protozoan Parasite Chemotherapy. *Curr Med Chem* 2015;**22**:2186–98.

Malby S, Pickering R, Saha S *et al.* The first epidermal growth factor-like domain of the low-density lipoprotein receptor contains a noncanonical calcium binding site. *Biochemistry* 2001;**40**:2555–63.

Mani P, Rohatgi A. Niacin Therapy, HDL Cholesterol, and Cardiovascular Disease: Is the HDL Hypothesis Defunct? *Curr Atheroscler Rep* 2015;**17**:43.

Manno CS, Pierce GF, Arruda VR *et al.* Successful transduction of liver in hemophilia by AAV-Factor IX and limitations imposed by the host immune response. *Nat Med* 2006;**12**:342–7.

Marais AD. Familial hypercholesterolaemia. *Clin Biochem Rev* 2004;**25**:49–68.

Marais AD, Blom DJ, Firth JC. Statins in homozygous familial hypercholesterolemia. *Curr Atheroscler Rep* 2002;**4**:19–25.

Matsunaga A, Sasaki J, Takada Y *et al.* Effect of simvastatin on receptor mediated metabolism of low density lipoprotein in guinea pigs. 1991;**90**:31–7.

McBride JL, Boudreau RL, Harper SQ *et al.* Artificial miRNAs mitigate shRNA-mediated toxicity in the brain: implications for the therapeutic development of RNAi. *Proc Natl Acad Sci U S A* 2008;**105**:5868–73.

McKenzie R, Fried MW, Sallie R *et al.* Hepatic failure and lactic acidosis due to fialuridine (FIAU), an investigational nucleoside analogue for chronic hepatitis B. *N Engl J Med* 1995;**333**:1099–105.

Methia N, André P, Denis C V. *et al.* Localized reduction of atherosclerosis in von Willebrand factor-deficient mice. *Blood* 2001;**98**:1424–8.

Miki T, Kori M, Mabuchi H *et al.* Synthesis of Novel 4,1-Benzoxazepine Derivatives as Squalene Synthase Inhibitors and Their Inhibition of Cholesterol Synthesis. 2002, DOI: 10.1021/JM020234O.

Mingozzi F, High KA. Immune responses to AAV vectors: overcoming barriers to successful gene therapy. *Blood* 2013;**122**:23–36.

Mitchell RS, Beitzel BF, Schroder ARW *et al.* Retroviral DNA integration: ASLV, HIV, and MLV show distinct target site preferences. *PLoS Biol* 2004;**2**:E234.

Moore KJ, Sheedy FJ, Fisher EA. Macrophages in atherosclerosis: a dynamic balance. *Nat Rev Immunol* 2013;**13**:709–21.

Morales M, Santana N, Soria A *et al.* Effects of tamoxifen on serum lipid and apolipoprotein levels in postmenopausal patients with breast cancer. *Breast Cancer Res Treat* 1996;**40**:265–70.

Muller C. Xanthomata, Hypercholesterolemia, Angina Pectoris. *Acta Med Scand* 1938;**89**:75–84.

Nagashima S, Yagyu H, Tozawa R *et al.* Plasma cholesterol-lowering and transient liver dysfunction in mice lacking squalene synthase in the liver. *J Lipid Res* 2015;**56**:998–1005.

Nakamura S, Maehara T, Watanabe S *et al.* Improvement of Hydrodynamics-Based Gene Transfer of Nonviral DNA Targeted to Murine Hepatocytes. 2013;**2013**.

Nakashima Y, Plump AS, Raines EW *et al.* ApoE-deficient mice develop lesions of all phases of atherosclerosis throughout the arterial tree. *Arterioscler Thromb* 1994a;**14**:133–40.

Nakashima Y, Plump AS, Raines EW *et al.* the Arterial Tree. *Arteriosclerosis* 1994b:133–40.

Nakayama O, Hirosumi J, Chida N *et al.* FR146687, a novel steroid 5-reductase inhibitor: In vitro and in vivo effects on prostates. *Prostate* 1997;**31**:241–9.

Nayak S, Herzog RW. Progress and prospects: immune responses to viral

vectors. *Gene Ther* 2010;**17**:295–304.

Nayerossadat N, Maedeh T, Ali PA. Viral and nonviral delivery systems for gene delivery. *Adv Biomed Res* 2012;**1**:27.

Ness GC, Zhao Z, Lopez D. Inhibitors of cholesterol biosynthesis increase hepatic low-density lipoprotein receptor protein degradation. *Arch Biochem Biophys* 1996;**325**:242–8.

Neuvonen PJ, Niemi M, Backman JT. Drug interactions with lipid-lowering drugs: mechanisms and clinical relevance. *Clin Pharmacol Ther* 2006;**80**:565–81.

Nguyen AT, Dow AC, Kupiec-Weglinski J *et al.* Evaluation of gene promoters for liver expression by hydrodynamic gene transfer. *J Surg Res* 2008;**148**:60–6.

Nguyen TH, Ferry N. Liver gene therapy: advances and hurdles. *Gene Ther* 2004;**11**:S76–84.

Nilsson SK, Lookene A, Beckstead JA *et al.* Apolipoprotein A-V interaction with members of the low density lipoprotein receptor gene family. *Biochemistry* 2007;**46**:3896–904.

Nishimoto T, Amano Y, Tozawa R *et al.* Lipid-lowering properties of TAK-475, a squalene synthase inhibitor, *in vivo* and *in vitro*. *Br J Pharmacol* 2003a;**139**:911–8.

Nishimoto T, Tozawa R, Amano Y *et al.* Comparing myotoxic effects of squalene synthase inhibitor, T-91485, and 3-hydroxy-3-methylglutaryl coenzyme A (HMG-CoA) reductase inhibitors in human myocytes. *Biochem Pharmacol* 2003b;**66**:2133–9.

Nohturfft A, Brown MS, Goldstein JL. Sterols regulate processing of carbohydrate chains of wild-type SREBP cleavage-activating protein (SCAP), but not sterol-resistant mutants Y298C or D443N. *Proc Natl Acad Sci U S A* 1998;**95**:12848–53.

Nomura S, Merched A, Nour E *et al.* Low-density lipoprotein receptor gene therapy using helper-dependent adenovirus produces long-term protection

against atherosclerosis in a mouse model of familial hypercholesterolemia. *Gene Ther* 2004;**11**:1540–8.

Ochiai A, Miyata S, Shimizu M *et al.* Piperine Induces Hepatic Low-Density Lipoprotein Receptor Expression through Proteolytic Activation of Sterol Regulatory Element-Binding Proteins. *PLoS One* 2015;**10**:e0139799.

Ott MG, Schmidt M, Schwarzwaelder K *et al.* Correction of X-linked chronic granulomatous disease by gene therapy, augmented by insertional activation of MDS1-EVI1, PRDM16 or SETBP1. *Nat Med* 2006;**12**:401–9.

Otway S, Robinson DS. The use of a non-ionic detergent (Triton WR 1339) to determine rates of triglyceride entry into the circulation of the rat under different physiological conditions. *J Physiol* 1967;**190**:321–32.

Page MM, Ekinci EI, Jones RM *et al.* Liver transplantation for the treatment of homozygous familial hypercholesterolaemia in an era of emerging lipid-lowering therapies. *Intern Med J* 2014;**44**:601–4.

Paigen B, Svenson KL, Von Smith R *et al.* Physiological effects of housing density on C57BL/6J mice over a 9-month period. *J Anim Sci* 2012;**90**:5182–92.

Pandit J, Danley DE, Schulte GK *et al.* Crystal Structure of Human Squalene Synthase. *Biochemistry* 2000;**275**:30610–7.

Pandor A, Ara RM, Tumur I *et al.* Ezetimibe monotherapy for cholesterol lowering in 2,722 people: systematic review and meta-analysis of randomized controlled trials. *J Intern Med* 2009;**265**:568–80.

Parzych EM, Li H, Yin X *et al.* Effects of immunosuppression on circulating adeno-associated virus capsid-specific T cells in humans. *Hum Gene Ther* 2013;**24**:431–42.

Pecoraro V, Moja L, Dall'Olmo L *et al.* Most appropriate animal models to study the efficacy of statins: a systematic review. *Eur J Clin Invest* 2014;**44**:848–71.

Pedersen TR. Randomised trial of cholesterol lowering in 4444 patients with coronary heart disease: the Scandinavian Simvastatin Survival Study (4S).

Lancet 1994;**344**:1383–9.

Peng D, Hiipakka RA, Xie J-T *et al.* A novel potent synthetic steroidal liver X receptor agonist lowers plasma cholesterol and triglycerides and reduces atherosclerosis in LDLR(-/-) mice. *Br J Pharmacol* 2011;**162**:1792–804.

Perez de Isla L, Alonso R, Watts GF *et al.* Attainment of LDL-Cholesterol Treatment Goals in Patients With Familial Hypercholesterolemia. *J Am Coll Cardiol* 2016;**67**:1278–85.

Phillips PS, Haas RH, Bannykh S *et al.* Statin-associated myopathy with normal creatine kinase levels. *Ann Intern Med* 2002;**137**:581–5.

Piechaczek C, Fetzer C, Baiker A *et al.* A vector based on the SV40 origin of replication and chromosomal S/MARs replicates episomally in CHO cells. *Nucleic Acids Res* 1999;**27**:426–8.

Pijlman AH, Huijgen R, Verhagen SN *et al.* Evaluation of cholesterol lowering treatment of patients with familial hypercholesterolemia: a large cross-sectional study in The Netherlands. *Atherosclerosis* 2010;**209**:189–94.

Pilankatta R, Chawla T, Khanna N *et al.* The prevalence of antibodies to adenovirus serotype 5 in an adult Indian population and implications for adenovirus vector vaccines. *J Med Virol* 2010;**82**:407–14.

Poirier S, Mayer G, Poupon V *et al.* Dissection of the endogenous cellular pathways of PCSK9-induced low density lipoprotein receptor degradation: evidence for an intracellular route. *J Biol Chem* 2009;**284**:28856–64.

Poulter CD, Capson TL, Thompson MD *et al.* Squalene synthetase, inhibition by ammonium analogs of carbocationic intermediates in the conversion of presqualene diphosphate to squalene. *J Am Chem Soc* 1989;**111**:3734–9.

Powell-Braxton L, Véniant M, Latvala RD *et al.* A mouse model of human familial hypercholesterolemia: markedly elevated low density lipoprotein cholesterol levels and severe atherosclerosis on a low-fat chow diet. *Nat Med* 1998;**4**:934–8.

Prescott MF, McBride CH, Hasler-Rapacz J *et al.* Development of complex atherosclerotic lesions in pigs with inherited hyper-LDL cholesterolemia bearing mutant alleles for apolipoprotein B. *Am J Pathol* 1991;**139**:139–47.

Raal FJ, Goldstein J, Hobbs H *et al.* Lomitapide for homozygous familial hypercholesterolaemia. *Lancet* 2013;**381**:7–8.

Raal FJ, Pilcher GJ, Panz VR *et al.* Reduction in mortality in subjects with homozygous familial hypercholesterolemia associated with advances in lipid-lowering therapy. *Circulation* 2011;**124**:2202–7.

Raal FJ, Santos RD, Blom DJ *et al.* Mipomersen, an apolipoprotein B synthesis inhibitor, for lowering of LDL cholesterol concentrations in patients with homozygous familial hypercholesterolaemia: a randomised, double-blind, placebo-controlled trial. *Lancet* 2010;**375**:998–1006.

Raasch RH. Pravastatin sodium, a new HMG-CoA reductase inhibitor. *DICP* 1991;**25**:388–94.

Radisky ES, Poulter CD. Squalene synthase: steady-state, pre-steady-state, and isotope-trapping studies. *Biochemistry* 2000;**39**:1748–60.

Ramakrishnan VM, Yang J-Y, Tien KT *et al.* Restoration of Physiologically Responsive Low-Density Lipoprotein Receptor-Mediated Endocytosis in Genetically Deficient Induced Pluripotent Stem Cells. *Sci Rep* 2015;**5**:13231.

Ramasamy I. Recent advances in physiological lipoprotein metabolism. *Clin Chem Lab Med* 2014;**52**:1695–727.

Rashid S, Curtis DE, Garuti R *et al.* Decreased plasma cholesterol and hypersensitivity to statins in mice lacking Pcsk9. *Proc Natl Acad Sci U S A* 2005;**102**:5374–9.

Reuben A. Hy's law. *Hepatology* 2004;**39**:574–8.

Ridker PM, Danielson E, Fonseca FAH *et al.* Rosuvastatin to Prevent Vascular Events in Men and Women with Elevated C-Reactive Protein. *N Engl J Med* 2008;**359**:2195–207.

Rimando AM, Nagmani R, Feller DR *et al.* Pterostilbene, a new agonist for the peroxisome proliferator-activated receptor -isoform, lowers plasma lipoproteins and cholesterol in hypercholesterolemic hamsters. *J Agric Food Chem* 2005;**53**:3403–7.

Robinson DM, Keating GM. Colesevelam: a review of its use in hypercholesterolemia. *Am J Cardiovasc Drugs* 2007;**7**:453–65.

Robinson JG, Farnier M, Krempf M *et al.* Efficacy and safety of alirocumab in reducing lipids and cardiovascular events. *N Engl J Med* 2015;**372**:1489–99.

Robinson JG, Rogers WJ, Nedergaard BS *et al.* Rationale and design of LAPLACE-2: a phase 3, randomized, double-blind, placebo- and ezetimibe-controlled trial evaluating the efficacy and safety of evolocumab in subjects with hypercholesterolemia on background statin therapy. *Clin Cardiol* 2014;**37**:195–203.

Rodrigues JCF, Urbina JA, de Souza W. Antiproliferative and ultrastructural effects of BPQ-OH, a specific inhibitor of squalene synthase, on Leishmania amazonensis. *Exp Parasitol* 2005;**111**:230–8.

Rondini EA, Duniec-Dmuchowski Z, Cukovic D *et al.* Differential regulation of gene expression by cholesterol biosynthesis inhibitors that reduce (pravastatin) or enhance (squalestatin 1) nonsterol isoprenoid levels in primary cultured mouse and rat hepatocytes. *J Pharmacol Exp Ther* 2016;**1**:216–29.

Rozman D, Monostory K. Perspectives of the non-statin hypolipidemic agents. *Pharmacol Ther* 2010;**127**:19–40.

Santos PCJL, Gagliardi ACM, Miname MH *et al.* SLCO1B1 haplotypes are not associated with atorvastatin-induced myalgia in Brazilian patients with familial hypercholesterolemia. *Eur J Clin Pharmacol* 2012;**68**:273–9.

Sawada M, Matsuo M, Hagihara H *et al.* Effect of FR194738, a potent inhibitor of squalene epoxidase, on cholesterol metabolism in HepG2 cells. *Eur J Pharmacol* 2001;**431**:11–6.

Schick BA, Laaksonen R, Frohlich JJ *et al.* Decreased skeletal muscle

mitochondrial DNA in patients treated with high-dose simvastatin. *Clin Pharmacol Ther* 2007;**81**:650–3.

Schneider WJ, Beisiegel U, Goldstein JL *et al.* Purification of the low density lipoprotein receptor, an acidic glycoprotein of 164,000 molecular weight. *J Biol Chem* 1982;**257**:2664–73.

Schröder ARW, Shinn P, Chen H *et al.* HIV-1 integration in the human genome favors active genes and local hotspots. *Cell* 2002;**110**:521–9.

Scott LJ. Alipogene tiparvovec: a review of its use in adults with familial lipoprotein lipase deficiency. *Drugs* 2015;**75**:175–82.

SEARCH Collaborative Group, Link E, Parish S *et al.* SLCO1B1 variants and statin-induced myopathy--a genomewide study. *N Engl J Med* 2008;**359**:789–99.

Seidah NG, Benjannet S, Wickham L *et al.* The secretory proprotein convertase neural apoptosis-regulated convertase 1 (NARC-1): liver regeneration and neuronal differentiation. *Proc Natl Acad Sci U S A* 2003;**100**:928–33.

Shah AS, Tan L, Long JL *et al.* The proteomic diversity of high density lipoproteins: Our emerging understanding of its importance in lipid transport and beyond. 2016.

Sharma A, Slugg PH, Hammett JL *et al.* Clinical pharmacokinetics and pharmacodynamics of a new squalene synthase inhibitor, BMS-188494, in healthy volunteers. *J Clin Pharmacol* 1998;**38**:1116–21.

Shepherd J, Cobbe S, Ford I *et al.* Prevention of Coronary Heart Disease With Pravastatin in Men With. *Lancet (London, England)* 1995;**333**.

Shulman GI, et al. The New England Journal of Medicine. *N Engl J Med* 2016.

Sibbald B. Death but one unintended consequence of gene-therapy trial. *CMAJ* 2001;**164**:1612.

Sirvent P, Mercier J, Lacampagne A. New insights into mechanisms of statin-associated myotoxicity. *Curr Opin Pharmacol* 2008;**8**:333–8.

Skålén K, Gustafsson M, Rydberg EK *et al.* Subendothelial retention of atherogenic lipoproteins in early atherosclerosis. *Nature* 2002;**417**:750–4.

Sniderman AD, Tsimikas S, Fazio S. The Severe Hypercholesterolemia Phenotype: Clinical Diagnosis, Management, and Emerging Therapies. *J Am Coll Cardiol* 2014;**63**:1935–47.

Somanathan S, Jacobs F, Wang Q *et al.* Aav vectors expressing LDLR gain-of-function variants demonstrate increased efficacy in mouse models of familial hypercholesterolemia. *Circ Res* 2014, DOI: 10.1161/CIRCRESAHA.115.304008.

Spady DK. Reverse cholesterol transport and atherosclerosis regression. *Circulation* 1999;**100**:576–8.

Spady DK, Woollett LA, Meidell RS *et al.* Kinetic characteristics and regulation of HDL cholesteryl ester and apolipoprotein transport in the apoA-I-/- mouse. *J Lipid Res* 1998;**39**:1483–92.

Staels B, Dallongeville J, Auwerx J *et al.* Mechanism of action of fibrates on lipid and lipoprotein metabolism. *Circulation* 1998;**98**:2088–93.

Stamellos KD, Shackelford JE, Shechter I *et al.* Subcellular localization of squalene synthase in rat hepatic cells. Biochemical and immunochemical evidence. *J Biol Chem* 1993;**268**:12825–36.

Stary HC, Chandler AB, Dinsmore RE *et al.* A definition of advanced types of atherosclerotic lesions and a histological classification of atherosclerosis. A report from the Committee on Vascular Lesions of the Council on Arteriosclerosis, American Heart Association. *Circulation* 1995;**92**:1355–74.

Stary HC, Chandler AB, Glagov S *et al.* A definition of initial, fatty streak, and intermediate lesions of atherosclerosis. A report from the Committee on Vascular Lesions of the Council on Arteriosclerosis, American Heart Association. *Arterioscler Thromb Vasc Biol* 1994;**14**:840–56.

Starzl TE, Bilheimer DW, Bahnson HT *et al.* Heart-liver transplantation in a patient with familial hypercholesterolaemia. *Lancet (London, England)* 1984;**1**:1382–

3.

Di Stasi SL, MacLeod TD, Winters JD *et al.* Effects of statins on skeletal muscle: a perspective for physical therapists. *Phys Ther* 2010;**90**:1530–42.

Stein E a., Bays H, O'Brien D *et al.* Lapaquistat acetate: Development of a squalene synthase inhibitor for the treatment of hypercholesterolemia. *Circulation* 2011;**123**:1974–85.

Stein EA, Honarpour N, Wasserman SM *et al.* Effect of the proprotein convertase subtilisin/kexin 9 monoclonal antibody, AMG 145, in homozygous familial hypercholesterolemia. *Circulation* 2013;**128**:2113–20.

Stein EA, Swergold GD. Potential of proprotein convertase subtilisin/kexin type 9 based therapeutics. *Curr Atheroscler Rep* 2013;**15**:310.

Steinberg D, Avigan J, Feigelson EB. Effects of Triparanol (Mer-29) on cholesterol biosynthesis and on blood sterol levels in man. *J Clin Invest* 1961;**40**:884–93.

Steinberg D, Witztum JL. Oxidized low-density lipoprotein and atherosclerosis. *Arterioscler Thromb Vasc Biol* 2010;**30**:2311–6.

Steinbrecher UP, Parthasarathy S, Leake DS *et al.* Modification of low density lipoprotein by endothelial cells involves lipid peroxidation and degradation of low density lipoprotein phospholipids. *Proc Natl Acad Sci U S A* 1984;**81**:3883–7.

Suda T, Gao X, Stolz DB *et al.* Structural impact of hydrodynamic injection on mouse liver. *Gene Ther* 2007;**14**:129–37.

Südhof TC, Russell DW, Brown MS *et al.* 42 bp element from LDL receptor gene confers end-product repression by sterols when inserted into viral TK promoter. *Cell* 1987;**48**:1061–9.

Tabas I, Williams KJ, Borén J. Subendothelial lipoprotein retention as the initiating process in atherosclerosis: update and therapeutic implications. *Circulation* 2007;**116**:1832–44.

Takahashi S, Sakai J, Fujino T *et al.* The very low-density lipoprotein (VLDL)

receptor: characterization and functions as a peripheral lipoprotein receptor. *J Atheroscler Thromb* 2004;**11**:200–8.

Talmud PJ, Shah S, Whittall R *et al.* Use of low-density lipoprotein cholesterol gene score to distinguish patients with polygenic and monogenic familial hypercholesterolaemia: a case-control study. *Lancet (London, England)* 2013;**381**:1293–301.

Tansey TR, Shechter I. Structure and regulation of mammalian squalene synthase. *Biochim Biophys Acta - Mol Cell Biol Lipids* 2000a;**1529**:49–62.

Tansey TR, Shechter I. Squalene synthase: Structure and regulation. *Prog Nucleic Acid Res Mol Biol* 2000b;**65**:157–95.

Tavridou A, Kaklamanis L, Papalois A *et al.* EP2306 [2-(4-Biphenyl)-4-methyl-octahydro-1,4-benzoxazin-2-ol, hydrobromide], A Novel Squalene Synthase Inhibitor, Reduces Atherosclerosis in the Cholesterol-Fed Rabbit. *J Pharmacol Exp Ther* 2007;**323**:794–804.

Taylor RD, MacCoss M, Lawson ADG. Rings in drugs. *J Med Chem* 2014;**57**:5845–59.

Teupser D, Persky AD, Breslow JL. Induction of Atherosclerosis by Low-Fat, Semisynthetic Diets in LDL Receptor-Deficient C57BL/6J and FVB/NJ Mice: Comparison of Lesions of the Aortic Root, Brachiocephalic Artery, and Whole Aorta (En Face Measurement). *Arterioscler Thromb Vasc Biol* 2003;**23**:1907–13.

The Lipid Research Clinics Coronary Primary Prevention Trial results. I. Reduction in incidence of coronary heart disease. *JAMA* 1984;**251**:351–64.

Thompsen J, Thompson PD. A systematic review of LDL apheresis in the treatment of cardiovascular disease. *Atherosclerosis* 2006;**189**:31–8.

Thompson DO. Cyclodextrins--enabling excipients: their present and future use in pharmaceuticals. *Crit Rev Ther Drug Carrier Syst* 1997;**14**:1–104.

Thompson GR. LDL apheresis. *Atherosclerosis* 2003;**167**:1–13.

Thompson JF, Hayes LS, Lloyd DB. Modulation of firefly luciferase stability and impact on studies of gene regulation. 1991;**103**:171–7.

Timmins JM, Lee J-Y, Boudyguina E *et al.* Targeted inactivation of hepatic Abca1 causes profound hypoalphalipoproteinemia and kidney hypercatabolism of apoA-I. *J Clin Invest* 2005;**115**:1333–42.

Tonstad S, Knudtzon J, Sivertsen M *et al.* Efficacy and safety of cholestyramine therapy in peripubertal and prepubertal children with familial hypercholesterolemia. *J Pediatr* 1996;**129**:42–9.

Tsimikas S, Brilakis ES, Miller ER *et al.* Oxidized Phospholipids, Lp(a) Lipoprotein, and Coronary Artery Disease. *N Engl J Med* 2005;**353**:46–57.

Tsujita Y, Kuroda M, Shimada Y *et al.* CS-514, a competitive inhibitor of 3-hydroxy-3-methylglutaryl coenzyme A reductase: tissue-selective inhibition of sterol synthesis and hypolipidemic effect on various animal species. *Biochim Biophys Acta* 1986;**877**:50–60.

Tsurumi T, Fujita M, Kudoh A. Latent and lytic Epstein-Barr virus replication strategies. *Rev Med Virol* 2005;**15**:3–15.

Turunen TAK, Kurkipuro J, Heikura T *et al.* Sleeping Beauty transposon vectors in liver directed gene delivery of LDLR and VLDLR for gene therapy of familial hypercholesterolemia. *Mol Ther* 2015;**24**:620–35.

Ugawa T, Kakuta H, Moritani H *et al.* YM-53601, a novel squalene synthase inhibitor, reduces plasma cholesterol and triglyceride levels in several animal species. *Br J Pharmacol* 2000;**131**:63–70.

Ugawa T, Kakuta H, Moritani H *et al.* Effect of YM-53601, a novel squalene synthase inhibitor, on the clearance rate of plasma LDL and VLDL in hamsters. *Br J Pharmacol* 2002;**137**:561–7.

Umans-Eckenhausen MA, Defesche JC, Sijbrands EJ *et al.* Review of first 5 years of screening for familial hypercholesterolaemia in the Netherlands. *Lancet* 2001;**357**:165–8.

Urbina JA, Concepcion JL, Caldera A *et al.* In vitro and in vivo activities of E5700 and ER-119884, two novel orally active squalene synthase inhibitors, against Trypanosoma cruzi. *Antimicrob Agents Chemother* 2004;**48**:2379–87.

Varga T, Czimmerer Z, Nagy L. PPARs are a unique set of fatty acid regulated transcription factors controlling both lipid metabolism and inflammation. *Biochim Biophys Acta - Mol Basis Dis* 2011;**1812**:1007–22.

Véniant MM, Sullivan M a, Kim SK *et al.* Defining the atherogenicity of large and small lipoproteins containing apolipoprotein B100. *J Clin Invest* 2000;**106**:1501–10.

Veniant MM, Zlot CH, Walzem RL *et al.* Lipoprotein clearance mechanisms in LDL receptor-deficient “apo-B48- only” and “apo-B100-only” mice. *J Clin Invest* 1998;**102**:1559–68.

Venkateswaran A, Laffitte BA, Joseph SB *et al.* Control of cellular cholesterol efflux by the nuclear oxysterol receptor LXRalpha. *Proc Natl Acad Sci* 2000;**97**:12097–102.

Verma IM, Somia N. Gene therapy -- promises, problems and prospects. *Nature* 1997;**389**:239–42.

Wade-Martins R, Saeki Y, Chiocca EA. Infectious Delivery of a 135-kb LDLR Genomic Locus Leads to Regulated Complementation of Low-Density Lipoprotein Receptor Deficiency in Human Cells. , DOI: 10.1016/S1525-0016(03)00060-1.

Wade-Martins R, White RE, Kimura H *et al.* Stable correction of a genetic deficiency in human cells by an episome carrying a 115 kb genomic transgene. *Nat Biotechnol* 2000;**18**:1311–4.

Wang C-Y, Liu P-Y, Liao JK. Pleiotropic effects of statin therapy: molecular mechanisms and clinical results. *Trends Mol Med* 2008;**14**:37–44.

Wasko BM, Smits JP, Shull LW *et al.* A novel bisphosphonate inhibitor of squalene synthase combined with a statin or a nitrogenous bisphosphonate in vitro. *J Lipid Res* 2011;**52**:1957–64.

Watanabe Y. Serial inbreeding of rabbits with hereditary hyperlipidemia (WHHL-rabbit). *Atherosclerosis* 1980;**36**:261–8.

WHO | Cardiovascular diseases (CVDs). *WHO* 2016.

Wierzbicki AS, Hardman TC, Viljoen A. New lipid-lowering drugs: an update. *Int J Clin Pract* 2012;**66**:270–80.

Wierzbicki AS, Humphries SE, Minhas R *et al.* Familial hypercholesterolaemia: summary of NICE guidance. *BMJ* 2008;**337**:a1095.

Willard K-E. Clinical Feature: Diagnosis and Genetic Variance in Familial Hypercholesterolemia. *Off Publ Natl Lipid Assoc* 2010.

Williams JK, Wagner JD, Li Z *et al.* Tamoxifen Inhibits Arterial Accumulation of LDL Degradation Products and Progression of Coronary Artery Atherosclerosis in Monkeys. *Arterioscler Thromb Vasc Biol* 1997;**17**.

Wilson DJ, Gahan M, Haddad L *et al.* A World Wide Web Site for Low-Density Lipoprotein Receptor Gene Mutations in Familial Tabular , and Direct Submission Data Handling. **9149**:1509–11.

Yadav K, Sharma M, Ferdinand KC *et al.* Proprotein convertase subtilisin/kexin type 9 (PCSK9) inhibitors: Present perspectives and future horizons. *Nutr Metab Cardiovasc Dis* 2016;**0**:1747–57.

Yamamoto A, Sudo H, Endo A *et al.* Therapeutic effects of ML-236B in primary hypercholesterolemia. *Atherosclerosis* 1980;**35**:259–66.

Yamamoto T, Bishop RW, Brown MS *et al.* Deletion in cysteine-rich region of LDL receptor impedes transport to cell surface in WHHL rabbit. *Science* 1986;**232**:1230–7.

Yamamoto T, Davis CG, Brown MS *et al.* The human LDL receptor: a cysteine-rich protein with multiple Alu sequences in its mRNA. *Cell* 1984;**39**:27–38.

Yan H, Ma Y, Gui Y *et al.* MG132, a proteasome inhibitor, enhances LDL uptake in HepG2 cells in vitro by regulating LDLR and PCSK9 expression. *Acta Pharmacol Sin* 2014;**35**:994–1004.

Yang Y, Ertl HC, Wilson JM. MHC class I-restricted cytotoxic T lymphocytes to viral antigens destroy hepatocytes in mice infected with E1-deleted recombinant adenoviruses. *Immunity* 1994;**1**:433–42.

Yin W, Carballo-Jane E, McLaren DG *et al.* Plasma lipid profiling across species for the identification of optimal animal models of human dyslipidemia. *J Lipid Res* 2012;**53**:51–65.

Young IS, McEneny J. Lipoprotein oxidation and atherosclerosis. *Biochem Soc Trans* 2001;**29**:358–62.

Young JM, Florkowski CM, Molyneux SL *et al.* Effect of coenzyme Q(10) supplementation on simvastatin-induced myalgia. *Am J Cardiol* 2007;**100**:1400–3.

Youngblom E, Knowles JW. *Familial Hypercholesterolemia*. University of Washington, Seattle, 1993.

Zbaida S, Kariv R. Biomimetic models for monooxygenases. *Biopharm Drug Dispos* **10**:431–42.

Zhang G, Budker V, Wolff JA. High levels of foreign gene expression in hepatocytes after tail vein injections of naked plasmid DNA. *Hum Gene Ther* 1999;**10**:1735–7.

Zhang L, Reue K, Fong LG *et al.* Feedback Regulation of Cholesterol Uptake by the LXR-IDOL-LDLR Axis. *Arterioscler Thromb Vasc Biol* 2012a;**32**:2541–6.

Zhang L, Zhou GZ, Song W *et al.* Pterostilbene protects vascular endothelial cells against oxidized low-density lipoprotein-induced apoptosis in vitro and in vivo. *Apoptosis* 2012b;**17**:25–36.